

MOLECULAR ECOLOGY OF *PEROMYSCUS POLIONOTUS*

Except where reference is made to the work of others, the work described in this dissertation is my own or was done in collaboration with my advisory committee. This dissertation does not include proprietary or classified information.

Jeffrey L. Van Zant

Certificate of Approval:

F. Stephen Dobson
Professor
Biological Sciences

Michael C. Wooten, Chair
Professor
Biological Sciences

James B. Grand
Associate Professor
Forestry and Wildlife Science

Craig Guyer
Professor
Biological Sciences

Stephen L. McFarland
Acting Dean
Graduate School

MOLECULAR ECOLOGY OF *PEROMYSCUS POLIIONOTUS*

Jeffrey L. Van Zant

A Dissertation

Submitted to

the Graduate Faculty of

Auburn University

in Partial Fulfillment of the

Requirements for the

Degree of

Doctor of Philosophy

Auburn, Alabama
August 7, 2006

MOLECULAR ECOLOGY OF *PEROMYSCUS POLIONOTUS*

Jeffrey L. Van Zant

Permission is granted to Auburn University to make copies of this dissertation at its discretion, upon request of individuals or institutions and at their expense. The author reserves all publication rights.

Signature of Author

Date of Graduation

VITA

Jeffrey L. Van Zant, son of Leon and Patricia (Bridgers) Van Zant, was born April 20, 1961, in Roanoke Rapids, North Carolina. He attended Gulf Coast Community College and graduated magna cum laude with an AA degree in biology in 1994. He entered the University of Montana in 1994 and graduated cum laude with a degree in wildlife biology in December 1996. He became a doctoral student at Auburn University in January 2000. He married Alison J. Lovell, daughter of Douglas and Sandra Lovell, on May 22, 2004. They have a son, Brice Carden.

DISSERTATION ABSTARCT
MOLECULAR ECOLOGY OF *PEROMYSCUS POLIONOTUS*

Jeffrey L. Van Zant

Doctor of Philosophy, August 7, 2006
(B. S., University of Montana, 1996)
(A. A., Gulf Coast Community College, 1994)

337 Typed Pages

Directed by Michael C. Wooten

Lowe *et al.* (2004) describes ecological genetics as “the investigation of the origin and maintenance of genetic variation within and between populations, which ultimately leads to adaptation and speciation.” Thus, to gain a more complete understanding of a real world species an ecological genetics investigation must look across multiple levels and utilize different types of DNA markers as these processes occur on both a regional and microgeographic scale. A regional scale typically involves between population processes while the microgeographic level often investigates the same processes but at a much finer scale. Measures of genetic variation that are investigated at both scales include genetic diversity and genetic differentiation. Here, I investigated these two

measures of genetic variation on both a regional and microgeographic scale using two different DNA markers (mitochondrial and nuclear DNA).

First, mitochondrial DNA was used to investigate phylogenetic relationships within the species *Peromyscus polionotus* based on a previously proposed phylogenetic model. The relationships predicted using mtDNA genes cytochrome-b and the control region were incongruent with the previously proposed model. A revised model, then, indicates three distinct clades occupy the Gulf Coastal region of Florida and Alabama. Divergence among the clades may have occurred approximately 300 000 YBP. The Gulf Coastal region is comprised of two inland clades and a beach clade. Inland clades appear to integrate while beach subspecies are comprised of a single haplotype and do not appear to have recently integrated with adjacent inland populations. In fact, extant beach forms represent lineages that are older than the present dune systems they inhabit.

Secondly, on a local or microgeographic scale, genetic diversity and differentiation was investigated using nuclear microsatellite markers. It was discovered that genotypes are partitioned on a microgeographic scale (< 1000 m). Genotype partitioning has several evolutionary implications and has been recognized as such for the majority of the past century. Partitioning was apparently temporal, deteriorating through annual population declines and reorganizing during birth pulses. Also, genotype partitioning reorganized following a hurricane that kept population densities low for four years. Importantly, partitioning of genotypes was demonstrated to slow the rate of genetic decay within the population of Alabama beach mice.

ACKNOWLEDGMENTS

Funding from the U.S. Fish and Wildlife Service, the Auburn University College of Sciences and Mathematics, the Office of the Vice President for Research, Auburn University and the Alabama Agricultural Experiment Station supported this research. I express sincere gratitude to Dr. Michael C. Wooten for his guidance and friendship. He was patient yet persuasive and from him I learned much about biology and life. I also express gratitude to my Advisory Committee, Drs. James B. Grand, Craig Guyer, and F. Stephen Dobson for their ideas and constructive criticisms. They all demonstrated a great deal of patience as I worked my way through this project. I am greatly appreciative for the guidance I received from all of my mentors, as it was an instrumental part of my academic development. Also, I offer special thanks to Dr. Marie Wooten and members of the Wooten lab. Many undergraduates also gave their time to this project, unfortunately, there is not room here to mention them by name but their work is greatly appreciated. I am grateful to have spent these last few years at Auburn University. Many faculty, students and staff have contributed to this time being academically challenging, intellectually stimulating and generally enjoyable.

Finally, with deep conviction, I offer wife Alison and son Brice unending devotion. They have given me patience, understanding and have affirmed in me the greatest joys of life. Lastly, I dedicate this work to my parents, Leon Caleb and Patricia Ann Van Zant because my accomplishments are through their love and support.

Style manual or journal used Molecular Ecology

Computer software used Word 97, SAS 9.1, PAUP 4.0B.10, Powerpoint 97,
Arlequin 2.0, Genescan 3.7.

TABLE OF CONTENTS

LIST OF TABLES.....	x
LIST OF FIGURES.....	xiv
GENERAL INTRODUCTION.....	1
PLEISTOCENE EVENTS IMPACT MITOCHONDRIAL DNA LINEAGES AND HISTORICAL DEMOGRAPHY OF <i>PEROMYSCUS</i> <i>POLIONOTUS</i>	6
Introduction.....	6
Methods.....	16
Results.....	27
Discussion.....	60
SPATIOTEMPORAL DYNAMICS OF GENE DIVERSITY IN THE ALABAMA BEACH MOUSE (<i>PEROMYSCUS POLIONOTUS</i> <i>AMMOBATES</i>).....	154
Introduction.....	154
Methods.....	164
Results.....	169
Discussion.....	181
CUMULATIVE REFERENCES.....	275
APPENDICES.....	294
Appendix 1.....	295
Appendix 2.....	304
Appendix 3.....	310

LIST OF TABLES

Chapter 1

Table 1.	Key to specimens abbreviations relative to species and collection site.....	141
Table 2.	Measures of diversity for the two major sets of sequence data that were used for phylogenetic analyses.....	143
Table 3.	Permutational Chi-squared tests of geographical association of clades and the inferred biological explanation.....	144
Table 4.	Measures of diversity for the clades estimated by maximum likelihood.....	146
Table 5.	Measures of diversity for model I 5 th level clades estimated using nested clade analysis.....	147
Table 6.	Measures of diversity for model II 5 th level clades estimated using nested clade analysis.....	148
Table 7.	Measures of diversity for model III 5 th level clades estimated using nested clade analysis.....	149
Table 8.	Fu and Li's D and F tests for <i>Peromyscus polionotus</i> with <i>Peromyscus maniculatus</i> as the outgroup haplotype along with McDonald-Kreitman test used only with cytochrome-b <i>P. maniculatus</i> as the outgroup haplotype.....	150
Table 9.	Fu and Li's D and F tests for <i>Peromyscus polionotus</i> clades or groups with other <i>P. polionotus</i> as outgroup haplotypes.....	151
Table 10.	Fu and Li's D* and F* and Tajima's D tests for estimated clades and groups.....	152

Table 11. Coalescent based maximum likelihood estimates of N_e , theta (θ), and exponential growth rate (95% CI) under models of constant size and growth as implemented by Kuhner <i>et al.</i> (1998).....	153
---	-----

Chapter 2

Table 1. Characterization of the 11 microsatellite loci used for these analyses including primer sequence, accession number, repeat motif, annealing temperature (T_a), and the number of observed alleles.....	246
Table 2. Total captures, new captures per trapping period and the number of individuals from which tissues was obtained for the combined trapping periods.....	247
Table 3. Total captures, new captures per trapping period and the number of individuals from which tissue was obtained on Gazebo grid.....	248
Table 4. Total captures, new captures per trapping period and the number of individuals from which tissue was obtained on Vet Village grid.....	249
Table 5. The total number of alleles observed for each trapping period on each grid and combined.....	250
Table 6. Summary statistics for the trapping periods of February 1995 on Gazebo grid and March 1995 on Vet Village grid.....	251
Table 7. Summary statistics for the trapping periods of April 1995 on Gazebo grid and April 1995 on Vet Village grid.....	252
Table 8. Summary statistics for the trapping periods of June 1995 on Gazebo grid and June 1995 on Vet Village grid.....	253
Table 9. Summary statistics for the trapping periods of February 1996 on Gazebo grid and March 1996 on Vet Village grid.....	254

Table 10. Summary statistics for the trapping periods of April 1996 on Gazebo grid and April 1996 on Vet Village grid.....	255
Table 11. Summary statistics for the trapping periods of June 1996 on Gazebo grid and June 1996 on Vet Village grid.....	256
Table 12. Summary statistics for the trapping periods of February 1997 on Gazebo grid and March 1997 on Vet Village grid.....	257
Table 13. Summary statistics for the trapping periods of April 1998 on Gazebo grid and February on Vet Village grid.....	258
Table 14. Summary statistics for the trapping periods of March 2000 on Gazebo grid and March 2000 on Vet Village grid.....	259
Table 15. Summary statistics for the trapping periods of November 2000 on Gazebo grid and December 2000 on Vet Village grid.....	260
Table 16. Summary statistics for the trapping periods of March 2001 on Gazebo grid and March 2001 on Vet Village grid.....	261
Table 17. Summary statistics for the trapping periods of November 2001 on Gazebo grid and October 2001 on Vet Village grid.....	262
Table 18. Summary statistics for the trapping periods of March 2002 on Gazebo grid and February 2002 on Vet Village grid.....	263
Table 19. Mantel test for Gazebo and Vet Village grids along with the number of samples for each trapping period.....	264
Table 20. F_{ST} values based on various models of subdivision within Gazebo and Vet Village grids.....	265

Table 21. Summary statistics produced by the combined trapping periods of February/March 1995 along with combined trapping periods of April/April 1995 on Gazebo and Vet Village grids.....	266
Table 22. Summary statistics produced by the combined trapping periods of June/June 1995 along with combined trapping periods of February/March 1996 on Gazebo and Vet Village grids.....	267
Table 23. Summary statistics produced by the combined trapping periods of April/April 1996 along with combined trapping periods of June/June 1996 on Gazebo and Vet Village grids.....	268
Table 24. Summary statistics produced by the combined trapping periods of February/March 1997 along with combined trapping periods of April/February 1998 on Gazebo and Vet Village grids.....	269
Table 25. Summary statistics produced by the combined trapping periods of March/March 2000 along with combined trapping periods of November/December 2000 on Gazebo and Vet Village grids.....	270
Table 26. Summary statistics produced by the combined trapping periods of March/March 2001 along with combined trapping periods of November/October 2001 on Gazebo and Vet Village grids.....	271
Table 27. Summary statistics produced by the combined trapping periods of March 2002 on Gazebo grid and February 2002 on Vet Village grid.....	272
Table 28. Mantel tests for the combined trapping periods along with the number of samples for each trapping period.....	273
Table 29. Between grid measures of differentiation including F_{ST} , R_{ST} and the number of migrants per generation.....	274
Table 30. Population assignment using the jackknife method from the program WHICHRUN (Banks & Eichert 2000).....	275

LIST OF FIGURES

Chapter 1.

Figure 1.	Bowen's (1968) proposed evolutionary sequence of the Gulf Coastal and some Atlantic forms of <i>Peromyscus polionotus</i>	75
Figure 2.	Locations where <i>P. polionotus</i> samples were collected.....	77
Figure 3.	Insert region found within <i>P. polionotus</i> and its alignment with <i>P. maniculatus</i>	79
Figure 4.	Maximum likelihood topology using the cytochrome-b region and model HKY + Γ with outgroup <i>P. leucopus</i>	81
Figure 5.	Maximum likelihood topology using the cytochrome-b region and model TVM + Γ with outgroup <i>P. leucopus</i>	83
Figure 6.	Maximum likelihood topology using the cytochrome-b region and model HKY + Γ with outgroup <i>P. keeni</i>	85
Figure 7.	Maximum likelihood topology using the cytochrome-b region and model GTR + Γ with outgroup <i>P. keeni</i>	87
Figure 8.	Maximum likelihood topology using the D-loop and model HKY +I + Γ with outgroup <i>P. leucopus</i>	89
Figure 9.	Maximum likelihood topology using the D-loop and model HKY +I with outgroup <i>P. keeni</i>	91
Figure 10.	Maximum likelihood topology using the cytochrome-b region and D-loop from model HKY +I + Γ with outgroup <i>P. leucopus</i>	93
Figure 11.	Maximum likelihood topology using the cytochrome-b region and D-loop from model HKY +I + Γ with outgroup <i>P. keeni</i>	95

Figure 12.	Weighted maximum parsimony topology using the cytochrome-b region with outgroup <i>P. leucopus</i>	97
Figure 13.	Maximum parsimony topology using the cytochrome-b region with outgroup <i>P. leucopus</i>	99
Figure 14.	Weighted maximum parsimony topology using the cytochrome-b region with outgroup <i>P. keeni</i>	101
Figure 15.	Maximum parsimony topology using the cytochrome-b region with outgroup <i>P. keeni</i>	103
Figure 16.	Weighted maximum parsimony topology using the D-loop with outgroup <i>P. leucopus</i>	105
Figure 17.	Maximum parsimony topology using the D-loop with outgroup <i>P. leucopus</i>	107
Figure 18.	Weighted maximum parsimony topology using the D-loop with outgroup <i>P. keeni</i>	109
Figure 19.	Maximum parsimony topology using the D-loop with outgroup <i>P. keeni</i>	111
Figure 20.	Weighted maximum parsimony topology using the cytochrome-b and D-loop with outgroup <i>P. leucopus</i>	113
Figure 21.	Maximum parsimony topology using the cytochrome-b region and D-loop with outgroup <i>P. leucopus</i>	115
Figure 22.	Weighted maximum parsimony topology using the cytochrome-b region and D-loop with outgroup <i>P. keeni</i>	117
Figure 23.	Maximum parsimony topology using the cytochrome-b region and D-loop with outgroup <i>P. keeni</i>	119
Figure 24.	Bayesian analysis using the cytochrome-b region with model GTR + Γ and outgroup <i>P. leucopus</i>	121
Figure 25.	Bayesian analysis using the cytochrome-b region with model HKY + Γ and outgroup <i>P. keeni</i>	123
Figure 26.	Bayesian analysis using the cytochrome-b region with model GTR +I and outgroup <i>P. keeni</i>	125

Figure 27.	Bayesian analysis using the D-loop with model HKY +I + Γ and outgroup <i>P. leucopus</i>	127
Figure 28.	Bayesian analysis using the D-loop with model HKY +I + Γ and outgroup <i>P. keeni</i>	129
Figure 29.	Bayesian analysis using the cytochrome-b region and the D-loop with split models HKY + Γ (cyt-b) and HKY +I + Γ (cyt-b and D-loop) with outgroup <i>P. leucopus</i>	131
Figure 30.	Bayesian analysis using the cytochrome-b region and the D-loop with split models HKY + Γ (cyt-b) and HKY +I + Γ (cyt-b and D-loop) with outgroup <i>P. keeni</i>	133
Figure 31.	Statistical-parsimony network (NCA) of <i>P. polionotus</i> haplotypes.....	135
Figure 32.	Constant-rate model of time estimates for estimated divergence periods within <i>P. polionotus</i>	137
Figure 33.	Range map of <i>P. p. allophrys</i> and location of debated haplotype.....	139

Chapter 2

Figure 1.	Gazebo and Vet Village grids established during the fall of 2000.....	196
Figure 2.	Reduction of both grids after the 1997 trapping periods increased the distance between them to 920 m.....	198
Figure 3.	Observed and estimated heterozygosity for each trapping period on Gazebo grid.....	200
Figure 4.	Observed and estimated heterozygosity for each trapping period on Vet Village grid.....	202
Figure 5.	Gazebo grid correlograms from the trapping period of February 1995.....	204
Figure 6.	Gazebo grid correlograms from the trapping period of April 1995.....	206
Figure 7.	Gazebo grid correlograms from the trapping period of June 1995.....	208

Figure 8.	Gazebo grid correlograms from the trapping period of February 1996.....	210
Figure 9.	Gazebo grid correlograms from the trapping period of April 1996.....	212
Figure 10.	Gazebo grid correlograms from the trapping period of June 1996.....	214
Figure 11.	Gazebo grid correlograms from the trapping period of March 2002.....	216
Figure 12.	Vet Village grid correlograms from the trapping period of March 1995.....	218
Figure 13.	Vet Village grid correlograms from the trapping period of April 1995.....	220
Figure 14.	Vet Village grid correlograms from the trapping period of June 1995.....	222
Figure 15.	Vet Village grid correlograms from the trapping period of March 1996.....	224
Figure 16.	Vet Village grid correlograms from the trapping period of April 1996.....	226
Figure 17.	Vet Village grid correlograms from the trapping period of June 1996.....	228
Figure 18.	Vet Village grid correlograms from the trapping period of February 2002.....	230
Figure 19.	Correlograms from the combined trapping periods of February 1995 on Gazebo grid and March 1995 on Vet Village grid.....	232
Figure 20.	Correlograms from the combined trapping periods of April 1995 on Gazebo grid and April 1995 on Vet Village grid.....	234
Figure 21.	Correlograms from the combined trapping periods of June 1995 on Gazebo grid and June 1995 on Vet Village grid.....	236

Figure 22. Correlograms from the combined trapping periods of February 1996 on Gazebo grid and March 1996 on Vet Village grid.....	238
Figure 23. Correlograms from the combined trapping periods of April 1996 on Gazebo grid and April 1996 on Vet Village grid.....	240
Figure 24. Correlograms from the combined trapping periods of June 1996 on Gazebo grid and June 1996 on Vet Village grid.....	242
Figure 25. Correlograms from the combined trapping periods of March 2002 on Gazebo grid and February 2002 on Vet Village grid.....	244

GENERAL INTRODUCTION

An earnest investigation concerning the movement of genes both within and between populations probably began with Wright (1931). Wright and others (Wright 1943; Kimura 1955; Kimura & Weiss 1964; Levins 1969; Slatkin 1977) developed increasingly more complex models that were designed to infer gene flow between subpopulations. Models, however, represent indirect estimates of gene flow. Direct methods of estimating gene flow were, historically, based on observational studies, however, more recently, genetic methods of measuring gene flow are becoming more popular as molecular markers and methods become more efficient to use. Gene flow is influenced by at least two factors, the physical ability of a species to change location and the environment the organism exists in. For example, species ill adapted for water are unlikely to cross major bodies of water except in rare circumstances. The amount of gene flow between groups has predictable outcomes in regard to genetic differentiation of the groups (Hartl & Clark 1998). Gene flow, however, occurs both between and within populations. Understanding the genetic composition of a population requires an accurate assessment of genetic diversity and gene flow on both a regional and local scale.

My primary research interest and, thus, the focus of my dissertation involved understanding genetic diversity within and between populations. The project was marked by a unique opportunity to investigate the maintenance of genetic variation within a population that functions without any obvious means for partitioning genotypes. The

genetic architecture of a population, as well as the dynamics acting to direct and maintain this architecture, are part of a population's response to counteract the persistent decay of gene diversity. Thus, understanding these processes and their outcome(s) has important evolutionary and conservation implications. As the model system for my research, I used the old-field mouse (*Peromyscus polionotus* spp). This species exhibits a collection of features that, I believe, made it an excellent model for the questions examined here. The species is monogamous, forms strong pair bonds, exhibits limited dispersal and occupies a temporally dynamic habitat. In addition, over 10 years of tissue samples and detailed ecological data from a single natural population were available.

First, I examined biogeographic variation at the regional level. Gene flow from the mainland of Alabama into the beach populations had long been proposed (Bowen 1968). This hypothesized gene flow was important to understand in the evolutionary context of my primary study population of Alabama beach mice (*Peromyscus polionotus ammobates*). Thus, I conducted a biogeographic study of populations spanning the northern Gulf Coast. Despite biological studies dating back to the 1920's, the evolutionary relationships within and among beach and inland subspecies remains an open question. Various phylogenetic hypotheses have been proposed for the Gulf Coast populations but no definitive conclusions have been reached. For example, within beach mice, there are varying degrees of color morphs that range from mostly white forms in the Santa Rosa beach mouse (*Peromyscus polionotus leucocephalus*) to the much darker morph of the Alabama beach mouse (*Peromyscus polionotus ammobates*). Bowen (1968) suggested that this dichotomy of pelage color was the result of differing levels of historical gene flow. The Santa Rosa beach mouse has been effectively isolated on Santa

Rosa Island for at least 5000 years. In contrast, seemingly, a land bridge existed between the habitat of the Alabama beach mouse and the nearby inland populations until modern times. Bowen (1968) hypothesized that this land connection allowed regular gene flow into the beach population. However, results here indicate that this scenario is unlikely. It appears that two gene regions (cytochrome-b, control region) in the mtDNA genome are monomorphic in the Alabama beach mouse population. These results conflict with Bowen's hypothesis of beach mouse phylogeny because the nearby inland population is not monomorphic for these gene regions and sampled variations are relatively diverged from the beach forms. Interestingly, the data here suggest that the Alabama beach mouse and the Santa Rosa beach mouse may share a more recent ancestor with each other than they do all other forms, which is also very different than predicted by Bowen (1968). In general, beach forms appear to be more substantially diverged from inland forms than suggested by Bowen; thus, my data bring into question all previous phylogenetic conclusions.

Peromyscus polionotus is generally thought to be a young species having evolved after being isolated in the southeastern United States during a mid to late Pleistocene glacial cycle. New data presented here along with recent fossil evidence indicates that *P. polionotus* is far older than previously thought. Using these mitochondrial DNA data, *P. polionotus* may have been isolated in the southeastern United States since the late Pliocene or early Pleistocene. Thus determining which form of *Peromyscus maniculatus* that *polionotus* split from is difficult. In fact, my data suggest that the forms of *maniculatus* examined here split following a *polionotus* split from *maniculatus*. Thus,

the subspecies of *maniculatus* for which I have data are represent younger lineages than *polionotus*.

Bowen's model of the evolution of Gulf Coastal forms of *P. polionotus* ssp indicated a recent colonization of the present beach by inland forms. Thus, present beach forms should be relatively undifferentiated from extant inland forms. However, my data suggest a split among three extant clades of *polionotus* of approximately 300 000 YBP. This indicates that present forms of beach mice are significantly older than the approximately 10 000 years suggested by Bowen (1968). My data strongly suggest that populations of *polionotus* populating shorelines and barrier islands of the Gulf Coast are older than the dunes they now inhabit. Therefore, as an alternative to Bowen's recurrent invasion hypothesis, I propose the Shoreline-Tracking Hypothesis. My data suggest that beach forms, already diverged from inland forms, were able to track the shoreline as the water of the Gulf of Mexico rose due to melting glaciers.

The second, and central, focus of my dissertation involved examination of variation at the population level. Once I had developed a historical framework for my study population, I examined the fate of genetic variants at the microgeographic level. The idea for this portion of my research arose from two observations reported by my advisor. Dr. Wooten noted that, following Hurricane Opal and the resulting collapse in population density, individual heterozygosity increased in a population of Alabama beach mice. This result runs completely counter to what one would expect under bottleneck conditions, *unless* some form of significant genotype partitioning existed prior to the storm event. The immediate question that came to me was "How did this partitioning arise?" The simplistic breeding, dispersal and social systems reported for beach mice

have not traditionally been considered adequate to drive formation of extensive population structure. More interesting, how could such structure exist in a population where individuals could easily move across the entire habitat space? Based on preliminary genotype data, Dr. Wooten proposed that beach mice were capable of forming “genetic neighborhoods” and he hypothesized that genetic relatedness within these neighborhoods served as reservoirs of genetic variance. Starting with these ideas, I formulated a series of questions that served to guide the following portion of my dissertation work. First, I attempted to document and quantify both spatial and temporal genetic structure. Once patterns of variation were identified, I examined the potential for this structure to influence the rate of genetic decay. Using this approach, I demonstrated that genetic partitioning does occur in beach mice populations and that this phenomenon serves to slow the rate of decay of genetic variance in these populations. I believe that this is a broad phenomenon that is an important factor underlying the genetic architecture of many mammalian populations.

Chapter One

Pleistocene Events Impact Mitochondrial DNA Lineages and Historical Demography of *Peromyscus polionotus*

Introduction

The Pleistocene Epoch, covering approximately the last two million years, had a profound effect on the biota of Earth (Hewitt 1996, 2000). Cyclical glacial-interglacial periods caused range alterations (Hewitt 2000, Blondel & Aronson 1999) and exchanges of biota. These climatic events have been explored as a possible cause of numerous speciation events (Haffer 1969, Veith *et al.* 2003, Avise *et al.* 1998) and extinctions (Graham & Lundelius 1984). One important aspect of these fluctuations was that habitats were lost, gained, or repositioned in regions far beyond the physical ice sheet. Repeated rounds of range contraction, dispersal, and vicariance events were likely common. The last major geological event (a withdrawal of glaciers and a corresponding significant increase of sea level) produced a variety of effects on numerous species (Hoffman & Blouin 2004, Zamudio & Savage 2003, Arbogast 1999) many of which persist today. For such species, these historical processes often played central roles in defining present geographic distribution of genetic lineages (Pielou 1991, Hewitt 1993, Avise 2000).

Complex climatic and geographic processes essentially confirm a complicated evolutionary history for species within affected regions. Disentangling geographic from contemporary effects on genetic lineages has long been recognized as essential for gaining a more complete understanding of an organism's evolutionary history. Classical approaches to the study of genetics data in relation to spatial history began with Wahlund (1928) and Wright (1931, 1943). Wright developed F-statistics to quantify the subdivision of populations and estimate gene flow under the assumption of drift-migration equilibrium in an island model. However, F-statistics were not designed to make use of the temporal information inherently found within gene sequences. Elucidating past intraspecific cycles of contraction, isolation, and expansion is difficult. More recently, expanded use of molecular techniques and the emergence of mitochondrial DNA data placed an emphasis on intraspecific variation. These events have fostered the growth of a new discipline termed phylogeography (Avice *et al.* 1979, 1987; Avice 2000). Phylogeography is concerned with "historical aspects of the contemporary spatial distributions of gene lineages." (Avice 1996). Analytical methods that have aided the growth of phylogeography include, nested clade analysis (Templeton *et al.* 1987, 1992; Templeton & Sing 1993), estimates of historical demographic parameters (Emerson *et al.* 2001), and tests of neutrality (Fu 1997). Nested clade analysis (NCA) was used to test for geographical association of haplotypes by placing haplotypes in clades at different hierarchical levels until a final level was reached that contains all haplotypes. NCA then tests for geographical association among haplotype groups. If significant geographical associations are found, a decision key is used to infer a biological scenario through which the observed association may have occurred.

Historical demographic parameters, such as effective population size, can be estimated using coalescent theory (Kuhner *et al.* 1995). Neutrality tests, initially derived for testing the neutrality of genes, can also indicate other circumstances such as population growth. Together, these analyses can be used to estimate how historical mechanisms have influenced extant genetic structure within a population.

As glaciers advanced and retreated, Pleistocene climatic oscillations repeatedly altered vegetation types in the southeastern United States. Sea level changes as great as 100 m (Gates 1993) marked the occurrence of glacial cycles that moved shorelines by more than a hundred kilometers in some regions of the Gulf of Mexico (Wanless 1989). Invariably, organisms inhabiting this region were also affected. Intraspecific genetic structuring of terrestrial vertebrates has been investigated within the region (Avice 1996), with the predominate phylogeographic model being turtles (Walker & Avice 1998). Phylogeographic studies of mammals from the region have also been completed (Ellsworth *et al.* 1994; Hayes & Harrison 1992; Avice *et al.* 1983); however, few, if any, have combined phylogenetic, NCA, and historical demographic methods in an attempt to measure the effects of past geologic events on present genetic distribution. For a species intimately associated with such an unstable environment, application of multiple methods in the study of intraspecific variation is important for understanding and determining the significant pattern(s) that may be detectable using gene sequences.

Here, I examine a mammalian species (*Peromyscus polionotus*) that is restricted to the Southeastern United States and that has an evolutionary history closely tied to the Florida and Alabama coastline of both the Gulf of Mexico and Atlantic Ocean.

Peromyscus polionotus is a small fossorial mouse of the southeastern United States

probably derived from a grassland form of *Peromyscus maniculatus* (Osgood 1909; Sumner 1926; Blair 1950; Bowen 1968). Recent fossil evidence dates the appearance of *Peromyscus polionotus* to the late Pliocene or early Pleistocene Epoch (Ruez 2001) representing approximately two million years before present (YBP). This time frame is significantly different from the earlier widely held hypothesis of a late Pleistocene/early Holocene split (Hibbard 1968; Webb 1974). Webb (1974) reported fossils of *P. polionotus* occurring at sites that dated between 20 000-100 000 years and fossils of *Peromyscus* dating to the mid-Pleistocene. A late Pleistocene split seems to be the assumption accepted by most authors when investigating the biogeography of this group (Hibbard 1968; Bowen 1968). However, using restriction enzymes and mtDNA, Avise *et al.* (1983) estimated that *P. polionotus* and a form of *P. maniculatus* from southern California split 1.5 MaBP but considered this an interim estimate.

According to Osgood (1909) there are two major morphological variants among *P. maniculatus*. These consist of a long-tailed, large-eared, large-footed forest type and a short-tailed, small-eared, small-footed grassland type. While today a forest type (*P. m. nubiterrae*) is geographically closer, Osgood (1909) noted that *P. polionotus* was more similar to the two grassland types, *P. m. pallescens* of Texas and *P. m. bairdii* of Michigan, and most resembled *P. m. pallescens*. Since Osgood's time, two competing hypotheses have arisen concerning the origin of *P. polionotus*. Blair (1950) postulated that *P. maniculatus* moved east along the Gulf Coast Corridor during the Pleistocene glacial periods. The Gulf of Mexico was much lower than present during glacial periods, and the Gulf Coastal Plain connected Florida and Texas, thus allowing the migration of many mammals from North and South America into Florida (Webb & Wilkins 1984).

Bowen (1968), however, proposed a different hypothesis for the origin of *P. polionotus*. He suggested a northern origin for the *P. maniculatus* stock that gave rise to *polionotus*. Presently, *P. m. bairdii* is the grassland form occupying the area most consistent with Bowen's model (Southern Michigan). Bowen speculated that during a pre-Pleistocene dry period, a north-south grassy corridor could have formed allowing passage of the ancestral *polionotus* stock. Bowen cited the absence of *P. polionotus* from suitable habitat west of Mobile Bay and the Alabama River as evidence against Blair's hypothesis. Subsequently, however, *P. polionotus* has been determined to inhabit areas west of the Alabama River (M. C. Wooten, personal communication). This seems to be the extent to which this speciation event has been characterized in the literature. Based on the evidence and technology of the time, it was difficult to advance either theory. However, since 1968, numerous advances in biogeographic and genetic techniques have been made. Thus, at this time, it may be possible to determine with increased probability which *P. maniculatus* was involved in this speciation event, and if one of the extant grassland forms (*bairdii*, *pallescens*) is the most recent ancestor of *P. polionotus*.

Both the sequence of events leading to the speciation of *P. polionotus* and the radiation of subspecies within the *polionotus* group remain poorly understood. Clarifying the systematic relationships within *P. polionotus* requires identification of the ancestor of the group, but the geographic distribution and complex biogeographical events make this task difficult. Driven by glacial cycles, both shifting vegetation zones and changing shorelines have almost certainly influenced the present biogeographic structure of *P. polionotus*. Indeed, isolated in the southeastern coastal plain, the *polionotus* group clearly evolved considerable geographic variation throughout its range (Blair 1950;

Bowen 1968; Selander 1970a). In fact, phenotypic variation has given *P. polionotus* something of a storied history. Beginning early in the last century and continuing through the majority of it, studies of *P. polionotus* were critical in the growth of current concepts such as geographic variation and the adaptiveness of morphological characters. Osgood (1909) initiated the historical research of *P. polionotus* by listing it along with four subspecies, three of which previously had species status. Subsequent splitting of the *polionotus* group followed until 1968 when Bowen, in an attempt to clarify the taxonomy of the Gulf Coast forms named five new subspecies.

Sumner (1926), concentrating primarily on color morphs that ranged from brown in the interior populations to almost white in the insular populations used several of the subspecies in crossing experiments to analyze the genetic basis of morphological characters. His results were widely cited by many evolutionists (e.g. Mayr 1942, 1954; Huxley 1943; Haldane 1948; Ford 1954, 1960). Sumner (1929) noted an apparent cline from Santa Rosa Island extending inland approximately 64 km, where pelage changed from pale to dark. He characterized this cline as gene flow inland from the beaches. Huxley (1943) and Haldane (1948) used this apparent gradient to produce some of the first analyses of clinal variation. However, according to Bowen (1968), Sumner's results were misleading largely due to the inadequately studied taxonomy of forms along the Gulf Coast. Bowen argued conversely that gene flow was predominately from interior populations into the beach populations.

Based on the first broad geographic studies of electrophoretic protein polymorphism, Selander (1970b) and Selander *et al.* (1971) also concluded that gene flow was most likely from interior to insular populations. In 1971, Selander *et al.*

published a comprehensive investigation of protein polymorphism in *P. polionotus*. Their analysis showed significant geographical partitioning of polymorphic loci. They demonstrated that the proportion of polymorphic loci within insular populations along the Florida Panhandle (8.8%) was decidedly lower than that of the adjacent mainland populations (22.0%). Moreover, the interior populations of the Florida Peninsula were found to have the highest proportion of polymorphic loci (29.0%) while the insular populations of the Atlantic coast were lower (22.0%). Inland populations across Georgia and South Carolina were polymorphic at 20% of loci sampled. Selander (1970b) contented that a low proportion of polymorphic loci among insular populations was due to their isolation from one another and from interior populations and the amount of gene flow that did occur was not sufficient to overcome this. Their analysis also identified a north-south cline of increased polymorphic loci. One criterion used for hypothesizing a center of origin is the area of greatest variation. Thus, from the Selander *et al.* (1971) data one might postulate that the center of origin for *P. polionotus* was peninsular Florida where there is the greatest amount of protein polymorphism.

Under Bowen's evolutionary scenario for *P. polionotus* (Fig. 1) the beach forms are of recent origin (< 10 000 years). This implies that, at the genetic level, beach forms should be very similar to inland forms, especially, according to Bowen, *P. p. griseobractus*. *Peromyscus polionotus griseobractus* inhabits what is today the mainland area of Eglin AFB. Bowen believed that *griseobractus* and a modified form of *griseobractus* played a determining role in the evolution of all beach forms. However, according to Bowen, other inland forms were also involved in the founding and subsequent evolution of the beach subspecies. For example, the beach forms *allophrys*

and *peninsularis* were each considered to be derived from *P. p. sumneri* and a modified form of *griseobractus*. *Peromyscus polionotus ammobates*, in Alabama, was hypothesized to be a descendent of *griseobractus* modified by intermittent contact with *P. p. polionotus*. Bowen hypothesized that *P. p. trissyllepsis* and *P. p. leucocephalus* were the two most recent beach forms, with *leucocephalus* being derived from *griseobractus* (pre-*peninsularis* stock) and *trissyllepsis* resulting from the admixture of *griseobractus*, *ammobates*, and *leucocephalus*.

Bowen (1968) further hypothesized that *P. polionotus* had originated from *maniculatus* stock, and that at least two forms of *polionotus* existed by the Yarmouth interglacial stage of the Pleistocene. He based his phylogeny on the occurrence of relict shorelines that were associated with interglacial cycles. However, these shorelines are today thought to be older than previously estimated (Winker & Howard 1977) thus, Bowen's use of relict shoreline refugia may be correct but his time periods may be significantly incorrect. Bowen also focused primarily on retreating sea levels to devise his phylogeny. He believed that encroaching sea levels would inundate marshes to the north of frontal dunes creating islands. Beach forms would then be isolated on these islands and eventually lost as the islands were submerged. Thus, with each marine encroachment existing beach forms were lost, which, during glacial periods, inland forms would again colonize more typical beach habitat. Differentiation of beach and inland forms was hypothesized to have occurred because selection pressures within the beach habitat favored pigment reduction.

In relation to extant beach forms, Bowen's latest and most significant shoreline (Silver Bluff) arose 6000 to 4000 YBP. This is significant because it was viewed as the

predominant event that allowed the recent colonization of the beach, thus leading to the present day beach forms. However, there is some debate concerning the origin of the Silver Bluff shoreline. The Silver Bluff Sequence may be the result of a significant slowing in the rise of the sea level, thus, allowing the accretion rate to increase (Wanless *et al.* 1994). This suggests that rather than a decrease in sea level an increase in beach deposition occurred, which could have a significant effect on the inferred biogeography of beach forms. Whether the sea level has risen and fallen or whether the sea level rise slowed remains under debate (Otvos 1995; Donoghue *et al.* 1998). Regardless, Bowen's conclusion of a very recent divergence of extant beach forms and their relation to one another through a common ancestor (*P. p. griseobractus*) is a testable hypothesis.

My original questions concerning *P. polionotus* were intended to explore microgeographic genetic structuring. As part of this I sequenced a hypervariable region, D-loop, of the mitochondrial DNA intending to track maternal lineages within a population of the Alabama beach mouse (*P. p. ammobates*). It soon became apparent, however, that the *P. p. ammobates* population was probably comprised of a single mitochondrial lineage. I viewed this as significant because this beach population was widely believed to have experienced recent, recurring gene flow from the adjacent mainland (Howell 1920; Bowen 1968; Selander 1970b) until 100 years ago when the intracoastal canal was opened. In fact, *P. p. ammobates* has been offered as an example of an organism in a unique environment that failed to change phenotypically because of sufficient gene flow from the more typical environment of the organism (Howell 1920). Given the initial result, it became obvious that I needed to sample and sequence the same mtDNA region of the adjacent mainland population, as well as, other *polionotus*

subspecies/populations. It also became apparent from the accumulating data that empirical results on the patterns of divergence, timing of divergence events and geographical genetic variation were not consistent with Bowen's (1968) postulated evolution of *P. polionotus*. Resolution of these issues became a major focus for my dissertation because of the direct implications for my primary research model, genetic structuring within a *P. p. ammobates* population. Before I could fully investigate microgeographic structuring and its effects on retarding the loss of genetic variation in a semi-isolated population I needed to be confident in my understanding of historical dynamics. My preliminary results suggested little evidence of gene flow into the *P. p. ammobates* population from the adjacent mainland population. In fact, adjacent interior haplotypes appeared to be quite diverged from the beach haplotype. Therefore, I viewed it as critical that the hypotheses put forth by Bowen (1968) and others concerning genetic variation within *P. polionotus* and its geographic placement throughout the Florida panhandle region be tested. Resolution, or clarification, of past premises or disputes is likely to be possible using gene sequence data with contemporary analytical methods of analyses. Most importantly, my results should have important implications broader questions concerning genetic structure of insular populations.

My goal, then, was to investigate phylogenetic relationships, gene flow, and geographical arraignment of genetic diversity within *P. polionotus* using Bowen's (1968) hypothesized phylogeny as the initial model. Bowen focused primarily on subspecies of the Florida Panhandle and used crossing experiments, standard body measurements and pelage reflectance values to construct his phylogeny. However, at the time of his publication, the crossing experiments were unfinished, thus, they only partially

contributed to his results. Regardless, he offered the hypothesis that *P. maniculatus* gave rise to *P. colemani* in turn giving rise to *P. polionotus*. Bowen then postulated the evolution of other inland forms, as well as, beach forms. All of the beach subspecies, according to Bowen, were derived from inland forms during the Holocene, thus, leading to the conclusion that they are less than 10 000 years old. To test these hypotheses, I made use of contemporary gene sequence analyses such as phylogenetic reconstruction, nested clade analysis, and estimated historical demographic parameters and population trends. Using these methods, I evaluated genetic variation of *P. polionotus* within the Gulf Coast region to: infer relationships among populations of insular and interior populations; test biogeographical scenarios concerning geographical placement of genetic variation; infer patterns and degrees of gene flow and finally to estimate approximate times when lineages may have split.

Methods

Samples

Tissue samples of *Peromyscus polionotus* were primarily obtained from toe clips. Additional muscle/organ tissue was collected from trap mortalities and/or museum specimens. *Peromyscus maniculatus* tissue was obtained from tail snips, muscle, and organs from wild caught or museum specimens. Samples of *Peromyscus maniculatus bairdii* {approximate location Ann Arbor, Michigan, BW1 (PMB01), BW2 (PMB02), BW3 (PMB03)}, *Peromyscus maniculatus sonoriensis* {approximate location White Mountain Research Station, California, SM4 (PMS04), SM5 (PMS05), SM6 (PMS06)}, and *Peromyscus polionotus subgriseus* {Ocala National Forest, Florida, PO10076 (MCFL76), PO10077 (MCFL77), PO10078 (MCFL78), PO10299 (MCFL99)} were

obtained from the Peromyscus Genetic Stock Center (University of South Carolina). Tissue samples of *Peromyscus polionotus niveiventris* {Ppn-2917 (NIV17), Ppn-2936 (NIV36), Ppn-762 (NIV62)} were obtained from Dr. Christopher L. Parkinson (University of Central Florida). Tissue samples from *Peromyscus keeni* {Kittitas Co, Washington, GK6601 (PK01), GK6621 (PK21), GK6622 (PK22), GK6623 (PK23)} and *P. maniculatus pallescens* {Robertson Co, Texas, GK6590 (PMP90), GK6592 (PMP92), GK6593 (PMP93), GK6594 (PMP94)} were obtained from Dr. Ira Greenbaum (Texas A & M University). Most tissue samples were preserved in 1.5-ml microcentrifuge tubes filled with 100% ethanol. DNA was isolated from 145 *P. polionotus* ssp, along with three *P. m. bairdii*, three *P. m. sonoriensis*, four *P. keeni*, four *P. m. pallescens*, six *P. gossypinus*, and three *P. leucopus* for this study. A total of seventy-eight individuals (Table 1) were used in at least one of the analyses presented here.

DNA was extracted using QUIAGEN DNeasy® tissue kits (QUIAGEN®, Valencia, California). A fragment of approximately 2.7 kb was amplified and 2452 base pairs were used for analyses. This fragment contained partial 12s rRNA (137 bp), partial cytochrome-b (1137 bp), and complete D-loop region (971 bp) along with tRNA-threonine (68 bp), tRNA-proline (66 bp), and tRNA-phenylalanine (68 bp). It was amplified using primer CB3R-L (5'-CATATTAAACCCGAATGATATTT-3') and primer 12SAR-H (5'-ATAGTGGGGTATCATATCCCAGTT-3') (Palumbi *et al.* 1991). Lengths of gene regions within the sequence are approximate as they varied among species. Identification of regions was based on alignment with positions 14 152 - 1024 of the *Mus musculus* mtDNA genome (GenBank accession number, AB042432). Not all of the nucleotides contained within the *P. polionotus* sequences were assigned using the *M.*

musculus alignment. For example, two nucleotides (1206, 1207) either at the end of tRNA-Thr or the beginning of tRNA-Pro were not accounted for in the *Mus* sequence inferring that one or both *polionotus* tRNAs are longer. To sequence the entire 2.7 kb region internal sequencing primers developed within the lab of M. C. Wooten (Auburn University) and consisted of DIs-01F (5'-AAGGACTAACCCCCACCATC-3'), and Dle-01R (5'-ATAAGGCCAGGACCAAACCT-3'), PL276-R (5'-TAACCCTGCTTGTCCAAATG-3'), PL792-F (5'-TTTGGGGTTTGTCAAGGATA-3'), BF1; (5'-AGGACAACCAGTCGAACACCCATT-3') and BR1; (5'-TGGCTGGCACGAAATTTACCAACC-3') were used. These primers are approximately 200 nucleotides internal of CB3R-L and 12SAR-H respectively. To sequence more of cytochrome-b gene (approximately 1 kb) another amplification using primer 14 724-F (5'-CGAAGCTTGATATGAAAAACCATCGTTG-3') (Palumbi *et al.* 1991) and primer TD20-R (5'-ACTATCAGGGCAATGGGTGA-3') was carried out.

The Polymerase Chain Reaction (PCR) method was used to amplify specific regions of DNA to determine the nucleotide sequence. PCR reactions were conducted using QUIAGEN Taq PCR Core Kit and Promega PCR Nucleotide Mix. Reactions were run in a Perkin Elmer GeneAmp PCR System 2400, a Hybaid Omn-E HBTRE02, or a MJ Research PTC-200. Amplification reactions were conducted in 31 *ul* volumes containing, 12.6 - 241.8 ng DNA, 0.32 *uM* primer, 0.75 mM MgCl₂, 200-*uM* dNTPs, 1X buffer, 1.25 U *Taq*. PCR conditions were: 35 cycles of 94° C (30 s) denaturing, 56° C (45 s) annealing, and 72° C (45 s) extension, followed by one 6 min period at 72° C. Product was determined to be present or absent by means of UV visualization. Product from successful reactions was cleaned using QUIAGEN QIAquick® PCR Purification Kit

or QUIAGEN QIAquick[®] Gel Extraction Kit and sequenced by the Auburn Genomics and Sequencing facility (Auburn University). Nucleotide sequence determination was completed using an ABI Prism[®] 3100 Genetic Analyzer (Applied Biosystems[®], Inc., Foster City, California). BIOEDIT v5.0.9 (Hall 1999) software was used to manipulate, proof and hand manipulate sequence data. CLUSTALX v1.81 (Thompson *et al.* 1997) was used to create global alignment files in NEXUS format.

A total of 145 samples were obtained from 32 locations across the southeastern United States (Fig. 2). A majority of the inland tissue samples were obtained from the Auburn University tissue stock collection. Florida samples were obtained from various inland localities including Okaloosa County, Walton County, Jackson County, Liberty County, Wakulla County, Suwannee County, and Marion County (Fig. 2). Inland Alabama samples were obtained from South Baldwin County, Lee County, Geneva County, and Russell County. Georgia samples were obtained from Talbot County. Beach locations included samples from Florida and Alabama. Samples were collected from Santa Rosa Island, Florida (*P. p. leucocephalus*), Topsail Hill State Preserve, Florida, Grayton Beach State Recreation Area, Florida, and Shell Island, Florida (*P. p. allophrys*). In addition, tissues from obtained from St. Joseph State Park, Florida (*P. p. peninsularis*), Florida Point, Florida, Perdido Key, Florida, Johnson Beach, Florida, Perdido Key, Florida (*P. p. trissyllepsis*), Cape Canaveral National Air Force Station (*P. p. niveiventris*), and Bon Secour National Wildlife Refuge, Alabama (*P. p. ammobates*).

Phylogenetic Hypothesis

Phylogenetic topologies were constructed using maximum parsimony (MP) and maximum likelihood (ML) optimality criterion in PAUP* v4.0b10 (Swofford 2002). A

Bayesian analysis was conducted using MRBAYES v3.0 (Huelsenbeck & Ronquist 2001). Phylogenetic reconstruction was limited to unique haplotypes and homologous haplotypes from different geographic locations. Within *P. polionotus* alignments, two single base insertions-deletions were removed from 13 samples as they were considered to be artifacts from the sequencing process. However, apparent insertions-deletions between species were considered likely to actually have occurred and, thus, were retained in the analysis. The fragment that was sequenced consisted primarily of cytochrome-b gene (coding) and the D-loop region (noncoding), separate phylogenies were developed using cytochrome-b gene, the D-loop region and the two sequences together. Each data set was analyzed twice, once with *P. leucopus* and *P. gossypinus* as outgroups and once with *P. keeni* as the outgroup. For both the MP and ML analysis, robustness and nodal support were evaluated using 1000 bootstrap iterations (Felsenstein 1985). To search for the best tree, a heuristic search was conducted using 100 random additions and TBR branch swapping in the parsimony analysis and 10 random additions and TBR branch swapping in the maximum-likelihood analysis. When applicable in Bayesian analysis, data sets were analyzed by assigning each partition (gene region) its individual model and prior probability distributions. Partitions were unlinked to conduct partitioned likelihood analyses.

For the MP analysis, weighted and unweighted phylogenies were generated. Weighting for the parsimony analysis was based on estimating a transition/transversion ratio and 1st, 2nd, 3rd codon position changes for cytochrome-b. These were estimated using the Hasegawa, Kishino, and Yano model (HKY85: Hasegawa *et al.* 1985) within PAUP v4.0b10. Likelihood-ratio tests along with AIC scores derived using MODELTEST

v 3.5 (Posada & Crandall 1998) were used to select a nucleotide substitution model for ML analysis. When likelihood-ratio tests and AIC scores were in disagreement, an analysis was conducted using each selected model. Parameter abbreviations in MODELTEST are, the number of substitution types (Nst), transition/transversion ratio (Tratio), substitution model (Rmat), rate of evolution for variable sites (Rates), gamma distribution shape parameter (Γ), and the proportion of invariable sites (I). Models for the Bayesian analysis were chosen using MRMODELTEST v1.1b (Nylander 2002). Again, if the log likelihood score and the AIC score were in disagreement each model was used and a separate analysis was conducted. For the Bayesian analyses, four chains were run for two million generations. Sampling occurred every 10 generations to produce a posterior probability distribution of 200 001 trees. A burn-in value was determined by graphing the log likelihood scores and determining the point at which relative stationarity had been achieved. Once stationarity was reached, a 50% majority-rule consensus tree was constructed from the remaining trees.

Nested Clade Analysis

Following the method of Templeton *et al.* (1995), a nested clade analysis was conducted. Nested clade analysis (NCA) tests the assumption, or null hypothesis, that haplotypes or clades of haplotypes are randomly dispersed with respect to space. Primarily, NCA allows one to infer historical causes for the present spatial distribution of haplotypes (i.e. range expansion, colonization, or vicariance events) through the genetic marker under analysis. Thus, individual effects of recurrent gene flow and historical events can be identified and inferences made about their role in the present phylogeographic structure. Based on work by Hudson (1989) using coalescent theory,

this method was designed to resolve population level divergence by calculating the overall limits of parsimony and developing a diagram of haplotype relationships. This is accomplished through the construction of a 95% statistical parsimony network of haplotypes (Templeton *et al.* 1992). Haplotypes are then hierarchically subdivided into nested clades using the algorithm and following the rules of Templeton *et al.* (1987) and Templeton & Sing (1993).

In order to employ this method, it first must be shown that the use of parsimony is justified (Sober 1988). This assumption can be tested by estimating the parameter Theta (θ) (Watterson 1975) where $\theta = 4N_e\mu$, N_e is the effective population size and μ is the mutation rate per nucleotide. For the mitochondrial genome $\theta = 2N_e\mu$. For this analysis θ was estimated using the software DNASP version 4.0 (Rozas *et al.* 2003) then used to solve for H in equation 1 of Templeton *et al.* (1992). Program TCS version 1.18 (Clement *et al.* 2000) was used to construct the cladogram and estimate probabilities. TCS uses the algorithm of Templeton *et al.* (1992). Clades are nested by moving one mutational step inward from the tips uniting haplotypes into one-step clades. After the tip clades have been nested, interior clades are nested as additional one-step clades. The next round of nesting unites two-step clades, again, beginning with the tips. The nesting continues until the final round results in a single clade that encompasses all haplotypes.

The final hierarchical clades were analyzed in GEODIS (Posada *et al.* 2000). The GEODIS analysis investigates the association of clades and nested clades in two different ways. First, locations are treated as categorical variables, and a permutational contingency analysis is used to test clades against their geographical location. Secondly, a more conclusive test is conducted utilizing geographical distances (Templeton *et al.*

1995). Within this analysis two primary parameters are calculated, clade distance (D_c) and nested clade distance (D_n). D_c is a measure of the geographical spread of a clade and D_n measures the distribution of a clade relative to clades of the same nesting level. GEODIS begins with the null hypothesis that haplotypes are dispersed randomly with respect to geographical location. When the null was rejected (5% level) an inference key (http://darwin.uvigo.es/download/GEODISkey_14Jul04.pdf) was used to draw inferences concerning population processes that may underlie the observed contemporary patterns. Nested clade analysis was used here to test for geographical associations of haplotypes using three different models of phylogeny based on TCS parsimony networks. The first model used the statistical parsimony network generated by the program TCS (Model I). Secondly, haplotypes from the Florida peninsula were removed prior to generating a parsimony network through TCS (Model II). Finally, a third model was analyzed with the parsimony network generated by TCS without the Florida peninsula haplotypes (Model III); however, the branch containing haplotypes from central Alabama and Georgia (LCAL01, LCAL02, and TCGA01) was manually moved to branch from a node basal to the beach clade. This branch was moved to be consistent with the core phylogeny estimated by Bayesian, MP, and ML analyses.

Neutral evolution and demographic analysis

For clades or groups identified by phylogenetic analysis, measures of diversity were estimated for cytochrome-b, D-loop, and the combined gene regions. Measures of diversity were estimated using DNASP version 4.0 (Rozas *et al.* 2003) and included the number of haplotypes (h), the number of polymorphic sites (S), the total number of mutations (Eta), haplotype diversity (Hd), nucleotide diversity (π), theta (θ), and the

average number of nucleotide differences (k). The assumption of neutrality for the genetic markers under analysis was tested using several neutrality test statistics.

However, there is the potential for multiple processes to occur within a population that may produce similar outcomes from some neutrality test statistics (i. e. selection, population expansion/contraction, population admixture, population subdivision).

Neutrality tests were conducted using DNASP version 4.0 (Rozas *et al.* 2003). These tests included Tajima's D (Tajima 1989), Fu & Li's D, Fu & Li's D*, Fu & Li's F, and Fu & Li's F* (Fu & Li 1993), and McDonald-Kreitman (McDonald & Kreitman 1991).

Tajima's D (Tajima 1989) statistic tests for violations of neutrality by comparing two measures of θ and does not require an outgroup. Neutral evolution predicts that both estimates of θ would be the same. Tajima's D statistic can be either positive or negative. Values greater than zero indicate higher average heterozygosity than expected which can indicate heterozygote advantage or population contraction. Values less than zero indicate a lower than expected average heterozygosity, as expected to result from events such as purifying selection, population expansion, or population admixture.

While Fu & Li's tests permit but do not require an outgroup, the analysis was conducted both with an outgroup (D, F) and without an outgroup (D*, F*). Because Fu & Li's tests compare mutations that occurred in the distant past with mutations that occurred in the recent past, an outgroup if available is preferred (Fu & Li 1993). Fu & Li's D and F tests were conducted for each *P. polionotus* clade using *P. maniculatus* as an outgroup and for selected each *P. polionotus* clades using a *P. polionotus* from a different clade as an outgroup and for each *P. polionotus* clade without an outgroup. A final neutrality test, the McDonald-Kreitman test (McDonald & Kreitman 1991) classifies

polymorphic sites in two ways, as differences between species or differences within species and whether the change is synonymous or nonsynonymous. This test does not assume that the population has reached equilibrium (i.e. the population may be expanding or in stasis). The McDonald-Kreitman test tests whether the ratio of nonsynonymous to synonymous changes between species is equal to that within a species. Neutrality tests were primarily intended to test the neutrality of nucleotide variation. However, they have inherent issues with limiting assumptions, and their outcomes may be open to competing interpretations. For instance, positive and negative values of Tajima's D statistic can simultaneously reflect different types of selection, population expansion, or population contraction.

Analysis of intraspecific demographic parameters was conducted using between clade comparisons. Clades that were analyzed were derived through statistical parsimony (TCS), maximum parsimony, maximum likelihood, and Bayesian phylogenetic analysis. Maximum likelihood (ML) estimates of the population parameters θ and exponential growth rate (g , scaled to reflect the number of mutations) were obtained using the program FLUCTUATE (Kuhner *et al.* 1998). FLUCTUATE is available from <http://evolution.genetics.washington.edu/lamarc.html>. FLUCTUATE assumes there is no selection or recombination. It utilizes the Metropolis-Hastings sampler to search the space of possible genealogies. Under the assumption of growth, the program accepts an initial genealogy, θ , and g which it then rearranges. It accepts or rejects the rearranged genealogy based on the probability of the data given the genealogy. FLUCTUATE can estimate its own beginning genealogy or have one entered along with an initial θ and g values. In my analysis, a method of 10 short chains with 100 000 steps and 2 long chains

with 200 000 steps while sampling every 20th step was used. DNASP version 4.0 was used for initial estimates of θ and when the population was allowed to grow the initial value of g was set at 1. Genealogies for selected clades were estimated under the assumption of growing and stationary population models. The growth models were compared and assessed by the 95% confidence intervals derived using the companion zero-growth model.

Molecular clock

As an initial estimate of time since *P. polionotus* and *P. maniculatus* last shared a common ancestor, percent divergence between a representative *P. polionotus* haplotype (*P. p. ammobates*) and the three *P. maniculatus* subspecies (*pallescens*, *bairdii*, *sonoriensis*) was estimated. For comparison, percent divergence was estimated for *P. p. ammobates* between a sample of other *polionotus*, as well as, an estimate between the *maniculatus* subspecies. *Peromyscus keeni* was compared with *ammobates*, *sonoriensis*, and *leucopus*. Also, percent divergence was estimated between *P. leucopus* and *P. gossypinus*. Likelihood ratio tests (LRT) were conducted to determine the appropriateness of adding a molecular clock to the nucleotide substitution models. For each ML data set, a clock assumption was added to the model selected by MODELTEST. The log-likelihood values of each data set with and without a clock assumption were compared and P-values calculated. Fossil dates of *P. polionotus* (Ruez 2001) were used to infer absolute times from genetic distances. Unfortunately, only one fossil calibration point was available, it was based on the estimated age of the Florida sinkhole locale (Inglis 1C). Ruez (2001) estimated the age of fossil deposits at the Inglis IC site to be between 2.01 - 1.78 Ma. For inferring time back to specific nodes, branch lengths were

estimated using maximum likelihood. To infer the age of nodes by a second method, a substitution rate (r) was measured using equation 5.10 (Li & Graur 1991) and equation 5.12 (Nei 1987). The estimated substitution rate could then be used to produce estimates of time to nodes for which there was no fossil evidence.

RESULTS

Phylogenetic analysis

The majority of this project was conducted using portions of mtDNA sequences that were 2449 base pairs in length. However, phylogenetic analysis of the complete sequence with *Peromyscus leucopus* and *Peromyscus gossypinus* as outgroups was conducted using sequences of 2452 base pairs in length. The additional three nucleotides were gained when *leucopus* and *gossypinus* were added to the alignment. Pairwise analyses of the D-loop of *P. polionotus*, *P. maniculatus*, *P. leucopus*, *P. keeni*, and *P. gossypinus* indicate an insert in *P. polionotus* that is approximately 74 base pairs in length. This insert, based on sequence alignment data with *Mus musculus* (GenBank ABO42432), appears to be located near the two ETAS regions of the D-loop (Sbisa *et al.* 1997) and may be a repeat of either ETAS region 1 or ETAS region 2. For phylogenetic analyses of *P. polionotus* using other *Peromyscus* as outgroup haplotypes, the large insert created alignment problems. Because the principle goal of this project was to determine the relationship within *P. polionotus*, a consensus sequence of the insert was created from the *polionotus* alignment and placed within outgroup haplotypes at the corresponding portion of the sequence. I feel confident in the placement of the insert within outgroup haplotypes due to the strong alignment on either side of the insert (Fig. 3).

Regions of the mtDNA sequence used in this study were as follows, partial cytochrome-b gene is 1 - 1137, tRNA-Thr is 1138 - 1205, tRNA-Pro is 1208 - 1273, the D-loop region is 1274 - 2244, tRNA-Phe is 2245 - 2312, and 12s rRNA is 2316 - 2449 or 3452. Using the complete mtDNA sequence of *Mus musculus* (GenBank AB042432) the corresponding genes or gene regions would be: partial cytochrome-b 14 152 - 15 289, tRNA-Thr 15 290 - 15 356, tRNA-Pro 15 357 - 15 423, D-loop 15424 - 16 395, tRNA-Phe 1 - 68, and 12s rRNA 70 - 1024. There are two bases between tRNA-Thr and tRNA-Pro and three bases between tRNA-Phe and 12s rRNA that are not accounted for based on the alignment with *Mus*. The 74 bp insert appears to be, from base 1428-1502 of my fragment to 15 578 - 15 650 in the *Mus* alignment.

Phylogenetic topologies were constructed under two outgroup scenarios. Dependent upon the haplotype used as the outgroup, either 44 sequences or 42 sequences were used for each estimated topology. Outgroup samples were from *P. maniculatus bairdii*, *P. m. sonoriensis*, *P. keeni*, *P. m. pallescens*, *P. gossypinus*, and *P. leucopus*. The data used for constructing topologies consisted of different *polionotus* haplotypes, individual *polionotus* with the same haplotype but from different geographic locations, and outgroup individuals. The data set using *P. gossypinus*, and *P. leucopus* as outgroup haplotypes consisted of 44 sequences comprised of 2452 nucleotides. For analysis, the sequence data was divided into three primary sets, the total sequence (2452 bp) partial cytochrome-b gene (1137 bp) and the complete D-loop region (971 bp). The entire sequence was composed of a portion of cytochrome-b, the D-loop region, three transfer RNA's (~204 bp), and ~140 bp of 12s rRNA gene. The cytochrome-b sequence data set consisted of 33 haplotypes, $S = 193$, $\pi = 0.0202$, $k = 22.99$, and $Hd = 0.977$. The D-loop

region consisted of, 36 haplotypes, $S = 241$, $\pi = 0.0294$, $k = 28.37$, and $Hd = 0.994$. Diversity analysis of the complete sequence consisted of 39 haplotypes, $S = 434$, $\pi = 0.0217$, $k = 52.97$, and $Hd = 0.994$. Another set of analyses was conducted with *P. keeni* as the outgroup along with individuals of *P. m. bairdii*, *P. m. sonoriensis*, and *P. m. pallescens* (Table 2). The total sequence length was 2449 base pairs with 38 haplotypes, $S = 267$, $\pi = 0.0141$, $k = 34.54$, and $Hd = 0.993$. Cytochrome-b gene consisted of 31 haplotypes, $S = 121$, $\pi = 0.0126$, $k = 14.27$, and $Hd = 0.974$. The D-loop portion of the sequence consisted of 34 haplotypes, $S = 132$, $\pi = 0.0198$, $k = 19.21$, and $Hd = 0.988$. These two data sets were analyzed using maximum parsimony, maximum likelihood, and Bayesian methods.

The ML model selection results were: cytochrome-b gene with an outgroup of *P. leucopus* and *P. gossypinus*, the HKY + Γ (Γ : shape parameter of the gamma distribution) model was identified by log likelihood score ($-1nL = 2994.17$) and the TVM + Γ model was identified by AIC analysis (AIC = 5987.24). Estimates of parameters for the HKY + Γ (Hasegawa *et al.* 1985) model were, base frequencies A = 0.3282, C = 0.2807, G = 0.1222, and T = 0.2689, Nst = 2, Tratio = 5.8576, rates = gamma, $\Gamma = 0.0672$, and I = 0.0000. Estimated parameters for the TVM + Γ model were, base frequencies A = 0.3232, C = 0.2766, G = 0.1261, and T = 0.2740, the substitution rate matrix was, [A-C] = 26126.14, [A-G] = 170050.33, [A-T] = 8973.04, [C-G] = 6208.09, [C-T] = 170050.33, and [G-T] = 1.0000, rates = gamma, $\Gamma = 0.0812$, and I = 0.0000.

For the cytochrome-b region with *P. keeni* as the outgroup, the selected model by log likelihood ($-1nL = 2427.31$) was HKY + Γ and by AIC score (AIC = 4859.24) was GTR + I (I: proportion of invariable sites) (Lanave *et al.* 1984). The parameters from the

HKY + Γ model were, base frequencies A = 0.3242, C = 0.2666, G = 0.1328, and T = 0.2764, Nst = 2, Tratio = 9.7396, rates = gamma, Γ = 0.0131, I = 0.0000, and for the GTR + I model, base frequencies A = 0.3208, C = 0.2677, G = 0.1295, and T = 0.2819, Nst = 6, rate matrix = [A-C] = 12981416.00, [A-G] = 169401536.00, [A-T] = 3301110.75, [C-G] = 3204468.50, [C-T] = 112213536.00, and [G-T] = 1.00, rates = equal, and I = 0.7866. For the D-loop region with *P. leucopus* and *P. gossypinus* as the outgroup, MODELTEST selected the model HKY + I + Γ from both log likelihood score (-1nL = 3063.81) and AIC score (AIC = 6139.61). Parameters for this model were, base frequencies A = 0.3375, C = 0.2242, G = 0.1127, and T = 0.3256, Nst = 2, Tratio = 3.2048, rates = gamma, Γ = 0.7973, I = 0.4977. For the D-loop region with *P. keeni* as the outgroup, MODELTEST selected HKY + I + Γ (-1nL = 2455.72) by both log likelihood score and AIC score (AIC = 4923.43). Parameters for these models were, base frequencies A = 0.3285, C = 0.2279, G = 0.1152, and T = 0.3284, Nst = 2, Tratio = 5.1041, rates = gamma, Γ = 0.8933, I = 0.6216.

For the combined cytochrome-b gene and D-loop region with *P. keeni* as the outgroup, MODELTEST selected HKY + I + Γ by both log likelihood (-1nL = 5555.24) and AIC score (AIC = 11122.48). Parameters for the model were, base frequencies A = 0.3345, C = 0.2434, G = 0.1289, and T = 0.2932, Nst = 2, Tratio = 6.5150, rates = gamma, Γ = 0.9817, I = 0.6719. Finally, using cytochrome-b gene and the D-loop region with an outgroup of *P. leucopus* and *P. gossypinus* MODELTEST selected a single model, HKY+I+ Γ (-1nL = 6822.79, AIC = 13657.59). Parameters for the model were, base frequencies A = 0.3386, C = 0.2475, G = 0.1232, and T = 0.2907, Nst = 2, rates =

gamma, $\Gamma = 0.8185$, $I = 0.5795$. These maximum likelihood models were used to construct phylogenies using PAUP.

MRMODELTEST v1.1b (Nylander 2002) was used to determine appropriate models for Bayesian analysis using the software MRBAYES 3.0 (Huelsenbeck & Ronquist 2001).

Using the sequence containing both cytochrome-b and the D-loop regions

MRMODELTEST selected the HKY + I + Γ model by both log likelihood score ($-1nL = 6822.79$) and AIC score (AIC = 13657.59). Parameters for the model were: base

frequencies A = 0.3386, C = 0.2475, G = 0.1232, and T = 0.2907, Nst = 2, Tratio =

4.0029, rates = gamma, $\Gamma = 0.8185$ and $I = 0.5795$. Again, using both cytochrome-b and

the D-loop but with *P. keeni* as the outgroup MRMODELTEST selected the HKY + I + Γ

model as the best fitting model by log likelihood ($-1nL = 5551.71$) and AIC score (AIC =

11115.41). The parameters were: base frequencies A = 0.3337, C = 0.2437, G = 0.1291,

and T = 0.2935, Nst = 2, Tratio = 6.5150, rates = gamma, $\Gamma = 0.9816$, and $I = 0.6717$.

Using the D-loop region with *P. leucopus* and *P. gossypinus* as outgroups,

MRMODELTEST selected the HKY + I + Γ model by log likelihood ($-1nL = 3063.80$) and

AIC score (AIC = 6139.61). The parameters were: base frequencies A = 0.3375, C =

0.2242, G = 0.1127, and T = 0.3256, Nst = 2, Tratio = 3.2048, rates = gamma, $\Gamma =$

0.7973, and $I = 0.4977$. Using the D-loop region with *P. keeni* as the outgroup

MRMODELTEST selected HKY + I + Γ model by log likelihood ($-1nL = 2455.72$) and AIC

score (AIC = 4923.43). The parameters were: base frequencies A = 0.3285, C = 0.2279,

G = 0.1152, and T = .03284, Nst = 2, Tratio = 5.1041, rates = gamma, $\Gamma = 0.8933$, and $I =$

0.6216. Using cytochrome-b gene and *P. leucopus* and *P. gossypinus* as outgroups

MRMODELTEST selected GTR + Γ by log likelihood score ($-1nL = 2985.61$) and AIC

score (AIC = 5989.23). The parameters were: base frequencies A = 0.3233, C = 0.2764, G = 0.1265, and T = 0.2738, Nst = 6, rate matrix was [A-C] = 5599042.50, [A-G] = 35834508.00, [A-T] = 1921158.63, [C-G] = 1327221.00, [C-T] = 36681148.00, and [G-T] = 1.00, rates = gamma, Γ = 0.0825, and I = 0.0000. Using cytochrome-b gene with *P. keeni* as the outgroup MRMODELTEST selected the HKY + Γ model by log likelihood score (-lnL = 2427.31) and GTR + I model by AIC score (AIC = 4859.24). Parameters for the models were, respectively: base frequencies A = 0.3242, C = 0.2666, G = 0.1328, and T = 0.2764, Nst = 2, Tratio = 9.7396, rates = gamma, Γ = 0.0160, I = 0.0000, base frequencies A = 0.3208, C = .02677, G = 0.1295, and T = 0.2819, Nst = 6, rate matrix was [A-C] = 35658768.00, [A-G] = 465339968.00, [A-T] = 9067707.00, [C-G] = 8802202.00, [C-T] = 308245280.00, and [G-T] = 1.0000, rates = equal, and I = 0.7866.

Twenty-seven topologies were developed that depict the hypothesized phylogenies generated from the multiple phylogenetic approaches. While the topologies vary substantially, significant agreement was observed (Fig. 4 - 30). Consistent among the MP and ML trees was the 100% bootstrap support for *P. polionotus* as a monophyletic clade indicating reciprocal monophyly. Bayesian models also strongly supported *P. polionotus* as a monophyletic clade with 100% posterior probability. Twenty-eight topologies were estimated based on maximum likelihood, maximum parsimony, Bayesian, and statistical parsimony methods. Eight maximum likelihood topologies were constructed (Fig. 4 - 11). Maximum likelihood analysis of cytochrome-b region (1137 bp), produced four topologies that were constructed from the best-fit models selected by MODELTEST v3.5. The number of models (28) resulted from testing the assumption of different outgroups, and, under each outgroup different models may have

been selected by likelihood ratio tests and AIC scores. Model selection for the cytochrome-b gene was the most variable. Using the ML method, four separate models were selected as best-fit models. With *P. leucopus* and *P. gossypinus* as outgroups the likelihood ratio tests (LRT) selected the HKY + Γ model, but the AIC score best-fit model was TVM + Γ . Using *P. keenii* as the outgroup the LRT best-fit model was the HKY + Γ while the AIC best-fit model was GTR + Γ . Using these different outgroups did not change the log likelihood model selection for the cytochrome-b portion of the sequence. However, with both outgroups the AIC method concluded adding more parameters was appropriate and selected a different model for each outgroup. All models, however, were in agreement concerning rate heterogeneity across sites. Using MRMODELTEST for model selection by Bayesian analyses with the cytochrome-b region, the only disagreement in model choice occurred when *P. keenii* was used as the outgroup. In this case, LRT selected GTR + I as the best-fit model while the AIC method selected the HKY + Γ model as most appropriate.

Model selection for the D-loop region was more congruent. For the ML method, model selection using different outgroups did not change the model (HKY). However, using *P. leucopus* and *P. gossypinus* as outgroups added the parameter of rate heterogeneity (Γ) and proportion of invariable sites (I) while using *P. keenii* as the outgroup added only the parameter of I. For the D-loop region, LRT and AIC were in agreement with model selection for each outgroup. Model selection resulting from Bayesian analyses of the D-loop region was in agreement regardless of the outgroup (HKY + Γ + I). When combining the cytochrome-b gene and the D-loop region for the ML phylogeny estimation, model selection by both LRT and AIC was in agreement

(HKY + Γ + I). Maximum likelihood model selection for the combined genes was not changed by either outgroup. The Bayesian analysis of the complete sequence was conducted using the substitution model that was selected for each of the separate regions.

Using ML methods for phylogenetic estimation from cytochrome-b gene with *P. gossypinus* and *P. leucopus* as outgroup haplotypes, LRT indicated that the best-fit model was HKY + Γ . However, the AIC score identified TVM + Γ as the most appropriate model. The HKY + Γ substitution model was somewhat more resolved (Fig. 4). It shows the presence of a clade comprised of seven haplotypes (inland clade II) that was not present in the TVM + Γ model (Fig. 5). However, the clade (inland clade II) has low (52%) bootstrap support value. Otherwise, the two models produced essentially the same topology. Bootstrap support values were generally low to moderate in both topologies. The HKY + Γ model indicated the possibility of four major clades emanating from a star phylogeny. The TVM + Γ model, however, suggested only three clades but again indicated a star phylogeny. The clades (HKY + Γ) were comprised of three inland groups and the partial formation of a beach clade. These clades were defined as inland clade I (BCAL05, RCAL01, TCGA03, BCAL04, OCFL03, BCAL01, WCFL04, MCAL01, and JCFL01), inland clade II (WCFL02, WCFL03, WCFL01, OCFL05, OCFL04, WCFL02, and OCFL06), the beach clade (PEN05, 89CI01, ALL02**, ALL05, and ALL02*). The third inland group was comprised of haplotypes WCFL01, WCFL06, JCFL03, OCFL01, and OCFL07.

Cytochrome-b topologies with *P. keeni* as the outgroup (Fig. 6, 7) were similar to the topologies identified with *P. leucopus* and *P. gossypinus* as outgroups. The model selection, HKY + Γ , by LRT for the both outgroups produced essentially the same

topology. Also, model selection by AIC score (TVM + Γ , GTR + Γ) with *leucopus/gossypinus* and *keeni* as outgroups, respectively, was in near complete agreement on the structure of the topology. Again, with *keeni* as the outgroup the HKY + Γ model was slightly more resolved but essentially the same as the HKY + Γ model with *P. leucopus* and *P. gossypinus* as outgroups. The same clades were present and the bootstrap values were only slightly different. Cytochrome-b established the presence of various relationships within *P. polionotus*, however, the amount of overall divergence was low and thus yielded inadequate resolution for solving my original question. Cytochrome-b is a moderately evolving gene, thus the lack of a defining topology was expected. However, cytochrome-b gene did establish *P. polionotus* as a monophyletic clade within a group of its sister taxa, and did indicate that *P. polionotus* is a significantly older taxon. This finding is more in agreement with recent fossil evidence (Ruez 2001) than previously hypothesized by biogeographic models.

Topologies based on data from the D-loop region (971 bp), were more resolved (Fig. 8, 9) than for cytochrome-b. This outcome was expected as the D-loop contains hypervariable regions (Vigilant *et al.* 1991) that were expected to provide greater phylogenetic signal at the subspecific level. Unlike the cytochrome-b region, a single best-fit model was identified for both outgroups (by both LRT and AIC scores). This model was HKY. However, when using *keeni* as the outgroup, the parameter I (proportion of invariable sites) was included. When *gossypinus* and *leucopus* served as outgroups two parameters, I and Γ (shape parameter of the gamma distribution) were components of the HKY model. The two resulting topologies exhibited the same branching configuration with only slight differences in bootstrap values. Haplotypes

placed within Inland clade I did not change regardless of gene region, model, and outgroup indicating strong support for this clade by the ML method. Inland clade II differed slightly between D-loop and cytochrome-b topologies. The D-loop topology placed haplotypes LCFL01 and SCFL01 within inland clade II but with low (model HKY + Γ + I 50%; model HKY + I 52%) bootstrap support. In contrast, the beach clade produced by the D-loop analysis was substantially different from the cytochrome-b beach clade (either model). Haplotypes (PEN05, CCFL01, TRI07, AMM01, LEU08, OCFL01, WCFL01, WCFL06, OCFL07, and JCFL03) comprised the D-loop beach clade while haplotypes (PEN05, PEN02*, ALL02**, ALL05, and ALL02*) comprised the cytochrome-b beach clade.

While there was added clarification from the analyses of the D-loop region, the overall topology was not fully resolved. I attempted to improve the stability of the topology by conducting a third round of analysis utilizing the combined gene regions (2449 bp). Again, neither of the outgroup haplotypes affected model selection. When either *leucopus/gossypinus* or *keeni* were used as outgroups, the model HKY + Γ + I was selected by both LRT and AIC scores (Fig. 10, 11). The complete fragment analyses yielded topologies that were most similar to the separate ML analyses of the cytochrome-b region and D-loop that were devised through the HKY model with *leucopus/gossypinus* as outgroups. However, combining the regions produced topologies that were more resolved than the analyses of either single region. Indeed, the beach clade now consisted of 16 haplotypes (LCAL01, TCGA01, PEN05, AMM01, LEU08, OCFL01, WCFL01, WCFL06, OCFL07, JCFL03, CCFL01, TRI07, PEN02*, ALL02**, ALL05, and ALL02*). Inland haplotypes LCAL01 and TCGA01 (central Alabama and central

Georgia respectively) branched from the basal node within the beach clade. Also, another group of inland haplotypes (OCFL01, WCFL01, WCFL06, OCFL07, and JCFL03) was placed within the beach clade. Conversely, haplotypes found in Gulf Coastal beach populations are not found outside of the beach clade. Inland clade I had the same haplotypes as the ML D-loop and cytochrome-b topologies, however in the combined analyses it was more strongly supported by bootstrap values. Inland clade I was then supported by all the topologies and was apparently quite robust. The HKY model from the cytochrome-b region supported the possible existence of at least two major inland clades. The D-loop analysis also supported two major inland clades and, minus six haplotypes, the beach clade. The D-loop included two new haplotypes within inland clade II while significantly altering the beach clade. The combined data set of cytochrome-b and the D-loop identified divergence points for at least three major lineages within *P. polionotus*, two inland clades and a single beach clade comprised of haplotypes found only within populations of subspecies along the Gulf Coast of Florida and Alabama.

For the maximum parsimony (MP) analysis, six weighted and six unweighted topologies were constructed (Fig. 12 - 23). Again, cytochrome-b and the D-loop were analyzed independently and combined into a single sequence. Also, where applicable, analyses were conducted using weighted characters such as transition/transversion ratio and nucleotide substitutions based on codon position bias. Weighting values for each data set were calculated using an HKY85 model of nucleotide substitution (PAUP* v 4.0b10). Analyses of cytochrome-b with *P. leucopus* and *P. gossypinus* as outgroups included 44 individual sequences of 1137 bp each. Among the 44 sequences were 33

haplotypes with 193 variable sites of which 126 were parsimony informative. A second set of cytochrome-b sequence data with *P. keeni* as the outgroup consisted of 42 sequences of 1137 bp each. The 42 sequences produced 31 haplotypes consisting of 121 variable sites of which 65 were phylogenetically informative.

The weighted MP analysis of cytochrome-b gene with *P. leucopus* and *P. gossypinus* as outgroups (Fig. 12) yielded 28 equally parsimonious trees (1646 steps) with a consistency index (CI) of 0.9195, a retention index (RI) of 0.9071 and a rescaled consistency index (RC) of 0.8341. Weighting consisted of a 9.5:1 transition/transversion ratio, 1st codon positions were weighted 5:1 and 2nd codon positions 40:1. The unweighted analysis of cytochrome-b with *leucopus* and *gossypinus* as outgroups revealed 77 equally parsimonious trees (272 steps) with a CI of 0.7684, a RI of 0.8205, and a RC of 0.6305. Using *leucopus* and *gossypinus* as outgroups, the MP weighted and unweighted cytochrome-b analyses produced similar results. Interestingly, the weighted topology placed haplotype NIV17 (*P. p. niveiventris*) branching from a basal node in the *P. polionotus* clade, however, at low (51%) bootstrap support. Weighting the analysis produced an inland clade I with the same haplotypes as estimated by the ML analyses with the addition of haplotype LCAL01. Removing the constraints of the weighted parameters (Fig. 13), inland clade I contained only the haplotypes BCAL04, OCFL03, BCAL01, WCFL04, MCAL01, and JCFL01. Inland clade II, however, was comprised of haplotypes LCFL01, WCFL02, WCFL03, WCFL01, OCFL05, OCFL04, WCFL02, and OCFL07. Thus, inland clade II differed from the cytochrome-b ML analyses with the addition of haplotype LCFL01. The D-loop ML analyses placed the LCFL01 haplotype within inland clade II where it remained throughout the remainder of the ML analyses.

Within the weighted and unweighted MP analyses of cytochrome-b using *P. leucopus* and *P. gossypinus* as outgroups, the beach clade fragmented in the same manner as the ML cytochrome-b analyses (Fig. 12, 13). Like the ML analyses, this analysis produced multiple, single long branches and placed haplotypes PEN05, PEN02*, ALL02**, ALL05, ALL02* in one clade and haplotypes WCFL01, WCFL06, JCFL03, OCFL01, and OCFL07 in a second clade. The previous two groups of haplotypes were placed in the beach clade in the ML analysis combining the cytochrome-b and D-loop region. Inland clade II contained the same haplotypes in both MP cytochrome-b analyses. Bootstrap values were essentially the same between the analyses for the two beach groups but were somewhat higher in the weighted analysis for inland clade II. Results from the two analyses, weighted and unweighted, were essentially the same with the exception of the removal of haplotypes LCAL01, BCAL05, RCAL01, and TCGA03 from inland clade I in the unweighted tree. While bootstrap values were very similar, (CI, RI, and RC) were higher in the weighted analysis. The weighted analysis produced 49 fewer equally parsimonious trees but was 1374 steps longer.

Maximum parsimony analysis of cytochrome-b using *P. keeni* as the outgroup (Fig 14, 15) included 42 sequences of 1137 bp. Among the 42 sequences were 31 haplotypes with 121 variable sites of which 65 were parsimony informative. The weighted analysis resulted in 14 equally parsimonious trees (805 steps) with a CI of 0.9553, a RI of 0.9439, and a RC of 0.9017. Weighting consisted of transition/transversion ratio of 18:1, 1st codon position changes 5:1, and 2nd codon position changes 37:1. Removing the weight assumptions produced 38 equally parsimonious trees (149 steps) with a CI of 0.8389, a RI of 0.8863, and an RC of 0.7435.

The unweighted tree with *P. keeni* as the outgroup placed fewer of the haplotypes into clades. Inland clade II and the beach clade were identical between the analyses, however, inland clade I differs by four haplotypes (BCAL05, LCAL01, RCAL01, TCGA03) which were absent from inland clade I in the unweighted analysis. With *keeni* as an outgroup for the cytochrome-b topologies, as opposed to *leucopus* and *gossypinus*, the topologies were not quite as resolved for the unweighted tree but were highly congruent between the weighted trees. However, bootstrap values for cytochrome-b with outgroup *keeni* were similar for congruencies that do occur.

Two topologies (weighted and unweighted) were generated for the D-loop region using *P. leucopus* and *P. gossypinus* as outgroups (Fig. 16, 17). The data set was comprised of sequences from 45 individuals (971 bp). Again, an artificial insert (74 bp) was placed in the D-loop region of outgroup haplotypes. Among the 45 samples were 37 haplotypes that consisted of 208 variable sites of which 136 were informative. Because the D-loop is not a coding region, only the transition/transversion ratio was weighted (6:1). The weighted analysis consisted of 17 equally parsimonious trees (745 steps) a CI of 0.8631, a RI of 0.8922, and a RC of 0.7700. The unweighted topology with *P. leucopus* and *P. gossypinus* as outgroups consisted of the same number of haplotypes and variable sites but the number of parsimony informative sites was reduced over the weighted topology to 132 from 136. The unweighted analysis consisted of 22 equally parsimonious trees (311 steps) with a CI of 0.7653, a RI of 0.8433, and an RC of 0.6454. While the two trees are highly congruent, there were some differences. Haplotype composition of inland clade I was not changed between weighted and unweighted analyses and contained haplotypes BCAL05, BCAL01, MCAL01, BCAL04, JCFL01,

OCFL03, WCFL04, RCAL01, TCGA03. Inland clade II differed between the two topologies by a single haplotype (LCFL01). Otherwise they consisted of the same sequences (OCFL04, OCFL06, WCFL01, WCFL02, WCFL02, OCFL05, WCFL03). Both analyses identified a beach clade consisting of haplotypes LCAL01, TCGA01, CCFL01, TRI07, PEN05, AMM01, LEU08, OCFL01, WCFL01, WCFL06, OCFL07, ALL05, ALL02*, PEN02*, ALL02**, and JCFL03. The weighted analysis grouped four haplotypes (SCFL01, MCFL76, WCFL07, WCFL09) that roughly comprise a Florida peninsula clade. The haplotypes WCFL07 and WCFL09 were collected near St. Marks, (south of Tallahassee, Florida), so the two haplotypes were geographically removed from the true Florida peninsula. Interestingly, the unweighted analysis placed the haplotype SCFL01 branching from a basal node in the *P. polionotus* group.

The D-loop analyses with *P. keenii* as the outgroup included 43 sequences with 971 bp (Fig. 18, 19). These sequences constitute 35 haplotypes with 132 variable sites where 81 were parsimony informative. The estimated transition/transversion ratio was 10:1. The weighted data set produced 32 equally parsimonious trees (482 steps) with a CI of 0.8465, a RI of 0.9094, and a RC of 0.7698. The unweighted data set yielded 520 equally parsimonious trees (184 steps) with a CI of 0.7500, a RI of 0.8682, and a RC of 0.6511. Both D-loop data sets supported the existence of the two hypothesized inland clades containing the same haplotypes as hypothesized by the prior (outgroup = *P. leucopus*) MP D-loop analyses. Using *keenii* as the outgroup, both the weighted and unweighted D-loop topologies supported inland clade I comprised of haplotypes (BCAL05, RCAL01, TCGA03, BCAL01, MCAL01, BCAL04, JCFL01, OCFL03, WCFL04). Again, only the weighted topology placed haplotype LCFL01 in inland clade

II, otherwise, inland clade II was comprised of the same haplotypes as the unweighted topology. These two analyses differed, however, in placement of haplotypes within the beach clade. The weighted topology placed haplotypes LCAL01, TCGA01, CCFL01, TRI07, PEN05, AMM01, LEU08, OCFL01, WCFL01, WCFL06, OCFL07, ALL05, ALL02*, PEN02*, ALL02**, and JCFL03 within the beach clade. However, the unweighted topology did not include haplotypes LCAL01, TCGA01, PEN02*, ALL02**, ALL05, and ALL02* within the beach clade. The weighted topology roughly supported the same peninsula clade. Neither the weighted nor the unweighted topology using *keeni* as the outgroup proposes a haplotype branching from a basal node among *polionotus* as the unweighted D-loop topology using *leucopus* and *gossypinus* as outgroups did. The D-loop topologies, despite the outgroup haplotype, were congruent when comparing weighted and weighted or unweighted and unweighted. The outgroup used to root the topology appeared to make little difference.

Combining the D-loop and cytochrome-b along with the three tRNAs and the 137 bp of 12s rRNA and using *P. leucopus* and *P. gossypinus* as outgroups, there were 44 sequences 2452 bp long (Fig. 20, 21). These data represented 39 haplotypes with 426 variable sites of which 265 were parsimony informative. The analysis produced 93 equally parsimonious trees (1668 steps) with a CI of 0.8639, a RI of 0.8718, and a RC of 0.7532. The cytochrome-b weighting scheme with *P. leucopus* and *P. gossypinus* as outgroup haplotypes consisted of 7:1 transition/transversion ratio, 1st positions weighted 5:1, and 2nd positions weighted 40:1. The unweighted analysis produced 26 equally parsimonious trees (614 steps) with a CI of 0.7687, a RI of 0.8273, and a RC of 0.6359. As with the previous topologies there was strong bootstrap support (100%) for *P.*

polionotus as a monophyletic clade. The weighted and unweighted topologies indicated an association among haplotypes BCAL05, RCAL01, TCGA03, BCAL01, MCAL01, OCFL03, WCFL04, BCAL04, JCFL01 to form inland clade I. The weighted topology placed haplotype LCAL01 and connected it to the basal node of the clade.

Both topologies created using the complete sequence represented inland clade II with haplotypes LCFL01, OCFL04, WCFL01, WCFL02, OCFL06, WCFL02, OCFL05, and WCFL03, as had many of the previous topologies. Also, both topologies contained beach clades with haplotypes AMM01, LEU08, WCFL01, WCFL06, OCFL01, OCFL07, JCFL03, PEN05, CCFL01, TRI07, PEN02*, ALL02**, ALL05, and ALL02*. However, the unweighted topology placed haplotypes LCAL01 and TCGA01 branching from a basal node in the beach clade. The unweighted topology did not group the haplotypes from the Florida peninsula, but the weighted topology did contain the peninsula clade (SCFL01, MCFL76, WCFL07, WCFL09). The weighted topology placed haplotype NIV17 branching at the basal node within the *polionotus* group. However, the unweighted topology placed haplotype SCFL01 branching from the basal node in the *polionotus* group.

Using *P. keeni* as the outgroup and weighting the data set produced 62 equally parsimonious trees (1002 steps) with a CI of 0.8752, a RI of 0.9092, and a RC of 0.7958. This data set was weighted as follows, transition/transversion ratio = 12:1, 1st positions weighted 5:1, and 2nd positions weighted 37:1. Removing the weighting assumptions from the data produced 440 equally parsimonious trees (354 steps) with a CI of 0.7853, a RI of 0.8645, and a RC of 0.6789. The topologies (weighted and unweighted) were similar to their counterparts with *leucopus* as the outgroup (Fig. 22, 23). In fact, inland

clades I and II contained exactly the same haplotypes but with bootstrap support values that differed slightly. However, with *keeni* as the outgroup neither topology placed haplotypes LCAL01 and TCGA01 branching from the basal node in the beach clade as had the unweighted topology with *leucopus* as the outgroup. The weighted data set identified a Florida peninsula clade with haplotypes SCFL01, MCFL76, WCFL07, and WCFL09 while the unweighted data set does not have this clade. The weighted data set places NIV17 branching from a basal node among *polionotus* while the unweighted data did not.

Bayesian analyses were carried out with cytochrome-b, D-loop and the both regions combined (Fig. 24 - 30). With *P. keeni* as the outgroup, LRT and AIC scores indicated different best fit models for the data, thus, including the data set with *leucopus* and *gossypinus* as outgroups there are three cytochrome-b phylogenies from the Bayesian analysis. The first cytochrome-b topology had *P. leucopus* as the outgroup and model GTR + Γ was selected by both log likelihood and AIC scores (Fig. 24). This tree also gave strong posterior probability support (95%) for inland clade I. Like the HKY + Γ model with *P. keeni* as the outgroup, the GTR + Γ model also placed haplotype LCFL01 within inland clade II and moderately supported (69%) the clade. This topology also placed haplotypes TCGA01 and LCAL01 within the beach clade but at similar support (54%) as the GTR + I model with *P. keeni* as the outgroup. With *P. keeni* as the outgroup, models GTR + I (AIC score) and HKY + Γ (LRT) were selected. The topology produced using the HKY + Γ model was a 50% majority-rule consensus of 191 840 trees (Fig. 25). The topology produced using model GTR + I was a 50% majority-rule consensus of 193 162 trees (Fig. 26). Both topologies gave strong posterior probability

support (100%) for *P. polionotus* as a monophyletic clade. Also, both topologies supported the existence of three major clades. The three clades (inland clade I, inland clade II, beach clade) were similar to the clades produced by maximum parsimony and maximum likelihood cytochrome-b phylogenies.

The two Bayesian cytochrome-b analyses were not, however, in complete agreement. Each inland clade I contained the same haplotypes, however, the HKY + Γ model had slightly higher posterior probabilities. The HKY + Γ model placed haplotype LCFL01 branching from the basal node in inland clade II but the GTR + I model did not place the LCFL01 haplotype in either clade. Inland clade II was much more strongly supported within the HKY + Γ model (83%) than within the GTR + I model (50%). Both models indicated the existence of a beach clade that is comprised of the same haplotypes. However, both gave low posterior probability support for the beach clade (HKY + Γ ; 56%; GTR + I; 51%). The GTR + I model also placed haplotypes TCGA01 and LCAL01 branching from the basal node in the beach clade while within the HKY + Γ model all haplotypes branch from a single node.

Both log likelihood and AIC scores identified a single model for the D-loop. Using either outgroup (*P. leucopus* or *P. keeni*) both AIC and log likelihood scores selected HKY+ Γ + I as the best-fit model. The D-loop Bayesian analysis with *P. leucopus* and *P. gossypinus* as outgroups produced a topology that is a 50% majority-rule of 191 313 trees (Fig. 27). The D-loop Bayesian analysis with *P. keeni* as the outgroup resulted in a 50% majority-rule of 191 737 trees (Fig. 28). The clades and node placement between the two topologies were essentially the same. However, using *P. leucopus* as the outgroup produced slightly stronger support for inland clade I (71% Vs

62%) and for inland clade II (92% Vs 73%). The posterior probability support for the beach clade remained essentially unchanged (65% Vs 64%). Using *P. keeni* as the outgroup, the model KHY + Γ + I supported inland clade I with the typical haplotypes although somewhat more resolved, but, uniquely placed inland clade I branching from the basal node in the *polionotus* group. Both of the Bayesian D-loop topologies placed haplotype LCFL01 within inland clade II and both also placed haplotype SCFL01 within inland clade II. The beach clade within these two topologies also contained haplotypes TCGA01 and LCAL01, however the beach clade was somewhat more resolved than the Bayesian cytochrome-b phylogenies.

The Bayesian topology combining cytochrome-b and the D-loop into a single fragment with *P. leucopus* and *P. gossypinus* as outgroups resulted in a 50% majority-rule consensus of 190 150 trees (Fig. 29). Using *keeni* for the outgroup, the 50% majority-rule represented 194 997 trees (Fig. 30). Combining cytochrome-b and the D-loop regions for the Bayesian analysis produced two topologies that are essentially the same. Inland clade I contained haplotypes consistent with other methods (BCAL05, RCAL01, TCGA03, BCAL01, MCAL01, OCFL03, WCFL04, BCAL04, JCFL01) as did inland clade II (SCFL01, LCFL01, OCFL04, WCFL01, WCFL02, OCFL06, WCFL02, OCFL05, and WCFL03). The beach clade as hypothesized by each topology was structurally the same. Posterior probability support was high and essentially the same between the topologies, however, the topology with *P. leucopus* and *P. gossypinus* as outgroups had slightly stronger support. The only haplotype that was not in agreement between the topologies was NIV17. With *P. leucopus* and *P. gossypinus* as outgroups, haplotype NIV17 branched from the basal node within the Florida peninsula clade.

However, with *keeni* as the outgroup, NIV17 was the only haplotype on a single branch. Posterior probabilities (PP) were generally higher for a given analysis than are bootstrap values (Huelsenbeck *et al.* 2002). Thus, posterior probability support is typically only considered strong at approximately 95%.

The total sequence analyses of maximum likelihood, maximum parsimony, and the Bayesian methods for phylogenetic analyses were largely in agreement concerning placement of haplotypes into clades. Comparing each region separately and combining the two regions for analyses using various methods also identified strikingly similar haplotype grouping. Minor differences among the analyses primarily involved the placement of single haplotypes. For instance, the unweighted MP analysis with *keeni* as the outgroup placed SCFL01 branching from the basal node in inland clade II. Haplotype SCFL01 was not placed in this position by any other MP analysis. However, this haplotype was placed in inland clade II in some of the ML analyses but with low bootstrap values suggesting that support for this placement was weak. Maximum parsimony analyses tended to leave haplotypes SCFL01, LCAL01, TCGA01, WCFL07, WCFL09, and NIV17 unresolved in a larger sense, but all of the analyses associate WCFL07 with WCFL08 and, separately, LCAL01 with TCGA01. These data supported the presence of three and possibly four lineages. The area of the fourth lineage (Florida peninsula), however, was poorly sampled because the intent of this study was to look for any similarities between beach forms from the Gulf Coast and Atlantic coasts of Florida.

The total sequence analyses indicated something of an unexpected outcome with respect to the relationship among the three *P. maniculatus* subspecies and their relationship to *P. polionotus*. Maximum likelihood analyses involving *P. m. pallescens*,

P. m. bairdii, and *P. m. sonoriensis* from cytochrome-b using *P. leucopus* as the outgroup and HKY + Γ , TVM+ Γ models of molecular evolution was unresolved. Concerning the three *maniculatus* subspecies, changing the outgroup to *P. keeni* using the HKY + Γ , and GTR + Γ models again left the relationship unresolved. However, ML analyses of the D-loop with *leucopus/gossypinus* and *keeni* as outgroups with substitution models HKY + I + Γ and HKY + I, respectively, indicated that *bairdii* split prior to the *pallescens/sonoriensis* split. Combining both gene regions and conducting a ML analyses produced two outcomes. With *P. leucopus* and *P. gossypinus* as outgroups and using the HKY + I + Γ model, the relationship between the three *maniculatus* subspecies was, again, unresolved. However, using *P. keeni* as the outgroup with the HKY + I + Γ model indicated that *bairdii* split prior to the *pallescens/sonoriensis* split.

Maximum parsimony (MP) strict-consensus trees were also used to investigate the relationship between the three *maniculatus* subspecies. Weighted and unweighted MP analyses of cytochrome-b using *leucopus* as the outgroup was unresolved. However, the same analyses with *keeni* as the outgroup indicated that *sonoriensis* split prior to the *pallescens/bairdii* split. Weighted and unweighted MP analyses of the D-loop with *leucopus* as the outgroup indicated *bairdii* split prior to the *pallescens/sonoriensis* split. Also, weighted and unweighted MP analyses of the D-loop with *keeni* as the outgroup suggested that *bairdii* split prior to a *pallescens/sonoriensis* split. However, combining the two gene regions in a weighted and unweighted analysis with *leucopus* as the outgroup leaves the relationship between the three unresolved. Weighted and unweighted MP analyses of the combined regions with *P. keeni* as the outgroup were also unresolved.

Finally, Bayesian 50% majority-rule consensus trees were used to investigate the relationship between the three *maniculatus* subspecies. Analysis of cytochrome-b using model GTR + Γ with *leucopus* as the outgroup shows that *pallescens* split prior to the *bairdii/sonoriensis* split. However, Bayesian analysis of cytochrome-b using model HKY + Γ and GTR + I with *keeni* as the outgroup was unresolved. Analyses of the D-loop using the model HKY + Γ + I with *leucopus/gossypinus* then *keeni* as the outgroup indicated a *bairdii* split prior to a *pallescens/sonoriensis* split. Combining the two gene regions within a Bayesian analysis using split models (cytochrome-b, HKY + Γ ; D-loop, HKY + Γ + I) with *leucopus* then *keeni* as outgroups and a 50% majority-rule consensus tree support the conclusion that *bairdii* split prior to a *pallescens/sonoriensis* split.

Nested Clade Analysis

Nested clade analysis were based on the parsimony network developed using an algorithm developed by Templeton *et al.* (1992). Prior to the nested clade analysis, fifty-five sequences consisting of 2449 nucleotides were analyzed in DNASP v4.0. This analysis identified 35 unique haplotypes. Theta (θ) estimated to be 0.01116, was then used to solve H in equation 1 of Templeton *et al.* (1992) ($H = 0.0290$). At the 5% level, this value indicated that the use of parsimony was justified for these data. For these data and assumptions, using a 95% statistical parsimony analysis, parsimony was exceeded for up to 21 mutational steps ($P_{21} = 0.9536$). However, the TCS generated parsimony cladogram contains ambiguities or two unresolved loops (Fig. 31). One single loop involves what is primarily a Florida peninsula clade. However, two haplotypes, one from central Alabama (LCAL01) and one from central Georgia (TCGA01), were placed within

this clade by the analysis. The other loop involved placement of a single Gulf Coast haplotype.

To resolve these ambiguities, three criterion based on predictions made by coalescence theory were used to discern more likely alternative solutions (Pfenninger & Posada 2002). Based primarily on geographic considerations, alternative parsimony connections labeled 1A, 1B, 1C, and 2 (Fig. 31) were broken. Loop 1A connects the Florida peninsula clade nearer to the basal haplotypes of the network. Loops 1B and 1C connect the disputed haplotypes nearer the tips of the network. Connections 1B and 1C were broken based on criteria 2 and 3 (Pfenninger & Posada 2002). The clade formed by haplotypes (MCFL76, MCFL77, WCFL08, WCFL09, WCFL10, NIV36, NIV17, LCAL01, LCAL01, and TCGA01) is unlikely to have evolved from within the Gulf Coastal beach clade. Leaving the clade connected to branch 1A as opposed to branch 1B or 1C seemed the most logical choice as it was more likely to have originated interior in the network rather than the interior of the beach clade. Also, given the amount of substitutions within the peninsular clade it was more likely to be an older clade. Thus, connections 1B and 1C that place a highly divergent clade within a less divergent clade from a different region seemed unlikely. The second loop (Connection 2) was broken based on criterion 3. The haplotype PEN02* was unlikely to have evolved within a clade from a different region. Therefore, connection 2 was broken on the assumption that this haplotype was most likely to have evolved within the clade from the same geographic region.

To be consistent with other analyses in this project, NCA was conducted both with and without haplotypes from the Florida peninsula. Also, with Florida peninsula

haplotypes removed, the analysis was conducted with haplotypes LCAL01 and TCGA01 placed in the network as suggested by statistical parsimony and branching manually placed from the basal node of the beach group as suggested by ML, MP, and Bayesian analyses. Thus, there were three separate NCA analyses conducted. One with haplotype placement as estimated by TCS (Model I), one with Florida peninsula haplotypes removed and again estimated by TCS (Model II), and one without Florida peninsula haplotypes and inland haplotypes LCAL01 and TCGA01 manually connected to a basal node of the beach clade (Model III). Within these three hypothetical topologies there were no significant associations between haplotypes and geographic distribution until the 2nd level (Table 3).

There was substantial agreement among the three models concerning several clades that showed a significant association of haplotypes within the geologic landscape. Clades that were the same between models may have different clade numbers; therefore, superscripting was used to indicate identical clades between models. Individually, model I indicated that clades 2-2¹, 3-3², 4-1³, 4-4⁴, 4-5⁵, 4-6⁶, 5-2, 5-3, and the total clade were significant. Biological explanations (Templeton 1998) include restricted gene flow with isolation by distance (2-2¹, 5-2), past fragmentation and/or long distance colonization (4-1³), contiguous range expansion (4-5⁵), allopatric fragmentation (4-6⁶), restricted gene flow with dispersal and with some long distance dispersal (total clade). Clades 3-3² and 4-4⁴ had inconclusive outcomes while clade 5-3 had no significant clade distances.

Model II, with Florida peninsula haplotypes removed and the LCAL01, LCAL02 and TCGA01 haplotypes with the inland group (per statistical parsimony), indicated that clades 2-2¹, 3-2², 4-1³, 4-3⁴, 4-4⁵, 4-5⁶, 5-1, 5-2, and the total clade were significant. The

chain of inference indicated restricted gene flow with isolation by distance (2-2¹), past fragmentation and/or long distance colonization (4-1³), contiguous range expansion (4-3⁴), and allopatric fragmentation (4-5⁶). Clades 3-2² and 4-3⁴ had inconclusive outcomes and clades 5-1, 5-2, and the total clade had no significant clade distances. Model III, with the Florida peninsula haplotypes removed and LCAL01, LCAL02, and TCGA01 manipulated to branch from a basal node of the beach clade indicated that clades 2-2¹, 3-2², 4-1³, 4-2⁴, 4-4⁵, 4-5⁶, 5-2, and the total clade were significant. The chain of inference identified a pattern consistent with restricted gene flow with isolation by distance (2-2¹), past fragmentation and/or long distance colonization (4-1³), contiguous range expansion (4-4⁵), and allopatric isolation (4-5⁶). Clades 3-2², 4-2⁴ had no conclusive outcome while clades 5-2 and the total clade had no significant clade distances.

Neutral evolution and demographic analysis

Overall, the phylogenetic analyses suggested the presence of at least three major clades within *P. polionotus*. Measures of genetic diversity within and between clades include: the number of polymorphic sites (S), the total number of mutations (Eta), haplotype diversity (Hd), nucleotide diversity (π), average number of nucleotide differences (k), number of haplotypes (h), and theta (θ). As expected, haplotype and nucleotide diversity decreased within groups when multiple samples were identical. The effect was most noticeable when sample size is small. The average number of nucleotide differences is much less influenced by the addition of identical samples and, within these data, may be a more reliable indicator of sequence variation among samples or groups. Table 2 gives estimates of diversity of both the data set containing *P. leucopus* and *P. gossypinus* as outgroups and the data set with *P. keeni* as the outgroup. An obvious

decline in diversity measures occurred when *P. leucopus* and *P. gossypinus* were removed. The group containing *P. keeni* and the three *maniculatus* subspecies is consistent with variation likely expected among closely related species. Both groups indicate more variation within the D-loop portion of the sequence. This was expected due to regions of the D-loop that are hypervariable.

Table 4 gives measures of diversity for clades derived from maximum likelihood phylogenetic analyses. Tables 5 - 7 show measures of diversity for 5th level clades for NCS models 1 - 3 respectively. The statistical parsimony network generated for the nested clade analysis (NCA) was similar to the phylogenetic analyses but did uniquely place some haplotypes. Haplotype diversity (Hd) and nucleotide diversity (π) were variable among the all clades and gene regions. Measures of diversity for cytochrome-b and the D-loop separately and combined produced generally predictable results. The D-loop region when compared with cytochrome-b gene region tended to be more diverse among all groups. Interestingly, a comparison of the beach clade and the two inland clades revealed that the D-loop π in the beach clade was significantly higher than either inland clade, however, inland clade I has a higher π within cytochrome-b than the beach clade. Nucleotide diversity within the D-loop of inland clade I was only slightly higher than π within cytochrome-b while in all other clades/groups it was approximately twice as high. For the complete fragment, the average number of pairwise differences was twice as high in the beach clade (12.28) as in inland clade II (6.47) and almost 1.5 times as high as in inland clade I (8.73). However, for cytochrome-b, the average number of pairwise differences for the beach clade was 3.70, inland clade I 3.83, and for inland clade II 1.03. Estimates of diversity for the beach clade were also calculated without the

haplotypes LCAL01, LCAL02, and TCGA01. These estimates for the total sequence, cytochrome-b, and the D-loop are 10.74, 2.98, and 7.16 respectively. Measures of diversity (Table 4) were also calculated for the entire *polionotus* group, the *polionotus* group (complete) without the Florida peninsula haplotypes (complete*).

The models analyzed using NCA resulted in seven 5th level clades. Measures of diversity were estimated for each clade (Tables 5 - 7). Not unexpectedly, the greatest amount of nucleotide diversity for cytochrome-b, D-loop, and the complete fragment was found within clade 5-2 of model one. This clade includes the haplotypes from the Florida peninsula. Florida peninsula haplotypes were removed in the analyses of models two and three. The haplotypes LCAL01, LCAL02, and TCGA01 are placed within the clade containing inland forms by statistical parsimony analysis resulting in model II. To be consistent with the phylogenetic analyses these haplotypes were placed on a branch extending from a basal node of the beach clade. In model II, measures of diversity are approximately 1.5 times higher in clade 5-1, which contains inland haplotypes along with LCAL01, LCAL02, and TCGA01. Model three was similar to model two, however, the haplotypes LCAL01, LCAL02, and TCGA01 are within clade 5-2 containing beach haplotypes. In model three clade 5-1 measures of diversity are higher, however, this model tends to decrease the difference.

Neutrality tests of cytochrome-b and the D-loop were conducted separately and as a complete sequence. Interpretations of the neutrality tests are influenced by the measuring statistic and by DNA region. If a gene under selection is linked to a neutral site the value of D could be affected (Tajima 1989). Neutrality statistics were calculated using DNASP v4.0 (Rozas *et al.* 2003) and were calculated using the number of

segregating sites. Clades for demographic analyses were chosen based on the outcome of the ML, Bayesian, and MP phylogenetic analyses along with the nested clade analysis. These clades were analyzed using various neutrality tests and are comprised of the following haplotypes, inland clade I, BCAL05, RCAL01, TCGA03, BCAL04, JCFL01, BCAL01, MCAL01, OCFL03, and WCFL04; inland clade II, SCFL01, LCFL01, OCFL04, WCFL01, WCFL02, OCFL06, WCFL01, OCFL05, WCFL03; beach clade, LCAL01, TCGA01, PEN05, AMM01, LEU08, OCFL01, WCFL01, WCFL06, OCFL07, JCFL03, CCFL01, TRI07, PEN02*, ALL02**, ALL05, and ALL02*. Because haplotypes LCAL01 and TCGA01 were found in central Alabama and central Georgia respectively, analyses of the beach clade was conducted both with and without these haplotypes (clade beach and clade beach* respectively). As expected, outcomes of neutrality analyses varied by gene region and statistic. The Cytochrome-b region tended to produce more negative values with the d-loop region being less negative.

Fu & Li's D and Fu & Li's F tests were conducted twice, once using *P. maniculatus* as an outgroup (Table 8) and once using *polionotus* haplotypes from other clades as outgroups (Table 9). With *maniculatus* as the outgroup, none of the tests produced significant results. However, again, all values were negative with one exception, Fu & Li's D test for the D-loop region of inland clade II. Fu & Li's D and F tests on *polionotus* groups with *polionotus* haplotypes as the outgroup were also not significant, however, testing the beach clade with inland clade I as the outgroup did approach significance. McDonald-Kreitman neutrality tests were conducted for cytochrome-b region only (Table 8). These tests were conducted using *maniculatus* for between species ratio estimates and clades or groups of *polionotus* as populations for

nonsynonymous to synonymous ratio estimate. The results of Fu & Li's D* and Fu & Li's F* tests of *polionotus* clades were, like the prior analysis, negative values (Table 10). While the tests were not significant, the tests using all available *polionotus* haplotypes and all regions (minus Fu & Li's D* for the D-loop region) produced near significant values ($0.1 > P > 0.05$). Without the four haplotypes from the Florida peninsula clade Fu & Li's F* and D* still approached significance when testing cytochrome-b ($0.10 > P > 0.05$). Tajima's D was not found to be significant in any analyses (Table 10). Use of the complete *P. polionotus* data set produced the most negative value of Tajima's D. However, Tajima's D statistic for clade beach produced the most negative values relative to all other clades minus the complete *polionotus* analysis. There are multiple ways to interpret neutrality statistics. Nevertheless, along with other evidence, the neutrality tests here suggest that *polionotus*, or clades of *polionotus*, have undergone demographic expansion.

Six clades or groups of haplotypes were analyzed using program FLUCTUATE (Table 11). All available *polionotus* haplotypes were analyzed (complete). Florida peninsula haplotypes were removed and analyzed (complete*). Inland clades I and II were analyzed along with clades beach and beach* (haplotypes LCA01 and TCGA01 removed). Each clade or group that contained the Florida peninsula haplotypes was analyzed both with and without these haplotypes. Also, the beach clade was analyzed with and without haplotypes LCAL01 and TCGA01. An asterisk (*) was used to indicate groups or clades where haplotypes have been removed. The results of the analyses were not significantly changed by removal of the haplotypes. To determine N_e , a substitution rate of 1.1×10^{-8} substitutions per site per year was calculated from the combined data.

The analysis of the complete or complete* set of *P. polionotus* haplotypes indicated that the N_e estimate without growth (2 657 062) was significantly different from the N_e of the growth model (5 120 272). Effective population size predictions for the beach (constant 768 109, growth 2 674 778) and beach* clades (constant 549 775, growth 1 729 500) were also significantly different. Other clades analyzed using FLUCTUATE included inland clade I (constant 326 013; growth 505 056) and inland clade II (constant 164 478; growth 158 444), clade 5-1 (constant 830 388; growth 1 176 722) and 5-1* (constant 527 952; growth 724 000). These clades were not significantly different in their constant or growth estimates of N_e (values). Inland clade II was the only clade with an estimated negative growth rate (values).

Molecular clock

Comparisons of percent divergence of the 1137 bp cytochrome-b gene between *P. p. ammobates* (AMM01) and *P. m. sonoriensis*, *P. m. bairdii*, and *P. m. pallescens* revealed 52 differences (4.57%), 49 differences (4.31%), and 45 differences (3.96%) respectively. *Peromyscus polionotus ammobates* was also compared to *P. leucopus* (111 differences; 9.76%) and *P. gossypinus* (113 differences; 9.94%). Estimates of percent divergence between the subspecies of *maniculatus* were, *bairdii* and *pallescens* with 13 differences for 1.14%, *pallescens* and *sonoriensis* with 18 differences for 1.58%, and *bairdii* and *sonoriensis* with 17 differences for 1.50%. A comparison between *P. leucopus* and *P. gossypinus* produced 57 differences for 5.01% divergence estimate. Comparison between *P. m. bairdii* and *P. leucopus* and *P. m. sonoriensis* and *P. gossypinus* revealed 102 differences for 8.97% divergence and 108 differences for 9.50% divergence respectively. Comparisons between *P. keeni* and the following, *P. p.*

ammobates, *P. m. sonoriensis*, and *P. leucopus* revealed 56 differences for 4.93% divergence, 54 differences for 4.75% divergence and 102 differences for 8.97% divergence respectively. Finally, divergence within *P. polionotus* was estimated using a haplotype from the beach clade (*P. p. ammobates*, AMM01) and a haplotype from each of the hypothesized clades, (inland clade I, inland clade II, and the Florida peninsula), as well as, a haplotype from the beach clade. Haplotypes used for comparisons were AMM01 to, NIV17, JCFL01, WCFL02, and PEN05 producing estimates of 5 differences for 0.44%, 8 differences for 0.70%, 5 differences for 0.44%, and 2 differences for 0.18% respectively.

Likelihood ratio tests (Felsenstein 1981) were conducted to determine if substitution rates were consistent among lineages within different phylogenies. Likelihood ratio tests (LRT) tests ($2\Delta\ell$) were conducted for all four nucleotide substitution models used in the analysis of cytochrome-b, the two models used to conduct the D-loop analyses, and the two models used to conduct the analysis with the complete sequence. For cytochrome-b with *P. keeni* as the outgroup under the HKY + Γ model, log likelihood values with and without a clock assumption were 2427.31 and 2442.32 respectively. Thus, the LRT test [$2(2442.32 - 2427.31) = 30.02$, $df = 40$, and $P = 0.8620$] indicated that the two models are not significantly different. Cytochrome-b data with *keeni* as the outgroup under the GTR + I model with and without the clock produced log likelihood values of 2420.62 and 2435.66 respectively. Here $2(2435.66 - 2420.62) = 30.08$, $df = 40$, and $P = 0.8729$ indicating the two models are not significantly different. Cytochrome-b with *P. leucopus* as the outgroup under the TVM + Γ model with and without a clock assumption produced log likelihood values of 2985.62 and 3001.73

respectively, then, $2(3001.73 - 2985.62) = 32.22$, $df = 42$, and $P = 0.8620$. Cytochrome-b with *leucopus* as the outgroup under the HKY + Γ model with and without the clock assumption produced log likelihood values of 2994.17 and 3010.22 respectively, then $2(3010.22 - 2994.17) = 32.10$, $df = 42$, and $P = 0.8653$.

The D-loop data set with *leucopus* as the outgroup under the HKY + I + Γ model with and without the assumption of a clock produced log likelihood values of 3063.81 and 3091.98 respectively, then, $2(3091.98 - 3063.81) = 56.35$, $df = 43$, and $P = 0.0833$. The D-loop with *keeni* as the outgroup under the HKY + I model with and without the clock assumption produced log likelihood values of 2455.72 and 2478.70 respectively, then, $2(2478.70 - 2455.72) = 45.96$, $df = 41$, and $P = 0.2742$. Combining cytochrome-b and the D-loop regions and using the HKY+ I + Γ model with *leucopus* as the outgroup produced log likelihood values of 6822.79 and 6845.90 respectively, then, $2(6845.90 - 6822.79) = 46.21$, $df = 42$, and $P = 0.3025$. The combined data set with *keeni* as the outgroup with the HKY + I + Γ model with and without the clock assumption produced log likelihood values of 5555.24 and 5572.78 respectively, then, $2(5572.78 - 5555.24) = 35.08$, $df = 40$, and $P = 0.6911$. Based on log likelihood ratio tests at the 5% level the molecular clock assumption was not rejected under any scenario.

Analysis of the complete sequence with *P. keeni* as the outgroup produced an estimated substitution rate of 1.8×10^{-8} substitutions per site per year. This rate was obtained by adding branch lengths from the *maniculatus/polionotus* split (t1; Fig. 32) to each tip then dividing by the estimated age of the sinkhole. Estimated substitution rates ranged from 1.3×10^{-8} to 2.4×10^{-8} . However, the two predominate estimates were 1.4×10^{-8} and 2.2×10^{-8} . Thus, the two most frequent estimates were averaged obtaining

1.8×10^{-8} . This rate was then used to convert other distances into time (Fig. 32). Times to nodes were estimated by calculating the distance from a node to the branch tip for each branch that extended from that node. These distance values were converted into time estimates to allow calculation of summary statistics. For example, the node involving the divergence of extant forms of *P. polionotus* (t1; Fig. 32) was estimated at $306\,000 \pm 48\,000$ YBP. For comparison, time to nodes involving the three *maniculatus* subspecies were also estimated under the assumption of the same substitution rate. The split of *bairdii* from the other two *maniculatus* subspecies was estimated at $430\,000 \pm 144\,534$ YBP. The constant-rate model tends to overestimate small distances (Yang 1996). Thus, when possible, conservative estimates of parameters were used in an attempt to minimize overestimating times. Using the equation 5.12 from Nei (1987) $r = K/(2T)$, a substitution rate of 1.1×10^{-8} per site per year was obtained. This estimate was similar to the previous estimate but was not used in favor of the more conservative estimated substitution rate of 1.8×10^{-8} .

Discussion

Divergence of polionotus/maniculatus

The multiple phylogenetic analyses used here indicate that *P. polionotus* forms a reciprocally monophyletic clade with respect to *P. maniculatus*. These data also indicate a much older *maniculatus/polionotus* split than was anticipated. While Blair (1950) and Bowen (1968) offered opposing theories concerning the ancestral lineage of *P. polionotus*, both inferred a relatively recent divergence ($< 500\,000$ YBP) of *polionotus* from a *maniculatus* stock. However, based on the results produced in this study it is unlikely that the ancestral lineage of *polionotus* is one of the three *maniculatus*

subspecies included in this analysis (*bairdii*, *pallescens*, *sonoriensis*). Instead, the most likely scenario is a *maniculatus/polionotus* split that preceded the divergence of the *maniculatus* subspecies *sonoriensis*, *pallescens*, and *bairdii*. *Avise et al.* (1983) analyzed mtDNA from 82 *maniculatus* and *polionotus* individuals collected across the United States portion of their range and concluded that their data best fit a model with *polionotus* as a monophyletic group with respect to *maniculatus* and *maniculatus* as a paraphyletic group with respect to *polionotus*. Here, however, results from this study indicate both *polionotus* and *maniculatus* as monophyletic groups with respect to one another. However, there were only three subspecies of *maniculatus* represented within my analysis. From these data, it could not be accurately determined if the ancestral *polionotus* stock entered the Southeastern US through a northern (Bowen 1968) or western route (Blair 1950). The phylogenies produced from different methods do not agree concerning a western or northern route for pre-*polionotus* stock. *Avise et al.* (1983) conducted a restriction enzyme analysis of mtDNA that demonstrated the *polionotus* divergence from *maniculatus* might be more difficult to elucidate than had previously been thought. In fact, their data suggested *polionotus* might be most similar to a *maniculatus* form presently found in Southern California. If the earlier divergence of *maniculatus/polionotus* stock is accurate, it may explain why the speciation event is difficult to characterize.

I hypothesized that the ancestral lineage of *P. polionotus* became isolated in the Southeastern US approximately two million years ago. Under this scenario, isolation of the ancestral form of *polionotus* may have occurred near the time of the Pliocene/Pleistocene border as temperature changes shifted vegetation zones. Again, this

represents a longer period than most previous researches had hypothesized. However, Avise *et al.* (1983) used a *maniculatus* form from Southern California and estimated a *polionotus/maniculatus* split at 1.5 million years. My data support their time and even conclude that it was likely to have occurred earlier. This conclusion is supported by recent fossil evidence of (Ruez 2001) dating *polionotus* to at least the late Pliocene or early Pleistocene. The degree of divergence of mtDNA between *maniculatus* and *polionotus* indicated an early split as well. While realizing that 2% divergence per million years for mammalian mitochondrial DNA (Brown *et al.* 1979) may be a limited estimate, it does seemingly fit these data. Percent divergence between *polionotus* and the three subspecies of *maniculatus* used within this analysis estimate a separation date of approximately two MYB.

Phylogenetic analysis

The three phylogenetic methods utilized in my study support the presence of at least three major clades with extant *P. polionotus*. These clades form polytomy in most topologies. In the present geologic state of the region there is not an obvious geographical feature that physically separates the clades. Molecular data suggest the three clades last shared a common ancestor approximately 300 000 YBP. Assuming a *polionotus/maniculatus* split two million years ago as fossil and molecular data suggest, it is intriguing that the divergence of extant forms would date to only 300 000 YBP. Such a date would suggest that extant lineages of *polionotus* began diverging during a pre-Illinoian glacial period of the Pleistocene Epoch. Interestingly, the initial divergence within the beach clade (243 000 YBP) appears to have occurred prior to divergence within the two inland clades (Fig. 32). However, the estimates of initial divergence

within the three primary clades are all within the same confidence intervals. Interval t5 within the beach clade and interval t6 within inland clade II are approximately the same age and interval t7 within inland clade I occurs approximately 63 000 years ago.

It is always difficult to determine the precise cause(s) that lead to divergence and cladogenesis within a taxonomic assemblage. Factors that have influenced between and within clade variation since divergence are also difficult to elucidate. However, climatic oscillations have clearly played a role within *P. polionotus*. If *P. polionotus* as a species has been present in the southeastern United States for the entire Pleistocene, the extant major lineage splits must be relatively recent. Thus, indicating either a long period of relative stasis or the loss of lineages that may have diverged prior to the last 300 000 years. A possible explanation for this lineage pattern is the cyclical nature of climatic phenomenon and its associated changes on the landscape. The pattern of lineage divergence observed within *P. polionotus* here is similar to other species whose range is limited to the southeastern United States and likely to have been driven by episodic climatic events that cyclically isolated lineages (Avice 2000). However, these same events may also isolate lineages in substandard habitat eventually leading to their extinction. Thus, while climatic cycles may be a principle factor isolating lineages leading to their divergence, levels of variation in these cycles (frequency, magnitude, timing) may also act to remove variant lineages thereby reducing variation and divergence within the species (i. e. lineage sorting). Traditionally, effects of Pleistocene climatic oscillations were generally characterized at the species level. However, contemporary genetics analyses have provided insight into genetic structure of species that had not been possible before. Climatic factors that influence species do so through

their effects on genetic lineages that comprise the species. Methods of phylogeographic analysis offer the ability to evaluate historical effects and their relationship to extant lineages. This is an important advance because the present lineages that comprise a species and their distribution have both a historical and contemporary component.

Haplotypes included in this analysis were primarily from the Florida panhandle region and constitute three primary lineages that form two inland clades and a beach clade. The geographic range of the three clades is overlapping. In fact, the Florida panhandle appears to be an area where haplotypes from the three clades integrate. The Freeport, Florida site, centrally located in the panhandle, was the only location where haplotypes from each clade were found. However, haplotypes from two different clades were found in several of the same inland locations. Repeatedly, from inland sites, haplotypes from different clades were found within the same burrow. Also, in some locations haplotypes collected in 1988 were still present after 13 years. There are two likely causes for this area of geographic concurrence, either natural dispersal and/or human mediated dispersal. Over the last 200 years, cultivation of fields and installation of railroad tracks, roads and power lines has almost certainly influenced the dispersal patterns of mainland *P. polionotus*. In fact, disturbed sites such as these are principle locations for obtaining samples and indeed account for the common name “oldfield mouse” (Hall 1981). Unfortunately, it is difficult to determine the degree to which dispersal of haplotypes was natural or human mediated. Within beach subspecies, however, populations appear to be comprised of a single haplotype. In fact, the following beach subspecies, *ammobates*, *trissyllepsis*, *leucocephalus*, and *peninsularis* are each comprised of a single different haplotype. An exception to this was a possible single

nucleotide substitution within the *ammobates* population. However, this substitution was present in only one individual and could easily be a sequencing artifact.

The subspecies *allophrys* was comprised of at least two and possibly three haplotypes. However, these haplotypes are found in populations that are now isolated from one another due to human development of the beaches. The *P. p. allophrys* subspecies appears to be the only beach subspecies that possesses multiple, extant haplotypes. Historically, it is likely that some level of gene flow did occur between the two, and possibly three, *allophrys* populations. The historical range of *allophrys* extended from Destin, Florida (Moreno Point) east to Shell Island, Florida and possibly as far east as Port St. Joe, Florida (Fig. 33). This length of beach was likely occupied by *polionotus (allophrys)* populations that were semi-isolated by drainages. The third haplotype placed within the *P. p. allophrys* subspecies group by multiple phylogenetic methods is from an extinct population (Crooked Island, FL). Crooked Island, Florida constitutes a portion of the described range of *P. p. peninsularis*. Bowen, (1968) delineated the subspecies distribution within the Gulf Coastal region based on breeding experiments and pelage reflectance values. His designation of the Crooked Island population, now a section of Tyndall Air Force Base, Florida, as *peninsularis* instead of *allophrys* now appears to have been incorrect. Regardless, during the mid 1990's *P. p. peninsularis* was determined to be extirpated from the Crooked Island, Florida portion of its range. The United States Fish and Wildlife Service (USFWS) determined translocation of individuals from the remaining *peninsularis* population on Cape San Blas, Florida to Crooked Island, Florida was an appropriate action. Thus, two translocations were conducted, and, within a few years, the Crooked Island population

multiplied and dispersed across the length of the area. The translocation effort appeared to be a success. However, prior to extirpation, tissue from individuals of the original Crooked Island population had been obtained. Therefore, that population was represented in these analyses. Unexpectedly, each of the three methods of phylogenetic analyses placed the original Crooked Island haplotypes within the *allophrys* group rather than with the *peninsularis* haplotype (Fig. 11, 23, 30). In fact, my analyses indicated that the Crooked Island haplotype shares a more recent ancestor with the Topsail Hill *allophrys* haplotype than the Topsail Hill haplotype shares with the Shell Island *allophrys* haplotype. This example highlights the necessity of genetic analyses prior to translocation of individuals between populations.

A possible fourth clade comprised of Florida peninsula haplotypes along with two haplotypes from near Crawfordville, Florida (south of Tallahassee, Florida) does not hold up in the majority of Bayesian, ML and MP analyses but was present in the statistical parsimony network. The Florida peninsula was not intended to be an area extensively represented within this study. It was intended to provide Atlantic Coastal haplotypes for comparison to Gulf Coastal haplotypes, and, possibly, an outgroup for Gulf Coastal haplotypes. The samples from the Florida peninsula are quite diverged relative to the divergence within *polionotus*. Selander *et al.* (1971) did find the Florida peninsula to possess the greatest amount of protein polymorphism. They also showed that insular populations of the Atlantic coast possessed the same amount of protein polymorphism as inland populations of the Florida panhandle and more than inland populations of Georgia and South Carolina. This is compatible with the findings here that show the *P. p. niveiventris*, a beach subspecies from the Cape Canaveral Air Force

Station, with at least two haplotypes within the population. *Peromyscus polionotus niveiventris* represents a large population that may be relatively undisturbed by human activities.

Nested clade analysis

The statistical parsimony network developed through NCA uniquely placed some haplotypes. Principally, however, it supported the phylogenies developed through Bayesian, ML, and MP methods. However, the results of NCA are based on a single network that was only one of multiple possibilities. The application of NCA to my data did allow the testing of hypotheses relative to geographic placement of haplotypes to help clarify the evolutionary history of *P. polionotus*. There were significant geographic associations of haplotypes within each model (Table 3). Some significant associations produced inconclusive outcomes and some P-values were significant but had no significant clade distances. Within all three models the first significant pattern of haplotype distribution is restricted gene flow with isolation by distance (clade 2-2¹). Haplotypes within this clade are found in the Florida panhandle, central and southern Alabama. Clade 2-2¹ was composed of haplotypes from inland clade I (MCAL01, BCAL01, BCAL03, OCFL03, WCFL04, WCFL05, JCFL01, JCFL02, and BCAL04). The second significant association common to the three models (clade 4-1³) was the inference of past fragmentation and/or long distance colonization involving the Florida panhandle and a single haplotype from the northern portion of the Florida peninsula. Another significant association (model I, clade 4-5⁵; model II and III clade 4-4⁵) infers contiguous range expansion as the biological explanation for haplotype placement. Clade 4-5⁵ from model I and the corresponding clade from models II and III, 4-4⁵ contain three

of the five Gulf Coast beach mice subspecies (*peninsularis*, *allophrys*, *leucocephalus*) and a single haplotype found in the central Florida panhandle. The final significant association common to the three models (model I clade 4-6⁶; model II and III clade 4-5⁶) implies allopatric fragmentation as the biological explanation and involves two of the beach subspecies and a group of haplotypes found within the Florida panhandle. Model I has two other significant patterns that produce biological scenarios for their causes. First, restricted gene flow with isolation by distance involving the Florida peninsula, central Alabama, and central Georgia (clade 5-2). The placement of haplotypes LCAL01, LCAL02, and TCGA01 within the Florida peninsula clade was unique to the statistical parsimony network. Model I was also significant at the total clade level. The biological scenario inferred for the geographical association of haplotypes is restricted gene flow with dispersal with some long distance dispersal. Model II and III do not have significant clade distance at the total clade level.

With respect to inland clade II (clade 4-1³), application of Templeton's criterion was most consistent with the hypothesis that dispersal has been into the Florida panhandle from the Florida peninsula. The dispersal direction for inland clade I is more difficult to determine. Branching patterns indicate two possible dispersal patterns of haplotypes from inland clade I. Dispersal was either from central Georgia or central Alabama into the Florida panhandle or within the south Alabama Florida panhandle region into central Alabama and central Georgia. The beach clade (model I, clade 5-3) supports dispersal was from central Alabama and central Georgia into the Florida panhandle. Although, removing haplotypes LCAL01, LCAL02 and TCGA01 from the beach clade forms a dispersal pattern that more closely reflects a beach clade that

originated in the present range of *P. p. allophrys*. However, *P. p. allophrys* appears to be older than the dune system it currently occupies, thus, a model suggesting the beach clade originated from that location is inconsistent. This demonstrates the difficulty of determining dispersal patterns when suitable habitat may be ephemeral due to climatic oscillations that cause haplotypes to make geographical shifts.

Neutral evolution and demographic analyses

Analysis of genetic variation within and between the three hypothesized clades of *P. polionotus* revealed the highest level of mtDNA variation as being within the beach clade. However, variation of cytochrome-b was approximately the same or slightly higher within inland clade I. Selander *et al.* (1971) found insular or beach populations to be monomorphic for most of the proteins they analyzed while inland populations tended to be heterozygous. However, they did find the situation reversed for some loci. Using mtDNA, the pattern of variation was essentially the same with beach populations being monomorphic and inland populations being heterozygous. However, if beach populations form a unique clade, variation within the clade is greater or at least equal to inland populations of the Florida panhandle region. Under this scenario the collective beach clade has the most variation but, viewed as single populations, the beach populations individually contain the least amount of variation. Each beach population appears to contain a single haplotype but when all the beach populations clade together, along with some inland haplotypes, it actually forms a diverse, growing population segment that may be the most dynamic segment of *polionotus* within the Florida panhandle region. In fact, if the entire population of the Florida panhandle region is growing as these data suggest, it appears to be predominately the beach clade driving the

expansion. Historical demographic analyses of each clade indicate the beach clade has been growing while the two inland clades appear to have been stationary over time. The FLUCTUATE growth rate (g) and theta (θ) values tend to be biased upward (Kuhner *et al.* 1998). However, given this, the estimates of effective population size are seemingly out of proportion with the amount of available habitat and the manner in which beach mice utilize available habitat. Even if the beach clade has not been growing the estimated effective population size is very large (Table 11). In fact, it is unlikely that the amount of historically available beach habitat could support such numbers.

Estimated divergence times

The mtDNA data consistently support the conclusion that three extant clades diverged approximately 300 000 YBP. Within clade divergence, however, does not appear to have occurred for approximately another 50 000 years, an effect possibly due to lineage sorting. Branching patterns of the topologies suggest that approximately 300 000 YBP, following an initial dispersal event, the three clades diverged in allopatry possibly occupying three refugia in southeastern North America. Dispersal might have been into the Florida peninsula from the panhandle or more interior regions of Alabama or Georgia. Contrarily, however, dispersal possibly occurred from the Florida panhandle into the interior and along the Gulf Coast. However dispersal occurred, it appears that extant genetic variation within *P. polionotus* arose from a single lineage over the last 300 000 years. The data are, however, inconclusive with respect to the location of a possible refugia. According to Delcourt & Delcourt (1981), at the last glacial maximum (~18 000 YBP) the Florida peninsula was primarily sand dune, scrub habitat. This habitat type could have served as refugia for *P. polionotus* during an earlier glacial maximum

approximately 300 000 YBP (Petit *et al.* 1999). Such a hypothesis is consistent with the findings of Selander *et al.* (1971) who reported protein polymorphism was highest in the Florida peninsula. Cain (1944) listed thirteen criteria that could be used in conjunction to indicate a center of origin. One criterion was the greatest amount of differentiation (i. e. number of species), however, taken here as the greatest amount of genetic variation, which, within *P. polionotus* is found in the Florida peninsula.

Comparisons among a priori hypotheses

Peromyscus polionotus was generally believed to be a young species having evolved after being isolated in the southeastern United States during a mid to late Pleistocene glacial cycle. However, the data presented here along with data from Avise *et al.* (1983) and recent fossil evidence (Ruez 2001) supports a conclusion that *P. polionotus* is far older and has likely been isolated in the southeastern United States since the late Pliocene or early Pleistocene. Correlated with this contention is the difficulty of determining which form of *maniculatus* that *polionotus* might have evolved from. Regardless of the *maniculatus/polionotus* split, the divergence among extent clades of *polionotus* probably occurred around 300 000 YBP. This is a relatively recent split in comparison to the estimated *maniculatus/polionotus* split and may be due to glacial cycles and how they effect a small mammal within a geographically limited region and that is restricted to open, sandy habitat. Organisms in the southeastern United States, limited in southward movement by the Gulf of Mexico, may have experienced a compression or packing effect controlled by the duration, rate and period of glacial cycles. In other words, organisms might have been isolated into single populations from which a solitary lineage emerged as the source of present genetic variation.

Bowen's model (1968) (the recurrent invasion hypothesis), contends that extant beach forms are the result of recent colonization events (< 10 000 YBP). As the water level of the Gulf of Mexico began to stabilize, coastal dunes and barrier islands were created. According to Bowen (1968), inland forms colonized these dune systems and then differentiated due to distinct selection pressures associated with the beach habitat. Bowen postulated both recent and repeated invasion of the dune systems by inland forms and contended that gene flow occurred in both a north/south and east/west pattern. However, the data presented here were not consistent with Bowen's model of gene flow involving the Gulf Coastal region of Florida and Alabama. In fact, my data strongly support a conclusion that beach subspecies are not the result of recent and repeated colonization events of the beach by inland forms. My analyses indicate that present day *polionotus* populating shorelines and barrier islands of the Gulf Coast form a monophyletic clade that is significantly older than the dunes they now inhabit. Thus, beach forms must have existed prior to the formation of current dune systems and shorelines. Based on the new findings, I propose an alternative hypothesis to explain the origin of the Gulf coastal forms. I refer to this hypothesis as the Shoreline-Tracking Hypothesis. Under this hypothesis, beach forms, already diverged from inland forms, were able to track the shoreline as the water of the Gulf of Mexico rose due to melting glaciers. This hypothesis explains why haplotypes are older than their habitat and infers that forms evolving under the selection pressures of a beach habitat were in existence prior to the formation of the present coastal strand and barrier islands.

A few inland haplotypes were placed in the beach clade, which suggests that gene flow, while limited, occurred. However, Bowen (1969) and Sumner (1929) disagreed

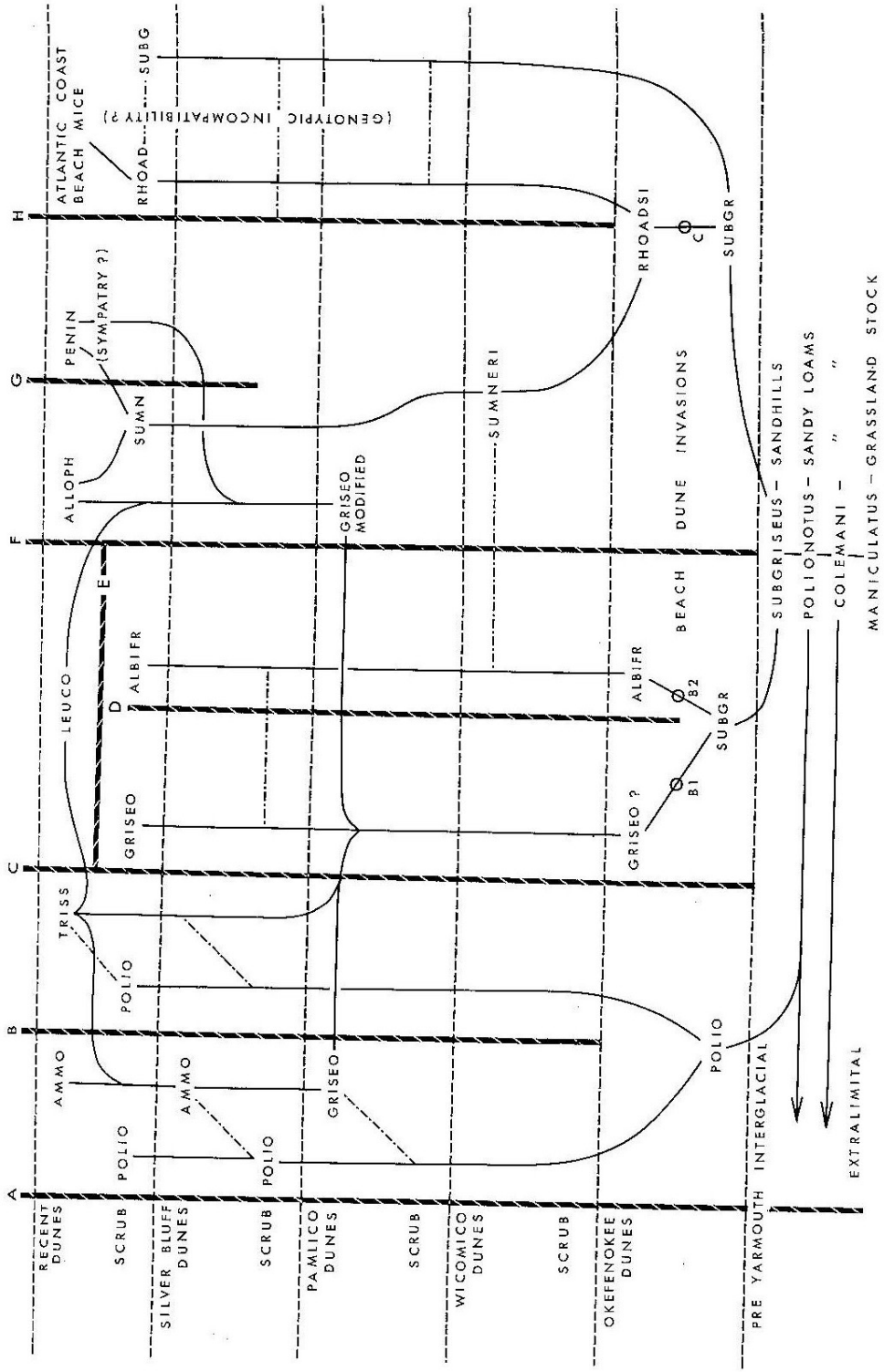
over the direction of gene flow. Placement of inland haplotypes within the beach clade (Fig. 21, Fig. 29), by some analyses, is consistent with the route of gene flow as Sumner hypothesized. However, while it does appear that gene flow has occurred between inland and beach clades it was probably not a recent event ($< 10\ 000$ YBP). On a larger geographic scale, nested clade analysis indicated that gene flow among major clades has likely been both into and out of the Florida panhandle. Given the limitations of my geographic collection sites, I was unable to further explore gene flow on a range wide geographic scale.

Conclusions

The application of multiple types of analyses that are designed to aid our understanding of evolutionary events revealed unexpected results for *P. polionotus*. In doing so, they provided a greater understanding of how the effects of Pleistocene glacial cycles have effected the evolution of a small, regionally isolated mammal that is restricted to a specific habitat type. Applying methods of phylogenetic analyses, nested clade analysis, neutrality tests and methods designed to estimate divergence times among diverse forms revealed these new insights. Using these analyses, I have shown that the evolutionary history of *P. polionotus* has in fact been quite complex. These data indicate *P. polionotus* as a monophyletic group that has probably been evolving in the southeastern United States for the entire Pleistocene. Also, there appear to be three major clades represented in the Gulf Coastal region of Florida and Alabama. Genetic data indicated that the clades diverged prior to the last glacial maximum ($\sim 18\ 000$ YBP) and possibly as far back as the prior glacial maximum ($\sim 120\ 000$ YBP). Presently the clades are not geographically isolated from one another and in fact do appear to integrate.

However isolated coastal populations appear to consist of a single mitochondrial haplotype, however, these populations form a clade that possesses the greatest amount of genetic variation based on these data. The three clades established here consist of two inland clades and a beach clade. While more than one geographic model was possible, my results were most consistent with the idea that inland clade I and the beach clade originated within the central Alabama/Georgia region while inland clade II originated within the Florida peninsula. Very importantly, beach forms that comprise the beach clade are clearly far older than had previously been hypothesized. This is significant because it refutes Bowen's (1968) hypothesis that extant beach forms recently (< 10 000 YBP) diverged from inland colonizers. Insular populations of *P. polionotus* comprise a unique and complex clade that forms an important segment of the regional population. In fact, extant beach forms represent lineages that have been evolving in a far different pattern than previously described. I hypothesize that beach lineages are older than the present dune system and formerly inhabited an area that is currently covered by the Gulf of Mexico. These conclusions and insights were gained through complementary genetic analyses that illustrate how genetic data can be used to disentangle past and present population processes to gain some understanding of current genetic structure within a population.

Fig. 1 Bowen's (1968) proposed evolutionary sequence of Gulf Coastal and Atlantic forms of *Peromyscus polionotus*. Broken diagonal lines indicate major barriers that likely limited gene flow. Bowen's model hypothesized recent, multiple invasions of the beach by inland forms and gene flow between beach populations.



SUBGRISEUS - SANDHILLS
 POLIONOTUS - SANDY LOAMS
 COLEMANI - "
 MANICULATUS - GRASSLAND STOCK

Fig. 2 Tissue samples of *Peromyscus polionotus* for these analyses were collected in Florida, Georgia and Alabama. Inland individuals are identified by the county and state they were obtained. The first three letters of their subspecific designation identify Beach subspecies.

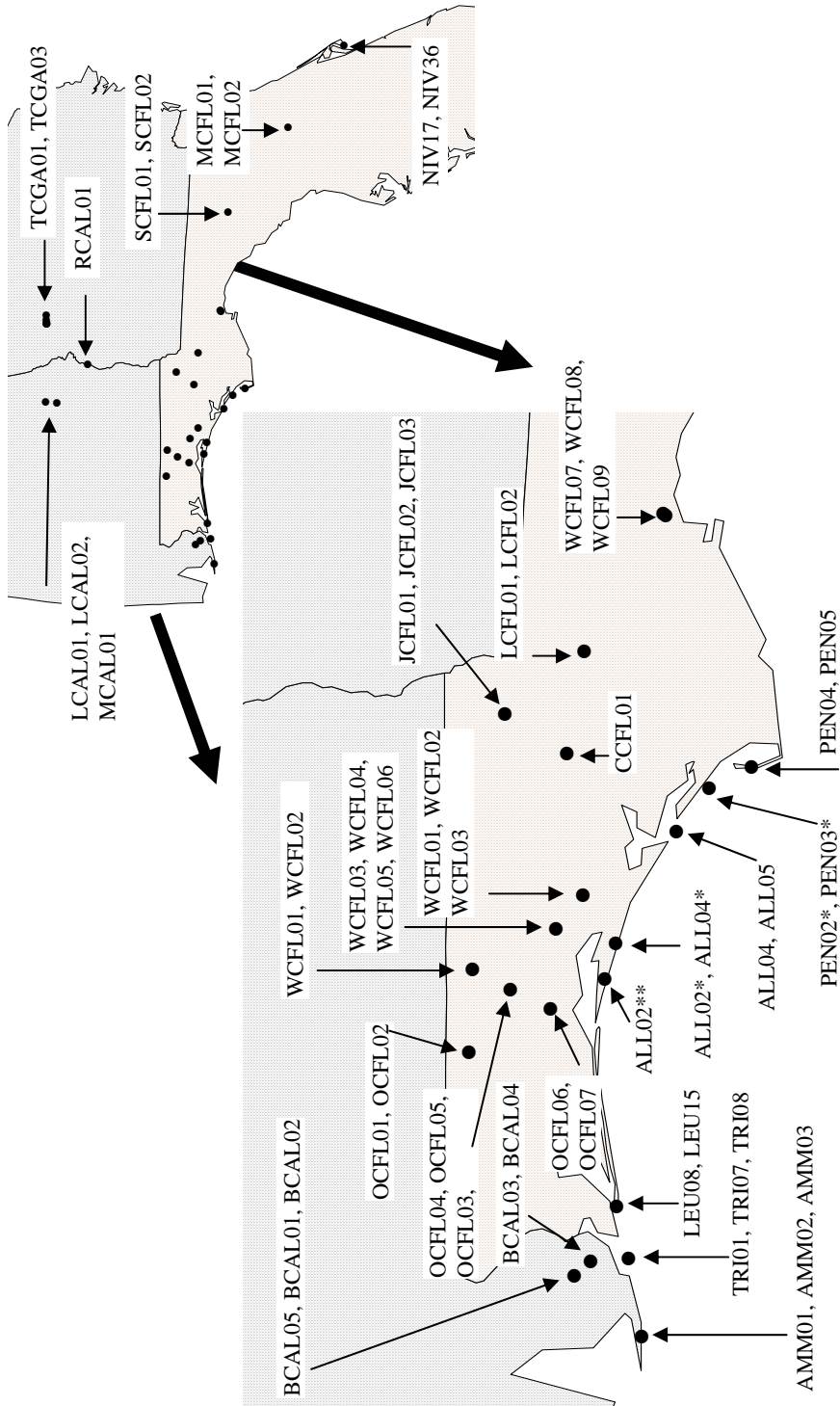


Fig. 3 Diagram depicting the section of mtDNA that was sequenced and placement of the insert found in *Peromyscus polionotus* but not found in the other *Peromyscus* used in this study.

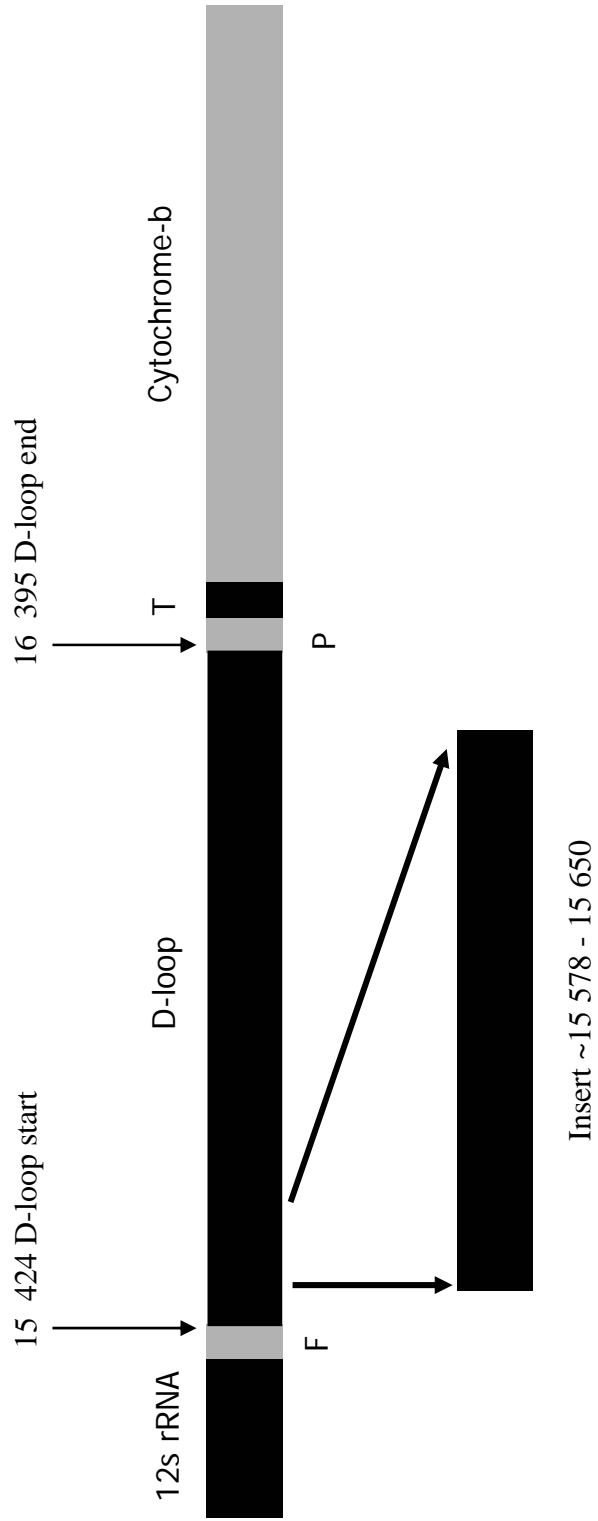


Fig. 4 Maximum likelihood topology using the cytochrome-b region and model HKY + Γ with outgroup *Peromyscus leucopus*. Model selection was based on log likelihood score. Numbers above branches are bootstrap values.

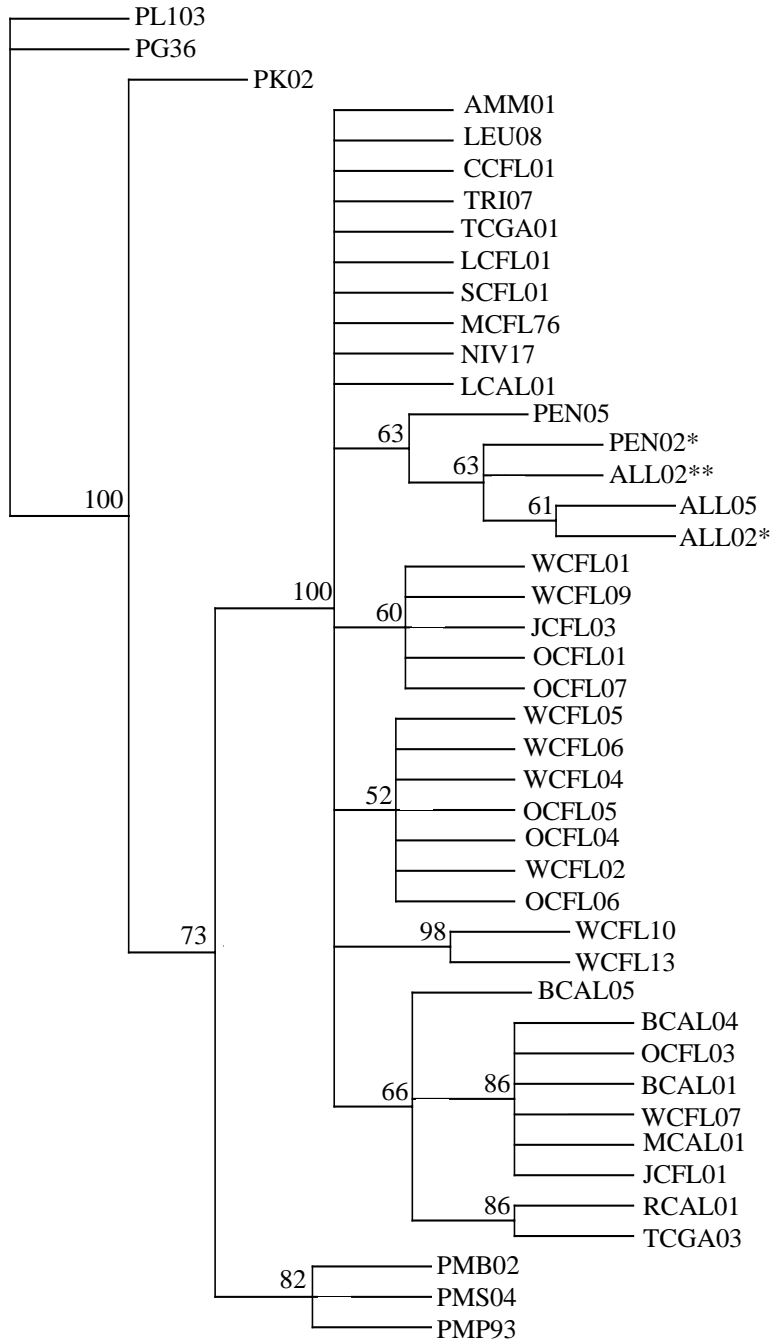


Fig. 5 Maximum likelihood topology using the cytochrome-b region and model TVM + Γ with outgroup *Peromyscus leucopus*. Model selection was based on AIC score. Numbers above branches are bootstrap values.

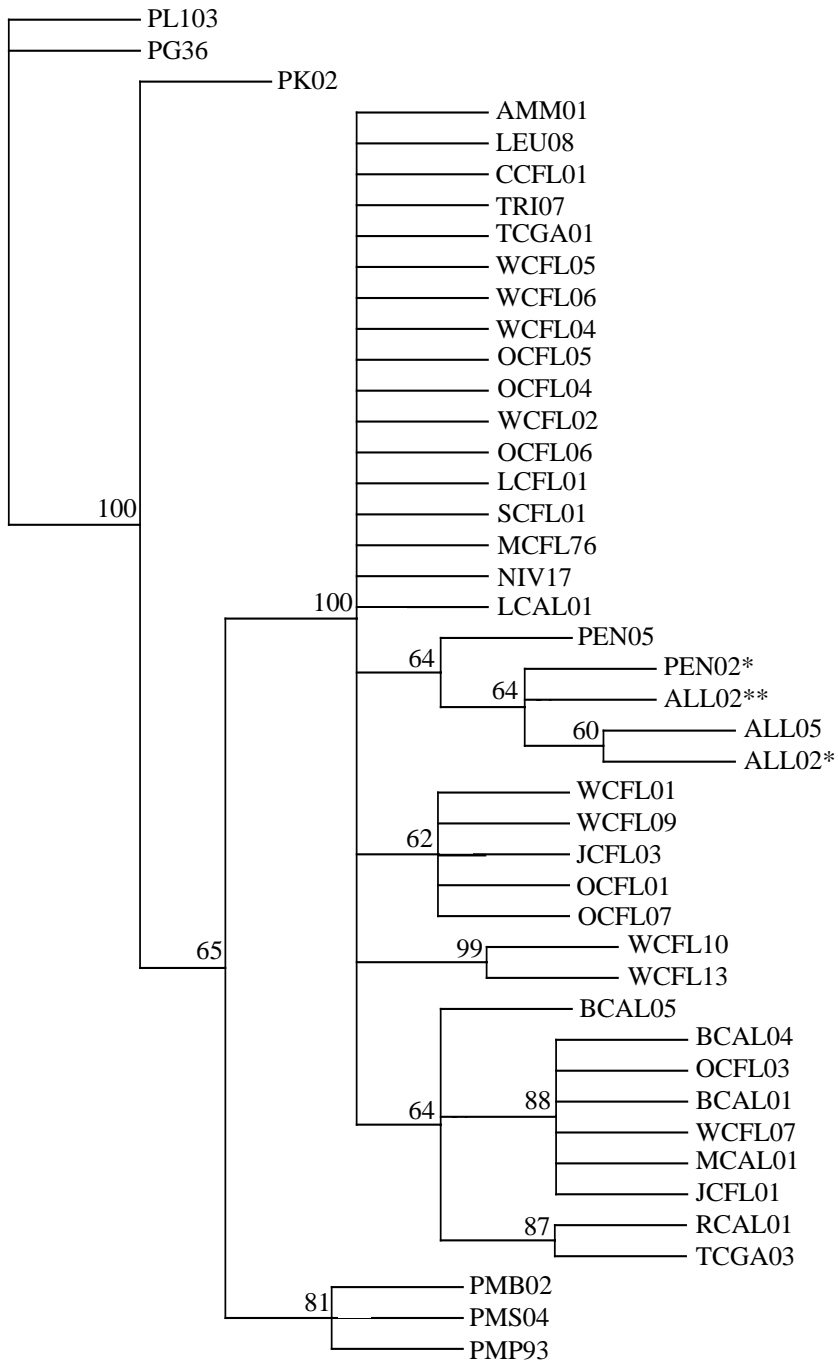


Fig. 6 Maximum likelihood topology using the cytochrome-b region and model HKY + Γ with outgroup *Peromyscus keeni*. Model selection was based on log likelihood score. Numbers above branches are bootstrap values.

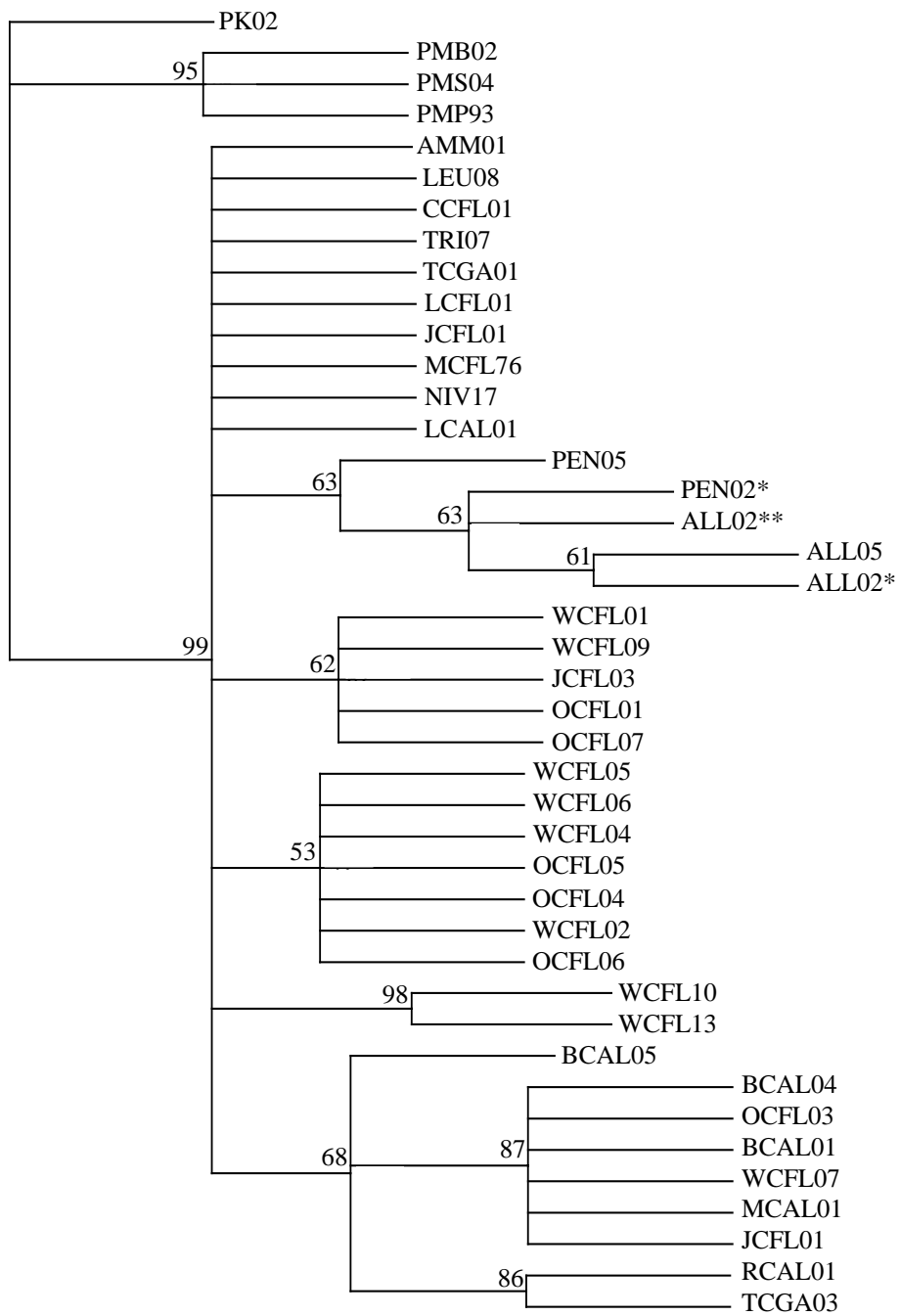


Fig. 7 Maximum likelihood topology using the cytochrome-b region and model GTR + Γ with outgroup *Peromyscus keeni*. Model selection was based on AIC score. Numbers above branches are bootstrap values.

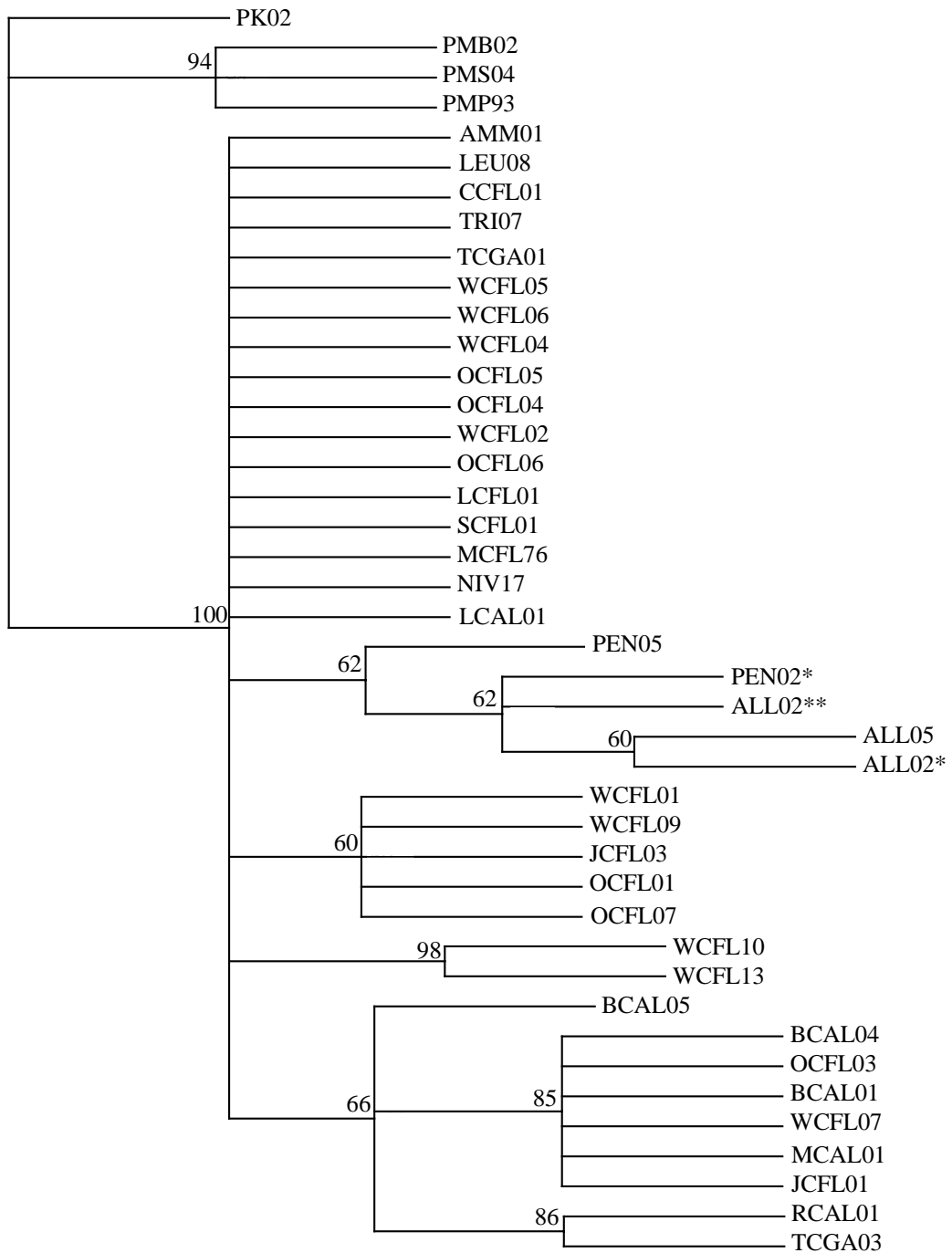


Fig. 8 Maximum likelihood topology using the D-loop and model HKY +I + Γ with outgroup *Peromyscus leucopus*. Model selection was based on both log likelihood and AIC scores. Numbers above branches are bootstrap values.

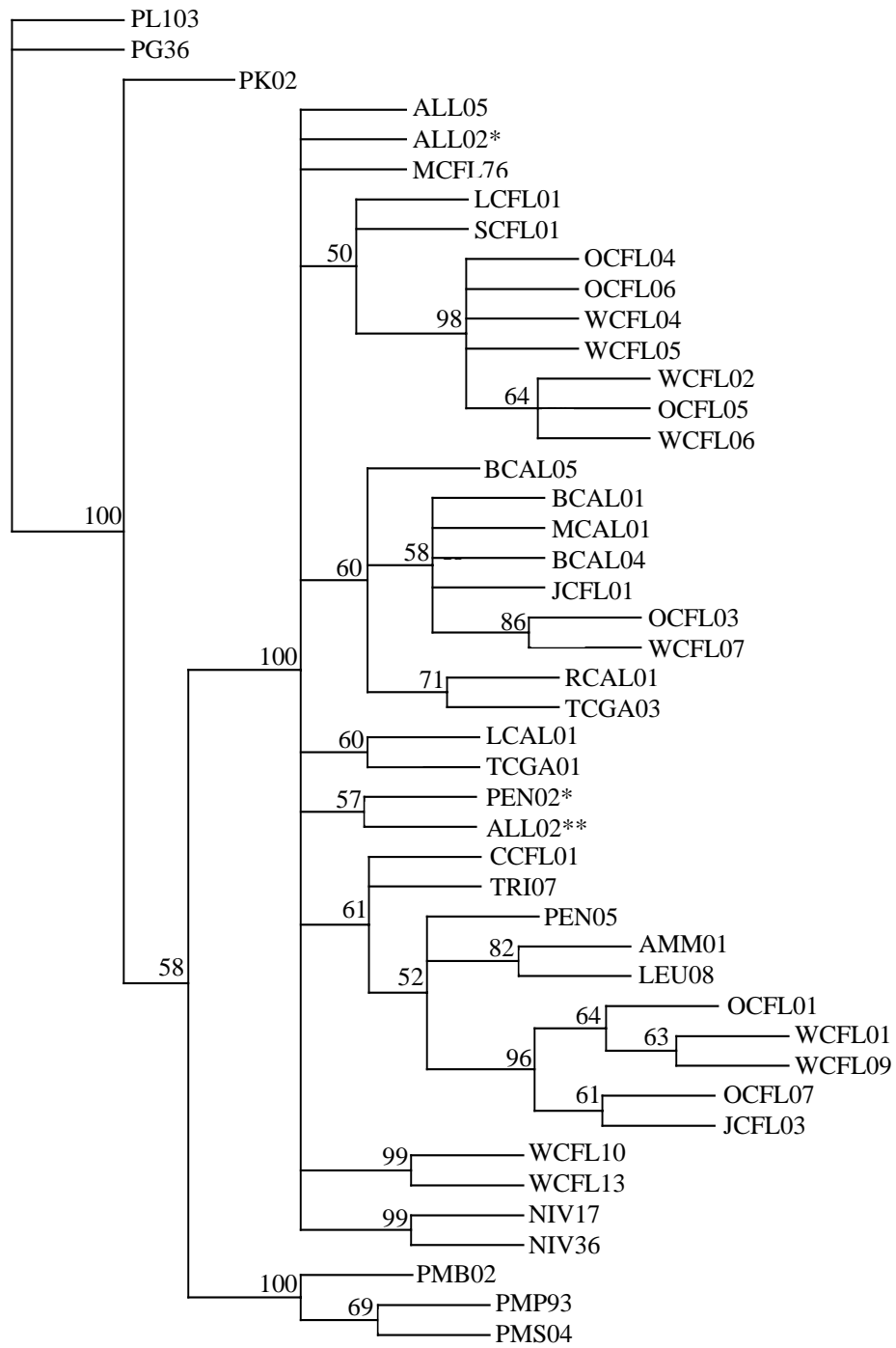


Fig. 9 Maximum likelihood topology using the D-loop and model HKY +I with outgroup *Peromyscus keeni*. Model selection was based on both log likelihood and AIC scores. Numbers above branches are bootstrap values.

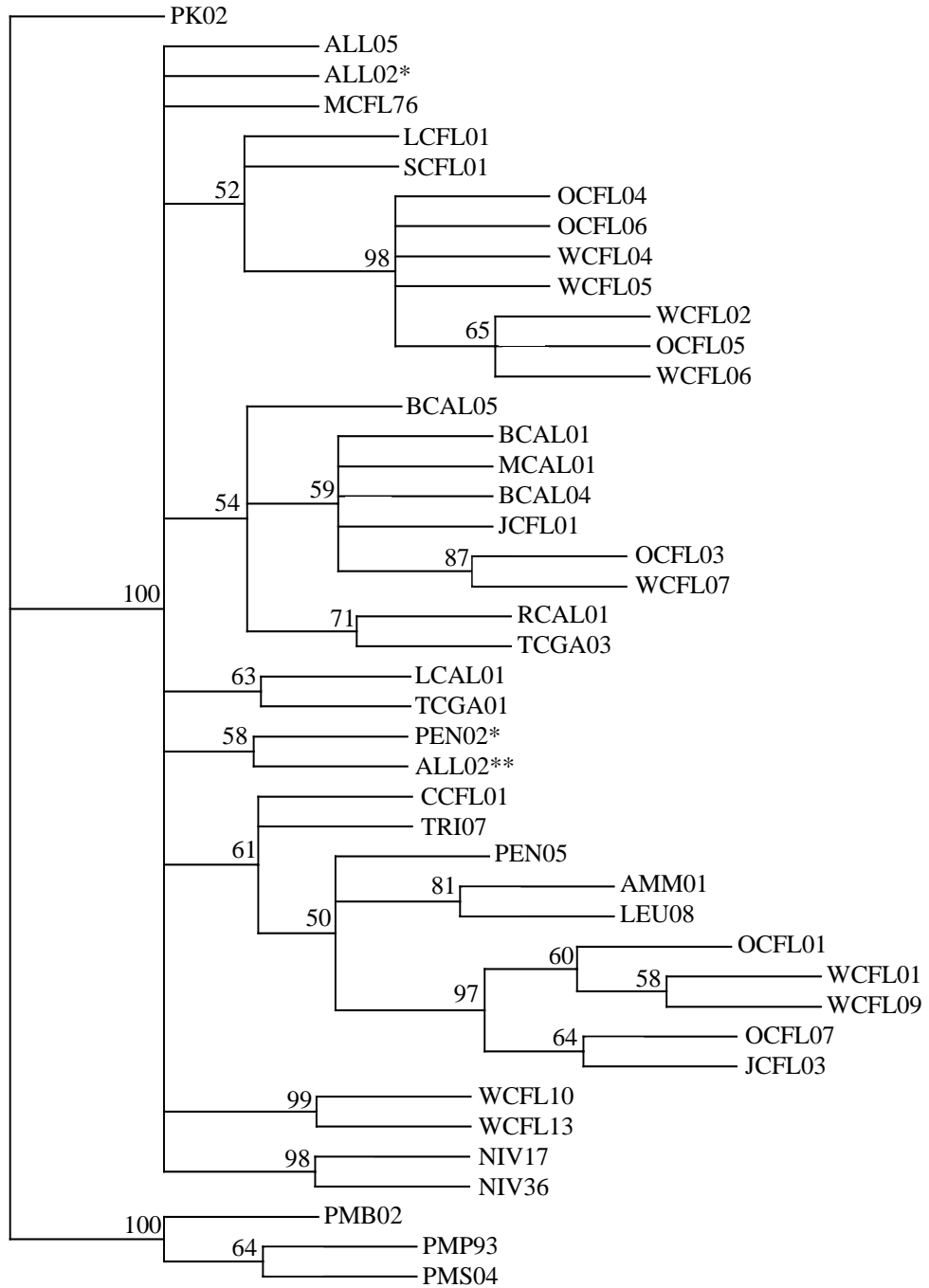


Fig. 10 Maximum likelihood topology using the cytochrome-b region and D-loop from model HKY +I + Γ with outgroup *Peromyscus leucopus*. Model selection was based on both log likelihood and AIC scores. Numbers above branches are bootstrap values.

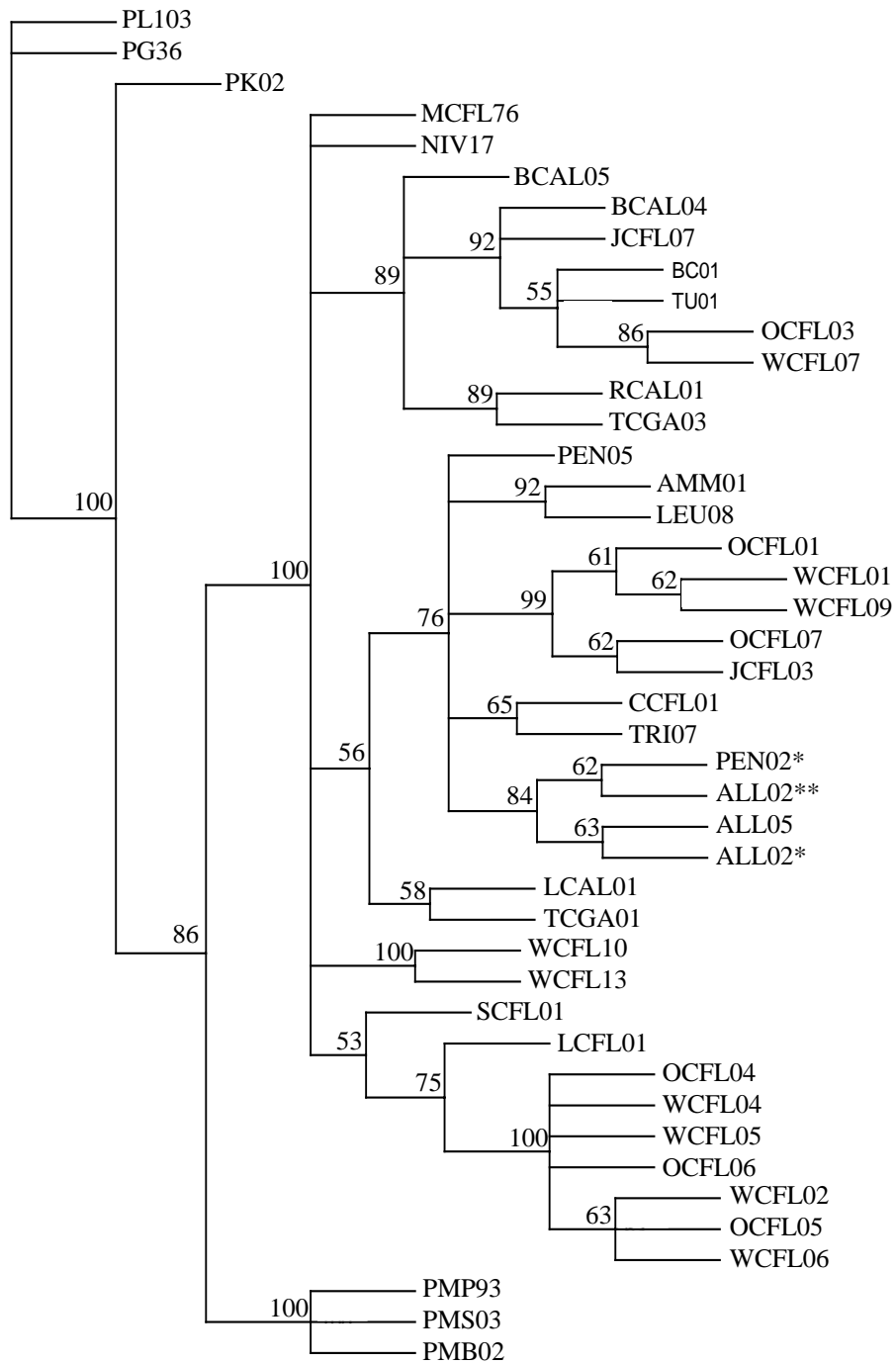


Fig. 11 Maximum likelihood topology using the cytochrome-b region and D-loop from model HKY +I + Γ with outgroup *Peromyscus keeni*. Model selection was based on both log likelihood and AIC scores. Numbers above branches are bootstrap values.

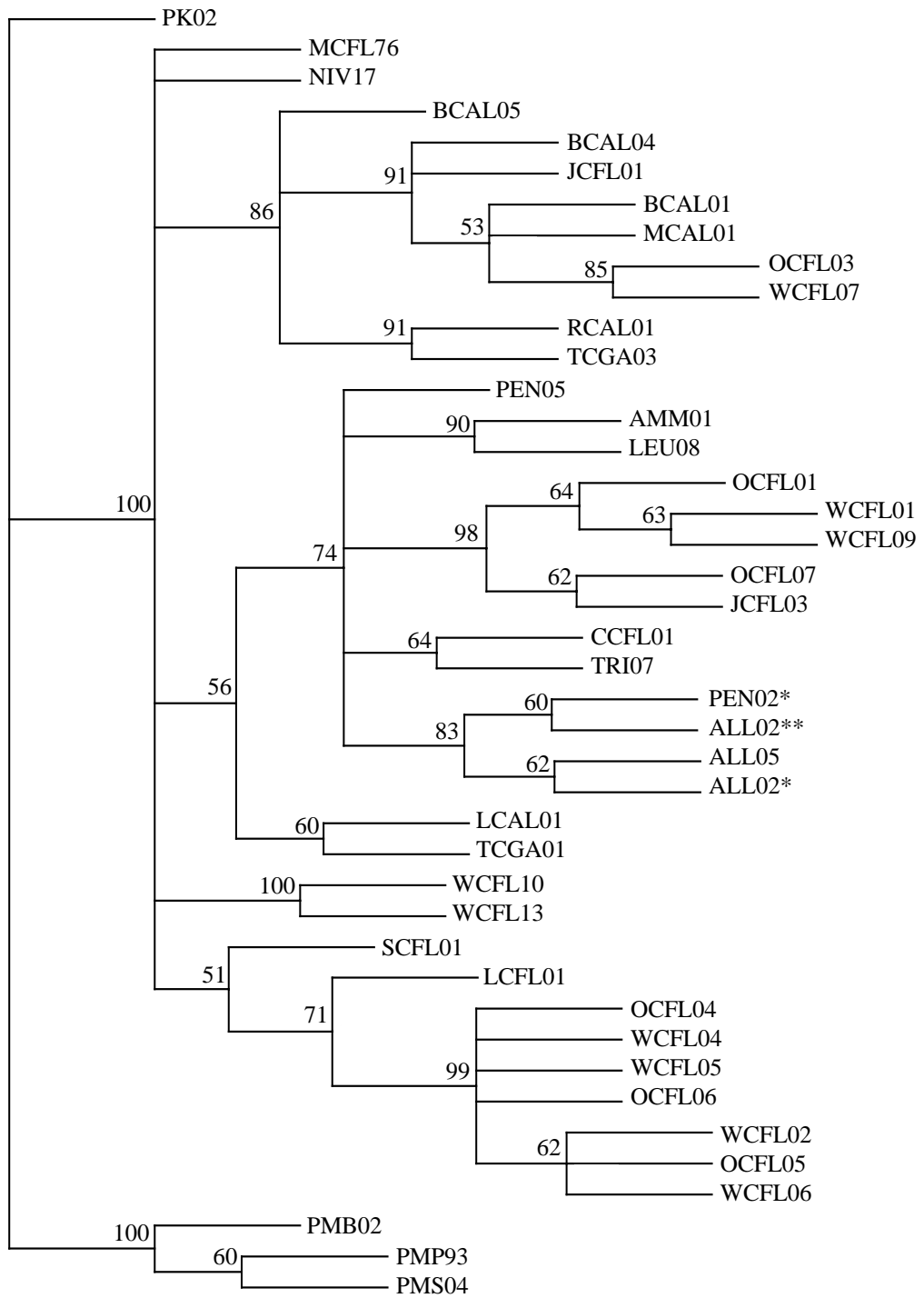


Fig. 12 Weighted parsimony topology using the cytochrome-b region with outgroup *Peromyscus leucopus*. The topology represents a strict consensus tree of 28 equally parsimonious topologies (CI = 0.9195, RI = 0.9071, RC = 0.8341, Tratio = 9.5:1, 1st position weight = 5:1, 2nd position weight = 40:1, Tree Length = 1646). Numbers above branches are bootstrap values.

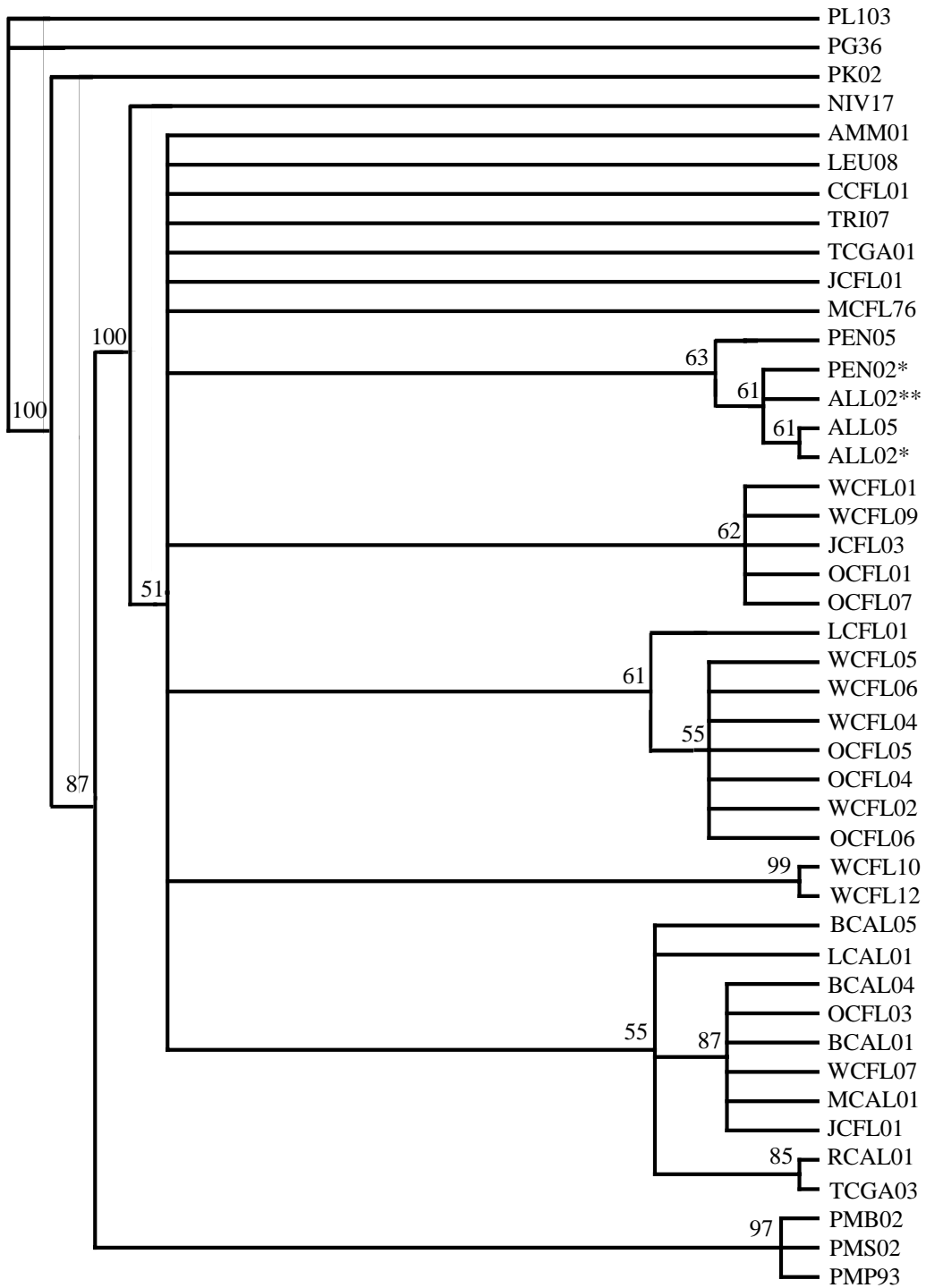


Fig. 13 Unweighted parsimony topology using the cytochrome-b region with outgroup *Peromyscus leucopus*. The topology represents a strict consensus tree of 77 equally parsimonious topologies (CI = 0.7684, RI = 0.8205 RC = 0.6305, tree length = 272). Numbers above branches are bootstrap values.

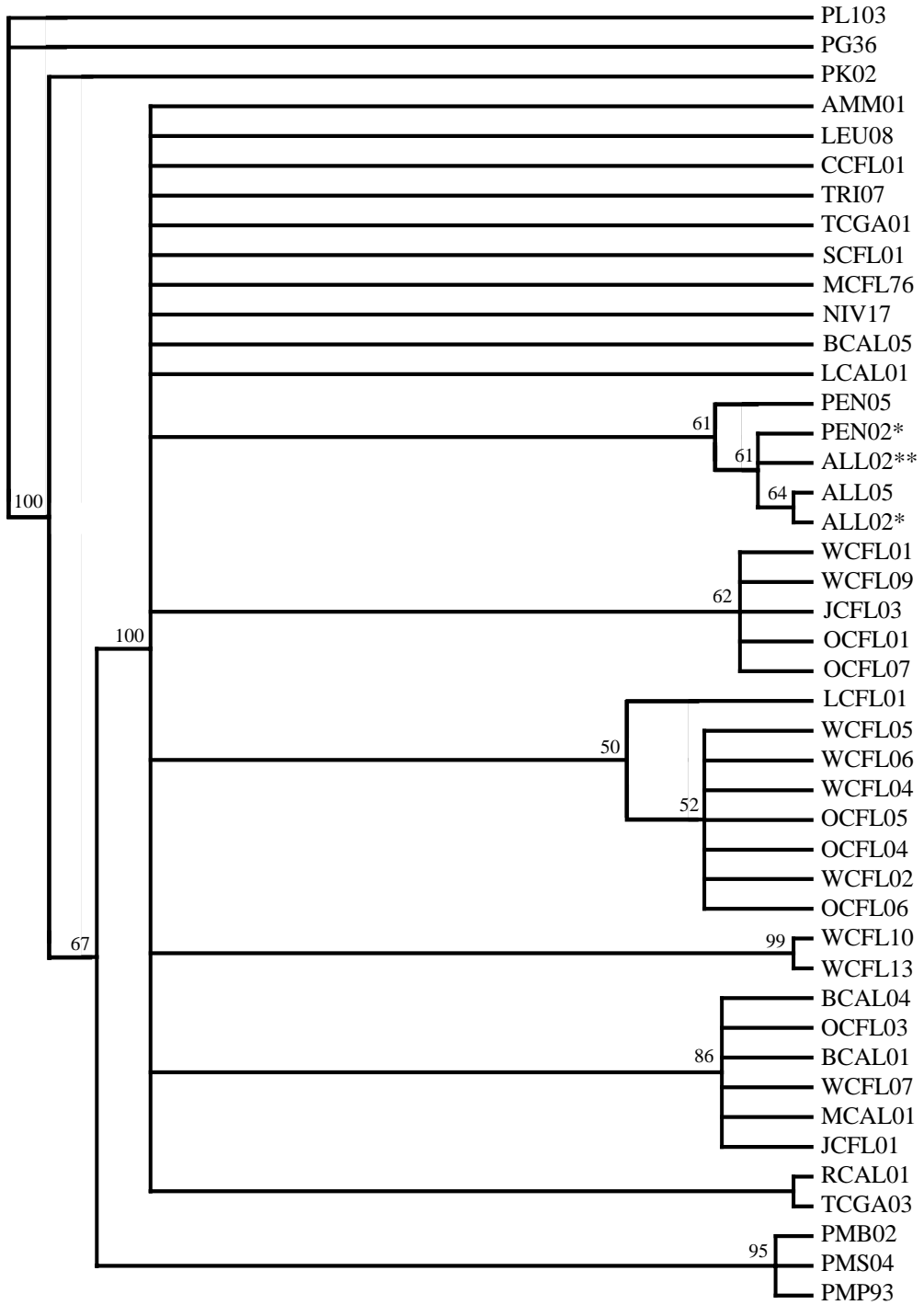


Fig. 14 Weighted parsimony topology using the cytochrome-b region with outgroup *Peromyscus keeni*. The topology represents a strict consensus tree of 14 equally parsimonious topologies (CI = 0.9553, RI = 0.9439, RC = 0.9017, Tratio = 18:1, 1st position weight = 5:1, 2nd position weight = 37:1, tree length = 805). Numbers above branches are bootstrap values.

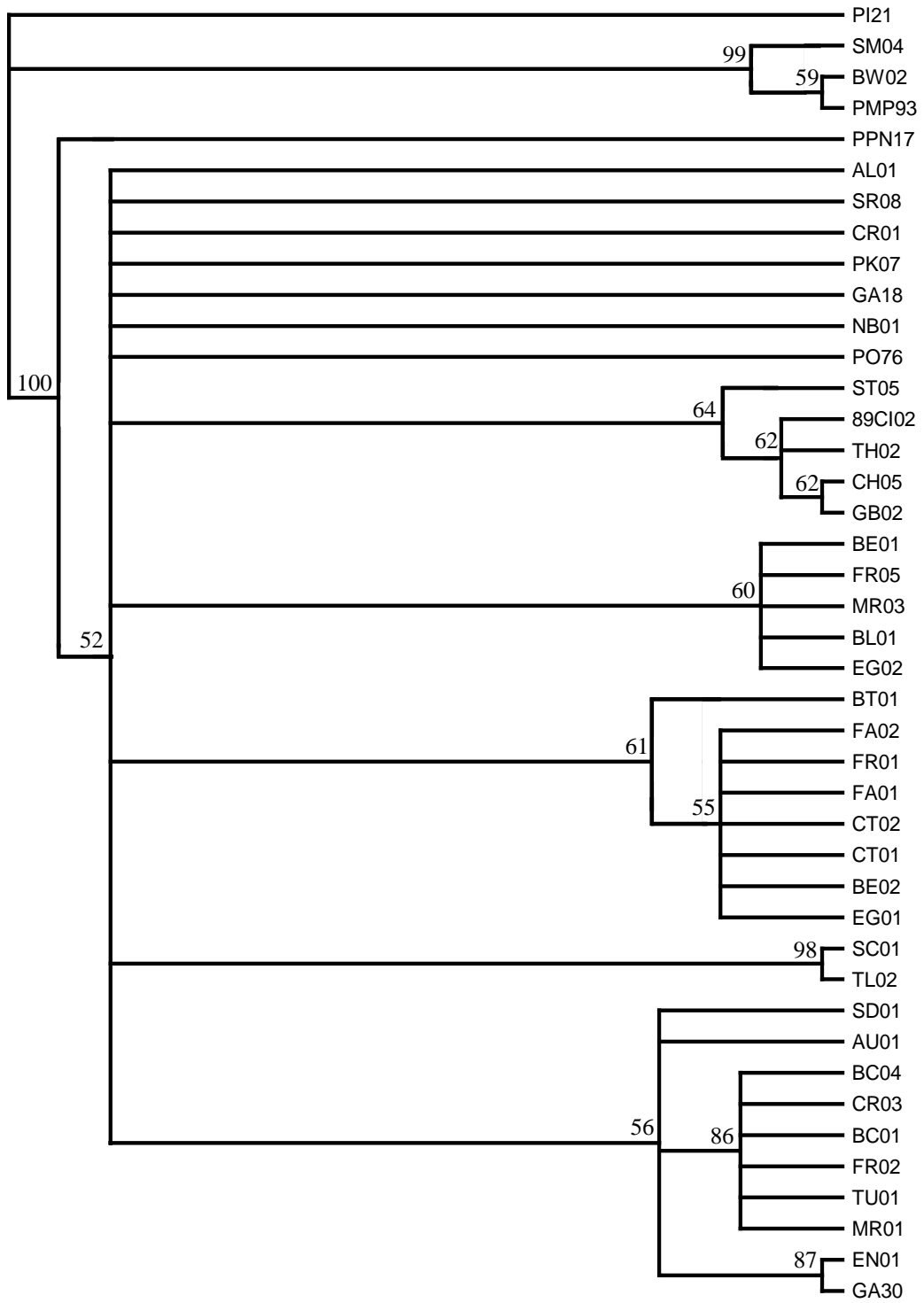


Fig. 15 Unweighted parsimony topology using the cytochrome-b region with outgroup *Peromyscus keeni*. The topology represents a strict consensus tree of 38 equally parsimonious topologies (CI = 0.8389, RI = 0.8863, RC = 0.7435, Tree Length = 149). Numbers above branches are bootstrap values.

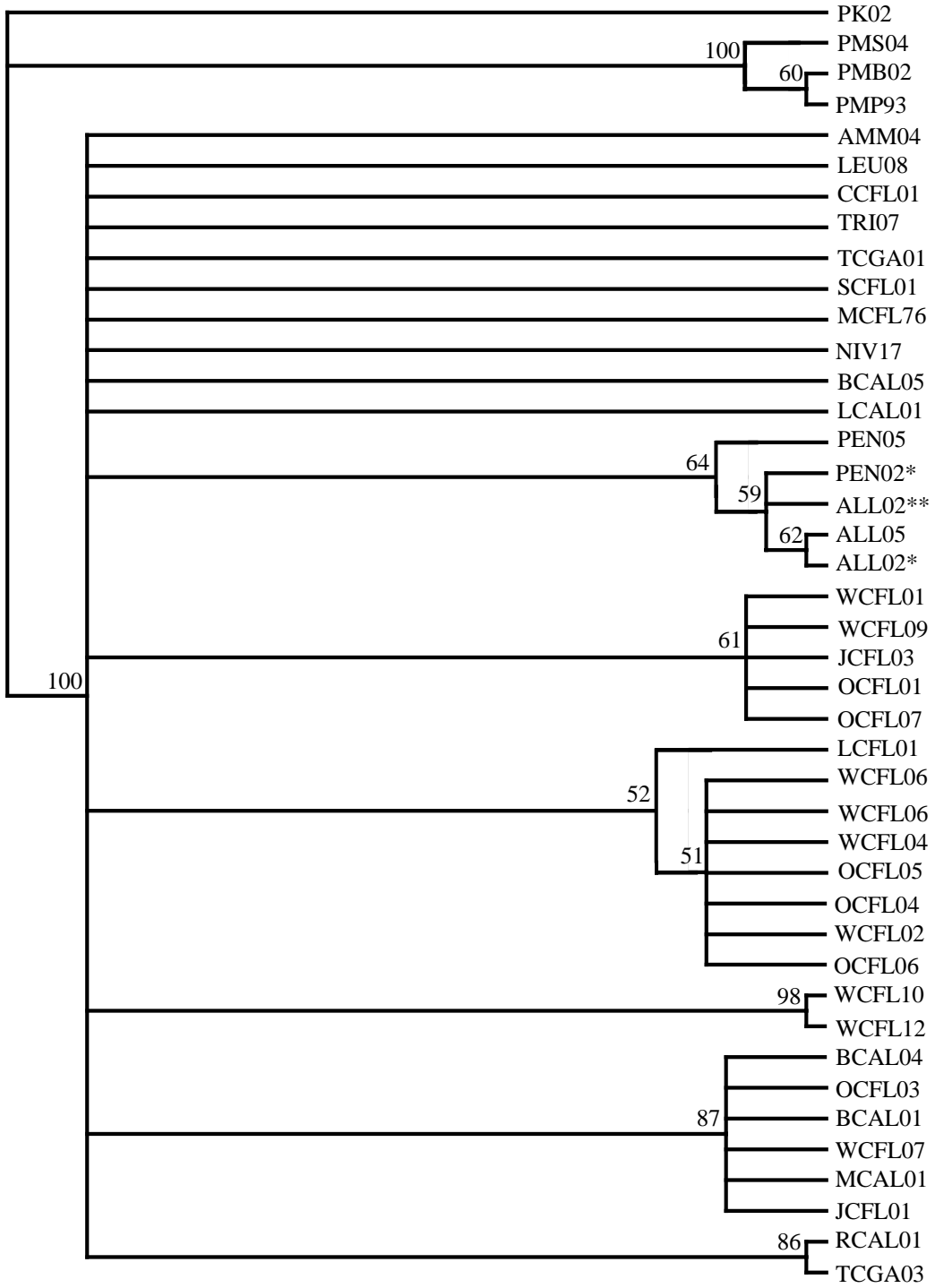


Fig. 16 Weighted parsimony topology using the D-loop with outgroup *Peromyscus leucopus*. The topology represents a strict consensus tree of 17 equally parsimonious topologies (CI = 0.8631, RI = 0.8922, RC = 0.7700, Tratio = 6:1, tree length = 745). Numbers above branches are bootstrap values.

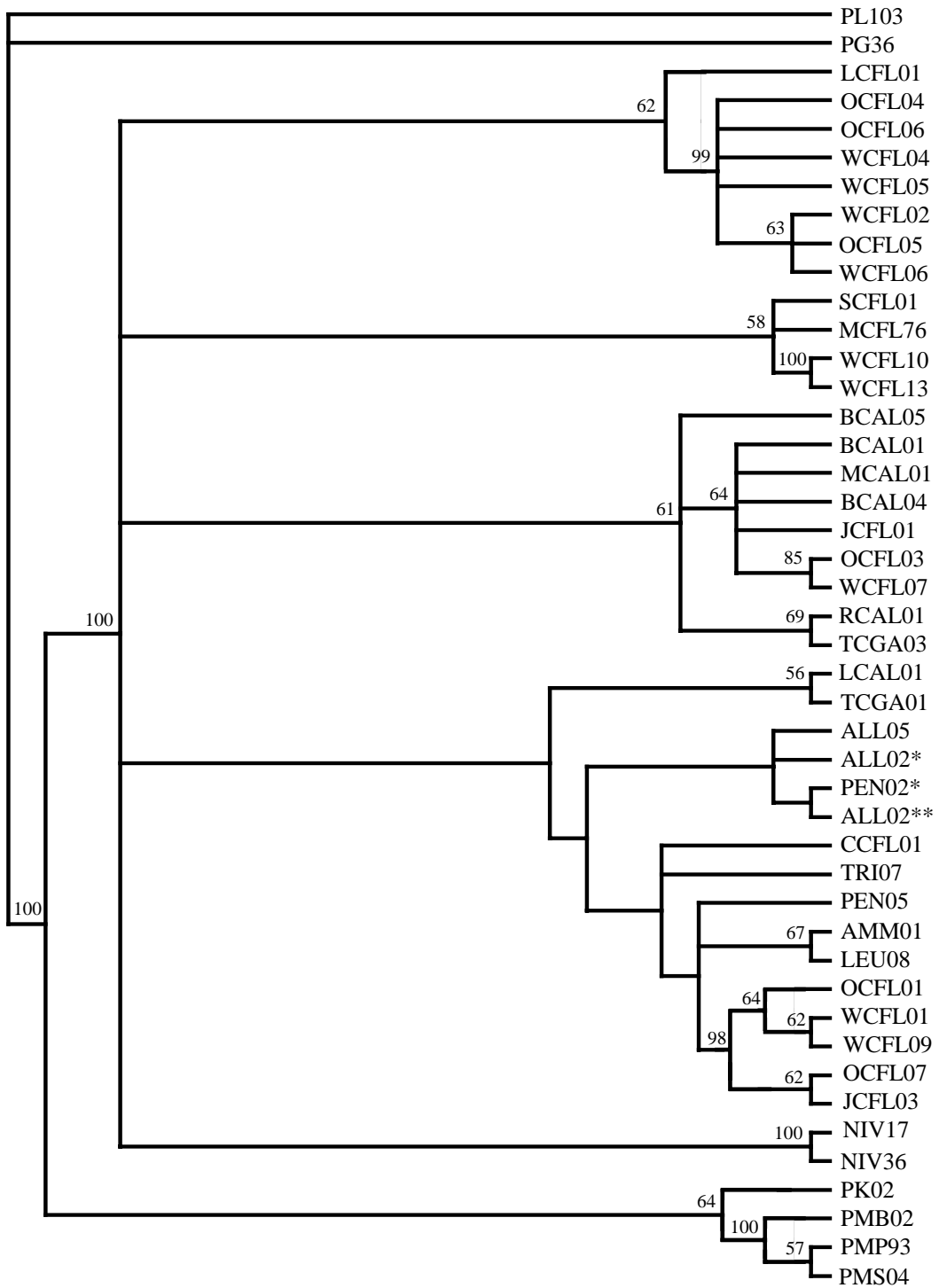


Fig. 17 Unweighted parsimony topology using the D-loop with outgroup *Peromyscus leucopus*. The topology represents a strict consensus tree of 22 equally parsimonious topologies (CI = 0.7653, RI = 0.8433, RC = 0.6454, tree length = 311). Numbers above branches are bootstrap values.

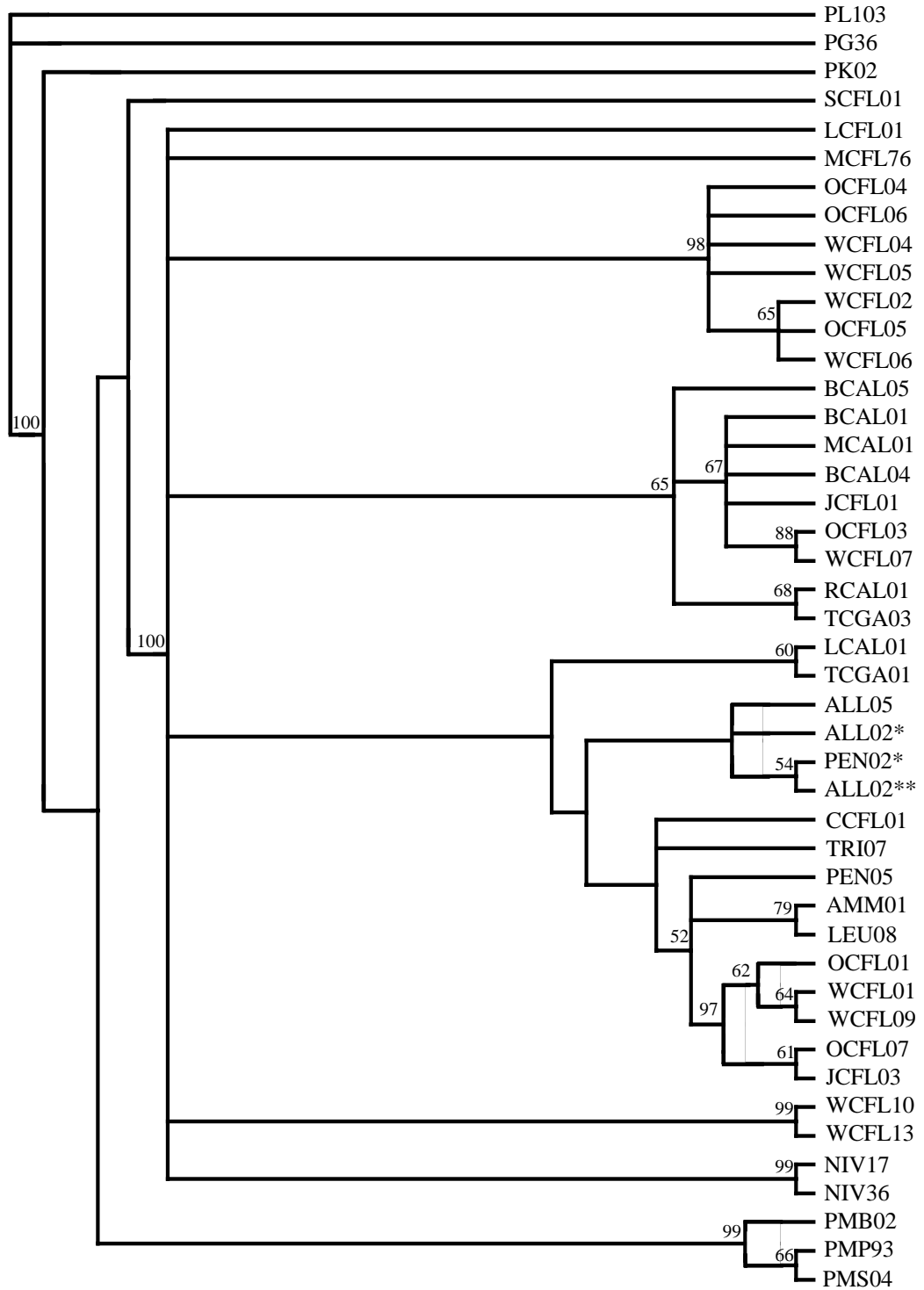


Fig. 18 Weighted parsimony topology using the D-loop with outgroup *Peromyscus keeni*. The topology represents a strict consensus of 32 equally parsimonious topologies (CI = 0.8465, RI = 0.9094, RC = 0.7698, Tratio = 10:1, Tree Length = 482). Numbers above branches are bootstrap values.

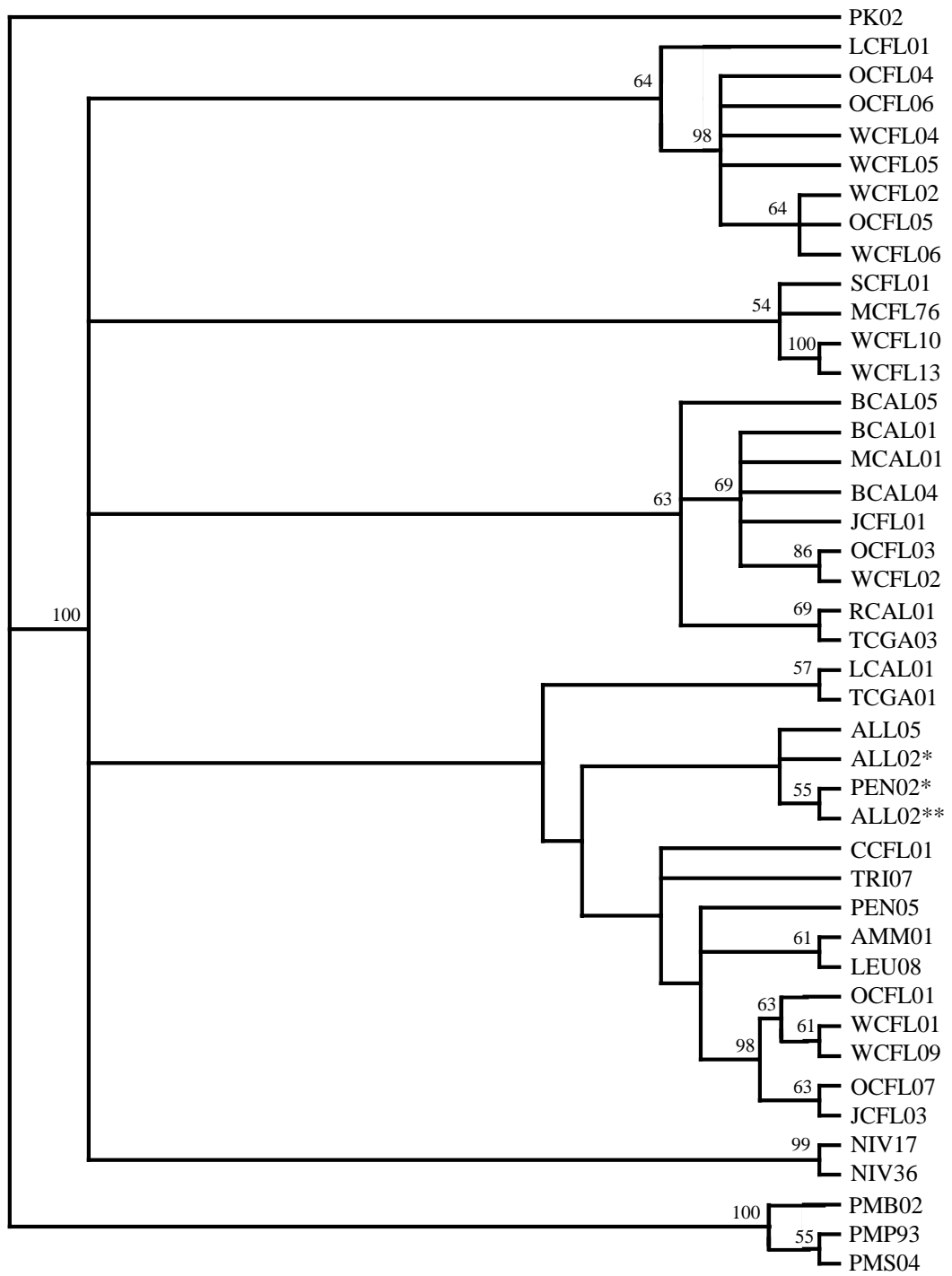


Fig. 19 Unweighted maximum parsimony topology using the D-loop with outgroup *Peromyscus keeni*. The topology represents a strict consensus tree of 520 equally parsimonious topologies (CI = 0.7500, RI = 0.8682, RC = 0.6511, tree length = 184). Numbers above branches are bootstrap values.

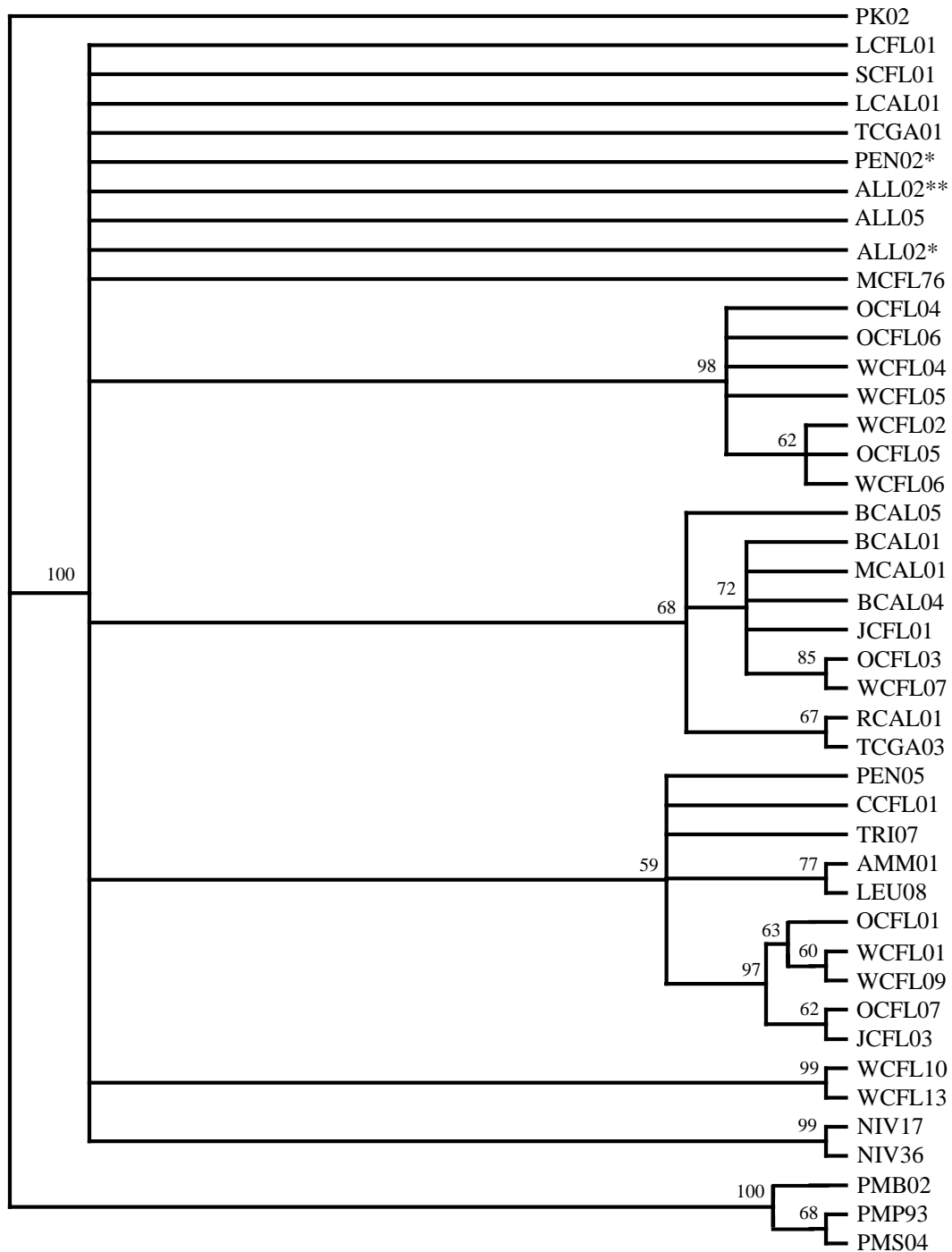


Fig. 20 Weighted parsimony topology using the cytochrome-b and D-loop with outgroup *Peromyscus leucopus*. The topology represents a strict consensus tree of 93 equally parsimonious topologies (CI = 0.8639, RI = 0.8718, RC = 0.7532, Tratio = 7:1, 1st position weight = 5:1, 2nd position weight = 40:1, tree length = 1668). Numbers above branches are bootstrap values.

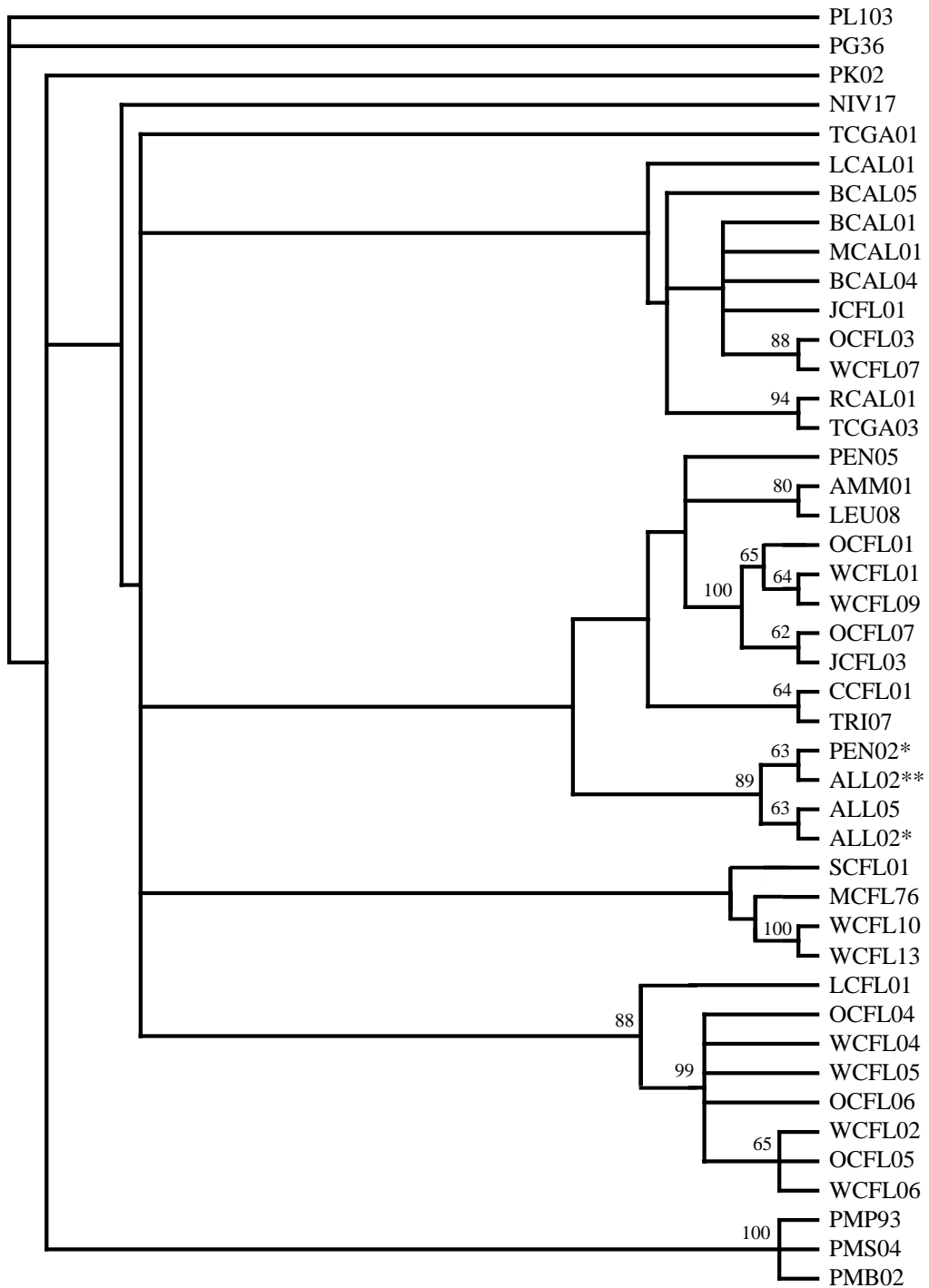


Fig. 21 Unweighted parsimony topology using the cytochrome-b region and D-loop with outgroup *Peromyscus leucopus*. The topology represents a strict consensus tree of 26 equally parsimonious topologies (CI = 0.7687, RI = 0.8273, RC = 0.6359, tree length = 614). Numbers above branches are bootstrap values.

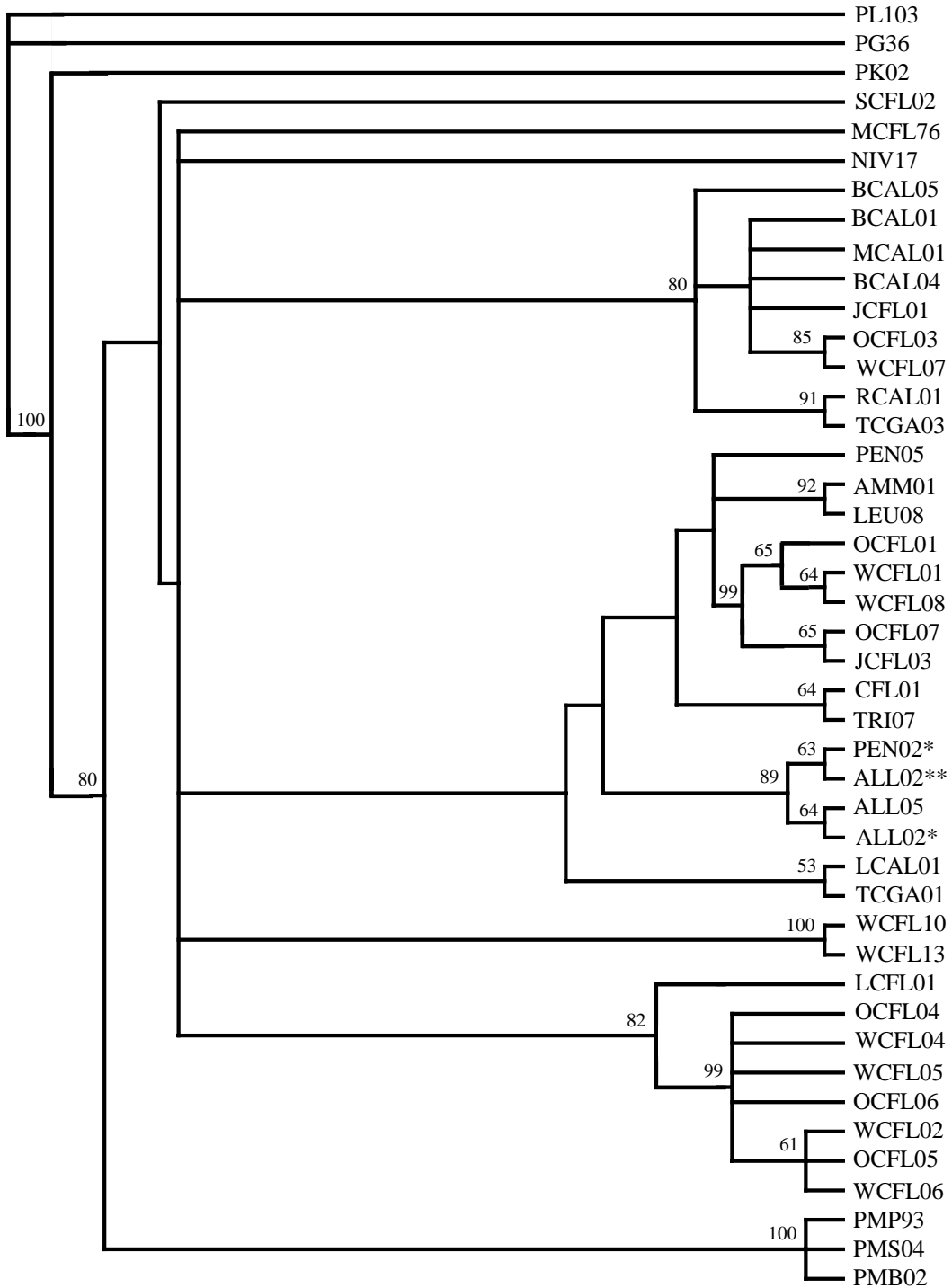


Fig. 22 Weighted parsimony topology using the cytochrome-b region and D-loop with outgroup *Peromyscus keeni*. The topology represents a strict consensus tree of 62 equally parsimonious topologies (CI = 0.8752, RI = 0.9092, RC = 0.7958, Tratio = 12:1, 1st position weight = 5:1, 2nd position weight = 37:1, tree length = 1002). Numbers above branches are bootstrap values.

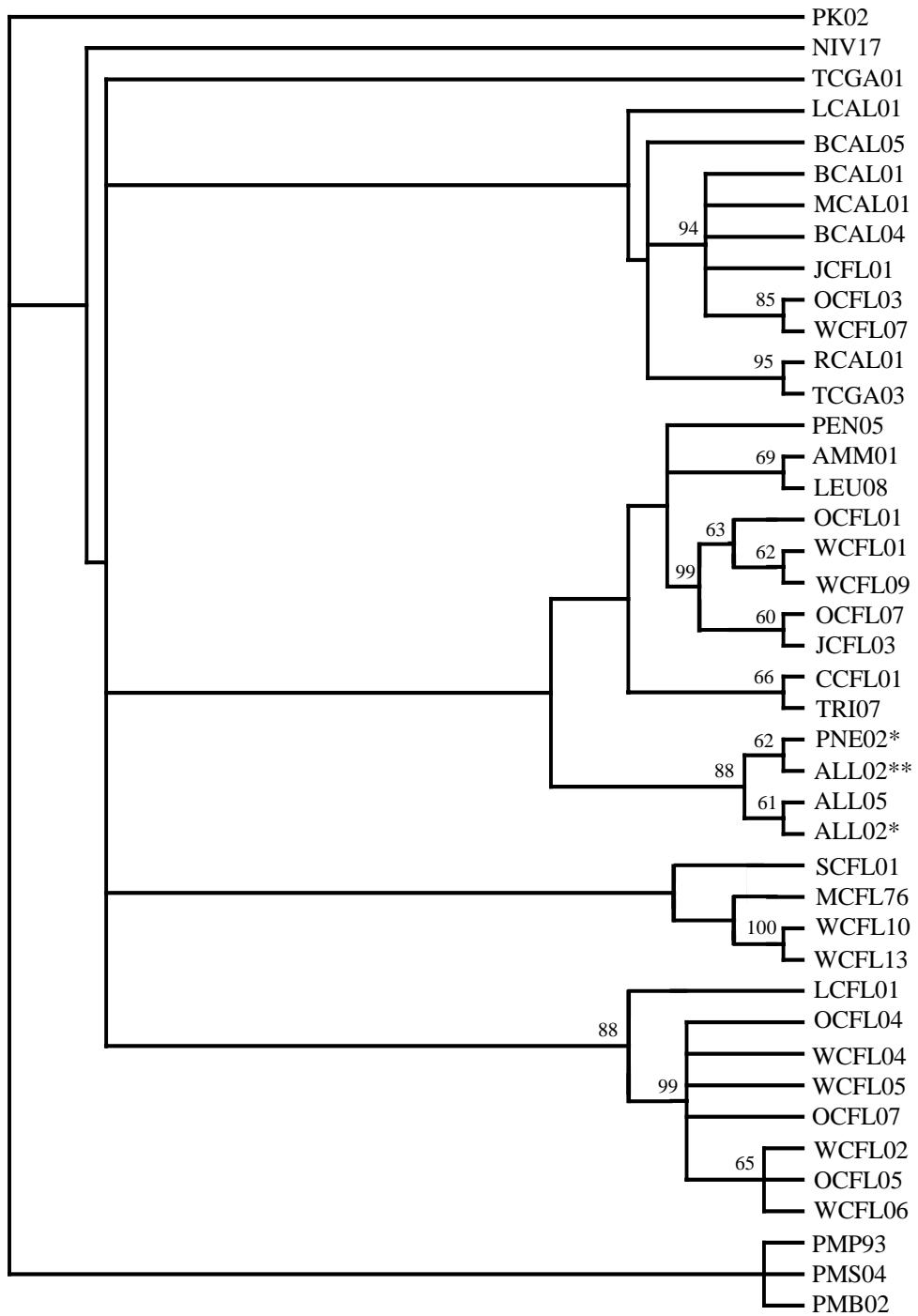


Fig. 23 Unweighted maximum parsimony topology using the cytochrome-b region and D-loop with outgroup *Peromyscus keeni*. The topology is represents a strict consensus tree of 440 equally parsimonious topologies (CI = 0.7853, RI = 0.8645, RC = 0.6789, tree length = 354). Numbers above branches are bootstrap values.

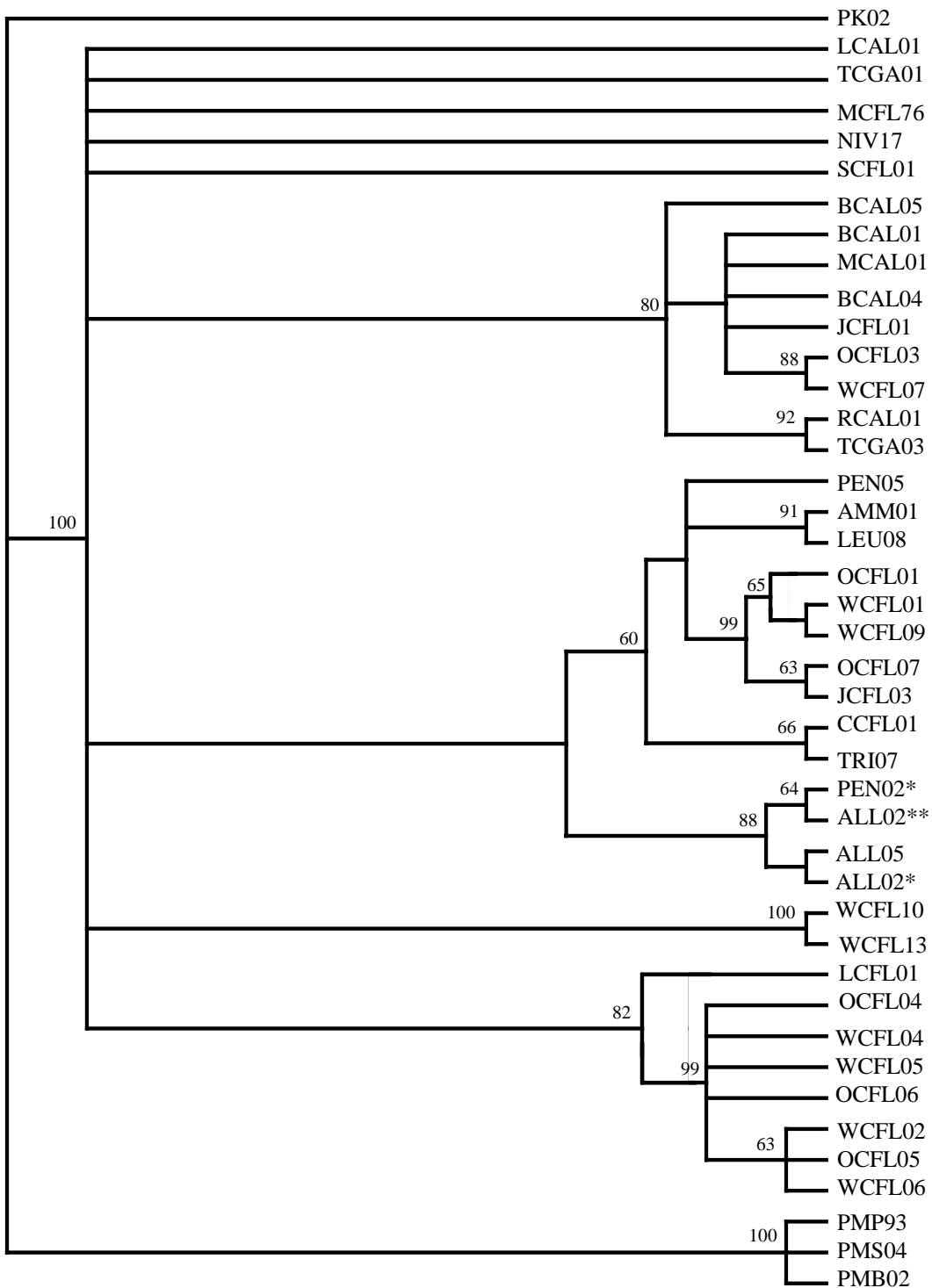


Fig. 24 Bayesian analysis using the cytochrome-b region with model GTR + Γ and outgroup *Peromyscus leucopus*. The topology represents a 50% majority-rule consensus of 192 186 topologies. Model selection was based on both log likelihood and AIC scores. Numbers above branches are bootstrap values.

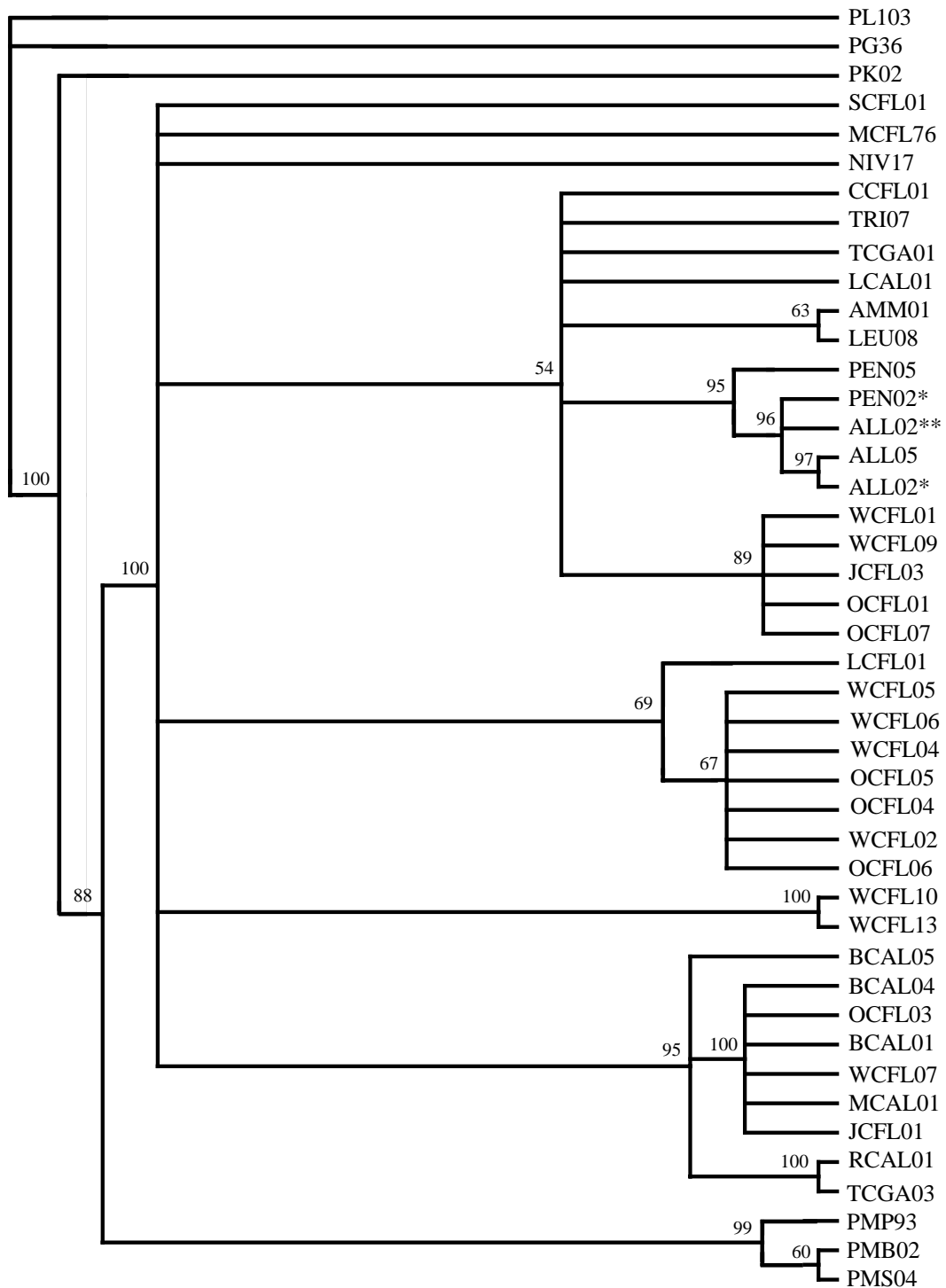


Fig. 25 Bayesian analysis using the cytochrome-b region with model HKY + Γ and outgroup *Peromyscus keeni*. The topology represents a 50% majority-rule consensus tree of 191 840 topologies. Model selection was based on log likelihood scores. Numbers above branches are bootstrap values.

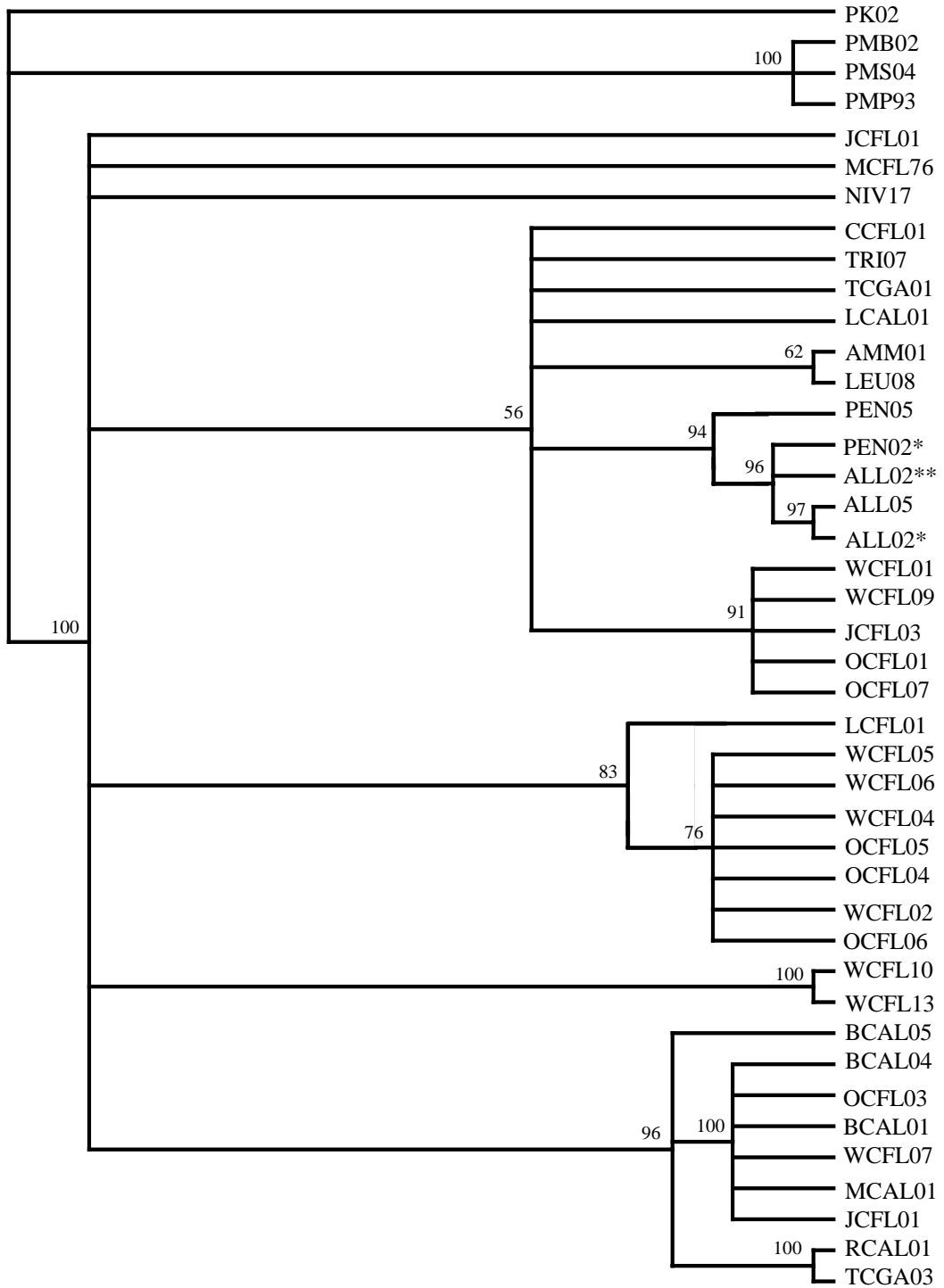


Fig. 26 Bayesian analysis using the cytochrome-b region with model GTR +I and outgroup *Peromyscus keeni*. The topology represents a 50% majority-rule of 193 162 topologies. Model selection was based on AIC score. Numbers above branches are bootstrap values.

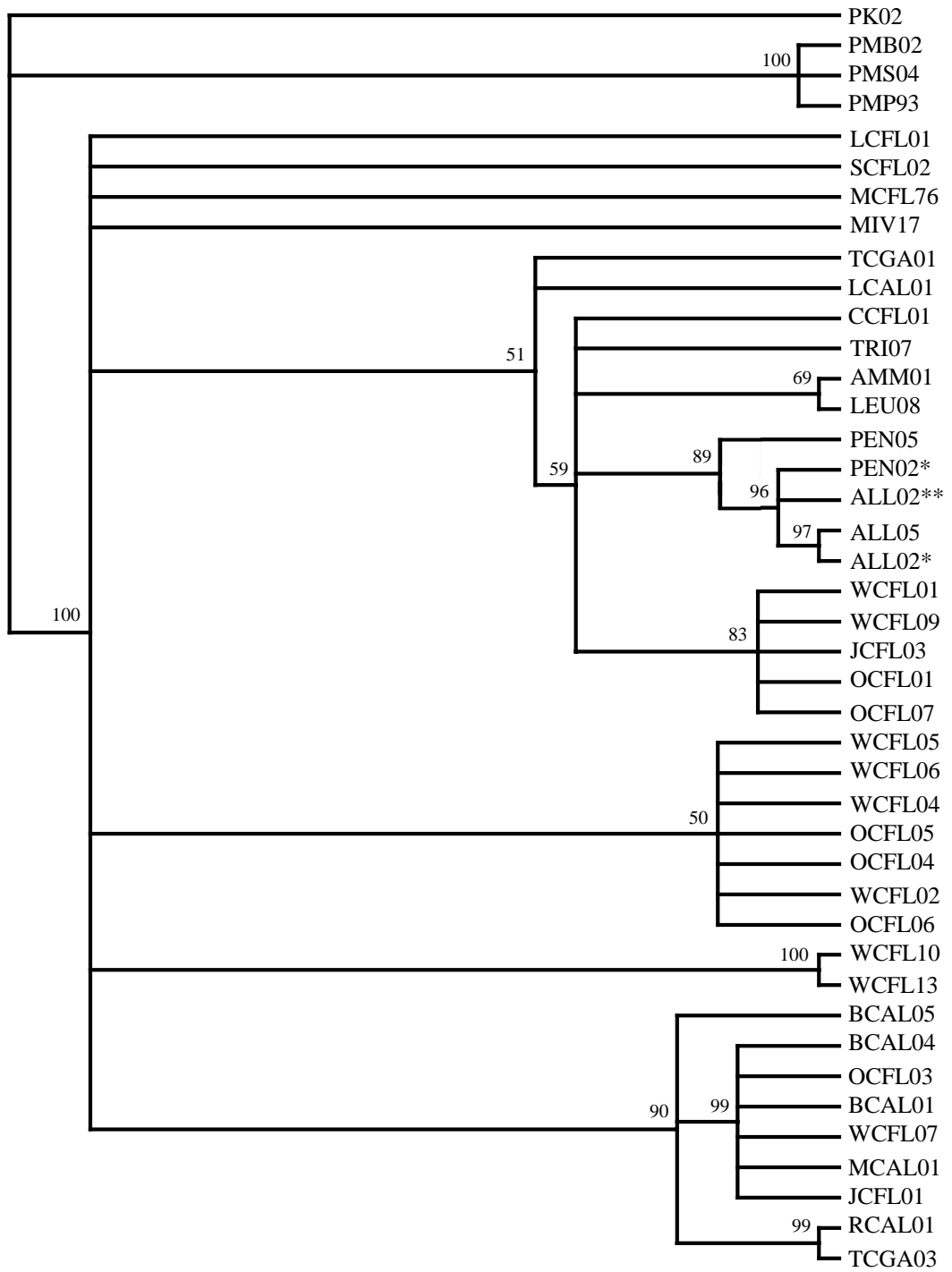


Fig. 27 Bayesian analysis using the D-loop with model HKY +I + Γ and outgroup *Peromyscus leucopus*. The topology represents a 50% majority-rule of 191 313 topologies. Model selection was based on both log likelihood and AIC scores. Numbers above branches are bootstrap values.

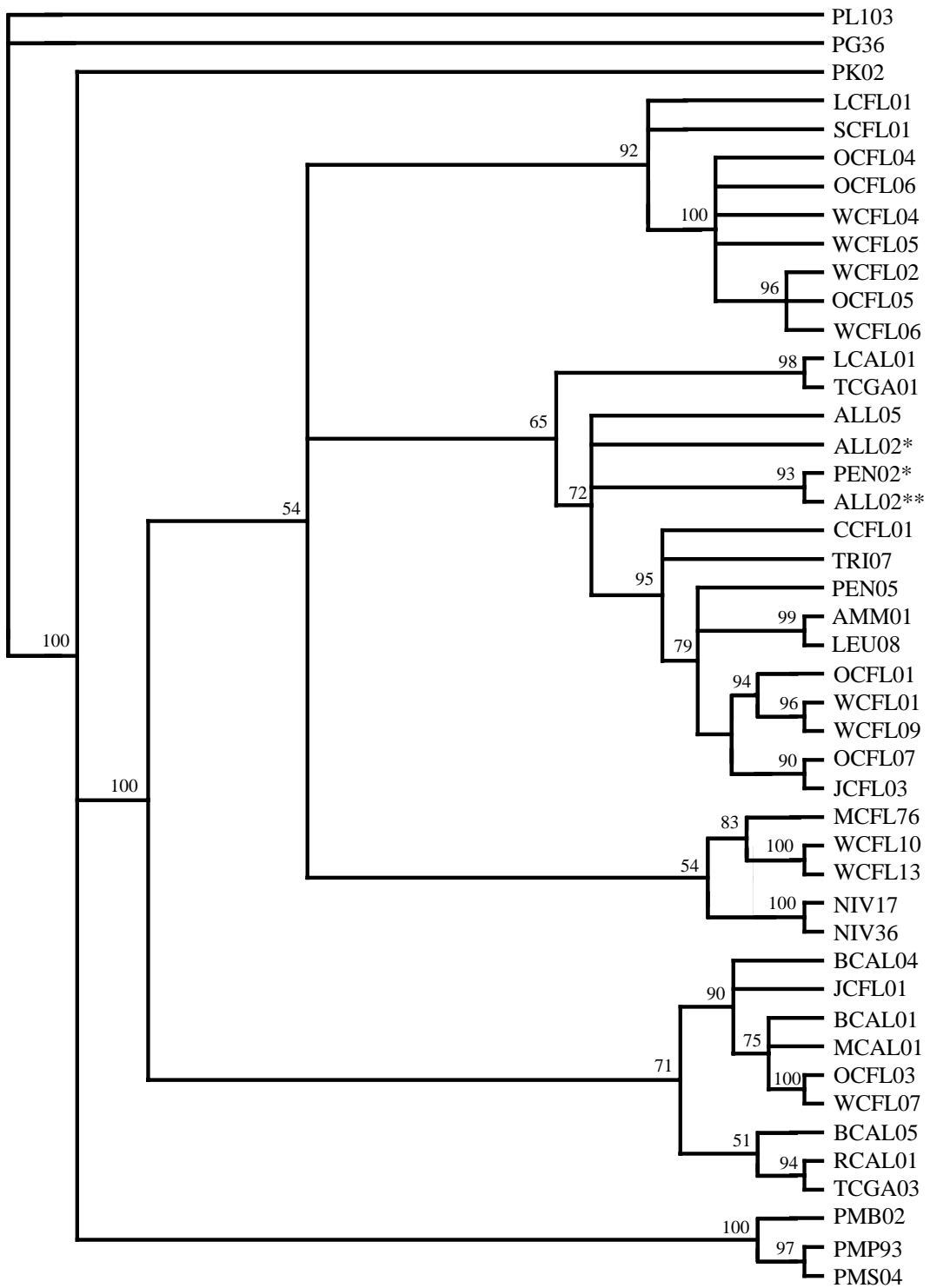


Fig. 28 Bayesian analysis using the D-loop with model HKY +I + Γ and outgroup *Peromyscus keeni*. The topology represents a 50% majority-rule of 191 737 topologies. Model selection was based on both log likelihood and AIC scores. Numbers above branches are bootstrap values.

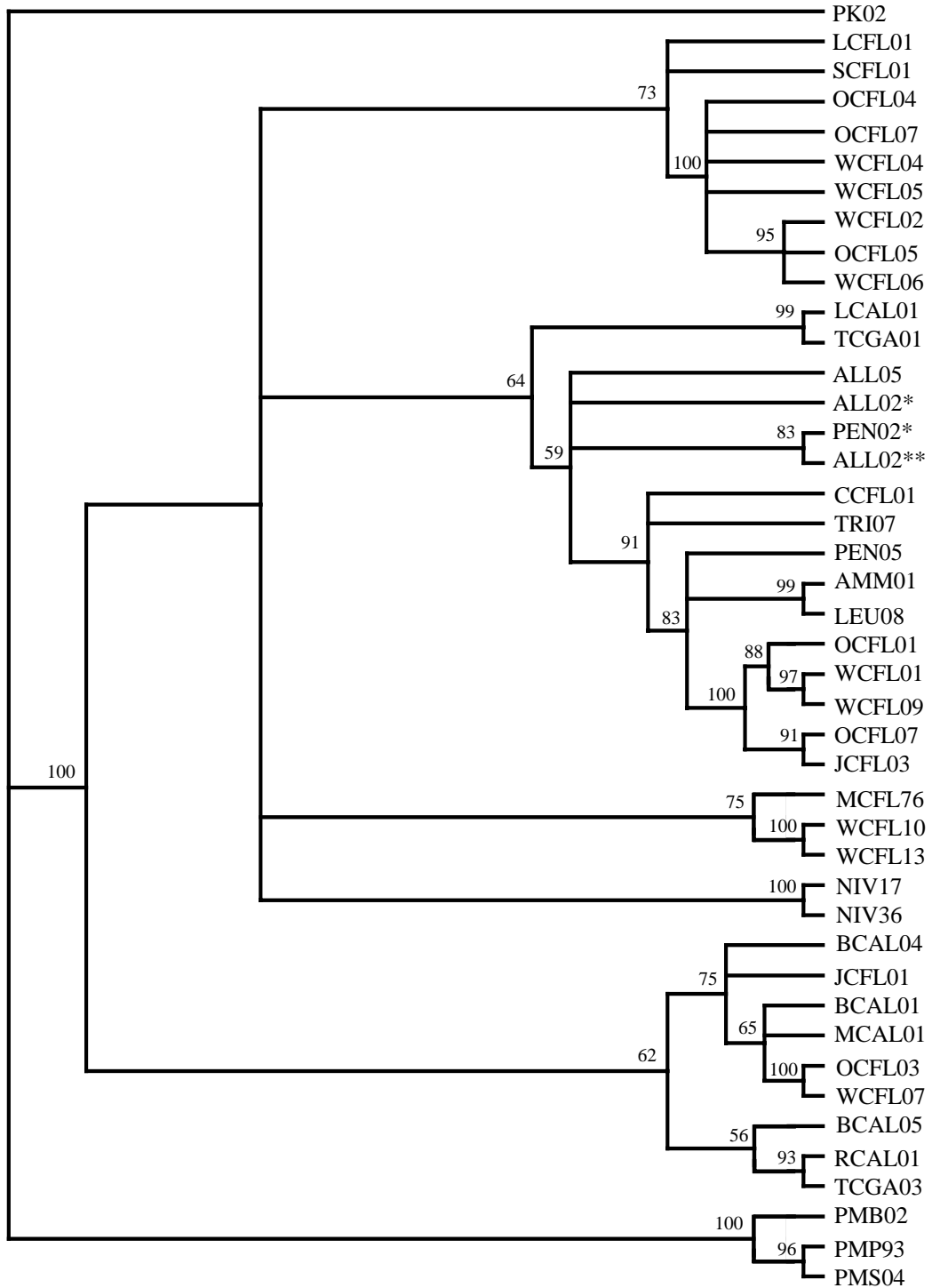


Fig. 29 Bayesian analysis using the cytochrome-b region and the D-loop with split models HKY + Γ (cty-b) and HKY +I + Γ (cyt-b and D-loop) with outgroup *Peromyscus leucopus*. The topology represents a 50% majority-rule of 190 150 topologies. Model selection is based on both log likelihood and AIC scores. Numbers above branches are bootstrap values.

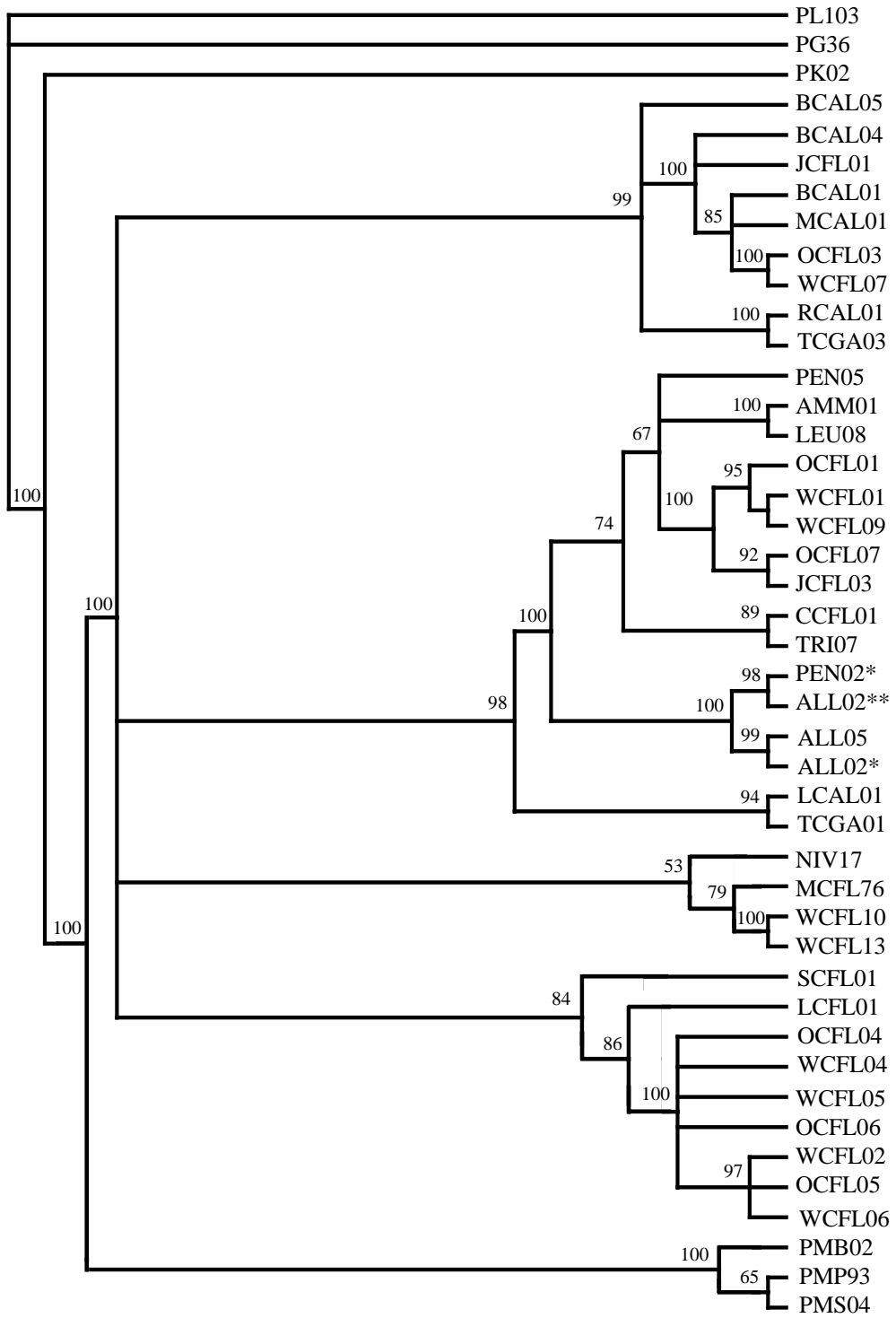


Fig. 30 Bayesian analysis using the cytochrome-b region and the D-loop with split models HKY + Γ (cyt-b) and HKY +I + Γ (cyt-b and D-loop) with outgroup *Peromyscus keeni*. The topology represents a 50% majority-rule of 194 997 topologies. Model selection is based on both log likelihood and AIC scores. Numbers above branches are bootstrap values.

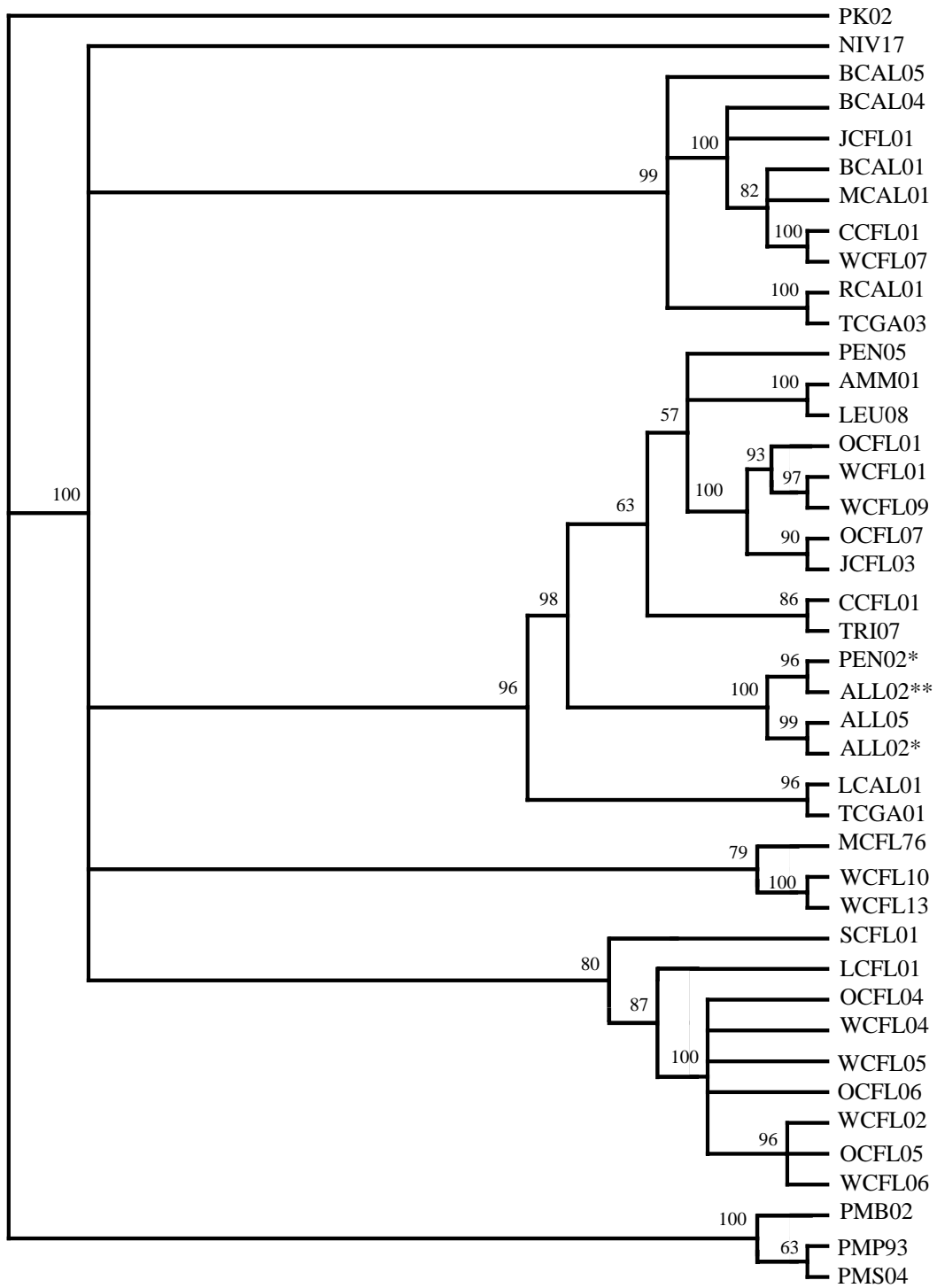


Fig. 31 Statistical parsimony network (Templeton *et al.* 1992) of *Peromyscus polionotus* haplotypes based on the number of substitutions. Numbers represent haplotypes as indicated in Table 1. Broken lines indicate alternative parsimony connections. Alternative loops are labeled 1A - 1C and 2. Solid circles represent inferred haplotypes that were not present in the sample. Lines between inferred and existing haplotypes represent a single mutational step.

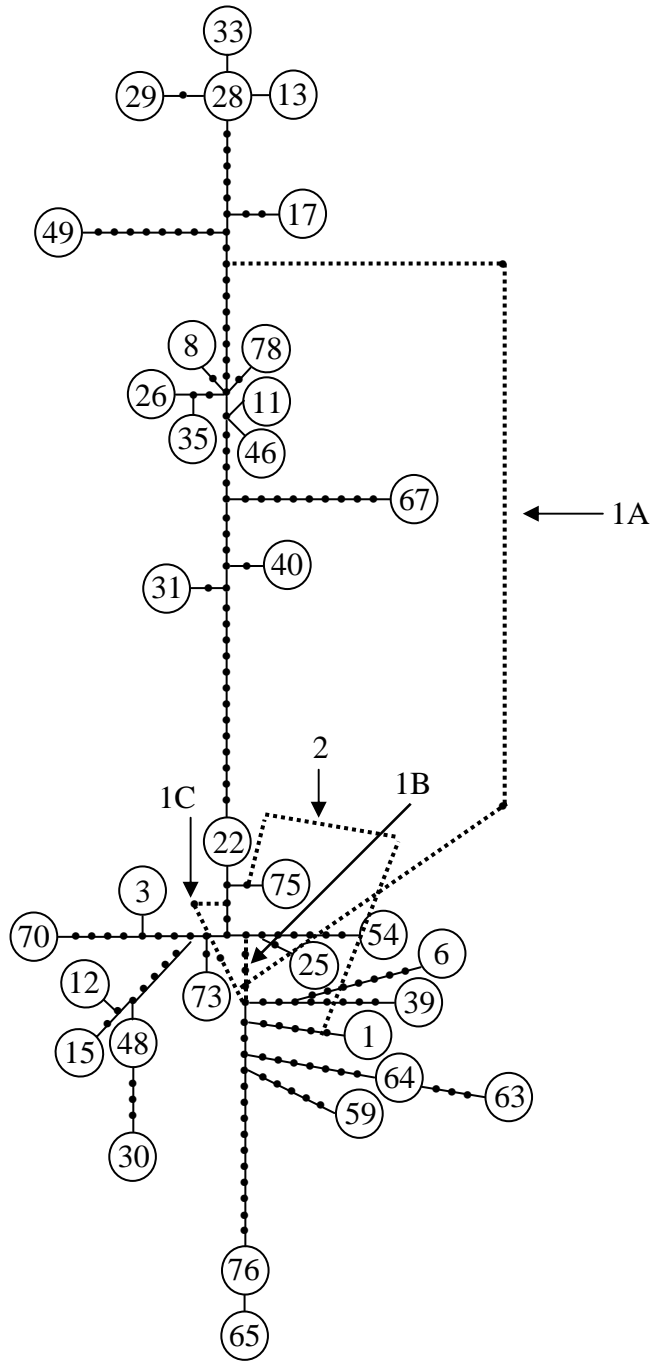


Fig. 32 Constant-rate time estimates for lineage divergence's within *Peromyscus polionotus* where $t_1 = 306,000 \pm 48,000$, $t_2 = 243,000 \pm 49,000$, $t_3 = 195,000 \pm 34,000$, $t_4 = 185,000 \pm 86,000$, $t_5 = 159,000 \pm 49,000$, $t_6 = 151,000 \pm 36,000$, $t_7 = 63,000 \pm 32,000$, $t_8 = 430,000 \pm 145,000$.

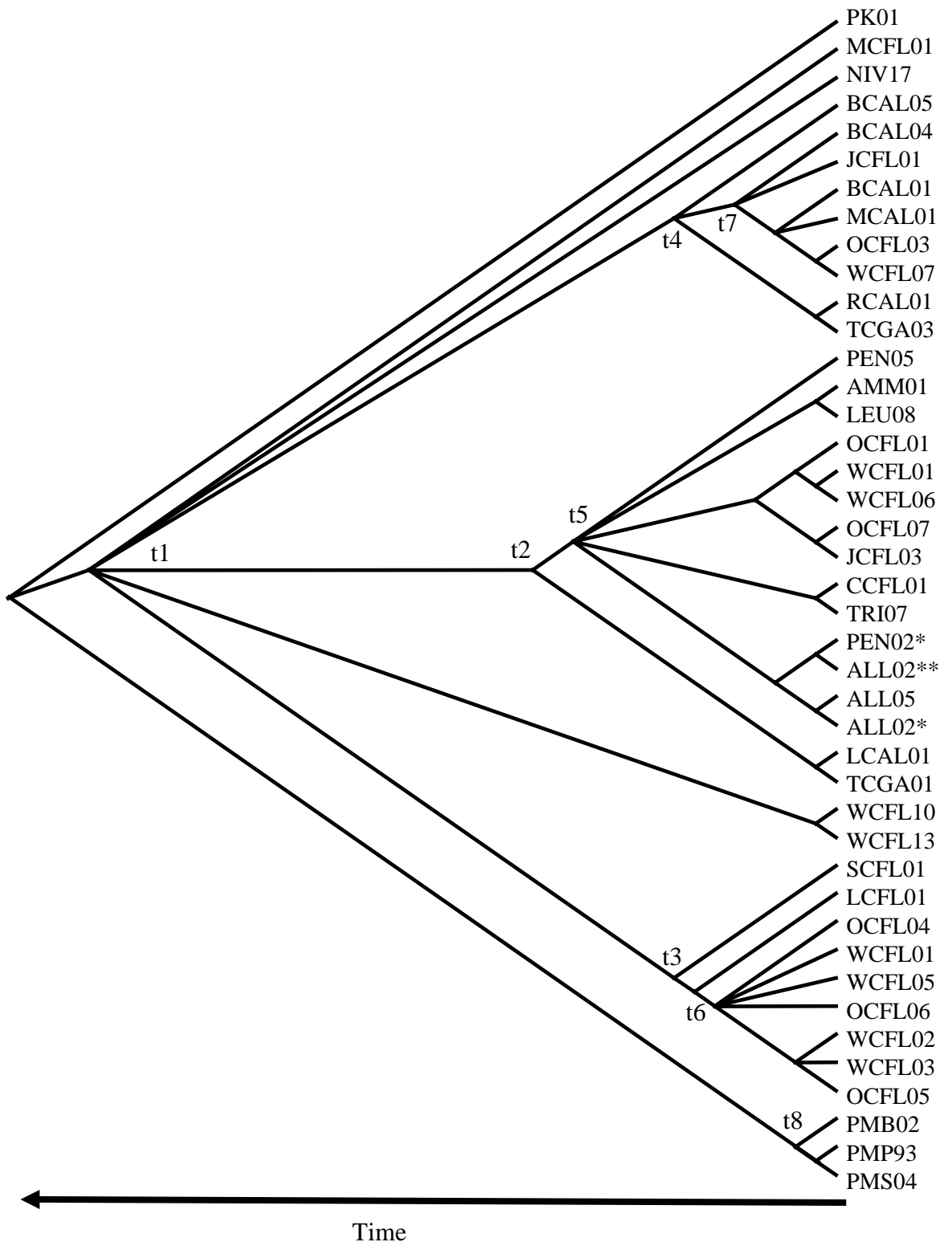


Fig. 33 Range map of *Peromyscus polionotus allophrys* (Bowen 1968) and location of the debated haplotype (Crooked Island, FL). Bowen (1968) concluded Crooked Island was a section of the range of *Peromyscus polionotus peninsularis*. However, phylogenetic analyses placed haplotypes from Crooked Island with haplotypes from *P. p. allophrys*.

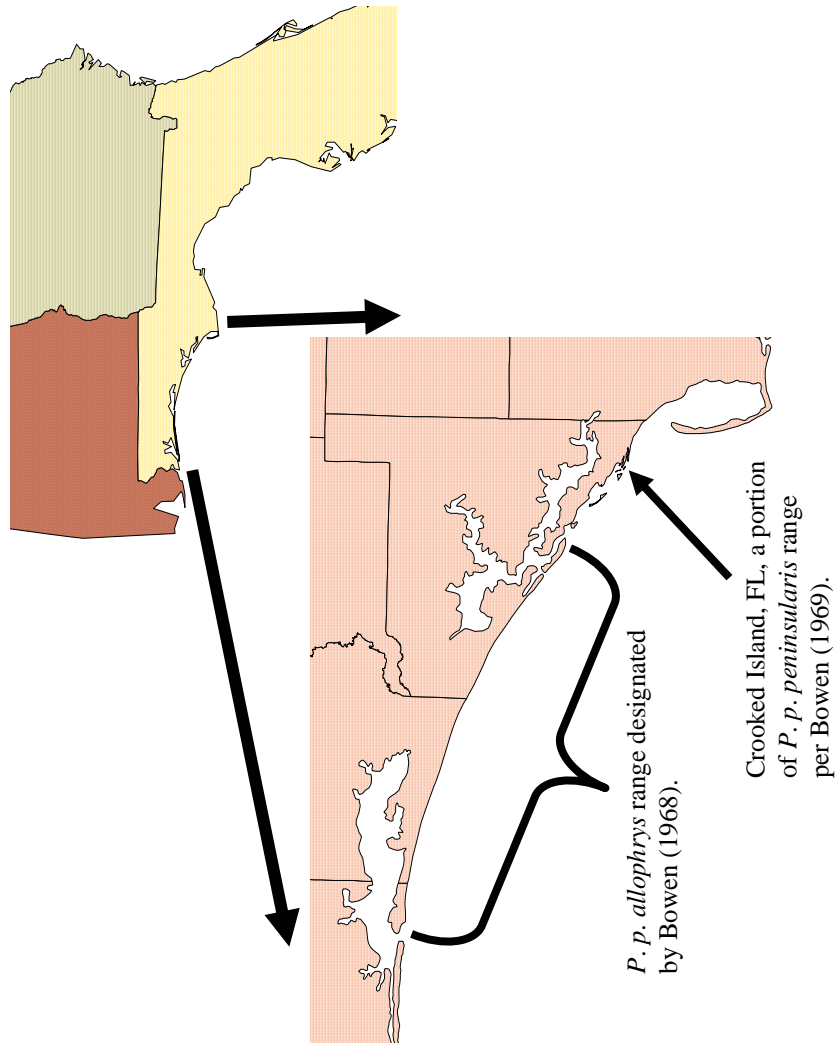


Table 1 Key to specimens abbreviations relative to species and collection site (BS = Bon Secour Wildlife Refuge, WMRS = White Mountain Research Station). The subspecific designation of some *polionotus* is uncertain as designated by ?

Number	Abbreviation	Species	Location
1	PEN02*	<i>P. p. peninsularis</i> ?	Crooked Island, FL
2	PEN03*	<i>P. p. peninsularis</i> ?	Crooked Island, FL
3	AMM01	<i>P. p. ammobates</i>	BS Perdue unit, AL
4	AMM02	<i>P. p. ammobates</i>	BS Fort Morgan Unit, AL
5	AMM03	<i>P. p. ammobates</i>	BS Fort Morgan Unit, AL
6	LCAL01	<i>P. p. polionotus</i>	Lee County, AL
7	LCAL02	<i>P. p. polionotus</i>	Lee County, AL
8	BCAL01	<i>P. p. polionotus</i>	Baldwin County, AL
9	BCAL02	<i>P. p. polionotus</i>	Baldwin County, AL
10	BCAL03	<i>P. p. polionotus</i>	Baldwin County, AL
11	BCAL04	<i>P. p. polionotus</i>	Baldwin County, AL
12	WCFL01	<i>P. p. sumneri</i> ?	Walton County, FL
13	WCFL02	<i>P. p. sumneri</i> ?	Walton County, FL
14	WCFL03	<i>P. p. sumneri</i> ?	Walton County, FL
15	OCFL01	<i>P. p. polionotus</i>	Okaloosa County, FL
16	OCFL02	<i>P. p. polionotus</i>	Okaloosa County, FL
17	LCFL01	<i>P. p. subgriseus</i>	Liberty County, FL
18	LCFL02	<i>P. p. subgriseus</i>	Liberty County, FL
19	PMB01	<i>P. maniculatus bairdii</i>	Near Ann Arbor, MI
20	PMB02	<i>P. maniculatus bairdii</i>	Near Ann Arbor, MI
21	PMB03	<i>P. maniculatus bairdii</i>	Near Ann Arbor, MI
22	ALL04	<i>P. p. allophrys</i>	Shell Island, FL
23	ALL05	<i>P. p. allophrys</i>	Shell Island, FL
24	ALL06	<i>P. p. allophrys</i>	Shell Island, FL
25	CCFL01	<i>P. p. sumneri</i> ?	Calhoun County, FL
26	OCFL03	<i>P. p. albifrons</i>	Okaloosa County, FL
27	OCFL04	<i>P. p. albifrons</i>	Okaloosa County, FL
28	OCFL05	<i>P. p. alibfrons</i>	Okaloosa County, FL
29	OCFL06	<i>P. p. griseobracatus</i>	Okaloosa County, FL
30	OCFL07	<i>P. p. griseobracatus</i>	Okaloosa County, FL
31	RCAL01	<i>P. p. polionotus</i>	Russell County, AL
32	WCFL04	<i>P. p. polionotus</i>	Walton County, FL
33	WCFL05	<i>P. p. polionotus</i>	Walton County, FL
34	WCFL06	<i>P. p. griseobracatus</i>	Walton County, FL
35	WCFL07	<i>P. p. griseobracatus</i>	Walton County, FL
36	WCFL08	<i>P. p. griseobracatus</i>	Walton County, FL
37	WCFL09	<i>P. p. griseobracatus</i>	Walton County, FL

38	TCGA06	<i>P. p. polionotus</i>	Taylor County, GA
39	TCGA01	<i>P. p. polionotus</i>	Taylor County, GA
40	TCGA03	<i>P. p. polionotus</i>	Taylor County, GA
41	TCGA04	<i>P. p. polionotus</i>	Taylor County, GA
42	TCGA05	<i>P. p. polionotus</i>	Taylor County, GA
43	ALL02*	<i>P. p. allophrys</i>	Grayton Beach, FL
44	ALL03*	<i>P. p. allophrys</i>	Grayton Beach, FL
45	ALL04*	<i>P. p. allophrys</i>	Grayton Beach, FL
46	JCFL01	<i>P. p. polionotus</i>	Jackson County, FL
47	JCFL02	<i>P. p. polionotus</i>	Jackson County, FL
48	JCFL03	<i>P. p. polionotus</i>	Jackson County, FL
49	SCFL01	<i>P. p. subgriseus</i>	Suwannee County, FL
50	SCFL02	<i>P. p. subgriseus</i>	Suwannee County, FL
51	PK01	<i>P. keeni</i>	Kittitas County, WA
52	PK02	<i>P. keeni</i>	Kittitas County, WA
53	TRI01	<i>P. p. trissyllepsis</i>	Johnson Beach, FL
54	TRI07	<i>P. p. trissyllepsis</i>	Florida Point, AL
55	TRI08	<i>P. p. trissyllepsis</i>	Florida Point, AL
56	PL103	<i>P. leucopus</i>	Unicoi County, TN
57	PMP92	<i>P. maniculatus pallescens</i>	Robertson County, TX
58	PMP93	<i>P. maniculatus pallescens</i>	Robertson County, TX
59	MCFL76	<i>P. p. subgriseus</i>	Marion County, FL
60	MCFL77	<i>P. p. subgriseus</i>	Marion County, FL
61	PG06	<i>P. gossypinus</i>	Baldwin County, AL
62	PG36	<i>P. gossypinus</i>	Baldwin County, AL
63	NIV17	<i>P. p. niveiventris</i>	Brevard County, FL
64	NIV36	<i>P. p. niveiventris</i>	Brevard County, FL
65	WCFL10	<i>P. p. roadsii</i>	Wakulla County, FL
66	WCFL11	<i>P. p. roadsii</i>	Wakulla County, FL
67	BCAL05	<i>P. p. polionotus</i>	Baldwin County, AL
68	PMS04	<i>P. maniculatus sonoriensis</i>	Near WMRS, CA
69	PMS05	<i>P. maniculatus sonoriensis</i>	Near WMRS, CA
70	LEU08	<i>P. p. leucocephalus</i>	Santa Rosa Island, FL
71	LEU15	<i>P. p. leucocephalus</i>	Santa Rosa Island, FL
72	PEN04	<i>P. p. peninsularis</i>	St. Joe State Park, FL
73	PEN05	<i>P. p. peninsularis</i>	St Joe State Park, FL
74	PEN06	<i>P. p. peninsularis</i>	St. Joe State Park, FL
75	ALL02**	<i>P. p. allophrys</i>	Topsail Hill SP, FL
76	WCFL12	<i>P. p. roadsii</i>	Wakulla County, FL
77	WCFL13	<i>P. p. roadsii</i>	Wakulla County, FL
78	MCAL01	<i>P. p. polionotus</i>	Macon County, AL

Table 2 Measures of diversity for two sets of sequence data that were used for phylogenetic analyses. The first group contained 44 sequences with *Peromyscus leucopus* and *Peromyscus gossypinus* as outgroup haplotypes. The second group contained 42 sequences and *Peromyscus keeni* as the outgroup haplotype.

Group	N	S	Mutations	Hd	Pi	k	h
<u><i>P. leucopus</i></u>							
Total	44	434	482	0.944	0.0217	52.97	39
Cyt-b:	44	193	209	0.977	0.0202	22.99	33
D-loop:	44	241	249	0.994	0.0294	28.37	36
<u><i>P. keeni</i></u>							
Total:	42	267	277	0.993	0.0141	34.54	38
Cyt-b:	42	121	125	0.974	0.0126	14.27	31
D-loop:	42	132	138	0.988	0.0198	19.21	34

Table 3 Permutation Chi-square tests of geographical association of clades and the inferred biological explanation. Inferences were based on the 14 July 2004 key (http://darwin.uvigo.es/download/geodisKey_14Jul04.pdf). Abbreviated inferences RGF, IBD, PF, LDC, and LDD are restricted gene flow, isolation by distance, past fragmentation, long distance colonization, and long distance dispersal respectively. Models were; all haplotypes, Florida peninsula haplotypes removed and peninsula removed with LCA01 and TCGA01 branching from a basal node of the beach clade.

Scenario	Clade level	Chi-square	P	Chain of inference	Inference
Model I	2-21	23.25	0.0535	1-19-202-11-17-4	RGF with IBD
	3-32	16.00	0.0203	1-2-11-17	Inconclusive outcome
	4-13	21.00	0.0321	1-19-20-2-3-5-15	PF and/or LDC
	4-44	17.33	0.2994	1-19-20-2-11-17-NO	Inconclusive outcome
	4-55	11.00	0.0782	1-2-11-12	Contiguous range expansion
	4-66	11.00	0.0433	1-19-20-2-3-4-9	Allopatric fragmentation
	5-2	20.00	0.0030	1-19-20-2-3-4	RGF with IBD
	5-3	22.00	0.0026		No significant clade distances
	Total Clade	91.50	<0.0000	1-2-3-5-6-7	RGFwith Dispersal with LDD
	Model II	2-21	23.25	0.0545	1-19-20-2-11-17-4
3-22		16.00	0.0212	1-2-11-17	Inconclusive outcome
4-13		21.00	0.0334	1-19-20-2-3-5-15	PF and/or LDC
4-34		17.33	0.2972	1-19-20-2-11-17-NO	Inconclusive outcome
4-45		11.00	0.0755	1-2-11-12	Contiguous range expansion
4-56		11.00	0.0457	1-19-20-2-3-4-9	Allopatric fragmentation
5-1		40.54	0.0082		No significant clade distances
5-2		22.00	0.0023		No significant clade distances
Total Clade		37.59	0.0015		No significant clade distances

Model III	2-21	23.25	0.0542	1-19-20-2-11-17-4	RGF with IBD
	3-22	14.00	0.0849	1-2-11-17	Inconclusive outcome
	4-13	21.00	0.0292	1-19-20-2-3-5-15	PF and/or LDC
	4-24	17.33	0.2960	1-19-20-2-11-17-NO	Inconclusive outcome
	4-45	11.00	0.0794	1-2-11-12	Contiguous range expansion
	4-56	11.00	0.0441	1-19-20-2-3-4-9	Allopatric isolation
	5-2	49.00	0.0001	1-2-3-4-9-NO	No significant clade distances
	Total Clade	35.65	0.0039		No significant clade distances

Table 4 Measures of diversity for clades estimated by maximum likelihood using the combined cytochrome-b and D-loop regions. Measurements include S = the number of variable sites, Eta = the number of mutations, Hd = haplotype diversity, π = nucleotide diversity, k = average number of nucleotide differences, h = the number of haplotypes. Clade beach* was without haplotypes LCAL01 and TCGA01. Clade complete* was without haplotypes from the Florida peninsula.

Clade	N	S	Eta	Hd	π	k	h	Theta
<u>Beach</u>								
Total:	23	57	59	0.963 ±0.02	0.0050 ±0.0004	12.28	15	0.0064
Cyt-b:	23	19	19	0.950 ±0.02	0.0033 ±0.0004	3.70	13	0.0044
D-loop:	23	34	36	0.953 ±0.02	0.0081 ±0.0006	8.05	13	0.0096
<u>Inland I</u>								
Total:	12	34	34	0.955 ±0.05	0.0036 ±0.0008	8.73	9	0.0046
Cyt-b:	12	16	16	0.939 ±0.05	0.0034 ±0.0010	3.84	8	0.0047
D-loop:	12	14	14	0.924 ±0.06	0.0042 ±0.0009	4.09	8	0.0048
<u>Inland II</u>								
Total:	11	23	23	0.855 ±0.09	0.0026 ±0.0008	6.47	6	0.0032
Cyt-b:	11	5	5	0.600 ±0.15	0.0012 ±0.0004	1.31	4	0.0015
D-loop:	11	17	17	0.818 ±0.08	0.0051 ±0.0017	4.20	5	0.0060
<u>Beach*</u>								
Total:	22	42	44	0.957 ±0.02	0.0044 ±0.0003	10.74	13	0.0049
Cyt-b:	22	12	12	0.939 ±0.02	0.0026 ±0.0002	2.98	11	0.0029
D-loop:	22	26	28	0.944 ±0.02	0.0074 ±0.0005	7.16	11	0.0079
<u>Complete</u>								
Total:	55	122	125	0.984 ±0.01	0.0074 ±0.0002	18.12	35	0.0112
Cyt-b:	55	45	45	0.969 ±0.01	0.0052 ±0.0003	5.91	28	0.0087
D-loop:	55	67	70	0.979 ±0.01	0.0120 ±0.0005	11.60	31	0.0158
<u>Complete*</u>								
Total:	48	103	106	0.980 ±0.01	0.0070 ±0.0002	17.20	30	0.0098
Cyt-b:	48	38	38	0.964 ±0.01	0.0051 ±0.0003	5.83	25	0.0075
D-loop:	48	57	60	0.974 ±0.01	0.0112 ±0.0004	10.84	26	0.0139

Table 5 Measures of diversity for 5th level clades estimated by the model I nested clade analysis. Measurements include S = the number of variable sites, Eta = the number of mutations, Hd = haplotype diversity, π = nucleotide diversity, k = average number of nucleotide differences, h = the number of haplotypes.

Clade	N	S	Eta	Hd	π	k	h	Theta
<u>Clade 5-1</u>								
Total:	23	63	63	0.957 \pm 0.03	0.0059 \pm 0.0004	14.47	15	0.0070
Cyt-b:	23	23	23	0.897 \pm 0.05	0.0044 \pm 0.0005	4.98	12	0.0055
D-loop:	23	35	35	0.941 \pm 0.03	0.0093 \pm 0.0007	8.98	13	0.0098
<u>Clade 5-2</u>								
Total:	10	46	46	0.933 \pm 0.06	0.0070 \pm 0.0006	17.04	7	0.0066
Cyt-b:	10	15	15	0.867 \pm 0.07	0.0048 \pm 0.0006	5.42	5	0.0047
D-loop:	10	29	29	0.933 \pm 0.06	0.0112 \pm 0.0011	10.91	7	0.0106
<u>Clade 5-3</u>								
Total:	22	42	44	0.957 \pm 0.02	0.0044 \pm 0.0003	10.74	13	0.0049
Cyt-b:	22	12	12	0.939 \pm 0.02	0.0026 \pm 0.0002	2.98	11	0.0029
D-loop:	22	20	28	0.944 \pm 0.02	0.0074 \pm 0.0005	7.16	11	0.0079

Table 6 Measures of diversity for 5th level clades estimated by the model II nested clade analysis. Measurements include S = the number of variable sites, Eta = the number of mutations, Hd = haplotype diversity, π = nucleotide diversity, k = average number of nucleotide differences, h = the number of haplotypes.

Clade	N	S	Eta	Hd	π	k	h	Theta
<u>Clade 5-1</u>								
Total:	26	75	75	0.963 \pm 0.02	0.0065 \pm 0.0004	15.79	17	0.0080
Cyt-b:	26	28	28	0.917 \pm 0.04	0.0048 \pm 0.0005	5.50	14	0.0065
D-loop:	26	42	42	0.951 \pm 0.02	0.0101 \pm 0.0007	9.84	15	0.0113
<u>Clade 5-2</u>								
Total:	22	42	44	0.957 \pm 0.02	0.0044 \pm 0.0003	10.74	13	0.0049
Cyt-b:	22	12	12	0.939 \pm 0.02	0.0026 \pm 0.0002	2.98	11	0.0029
D-loop:	22	26	28	0.944 \pm 0.02	0.0074 \pm 0.0005	7.16	11	0.0079

Table 7 Measures of diversity for 5th level clades estimated by the model III nested clade analysis. Measurements include S = the number of variable sites, Eta = the number of mutations, Hd = haplotype diversity, π = nucleotide diversity, k = average number of nucleotide differences, h = the number of haplotypes.

Clade	N	S	Eta	Hd	π	k	h	Theta
<u>Clade 5-1</u>								
Total:	23	63	63	0.957 \pm 0.03	0.0059 \pm 0.0004	14.47	15	0.0070
Cyt-b:	23	23	23	0.897 \pm 0.05	0.0044 \pm 0.0005	4.98	12	0.0055
D-loop:	23	36	36	0.941 \pm 0.03	0.0092 \pm 0.0007	9.15	13	0.0098
<u>Clade 5-2</u>								
Total:	25	57	59	0.963 \pm 0.02	0.0050 \pm 0.0004	12.28	15	0.0064
Cyt-b:	25	19	19	0.950 \pm 0.02	0.0033 \pm 0.0004	3.70	13	0.0044
D-loop:	25	34	36	0.953 \pm 0.02	0.0081 \pm 0.0006	8.05	13	0.0096

Table 8 Measures of diversity for clades estimated by maximum likelihood using the combined cytochrome-b and D-loop regions. Measurements include S = the number of variable sites, Eta = the number of mutations, Hd = haplotype diversity, π = nucleotide diversity, k = average number of nucleotide differences, h = the number of haplotypes. Clade beach* was without haplotypes LCAL01 and TCGA01. Clade complete* was without haplotypes from the Florida peninsula. For Fu and Li's D and F tests all P values were > 0.10.

Clade	Fu and Li's D	Fu and Li's F	McDonald-Kreitman
<u>Complete</u>			
Total:	-1.8272	-1.9972	
Cyt-b:	-1.4629	-1.8123	P-value: 0.0494
D-loop:	-1.3800	-1.4748	
<u>Beach</u>			
Total:	-1.4779	-1.6929	
Cyt-b:	-1.3924	-1.6934	P-value: 0.0585
D-loop:	-1.1325	-1.2717	
<u>Inland I</u>			
Total:	-0.6456	-0.9265	
Cyt-b:	-0.5636	-0.9037	P-value: 0.1956
D-loop:	-0.5040	-0.6088	
<u>Inland II</u>			
Total:	-0.2131	-0.4770	
Cyt-b:	-0.5795	-0.9078	P-value: 0.3909
D-loop:	0.1495	-0.0561	
<u>Beach*</u>			
Total:	-1.0777	-1.1911	
Cyt-b:	-1.0223	-1.1669	P-value:0.0771
D-loop:	-0.6596	-0.7183	
<u>Complete*</u>			
Total:	-1.6520	-1.7600	
Cyt-b:	-1.5003	-1.7170	P-value: 0.0460
D-loop:	-1.2056	-1.2479	

Table 9 Fu and Li's D and F tests for *Peromyscus polionotus* clades or groups with other *Peromyscus polionotus* as outgroup haplotypes. Clade beach* was without haplotypes LCAL01 and TCGA01. Significance is indicated by *.

Clade	Fu and Li's D	Fu and Li's F
<hr/>		
<u>Beach</u>		
(inland I)		
Total:	-1.7239	-1.8771
Cyt-b:	-2.0283	-2.2241
D-loop:	-1.1532	-1.2666
<hr/>		
<u>Beach*</u>		
(inland I)		
Total:	-1.3985	-1.4496
Cyt-b:	-1.4650	-1.5427
D-loop:	-0.9416	-0.9486
<hr/>		
<u>Beach</u>		
(inland II)		
Total:	-1.4800	-1.6720
Cyt-b:	-2.3462*	-2.4894*
D-loop:	-0.5711	-0.7845
<hr/>		
<u>Beach*</u>		
(inland II)		
Total:	-0.9366	-1.0633
Cyt-b:	-1.4650	-1.5427
D-loop:	-0.2361	-0.3557
<hr/>		
<u>Inland I</u>		
(inland II)		
Total:	-1.1633	-1.3696
Cyt-b:	-1.2261	-1.4749
D-loop:	-0.5040	-0.6088

Table 10 Fu and Li's D* and F* and Tajima's D tests for each clade or group. Within each clade or group the complete sequence and each major gene were tested. Clade beach* was without haplotypes LCAL01 and TCGA01. Clade complete* is without Florida peninsula haplotypes. All P values were > 0.05.

Clade	Singletons	Fu and Li's D*	Fu and Li's F*	Tajima's D
Beach				
Total:	32	-1.3361	-1.4797	-1.1319
Cyt-b:	13	-1.8340	-1.9784	-1.4039
D-loop:	16	-0.8193	-0.9389	-0.7910
Beach*				
Total:	22	-0.9734	-1.0399	-0.7199
Cyt-b:	7	-1.1252	-1.02023	-0.8395
D-loop:	12	-0.6400	-0.6649	-0.4155
Inland I				
Total:	18	-0.7489	-0.9336	-1.0174
Cyt-b:	9	-0.8461	-1.0655	-1.1938
D-loop:	6	-0.2790	-0.3830	-0.5016
Inland II				
Total:	13	-0.7920	-0.9010	-0.8031
Cyt-b:	3	-0.7638	-0.8976	-0.8933
D-loop:	9	-0.6271	-0.7125	-0.6345
Complete				
Total:	55	-1.9113	-2.0062	-1.2807
Cyt-b:	22	-2.0651	-2.2103	-1.4799
D-loop:	88	-1.7169	-2.0280	-0.8759
Complete*				
Total:	46	-1.7262	-1.7634	-1.0372
Cyt-b:	19	-1.9855	-2.0343	-1.1998
D-loop:	21	-1.0223	-1.0629	-0.6566

Table 11 Mitochondrial DNA polymorphism within different *Peromyscus polionotus* clades. Coalescent based maximum likelihood estimates of N_e , theta (θ), and exponential growth rate (95% CI) under models of constant size and growth as implemented by Kuhner *et al.* (1998). Clade beach* was without haplotypes LCA101 and TCGA01. Clade complete* was without Florida Peninsula haplotypes.

	Beach	Beach*	Inland I	Inland II	Complete	Complete*
Sample Size	17	15	12	11	44	40
Base pairs	2449	2449	2449	2449	2449	2449
Haplotypes	15	13	9	6	34	30
Polymorphic sites	57	42	34	23	122	103
?ML (constant size)	0.0138	0.0099	0.0059	0.0030	0.0292	0.0226
Ne (constant size)	1256906	899631	533476	269146	2657062	2051542
?ML (growth)	0.0481 ±0.0115	0.0311 ±0.0081	0.0091 ±0.0022	0.0029 ±0.0007	0.0563 ±0.0069	0.0433 ±0.0058
Ne (growth)	4 376 909	2 830 090	826 454	259 272	5 120 272	3 939 818
Growth rate	1066.39 ±172.95	1212.47 ±230.51	469.13 ±173.58	-30.24 ±206.18	524.24 ±68.65	578.52 ±83.65
Substitution rate (μ)	1.1 X 10 ⁻⁸	1.1 X 10 ⁻⁸	1.1 X 10 ⁻⁸	1.1 X 10 ⁻⁸	1.1 X 10 ⁻⁸	1.1 X 10 ⁻⁸
Models agree	No	No	Yes	Yes	No	No
?ML (constant)	0.008 - 0.0251	0.0055 - 0.0188	0.0029 - 0.0126	0.0014 - 0.0069	0.0209 - 0.0419	0.0157 - 0.0331

Chapter Two

Spatiotemporal Dynamics of Gene Diversity in the Alabama Beach Mouse (*Peromyscus polionotus ammobates*)

Introduction

The presence of genetic variation is an essential prerequisite for the evolutionary process. In order for any species to evolve, it must both accrue and maintain variation. In natural systems, this requirement represents an obstacle to evolution. Two key mechanisms that drive the evolutionary process, natural selection and genetic drift, both generally result in the removal of allelic variants. On an evolutionary timescale, these losses can be partially balanced by mutation, the ultimate source of all new variation. But, at best, the accumulation of variation via mutation is a slow process that contributes little to the genomic variance present at any given moment. In fact, as demonstrated by Fisher (1930), the ultimate fate of 99% of all new mutations is eventual loss from the gene pool. Clearly under these constraints, the evolution of mechanisms for genetic management is, for most species, as critical to long-term evolutionary success as are the classical studied markers of reproductive success. What avenues might be open to a species for gene pool “management”, given that the goal is to slow the rate of decay of

variation? If we view genetic variation as a resource that a species is attempting to protect, then biology provides us with one immediate answer. The most common approach used by any biological entity to conserve a resource, be it a community / a guild / a population, or a single cell, is to partition that resource. Isolation of the resource into separate subunits for management, while not necessarily the best approach in some cases, is clearly a natural response to many biological problems. The management of gene pool diversity appears to adhere to this rule. For example, the partitioning of the genetic blueprint into separate chromosomes by the earliest cellular forms eventually led to meiosis, recombination, and sexual reproduction; mechanisms which collectively work as one of the most effective variation generators known. At every level, this pattern continues. Many organisms partition their gene pools into male and female units, where environmental and physiological effects can be managed separately. These separations also provide the basis for higher-level units that are formed by organisms such as kin groups, breeding groups, pods, harems, coteries, etc, each representing a viable, additional subdivision of the gene pool (Dobson 1998). Following from these observations, organisms should be expected to produce and maintain systems that partition genotypes. As do many others, I view these systems as “traits”, subject to modification and refinement by the evolutionary process.

Contemporary concepts of genetic structuring through partitioning of genotypes are direct descendents of the theoretical framework established by Sewall Wright (1931, 1951, 1969, 1978). Wright recognized and promoted the importance of population subdivision. Theoretically, in large panmictic populations, the primary determinant of genetic variation is selection. However, as populations become smaller, such as through

partitioning or otherwise depart from panmixis, other factors can have a significant effect on genetic variation (Wright 1978). Primary of these is genetic drift, which, along with the related mechanisms of inbreeding, demographic bottlenecks, and founder events, tends to reduce genetic variation. As a legacy from Wright, population models have proven to be crucial in the study of evolution and population genetics. A principle question arising among these models is whether a population functions as a single entity moving along one evolutionary path, or as an amalgamation comprised of multiple entities exploring different evolutionary pathways. Understanding how populations are genetically structured is a vital step towards understanding and predicting the forces that shape populations of organisms (Wright 1931).

As the theoretical base for population models grew, the importance of spatial variance in migration among subpopulations and its genetic consequences were soon realized (Giles & Goudet 1997). This knowledge led to the development of a set of dispersal-based models (Hamrick & Nason 1996). One, the continent-island model, represents what is essentially one-way migration. This model is structured as a single large population (continent) and a small population (island) where migration occurs from the continent to the island. Dependent upon the amount of migration over-time, the island population is predicted to assume the allele frequency of the continent population. Because of their value to population genetics, other models followed, these include Wright's (1931) island model, the stepping-stone model (Kimura 1955; Kimura & Weiss 1964), and the isolation-by-distance model (Wright 1943). These models and their descendants vary in complexity, represent different types of population structure and begin to account for the possibility of nonrandom mating (Gile & Goudet 1997).

Wright's island model assumes that all populations are equal in size and contribute equally to the migrant pool. Spatially, each population is effectively equally close to all other populations; thus, each population receives a proportionate number of migrants. This model moves the complex of populations towards an equilibrium frequency.

Kimura (1955, 1964) proposed the stepping-stone model to incorporate the effects of spatial variance in migration rate. It assumes that migration is restricted to adjacent populations. Thus, a new allele or mutation could move to an adjacent population in one generation and move to a second population in the next generation. This model creates the greatest amount of genetic differentiation among the subpopulations. While the previous two models are composed of subpopulations that are panmictic, Wright developed the isolation-by-distance model (IBD) to account for population assemblages in which mating is nonrandom (Hamrick & Nason 1996). In the IBD model, migration occurs among local communities in a continuously distributed population. The IBD model is intermediate to the stepping stone model and the island model in producing levels of within population variation (Hamrick & Nason 1996). The three models discussed above do share important assumptions. Random mating is assumed to occur in each subpopulation or community and effective population size is expected to remain constant. Typically the models also assume that no selection or mutation occurs. Lastly, the basic models describe diploid, sexually reproducing organisms with nonoverlapping generations.

Dispersal models have continued to evolve and to incorporate more realistic assumptions. Wright (1940) suggested that extinctions of subpopulations might increase between population variation. Following this logic, Levins (1969), developed the

concept of a metapopulation. Within the metapopulation model, space is discrete and composed of suitable and unsuitable habitat. Extinction and recolonization on patches of suitable habitat is an essential component of metapopulation theory. Recolonization of patches is important in the overall genetic structure of the populations. The effects of recolonization on genetic structure depend on whether all populations or a single population contributed migrants. Slatkin (1977) modified Levins basic model to account for variation in patch size, variance of migrants between occupied patches, and to acknowledge that vacant patches may or may not be immediately recolonized (Giles & Goudet 1997). While metapopulation theory has evolved dramatically since its inception, its primary focus continues to be between subpopulation dynamics as driven by migration. Regardless of the assumptions of each model, they are all simplifications of spatial genetic structure.

Traditionally, empirical evaluations of spatial partitioning have focused on situations where clear patterns of partitioning existed (e. g. environmental barriers and mating systems). More recently, however, techniques such as spatial autocorrelation (Sokal & Oden 1978a, b) and Mantel's Test (Smouse *et al.* 1986) along with population assignment methods (Paetkau *et al.* 1995; Waser & Strobeck 1998; Banks & Eichert 2000) are increasingly being applied to hypervariable microsatellite data sets. Thus, detection of microgeographic genetic structuring along with assignment of individuals to their original population is now quite possible. Using autocorrelation analysis, populations characterized by limited dispersal and the lack of selection will demonstrate positive genetic association within smaller distance classes before becoming negative as distance classes increase (Sokal & Wartenberg 1983; Smouse & Peakall 1999).

Populations that are subdivided into microgeographic groups might be characterized by increased inbreeding and homozygosity and distinguished by microgeographic assemblages of like genotypes (Turner *et al.* 1982). However, little empirical work has focused on potential breeding units within a population that is not distinctly subdivided by a habitat matrix. Arguably, within contiguous populations, semi-independent breeding units may occur that are critical to the gene dynamics of populations. Nonrandom mating and individual dispersal events would be the major factors affecting the genetic structuring within such a population.

Theoretically, subdivision of a population can impact the maintenance of genetic diversity over time (Chesser *et al.* 1980; Karlin & Campbell 1980). Genetic partitioning is also hypothesized to increase the ability of a species to adapt to environmental changes more quickly (Wright 1969, 1978). Thus, species should be expected to evolve mechanisms to partition genotypes to counter factors that can act to reduce overall variation. According to Waser (1993), populations are genetically structured by the coevolution of mating systems, dispersal behavior, mate choice, and the fitness effects of mating. Studies have demonstrated that both spatial segregation and breeding structure can be important causal agents of genotype partitioning (Chesser 1991a; Chesser 1998; Gerlach & Musolf 2000; Tiedemann *et al.* 2000). However, many populations exist in more contiguous habitats than are normally considered in genetical structure studies.

The premise underlying my research is that within contiguous habitats, microgeographic structure can mimic higher-order breeding systems (coterries, harems, etc.) such that alleles are partitioned and genetic diversity is maintained at higher levels than would otherwise be expected. Most mammal species exhibit some type of

population structuring (Greenwood 1980). This has been demonstrated for house mice, *Mus musculus*, (Selander 1970a) deer mice, *Peromyscus maniculatus*, (Wright 1978) pocket gophers, *Thomomys bottae*, (Patton & Yang 1977) prairie dogs, *Cynomys ludovicianus*, (Chesser 1983) and the Australian bush rat, *Rattus fuscipes*, (Peakall *et al.* 2003). The reoccurrence of partitioning among species suggests that there are likely to be multiple mechanisms (dispersal patterns, single sex clusters, etc.) and, thus, multiple scenarios that favor the formation of such elements. One model (Isolation by Distance) invoked to explain such formations is characterized by short dispersal differences and nonrandom mating inferring some level of inbreeding may result (Wright 1943). Mammals, in particular, because of low reproductive rates, may benefit from maintaining high degrees of relatedness within social groups (Chesser 1998). Inbreeding may serve to increase the proportion of an individual's genome that is passed on to its offspring, and, if dispersal costs are high, it is potentially beneficial for related individuals to mate (Bengtsson 1978). Thus, low levels of inbreeding may be less costly than dispersal. Also, gene combinations that are selectively advantageous may increase in frequency more quickly in small inbreeding groups rather than in larger randomly mating populations (Slatkin 1976).

Historically, allozymes have been used to investigate genetic structuring within a population. However, allozymes are probably best suited for detection of structure on a larger scale or where some discernable form of isolation among populations is present. As might be expected, some of these studies have detected the presence of genetic structure on a local scale while others have not. Waser & Elliott (1991) failed to detect local structure within a population of bannertailed kangaroo rats (*Dipodomys spectabilis*).

However, van Staaen *et al.* (1996) demonstrated substantial structure within a population of Richardson's ground squirrels (*Spermophilus richardsonii*). A behavioral characteristic of Richardson's ground squirrels is philopatry by females. The clustering of related females strongly suggests that genetic structure will be present. While there are multiple means by which species might develop structure (behavioral, social, dispersal) rarely have populations been temporally examined to determine if and how structure is influenced temporally. However, Scribner & Chesser (1993) investigated genetic structuring in the eastern cottontail (*Sylvilagus floridanus*) and demonstrated significant nonrandom genetic structuring across multiple time periods. They also observed a cyclic temporal pattern where during some time periods autocorrelation was less evident. Importantly, spatial autocorrelation of genotypes was less evident during the winter season. This result was attributed to the winter season being the prereproductive season. While genetic structure has been demonstrated on a local scale, microgeographic structuring was difficult to assess. Recent application of large numbers of hypervariable microsatellite loci as markers in ecological studies have substantially increased the precision by which questions concerning spatial structure can be addressed. Microsatellite markers, found abundantly within the genome and possessing a high mutation rate, are now being applied to the investigation of microgeographic genetic structuring. Microsatellites have been used to investigate spatial structure at a fine-scale with some success in mammals, birds, snakes and fire ants, *Solenopsis invicta*, (Peakall *et al.* 2003; Albrecht *et al.* 2001; Double *et al.* 2000; Gibbs *et al.* 1997; Ross *et al.* 1997). Also, Double *et al.* (2005) used microsatellites to show sex-biased dispersal and positive spatial structure among males within a population of the superb fairy-wren (*Malurus*

cyaneus). Increased detection of genetic structuring within populations is beginning to provide key insights into such evolutionary factors as dispersal patterns. In particular, this new wave of data is fostering empirical examination of long-standing theories regarding the partitioning of genotypes as a means of preserving or slowing the rate of loss of global genetic variance (Chesser *et al.* 1980; Karlin & Campbell 1980). Rohlfs & Schnell (1971) used a single-locus two-allele model and showed local genetic differentiation can occur in a contiguous population. Models of noncontiguous populations have also yielded evidence for this critical element of spatial structuring (Maruyama 1970; Christensen 1974; Slatkin 1985).

My study animal, beach mice (*Peromyscus polionotus* ssp.) has not been reported to be territorial, form single sex clusters, or exhibit other characteristics that would normally drive behavioral partitioning of genotypes. All evidence to date indicates that beach mice are monogamous (Foltz 1981; Swilling & Wooten 2002). Monogamy may produce varying effects on population structure because it tends to limit reproductive variation among individuals. Contributing to their uniqueness are the habitat associations of beach mice. Along the Gulf Coast of Alabama, beachfront habitat is long, linear, and seemingly contained few areas that beach mice did not inhabit. Until recent decades, beach mouse populations appear to have existed in this semicontiguous habitat where spatial separation (i.e. a coarse habitat matrix) was not the defining characteristic. Thus, geographic boundaries would not seem to be the foremost agent in fine-scale genetic structuring within local beach mouse populations. Temporal variance is however a significant element among beach mouse populations as they experience pronounced demographic annual fluctuations that are compounded by cyclic patterns of tropical

storms and hurricanes that can reduce population size for several years. Such fluctuations in population size are known to have significant effects on genetic variation (Zhang *et al.* 2004). The recovery period following a hurricane Opal for the segment of the beach mouse population representing my study site was approximately four years. Theory predicts that the amount of genetic variation remaining in the population following a bottleneck is a function of the severity of the bottleneck and the rate of demographic change (Nei *et al.* 1975). Compounding the annual cycle, is the fact that a major hurricane affects the area, on average, every 10 years. Thus, bottlenecks arise through an annual cycle as well as through periodic hurricanes. This combination of conditions (i. e. cyclic bottleneck, behavioral tendencies, semicontiguous habitat) where each tends to elevate the rate of genetic decay gave rise to my central question, namely, what options are available to populations of beach mice to aid in mitigating the loss of genetic variance? In fact, it is due to such conditions that I believe beach mice (*Peromyscus polionotus* ssp.) represent an appropriate model organism for use in examining questions concerning genetic partitioning and the rate of loss of genetic variance. If partitioning occurs in a “system” such as beach mice it indicates that a level of partitioning other than that defined by spatial boundaries and mating systems (i.e. single sex clusters) can develop.

It was my supposition that the dynamics of gene diversity within beach mice populations are not panmictic or metapopulation but do share characteristics with each model. Within these insular populations experiencing regular and repeated factors that tend to reduce genetic variation, temporal partitioning of genotypes may occur if groups are formed by low dispersal rates, distances and some toleration of inbreeding. Under

these conditions, one might predict that, due to chance alone, individual familial lineages would be established across the habitat. Within any local region of a beach mouse population, structural population units are likely to be comprised of closely related individuals. Genetic structuring would be maintained through social dynamics, dispersal patterns, and, to a lesser degree, broken habitat. Within this model, local breeding clusters are familial and exist as smaller, interconnected units within the population. Genetic partitioning exists due to the temporal formation of familial breeding units on a microgeographic scale. An excess of homozygous individuals would be expected to characterize these familial lineages. Periodically, catastrophic events (e. g. hurricanes, tropical storms) increase mortality thus breaking down familial lineages and forcing individuals to seek new mating opportunities. If genotype partitioning exists, shortly following such events as hurricanes individual heterozygosity should increase, however over time familial lineages will reform with the genetic structuring again being characterized by an excess of homozygotes. The increase in heterozygosity likely represents “isolate breaking”. Spatial autocorrelation should be significantly positive prior to spikes in heterozygosity but significantly positive during spikes in heterozygosity. Wooten and Holler (1998) observed such an increase in heterozygosity following hurricane Opal within this population of Alabama beach mice. Their observation was based on three loci and while the pattern appeared to be real, adding loci would provide a more definitive test.

Here, I investigated not only genotype partitioning, but also the potential for this hypothesized system of genotype partitioning to be a significant component of the evolutionary process. Specifically, I examined how gene pool management occurs in a

natural population that is subject to multiple, severe events known to increase genetic decay. An important twist to this research is that my model species, *Peromyscus polionotus ammobates*, operates in a wildly unstable environment while maintaining a monogamous mating system, and no traditional breeding structures, within a locally contiguous habitat. First, I investigated predicted microgeographic spatiotemporal partitioning of genotypes based primarily on social dynamics (monogamy, increased inbreeding levels) and individual dispersal patterns exhibited by *P. polionotus*. Second, I investigated the effect of spatiotemporal gene partitioning on the rate of loss of genetic variation. My overall goal was to test the hypothesis that microgeographic spatial structuring alone could reduce the observed rate of genetic decay relative to a predicted rate. More globally, it is my contention that such structure plays a critical role as the core modulator of gene pool composition.

Methods

Tissue Collection

Tissue samples were obtained from mice captured on two permanent grids. Established in fall of 1994, the grids consisted of 25 stations set at 20 m intervals east to west and 12-13 stations at 20 m intervals extending south to north (Fig. 1). The two grids (Gazebo and Vet Village) began in the foreslope of the primary dunes and extended north into scrub habitat and were separated east and west by approximately 620 m (Swilling *et al.* 1998). Two Sherman live traps baited with rolled oats were placed at each station. Captured mice were weighed, sexed, aged (adult or subadult), and reproductive condition determined (scrotal or nonscrotal for males; not pregnant, pregnant, lactating, or pregnant and lactating for females). Each mouse was assigned a unique number for individual

identification. Mice were released at the capture site immediately after data collection. Traps were opened in the late afternoon and checked for captures prior to dawn unless temperatures were expected to drop below 13° C. All traps were left closed after predawn checking. Cotton was used inside traps to provide insulation during cool nights. Trapping periods were designed to run for five consecutive nights. However, trapping was stopped for nights of rain and/or temperatures deemed to be too cold. Interrupted trapping periods were resumed after passing of inclement weather.

For years 1995, and 1996 and half the year of 1997, the grids were trapped approximately bimonthly. For 1995 and 1996, I used tissue collected during February, April and June on Gazebo grid and March, April and June on Vet Village grid. Only a single trapping period for both grids from 1997 (March) was examined. In fall of 1997, both grids were reduced in size. This modification consisted of removing seven north/south lines from the western section of Gazebo grid and seven from the eastern section of Vet Village grid. The result was additional spacing of approximately 280 m between the two grids, extending the total separation to approximately 920 m (Fig. 2). Thus, all trapping periods from late 1997-2002 were conducted on smaller grids spaced farther apart. Only spring trapping periods from 1998 and 1999 were examined. For 2000 and 2001, both a spring and fall trapping period were available, and, from 2002, a single spring trapping period was available for analysis. The final data set represented 14 trapping periods spanning eight years (1995-2002).

DNA preparation

DNA was extracted from tissue samples using Qiagen DNeasy® tissue kits. The Polymerase Chain Reaction (PCR) method was used to amplify specific regions of DNA

to determine the nucleotide sequence and/or fragment length. For PCR reactions, Qiagen Taq PCR Core Kit and Promega PCR Nucleotide Mix were used. Reactions were run with a Perkin Elmer GeneAmp PCR System 2400, a Hybaid Omn-E HBTRE02, or a MJ Research PTC-200. Nucleotide sequence determination and fragment analysis was completed using an ABI Prism® 3100 Genetic Analyzer. GENESCAN® analysis software along with GENOTYPER® software was used for fragment scoring. Several of the microsatellites were sequenced to be sure of amplification of the proper alleles. BIOEDIT v5.0.9 (Hall 1999) software was used primarily to manipulate nucleotide sequence data.

Polymerase chain reactions (PCR) were conducted with 11 primer sets known to amplify dinucleotide repeat regions. These 11 loci were selected after testing 24 primer sets. Some of the initial primer sets did not amplify or generated inconsistent peaks where scoring was not reliable. The 11 loci that amplified and scored consistently were Ppa-01, Ppa-12 and Ppa-46 (Wooten *et al.* 1999), Pml-03, Pml-04, Pml-06 and Pml-11 (Chirhart *et al.* 2000) and PO3-85 and PO3-68 (Prince *et al.* 2002). Also, two primer sets, PO-25 (AF380236) and PO-71 (AF380240), were obtained directly from NCBI (Direct submission; Prince *et al.* 2001). Forward primers contained fluorescent dye-labeled either 5' 6-FAM™, 5' HEX™, and 5' NED™. Each primer set consisted of 25 µL total volume and contained 12.6-54.7 ng DNA, 0.25 µM primer, 0.5 mM MgCl₂, 100-µM dNTPs, 1X buffer, 1.0 U of *Taq*. PCR reactions were conducted using Taq PCR Core Kit (Qiagen®, Valencia, California) and PCR Nucleotide Mix (Promega®, Madison, Wisconsin). Characterization of the 11 microsatellite loci is reported in Table 1. Conformation of PCR product was determined by running electrophoresis on a 2% agarose gel at 75 milli amps and viewing under UV light. Fragment analysis was

conducted using an ABI 3100 Genetic Analyzer (Applied Biosystems, Foster City, CA) located at the Auburn University Genomics and Sequencing Lab (Auburn University). A total of 1085 individuals were examined at 11 loci resulting in 11 935 individual genotypes.

Statistical Analyses

Data from each trapping period for Gazebo and Vet Village grids were analyzed independently. Also, trapping periods from each grid covering approximately the same time period were combined and analyzed as a single population. Exact tests for deviations from Hardy-Weinberg equilibrium were performed using GENEPOP on the Web (Raymond & Rousset 1995). The Markov chain method (Guo & Thompson 1992) with the parameters dememorization, iterations set at 1000 and batches set at 100 were used to estimate P-values. GENEPOP was also used to test for heterozygote deficiency with dememorization and iterations set at 10 000 and batches set at 1000. Population differentiation as estimated by Analysis of molecular variance (AMOVA) (Excoffier *et al.* 1992), F_{ST} and R_{ST} values were calculated using the program ARLEQUIN version 2.0 (Schneider *et al.* 2000). Significance tests were based on 1000 permutations. ARLEQUIN performs an AMOVA based on the method of Excoffier *et al.* (1992). Differentiation was tested between grids, as well as among select trapping periods on individual grids. These models allow for the grids to be split into different subpopulations for analysis of differentiation within grids. Individual grid analyses were conducted by dividing each grid into four quadrants reflecting the four directional corners, north/south, and east/west (Fig. 1). Thus, one analysis consisted of four subpopulations (four corners) while the other two consisted of two populations (north/south, east/west). Also, for comparison,

twice I randomly assigned individuals into the same quadrants (four corners, north/south, east/west). Standard population genetic parameters (number of alleles, allele frequency, observed and expected heterozygosity, and fixation index) were calculated using the software program GENALEX (Peakall & Smouse 2005). GENALEX was also used to investigate spatial genetic structuring and conduct Mantel tests. For spatial genetic structure analysis, the method of Smouse & Peakall (1999) was used. This approach employs a multivariate method that combines alleles and loci rather than analyzing a single locus at a time. Spatial autocorrelation was tested at multiple distance classes within and among sites. To determine significance, the approach of Peakall *et al.* (2003) was used. Mantel tests are designed to test the correlation between two matrices. The two matrices used in GENALEX are genetic and geographic distance. For conducting Mantel tests GENALEX follows the methods of Smouse & Long (1992) and Smouse *et al.* (1986). Significance of the Mantel statistics were determined using 999 permutations. Population assignment tests were conducted using WHICHRUN version 4.1 (Banks & Eichert 2000). Population assignment was based on the jackknife method. The jackknife method samples an individual while recalculating allele frequencies without the previously sampled genotypes and then estimates the most likely source of that individual. The computer program POPGENE (version 1.32; University of Alberta, Edmonton, Canada) was used to calculate F_{IS} (Wright 1978). Program SAS (SAS Institute 2000) was used to compute means, standard errors, and random assignment of individuals. The program MICRO-CHECKER (van Oosterhout *et al.* 2004) was used to test for null alleles (nonamplifying alleles). MICRO-CHECKER uses the methods of Brookfield (1996) and others to determine if null alleles may be present. Two equations were used

to predict heterozygosity as a function of time. First, average heterozygosity was predicted for selected trapping periods (Gazebo, Feb-96, Feb-97, Apr-98, Feb-99, Mar-00, Mar-01, Mar-02; Vet Village, Mar-96, Mar-97, Feb-98, Mar-00, Mar-01, Feb-02) using equation 13.12 from Nei (1987). Effective population size was estimated using equation 7.22 in Hartl & Clark (1997). Population estimates were done using the jackknife method within program CAPTURE (Otis *et al.* 1978). Secondly, I used equation 7.14 in Hartl & Clark (1997) to estimate the rate of change in heterozygosity for all trapping periods. The upper limit of the 95th CI was used to estimate effective population size for equation 7.22 and the rate of change of heterozygosity for equation 7.14.

Results

Summary

Data were obtained during eight years from 14 trapping periods (28 sessions) on both Gazebo and Vet Village grids. A total of 14 112 trap nights were represented with 1869 captures of 1163 animals. Tissue was available from 1007 of these individuals (Table 2). Trapping on Gazebo grid resulted in a total of 890 captures of 539 animals with tissue being obtained from 477 individuals (Table 3). Captures per trapping period on Gazebo grid ranged from 9 to 145. Trapping on Vet Village grid produced 979 captures of 625 animals with tissue being obtained from 530 individuals (Table 4). Captures on Vet Village grid ranged from 7 to 152 animals over 14 sessions. Amplification was attempted for all 1007 individuals at 11 loci. The number of alleles per locus on Gazebo grid ranged from 3 to 10 and 3 to 8 on Vet Village grid (Table 5). To be conservative, I used predicted heterozygosity from equation 13.12 (Nei 1987) because it produced higher estimates than equation 7.14 (Hartl & Clark 1997).

Gazebo Grid

The March 1999 trapping period on Gazebo grid was not used due unsuccessful amplification of primer sets for those individuals. Tables 6-18 summarize genetic diversity information by trapping period for Gazebo grid for each of the 11 loci examined, including locus sample size, number of alleles, effective number of alleles per locus, average observed heterozygosity, expected average heterozygosity, and the fixation index (F_{IS}). The total number of observed alleles on Gazebo grid across all trapping periods was 70 (Table 5). The total number of alleles detected per locus across trapping periods ranged from 3 to 10. The number of alleles observed by trapping period on Gazebo grid ranged from 38 to 57. The highest number of alleles observed (57) was during the June 1996 trapping period while the lowest number (38) occurred three times (Feb-97, Nov-00, Nov-01). Typically, for a trapping period when sample size was large (number of captures) the observed number of alleles was also high relative to trapping periods with low captures. The average number of alleles per locus by trapping period ranged from 3.45 to 5.18. Allele frequencies by trapping period are presented in Appendix 1. Common alleles tended to persist across trapping periods. Nine alleles were present only in the June 1996 trapping period. Population pairwise F_{ST} values for trapping periods February 1995 and February 1996, April 1995 and April 1996, June 1995 and June 1996 were not significant, however, F_{ST} for the February 1995 and March 2002 trapping periods was significant ($F_{ST} = 0.0254$; $P = 0.0000$).

The average observed heterozygosity per trapping period ranged from 0.5187 to 0.6446 (Table 6-18). It was highest during the November 2001 trapping period (0.6446) and lowest during the March 2000 trapping period (0.5187). Average observed

heterozygosity oscillated throughout the study but temporally increased following hurricane Opal predominately in the June 1996 trapping period (Table 11). Predicted heterozygosity (equation 13.12 Nei 1987) did not increase following the hurricane. The predicted heterozygosity from equation 13.12 (Nei 1987) ranged from 0.5143 during March of 2002 to 0.5910 during February 1996 (Fig. 3). Using equation 7.14 (Hartl & Clark 1997) the predicted heterozygosity ranged from 0.4895 in March 2002 to 0.6069 during February 1995. The observed heterozygosity plotted as a linear best-fit line (H_O Net) indicates a lower rate of decay than predicted (H_T) (Fig. 3). The average expected heterozygosity ranged from 0.5441 to 0.6212 where the low occurred in March 2000 and the high in February 1996. Across all trapping periods the mean observed heterozygosity was 0.5909 and the mean expected heterozygosity was 0.5896. The fixation index, F_{IS} , occasionally indicated that inbreeding and outbreeding were occurring within the grid. However, estimates of F_{IS} did not typically coincide with predictions of when inbreeding or outbreeding may occur. Mantel tests were significant for four of the 14 trapping periods on Gazebo grid (Table 19) indicating that for these trapping periods (Feb-95, Mar-01, Nov-01, Mar-02) there was a positive relationship between genetic differentiation and geographic distance. Exact tests of Hardy-Weinberg expectations (HWE) across all trapping periods and loci revealed few significant deviations (0-2 loci per trapping period; Appendix 2). On Gazebo grid, three of the eleven loci were found to significantly deviate (5% level) from HWE across 14 trapping periods. However, these loci did not consistently deviate across trapping periods.

Investigation of possible structuring within the grid produced some interesting results (Table 20). For the February 1995 and March 2002 trapping periods, the four

corner quadrant estimate produced the highest values of F_{ST} (0.0143; 0.0159). Estimates from February 1996 and June 1996 were higher in the east/west (0.0125) and north/south (0.0220) analysis respectively. Only for the June 1995 trapping period was F_{ST} highest (0.0219) based on a random assignment of individuals to grids. While F_{ST} values were high considering the proximity of groupings, a particular group (e.g. four corner, etc.) was not consistently higher than other groups. Analysis of molecular variance (AMOVA) framework was used to estimate hierarchical analysis of genetic differentiation within and among quadrants of the grid for trapping periods February 1995, June 1995, February 1996, June 1996 and March 2002 and are reflected in the F_{ST} values (Table 20). The north/south sectioning of the grid produced the highest estimate of genetic variance (2.20%) within Gazebo grid. However, the east/west sectioning produced the highest estimate for the June 1995 trapping period (0.69%) while the four corner sectioning produced the highest estimate for February 1995 (1.43%) and March 2002 (1.59%). Significant estimates of F_{ST} from within grid, nonrandom associations were revealed for the February 1995, June 1996 and March 2002 trapping periods. The estimates of genetic variance between grids were generally higher than within grids.

Analysis of spatial genetic autocorrelation was conducted for each trapping period using multiple distance class sizes (20 m, 50 m, 100 m, 250 m). Significant spatial autocorrelation was found for eight of fourteen trapping periods and multiple distance classes on Gazebo grid (Appendix 3). However, for distance classes that were significant during the February 1996, February 1997, March 2001 (except the 100 m distance class) and November 2001 sample size was ≤ 24 . For six trapping periods significant autocorrelation was not found (Jun-95, Apr-96, Jun-96, Apr-98, Feb-99, Nov-00).

Autocorrelation patterns across trapping periods and distance classes were generally not consistent. However, this result was expected for trapping periods following hurricane Opal. Spatial autocorrelation data sets were comprised of males and females. This indicates that proximal individuals were more genetically similar regardless of sex. Individual trapping periods, typically at larger distance classes (250 m), were marked by an increasing autocorrelation coefficient (r). However, these particular analyses were limited due to small sample sizes.

Veterans Village Grid

Tables 6-18 summarize genetic diversity information by trapping period for Vet Village grid for each of the 11 loci examined, including locus sample size, number of alleles, effective number of alleles per locus, average observed heterozygosity, expected average heterozygosity, and the fixation index (F_{IS}). Through all trapping periods the total number of alleles on Vet Village grid was 59 (Table 5). A larger number of samples from Vet Village grid (530) produced 11 fewer alleles than 477 samples from Gazebo grid. The total number of alleles detected per locus across trapping periods was 3 to 8. The number of alleles found on Vet Village grid per trapping period ranged from 37 to 53. The highest number of alleles during a single trapping period on Vet Village grid (53) was from April 1995 while the lowest (37) was from December 2000. This is different from Gazebo grid when the most alleles during a trapping period was observed in June 1996. However, a low number of alleles observed during a single trapping period occurred at approximately the same time. Typically, when sample size was low so was the number of observed alleles. However, a larger overall sample size on Vet Village grid did not produce a larger number of alleles. The average number of alleles per

trapping period per locus ranged from 3.36 to 4.82. Allele frequencies by trapping period are presented in Appendix 1. As expected, common alleles tended to persist across trapping periods while rare alleles were not observed when sample size was small. Population pairwise F_{ST} values for the trapping periods of March 1995/March 1996 and June 1995/June 1996 were not significant, however, F_{ST} for the April 1995/April 1996 and March 1995/February 2002 trapping periods was significant ($F_{ST} = 0.0050$, $P = 0.0137$; $F_{ST} = 0.0254$, $P = 0.0000$ respectively).

The average observed heterozygosity per trapping period on Vet Village grid ranged from 0.4496 to 0.6669. The highest estimate of average observed heterozygosity was during the April 1996 trapping period while the lowest occurred in December of 2000. Highest and lowest estimates of mean heterozygosity occurred at approximately the same time period on both sample grids. However, even more dramatically than on Gazebo grid, observed heterozygosity temporarily increased in the first trapping period following hurricane Opal on Vet Village grid (Table 9). Estimates of predicted heterozygosity over time were slightly higher on Vet Village grid than on Gazebo grid. A linear trend line of observed heterozygosity (H_O Net) indicates a much reduced slope versus predicted loss of heterozygosity (H_T) (Fig. 4). Using equation 13.12 (Nei 1987) predicted heterozygosity ranged from 0.5500 during February of 2002 to 0.6009 during March 1996 (Fig. 4). Equation 7.14 (Hartl & Clark 1997) predicted heterozygosity was lowest February 2002 (0.5339) and highest during March 1995 (0.6109). Observed heterozygosity on Vet Village grid was higher than predicted following hurricane Opal and was higher than predicted for all but a single trapping period (Dec-00). The mean expected heterozygosity ranged from 0.6420 to 0.5196 and occurred during March 1996

and December 2000 respectively. Average observed heterozygosity across all trapping periods was 0.6084 while average expected heterozygosity was lower at 0.6000. These estimates are slightly higher than estimates for Gazebo grid. The fixation index F_{IS} , typically near zero, did not indicate a pattern of higher rates of inbreeding or outbreeding. Mantel tests were significant for four (Mar-96, Mar-01, Oct-01, Feb-02) of the 13 trapping periods on Vet Village grid (Table 19) indicating a periodic relationship between genetic distance and geographic distance. Mantel tests were significant for three of the same trapping periods on Vet Village and Gazebo grids indicating that a relationship between genetic and geographic distances occurred on both grids simultaneously. Exact tests of Hardy-Weinberg expectations per trapping period for each locus on Vet Village grid found significance deviations, similar to Gazebo, ranging from 0 to 2 loci per trapping period. Six of eleven loci deviated significantly from HWE across 13 trapping periods (Appendix 2), however, there was no obvious pattern associated with these deviations.

For select trapping periods (Mar-95, Jun-95, Mar-96, Jun-96, Feb-02) the fixation index (F_{ST}) was estimated for Vet Village grid by sectioning the grid into the four directional corners, north/south, and east/west quadrants and treating individuals in each quadrant as a subpopulation (Table 20). Also, for comparison, F_{ST} was estimated by twice randomly assigning individuals to these quadrants (Table 20). For the March 1995 and March 1996 trapping periods, the four corner estimate produced the highest F_{ST} value (0.0247, 0.0369 respectively). The F_{ST} estimate from the March 2002 trapping period was highest in the east/west analysis (0.0231). The June 1995 and June 1996 estimates of F_{ST} were highest based on random assignment of individuals into quadrants (0.0078,

0.0337 respectively). Similar to Gazebo grid, F_{ST} values were relatively high, but a particular quadrant (i. e. four corner, etc.) was not consistently higher than other groups. Similar to Gazebo grid, significant estimates of F_{ST} from within grid, nonrandom associations were revealed for the March 1995, March 1996 and March 2002 trapping periods. Analysis of molecular variance (AMOVA) framework was used to estimate hierarchical analysis of genetic differentiation within and among quadrants of the grid and are reflected in the F_{ST} values (Table 20). The sectioning of the grid into four corners produced the highest estimate of genetic variance (3.69%) within Vet Village grid. However, the east/west sectioning produced the highest estimates for the June 1996 (0.70%) and March 2002 (2.31%) trapping periods. As on Gazebo grid, some of the F_{ST} estimates were significant.

Analysis of spatial genetic autocorrelation was conducted for each trapping period using multiple distance class sizes (20 m, 50 m, 100 m, 250 m; Appendix 3). Significant patterns were identified. Significant spatial autocorrelation found during the March 1997 trapping period for the 20 and 50 m distance classes was most likely the result of small sample sizes (≤ 28). Spatial autocorrelation was not detected during all trapping periods. This outcome was expected based on predictions and spatial autocorrelation results were similar to Vet Village grid. For trapping periods where spatial autocorrelation was detected, not all distance classes were significant. Significant autocorrelation was found during seven of the thirteen trapping periods. Corresponding trapping periods where positive significant autocorrelation was found on both grids include six trapping periods covering winter and spring 1995, winter 1997, winter and fall 2001 and winter 2002. Significant positive autocorrelation was generally found at the same distance classes

between grids for corresponding trapping periods. Significant positive autocorrelation was not detected for all trapping periods and distance classes. Males and females were combined in all autocorrelation analysis indicating that regardless of sex, proximal individuals were more genetically similar. The correlograms, primarily for smaller distance classes (20 m to 50 m), show the autocorrelation coefficient (r) oscillating in a high to low pattern (Fig. 12-18). The pattern of larger distance classes (250 m) marked by an increasing autocorrelation coefficient (r) was not found on Vet Village grid when sample size was sufficient. Overall, the patterns of autocorrelation found on Vet Village grid were strikingly similar to the patterns observed on Gazebo grid.

Gazebo and Veterans Village combined

Trapping periods on Gazebo and Vet Village grids that occurred at approximately the same time were combined and analyzed as single trapping periods (e. g. Gazebo Feb-95 and Vet Village Mar-95, Gazebo Apr-95 and Vet Village Apr-95, etc.). Analyses of these data included exact tests of Hardy-Weinberg, spatial autocorrelation, F_{ST} , R_{ST} , number of migrants (N_M), AMOVA, Mantel tests, and Population assignment. Combining trapping periods from both Gazebo and Vet Village grids into single trapping periods resulted in captures ranging from 16 to 329 (Table 2). Tables 21-27 summarize information by trapping period for the combined trapping periods for each of the 11 loci examined, locus sample size, number of alleles per locus, effective number of alleles per locus, average observed heterozygosity, average expected heterozygosity, and the fixation index (F_{IS}). The total number of alleles observed for the global population was 73 (Table 5). The genetic variability for the combined data sets was moderate. The number of alleles per data set after combining ranged from 41 to 63. The high occurred

during the 3rd trapping period of 1996 (June for both grids), with the low in November 2000 on Gazebo grid and December 2000 on Vet Village grid. The average number of alleles per locus across trapping periods ranged from 3.73 to 5.73. The number of alleles per locus across trapping periods ranged from 3 to 10. Allele frequencies by trapping period are presented in Appendix 1. Twenty-seven of 73 alleles were observed during each trapping period. Population pairwise F_{ST} values for the combined trapping periods of the 1st trapping period of 1995/1st trapping period of 1996 and the 2nd trapping period of 1995/2nd trapping period of 1996 were not significant. F_{ST} values for the 3rd trapping period of 1995/3rd trapping period of 1996 and the 1st trapping period of 1995/1st trapping period of 2002 were significant ($F_{ST} = 0.0046$, $P = 0.0215$; $F_{ST} = 0.0327$, $P = 0.0000$ respectively).

The average observed heterozygosity per trapping period across both grids ranged from 0.5014 to 0.6455. It was highest during the 2nd trapping period of 1996 (April on both grids) and lowest during the 2nd 2000 trapping period (Gazebo November, Vet Village December). The mean expected heterozygosity ranged from 0.5770 to 0.6388. It was lowest during the 2nd 2000 trapping period (Gazebo November, Vet Village December) and highest during the 1st 1996 trapping period (Gazebo February, Vet Village March). For all trapping periods the average observed heterozygosity was 0.6015 and the average expected heterozygosity was 0.6085. F_{IS} values for the combined data sets ranged from -0.0268 to 0.1464. The lowest estimate occurred during the 2nd 1996 trapping period (April for both grids) while the highest estimate occurred during the 2nd 2000 trapping period (Gazebo November, Vet Village December). Mantel tests were significant for 11 of 13 trapping periods examined (Table 28). Thus, for the majority of

the trapping periods there was a relationship between genetic differentiation and geographic distance. Locus by locus exact tests for Hardy-Weinberg expectations for each combined trapping periods found significant deviations (5% level) ranging from 0 to 3 loci per trapping period (Appendix 2). For the combined data eight of the eleven loci were found to significantly deviate from HWE. However, there was not a consistent pattern of loci or a locus deviating from HWE.

The fixation index F_{ST} and an analog, R_{ST} , along with N_M were calculated for all combined trapping periods (Table 29). F_{ST} values for 10 of 13 trapping periods, while small, were significantly different from zero. R_{ST} values were similar to F_{ST} estimates. The number of migrants was also estimated for each combined trapping period and ranged from 9.4 to inf. Both F_{ST} and N_M suggest that gene flow among grids varied widely. Also, AMOVA was used to estimate hierarchical analysis of genetic differentiation for each combined trapping period (Table 29). The combined trapping periods from March 2000 produced the highest estimate of genetic variance between grids (5.05%) while the 1st 1998 trapping period was the lowest (0.00). Within grid AMOVA values were approximately equal to combined trapping periods. The percentage of individuals assigned to the population from which they were trapped for Gazebo grid ranged from 63.6% to 81.7% and Vet Village grid ranged from 59.1% to 81.2% (Table 30). The highest proportion of individuals correctly assigned on Gazebo grid was from the March 2002 trapping period while the lowest proportion were from the March 2001 trapping period. On Vet Village grid, the highest proportion of individuals correctly assigned was from the February 2002 trapping period and the lowest number correctly assigned were from the March 1996 trapping period.

Analysis of spatial genetic autocorrelation was conducted for each combined trapping period using unique distance classes and distance classes equal to those used for individual grids. Significance was demonstrated for at least one distance class over 12 of the 13 trapping periods (Appendix 3). Only the 2nd 2000 trapping period did not show significance for at least one distance class. For the 1998 trapping period only the 200 m distance class was significant and only at a marginal level. As with the previous analyses, males and females were combined again indicating that proximal individuals are more genetically similar regardless of sex.

Discussion

Differentiation among grids

Analyses were conducted to determine if genetical spatial structure could be detected within a population of the Alabama beach mouse (*Peromyscus polionotus ammobates*) and, if structure was present, to determine if it had an effect on the rate of genetic decay within the population. As previously discussed, the Alabama beach mouse displays none of the traditional mechanisms by which genetical structure might develop. Regardless, however, genetical spatial structure was demonstrated within this population. Structure was present on two levels. First, the total data set comprised of combined trapping periods on both Gazebo and Vet Village grids showed a consistent pattern of microgeographic genetic structure (Appendix 3). Second, genetical spatial structure was detected within each grid, however, less consistently than with the overall data set. It is also shown that the rate of genetic decay is reduced compared to a predicted loss of heterozygosity based on a simple drift model (Fig. 3, 4). Thus, genetical spatial structure was shown to be temporally present within this population of Alabama beach mice on a

microgeographic scale (<500 m), and importantly, the rate of genetic decay was effectively reduced.

Wooten & Holler (1999) noted an increase in observed heterozygosity within a population of Alabama beach mice following hurricane Opal in October 1995. Here, using a substantially larger data set of both individuals and loci, their observation is substantiated as these data also show a temporary increase in observed heterozygosity on both Gazebo and Vet Village grids during the year (1996) following hurricane Opal (Table 9 - 11). A possible explanation for this temporary increase in observed heterozygosity would be “isolate breaking” which occurs when subpopulations are forced to interbreed. This type of phenomenon is generally referred to as a Wahlund effect (Wahlund 1928) and can indicate the presence of subdivision within the population. The observed “isolate breaking” is notable in the context of genetical spatial structure because beach mice exist in a narrow, contiguous habitat where large-scale habitat heterogeneity is not typically evident. Clearly, narrow, linear beach habitat is not a system where genetical spatial structure would likely develop through landscape heterogeneity. However, within this system, consistent microgeographic spatial structure has been shown with positive autocorrelation detected across multiple time periods and distance classes. The spatial structure of genotypes is believed to be the reason for the reduced rate of genetic decay that was measured. Also, the recovery of spatial structure following recovery from a catastrophic event was observed. Based on a suite of analyses, I believe that the data are sufficient to warrant rejection of the null hypothesis that genotypes are randomly distributed within the Alabama beach mouse population and conclude that proximal beach mice share more similar genotypes than do more removed beach mice.

The fixation index (F_{IS}) values for the combined trapping periods were positive from February 1995 through February 1996 (1st trapping period post hurricane) then became negative for the remainder of the 1996 trapping periods as negative F_{IS} values suggest outbreeding. I interpret this as an indication that structure within the population had deteriorated. However, F_{IS} values, measured for each trapping period on both grids separately, were less clear concerning spatial structuring within grids. Measured over the total population F_{IS} values did indicate an excess of homozygotes prior to the hurricane and an excess of heterozygotes consistently following the hurricane. This finding is consistent with the hypothesized presence of genetical structure within the population. The recovery period, 1997 through 2001, was marked by both positive and negative F_{IS} values. The inconsistency in these values during the recovery period is likely, to some extent, a reflection of small sample size. Small sample size during the recovery period was primarily on Gazebo grid. F_{IS} values for separate grids across trapping periods demonstrated the difficulty of detecting a clear signal at such a microgeographic level. However, concerning F_{IS} values, it is also probable that the grid does not represent a single subpopulation but a composite of subpopulations. The grids were placed with only a basic knowledge of how breeding units within the population might be positioned both spatially and temporally. Tests for heterozygote deficiency were significant at some loci for trapping periods even when the average heterozygosity for those periods was high. Null alleles were unlikely to account for the observed patterns because significant heterozygote deficiency was inconsistent across trapping periods and loci. High levels of inbreeding were also not likely during this time, again due to the inconsistencies of

heterozygote deficiency across loci. Higher levels of inbreeding usually affect all loci (Hartl & Clark 1989).

Given the microgeographic scale of my analysis, it was of course difficult to distinguish true signal from noise. However, F_{ST} values, while not globally high, were significant between grids and exhibited a substantial range (0.006-0.051; Table 29). Calculation of R_{ST} produced results essentially the same as F_{ST} . Estimates of F_{ST} among populations (grids) were significant for all but the June 1996, winter/spring 1998 and fall 2000 trapping periods. Collectively, my results suggest that individuals inhabiting each grid, approximately 630-910 m apart, were arranged across space in a distinctive allelic pattern. Analyses of these data also suggest that the partitioning of alleles across space was temporal. On a scale of < 1 km, F_{ST} values reported by Peakall *et al.* (2003) for Australian bush rats ranged from 0.04 to 0.08. Also, on a scale of < 1 km, Root *et al.* (2003) calculated F_{ST} values for *P. maniculatus* at 0.031 and 0.043. Thus, F_{ST} values reported here were consistent with other microsatellite analysis. However, F_{ST} values for beach mice may be unparalleled in the context of the contiguous habitat pattern and small distance between grids. Mantel tests among grids were significant for all of the combined trapping periods except June 1996 and fall 2000 suggesting a pattern of restricted gene flow between grids. Typically, the association between genetic and geographic distance is not detected by a Mantel test unless the association is very strong (Peakall *et al.* 2003). These analyses (F_{IS} , F_{ST} , Mantel test) all suggest the presence of genetical spatial structure on a microgeographic scale within a contiguous population of Alabama beach mice. The AMOVA results, and microgeographic scale, are similar to those reported by Peakall *et al.* (2003). AMOVA results for the total population ranged

from 2% to 5% of genetic variance among groups, while within grids AMOVA values, under some scenarios, were as high as 3.69%. Thus, within grid differentiation (< 500 m through 1997; < 360 m through 2002) was similar to between grid differentiation (< 1600 m).

Spatial autocorrelation analyses demonstrated microgeographic structure both among and within grids. Within grids, the pattern of autocorrelation was not as consistent across seasons but was evident. The model predicted that autocorrelation would be present prior to the hurricane and deteriorate following the hurricane. When densities returned to prehurricane levels (2002), autocorrelation should have been strongly detected. In fact, this is essentially what occurred (Fig. 25). Prior to the hurricane spatial autocorrelation was detected at all distance classes except for the 20 m distance class during the combined trapping period of June 1995. Also during the June 1995 trapping period distance classes of 50 and 100 m were approaching nonsignificance. This may, in part, be due to the large annual population decline that beach mice experience each summer (Oli *et al.* 2001). A large population decline might produce the same effect as the hurricane but on a smaller scale. Significant spatial autocorrelation was detected for each trapping period up to approximately one year following the hurricane suggesting that the genetic spatial autocorrelation was left intact by the initial storm event. However, by the June 1996 trapping period structure was not detected. During the summer period, structure was expected to be weak at smaller distance classes. However, a further reduction in structure during June 1996 may also indicate that factor(s) resulting from the hurricane was/were responsible for driving the deterioration of genetical spatial structure.

There are several possible factors that could explain the presence of genetic spatial structure within the Alabama beach mouse population including selection, surges in reproduction, dispersal patterns and social structure (Peakall *et al.* 2003). In my case, selection is unlikely to explain the spatial autocorrelation because microsatellites are neutral loci and typically are spread throughout the genome (Jarne & Lagoda 1996). According to Epperson (1990), selection should generate spatial genetic structure through particular coding genes or loci linked to particular coding genes. It is unlikely that the 11 loci examined here are linked to coding genes that were each under similar selection. According to Scribner and Chesser (1993), the reproductive period of a population can lead to a clustering of similar genotypes. However, data sets here were comprised predominately of adults so it is unlikely that clustering of juveniles created positive spatial structure that deteriorated as juveniles dispersed. Rather, limited dispersal of juveniles promoted spatial structure. Swilling & Wooten (2002) showed that beach mice, on average, tend to disperse about 160 m or within a distance of one homerange of their natal site. The reproductive period of beach mice begins in November/December and juveniles begin entering the population en mass during January. The reproductive season typically continues into April; afterward the population begins a dramatic decline. Thus, one would expect spatial structuring to be strongest during the peak of the reproductive season because juveniles tend to remain associated with their natal site. This is in fact what was observed. Spatial structure was typically not detected during June trapping periods. The apparent break down of spatial structure follows a demographic decline that is likely to increase mate searching among the adult age class.

For the three trapping periods of 1995 and the three of 1996 spatial autocorrelation was detected at the largest distance class of 800 m. However, this pattern was not found during the recovery period (1997-2000). In fact, spatial structure was rarely detected during the recovery period. Lower survivorship and/or more frequent movement by individuals might account for this observation. However, during 2001 and into 2002 spatial structure was clearly evident on both grids. This may represent a point at which detrimental effects relating to the hurricane had diminished allowing population recovery. Most important to my model, this pattern does indicate that genetical spatial structure will reorganize following disruption by a catastrophic event. This is a critical point because it demonstrates that factors inherent in the population result in recurring spatial structure. The precise location of clusters may change over time but, importantly, groups do appear to have reformed in this population.

Within this population of Alabama beach mice, the most likely explanation for positive spatial autocorrelation is the social organization, nonrandom mating and the dispersal pattern of beach mice. A limited pattern of dispersal, by both sexes, along with a monogamous mating system would necessarily create familial clusters. Once established, kinship groups themselves can act to limit gene flow (Chesser 1991b; Scribner & Chesser 1993). Also, according to van Staaden *et al.* (1996), positive spatial genetic structure may not occur over short distances unless dispersal is limited. Here, when spatial structure was detected for the combined trapping periods, 58% of the time it was detected in the 20 m distance class. Independently, on Gazebo and Vet Village grids spatial structure was detected at the 20 m distance class in 75% and 57% of the trapping periods, respectively. Several authors have used computer simulations to demonstrate

that a vacillating pattern of positive and negative genetic structure can be brought about by restricted gene flow (Turner 1982; Sokal & Wartenburg 1983; Sokal *et al.* 1989; Epperson 1990; Epperson & Li 1997). Such vacillations, while not significant, were present in some analyses within smaller distance classes (20 m, 50 m). Thus, the pattern of genetic structure observed in beach mice is consistent with that predicted from a combination of social group formation, enforced by limited dispersal resulting in a clumped pattern of similar genotypes. The genetic data produced in my study were consistent with field observations concerning dispersal patterns made by Swilling & Wooten (2000). They showed that dispersal by juveniles was typically limited to within one homerange of their natal site or about 160 m.

Differentiation within grids

Gazebo

The increase of observed heterozygosity on Gazebo grid following hurricane Opal was not as pronounced as the Vet Village increase. However, patterns for both grids were consistent with the concept of isolate braking. F_{IS} values from each trapping period on Gazebo grid were not always consistent with expectations based on spatial structure. Average F_{IS} values for trapping periods were both positive and negative but not generally in a predictable pattern. However, it is unlikely that individuals captured on the grid represent a single, structurally distinct segment of the population. F_{ST} values derived by dividing the grid into various quadrants indicated that under some scenarios subdivision of the grid could produce relatively high values. On Gazebo grid, based on the three models of subdividing the population used here, the most likely scenario of spatial structure within the grid was the four corner quadrants and the east/west quadrants (Fig.

1). However, the north/south quadrants were consistently the highest F_{ST} estimates. The north/south quadrants reflect the primary and secondary dunes (south) and the scrub habitat (north). Swilling & Wooten (2000) showed that dispersal between the two habitat types was limited. My results support the idea that the fore and back dune habitats effectively function as separate units in spite of their close spatial relationship.

Mantel tests were significant for the February 1995, March 2001, November 2001 and March 2002 trapping periods. Thus, within grid Gazebo (Feb-95 < 500m; Mar-01, Nov-01, Mar-02 < 360 m), an association between genetic and microgeographic distances was demonstrated. The pattern of association detected by Mantel tests on Gazebo grid indicated that structure existed prior to the hurricane and reorganized following the recovery period (1997-2000). While the Mantel test for April 1995 was not significant, it did approach significance ($P = 0.057$). Mantel tests on Gazebo grid also indicated a pattern of association that is highest during late winter and declines throughout the remainder of the year. Analyses of spatial autocorrelation on Gazebo grid produced eight trapping periods with positive autocorrelation for at least one distance class. However, sample size was a limiting factor for four of these trapping periods. Regardless, similar to the Mantel tests, the spatial autocorrelation analyses indicated that spatial structure existed prior to the hurricane and reorganized following the recovery period. While the June 1995 trapping period occurred prior to the hurricane, not finding positive autocorrelation was consistent with other analyses that suggested a reduction in spatial genetic association during summer/fall. Again, this observation is likely due to factors related to the sharp annual demographic decline experienced each summer. Overall, the

seasonal pattern appears to be that structure within the grid is most defined during the late winter/spring then declines throughout the year as population recruitment wanes.

Vet Village

Analyses of Vet Village grid produced very similar results to Gazebo grid, however, some differences were observed. The increase of observed heterozygosity on Vet Village grid following hurricane Opal was more pronounced and immediate than the increase on Gazebo grid. The increase on Vet Village grid is, again, consistent with the concept of isolate braking. F_{IS} values from each trapping period on Vet Village grid were generally more consistent with expectations based on spatial structure than F_{IS} values from Gazebo grid. Typically, for trapping periods when F_{IS} was positive an excess of homozygotes was expected. Similar to Gazebo grid, estimates of F_{ST} derived by dividing Vet Village grid into quadrants showed that defining subpopulations within the grid could produce relatively high values. On Vet Village grid, the most likely scenario for demonstrating spatial structure was the four corner quadrants (Fig. 1). The four corner quadrant estimates of F_{ST} on Vet Village grid indicated that structure was most likely to occur under this scenario during March. This is consistent with a model that predicts structure is more defined during March but diminishes over summer. Unlike Gazebo grid, on Vet Village grid the east/west quadrants consistently produced the highest F_{ST} values.

Mantel tests for Vet Village grid data were significant for the March 1996, March 2001, November 2001 and March 2002 trapping periods. Thus, within Vet Village grid (Mar-96 < 500m; Mar-01, Nov-01, Mar-02 < 360 m), an association between genetic and geographic distances was demonstrated. On Vet Village grid, Mantel tests for five other

trapping periods approached significance suggesting an eight-year pattern indicating structure was more evident during winter/spring rather than summer/fall. The pattern of genetic and geographic association on Vet Village grid, like Gazebo grid, indicates that structure existed prior to the hurricane and reorganized following the recovery period (1997-2000). Analyses of spatial autocorrelation on Vet Village grid produced seven trapping periods with positive autocorrelation for at least one distance class. Sample size was limiting for only one of these trapping periods. Interestingly, spatial autocorrelation, unlike the Mantel test, was not significant during the March 1996 trapping period. Regardless, similar to the Mantel tests, the spatial autocorrelation analyses indicated that spatial structure existed on Vet Village grid prior to the hurricane and reorganized following the recovery period (1997-2000). As on Gazebo grid, the June 1995 trapping period on Vet Village grid did not produce significant positive autocorrelation supporting the idea that positive spatial structure abated throughout the summer and fall. This pattern has been observed on both Gazebo and Vet Village grids. This phenomenon is likely due to a reorganization of the population following a sharp demographic decline. The conclusions reached based on separate data and analyses from each grid are in agreement concerning genetical spatial structure. However, based on these analyses, spatial structure may have been more conspicuous on Vet Village grid than Gazebo grid. Following hurricane Opal, sections of Vet Village grid were fertilized and vegetation recovered more quickly than on Gazebo grid. Vet Village grid produced more captures than Gazebo grid thus effective population size (N_e) was higher on Vet Village grid. This may also be partially explainable by the fact that Vet Village grid is more difficult to

emigrate to. Water borders the north boundary of Vet Village grid effectively isolating the grid from the deep scrub habitat (Fig. 1).

Conclusions

Based on microsatellite analyses, beach mice exhibit moderate levels of genetic variation (Peakall *et al.* 2003; Williams *et al.* 2002; Kretzmann *et al.* 2001). This level of variation persists even under the pressure of intensive annual demographic bottlenecks compounded by hurricanes that can further reduce population size across multiple years. In many cases, severe, persistent bottlenecks reduce genetic variation (Nei *et al.* 1975) and coupled with a contiguous habitat that readily allows dispersal (up to several kilometers) genetic variance was expected to be low. These factors likely place immediate ecological stress on individuals as well as having evolutionary implications for the population. Given the annual reduction in population size, one might expect frequent, long distance dispersal by beach mice. However, in agreement with field observations, I found little evidence of a high rate of gene flow between grids (< 930 m). The observed low dispersal rates and distances were the predicted pattern for beach mice based on observation (Swilling & Wooten 1998) and genetics (Wooten & Holler 1998).

With such a restricted pattern of gene flow microgeographic structure should develop even within this contiguous population. Spatial autocorrelation analyses conducted for each grid, as well as combined data sets, indicated that beach mice populations were indeed comprised of clusters of similar genotypes as was predicted. These clusters, however, were apparently more temporal than anticipated as they were undetectable during the early summer and fall, even during periods of relatively high density. Two possible scenarios by which structure could erode are populations where

significant demographic declines tend to leave neighboring individuals that are on average less genetically similar and if individuals are more likely to disperse following population declines. However, field observations along with genetic data suggest dispersal is limited. Supporting limited dispersal, Mantel tests and spatial autocorrelation analyses indicated that between grid differentiation was generally significant.

Regeneration of spatial structure would occur through a reproductive cycle with limited dispersal by juveniles. However, further compounding a reforming of spatial structure are periodic hurricanes that place severe stresses on the population. Low population density during hurricane recovery periods might be characterized by higher dispersal rates than is typical. Recovery period trapping results were marked by small sample sizes that were generally difficult to interpret. Following the recovery period, however, structure reorganized both within and among grids. This indicates properties of the beach mouse population that lead to the formation and reformation of genetical spatial structure.

These properties that lead to genetical spatial structure appear to be an inherent aspect of the beach mouse population and are likely to have some evolutionary justification. My research suggests that spatial structure within this population of Alabama beach mice reduces the rate of genetic decay. Three of the main factors that can affect genetic diversity within populations are demographic bottlenecks, genetic drift and inbreeding. Beach mice populations experience regular and persistent demographic bottlenecks. Thus, genetic drift and inbreeding are likely, on some level, persistent forces within beach mice populations. Regardless, observed heterozygosity declined at a slower rate than the predicted loss of heterozygosity. Genetic diversity within beach mice populations appears to reside at a microgeographic level. By partitioning genetic

variation in this manner, beach mice are able to slow the rate of loss of genetic variation. Restricted dispersal and social structure within beach mice populations are evolutionary adaptations that aid in the preservation of genetic variation. I predict that genetic diversity resides at a microgeographic level for many species and represents an evolutionary adaptation by which genetic variation can be maintained at a higher level than would otherwise be expected. In doing so, microspatial structure sets the boundaries within which all evolution, including natural selection must operate.

Clearly, biological aspects of beach mice serve as a mechanism that functions to preserve genetic variation. These biological “traits” negate the effects of forces such as genetic drift that typically act to reduce genetic variation. The findings of microgeographic genetic structure and its relationship in preserving genetic variation establish a connection between microevolution and the ecology of beach mice. The dispersal “ability” and social interactions of beach mice has a clear association with the magnitude and spatial scale of genetic differentiation within the population of Alabama beach mice. The maintenance of genetic variation is essential for the evolutionary process, and genetic differentiation within the population provides the potential for local adaptation or even speciation.

Combining demographic and genetic data in a spatiotemporal manner has provided insights into population processes that might have been undetected by a single method. My results demonstrate that behavioral partitioning of genotypes can occur on a microgeographic scale in the absence of traditional breeding structures (e. g. single sex clusters, etc.). Importantly, following a catastrophic event genotype partitioning was shown to reorganize. Also, and unexpectedly, genotype partitioning deteriorated and

reorganized on an annual basis. This indicates that partitioning of genotypes is an intrinsic aspect of the population. Further, this partitioning of genotypes acts as a mechanism that slows the rate at which genetic variation is lost. Given the process of genetic partitioning, future studies might investigate both the spatial and temporal formation and decay of actual breeding groups. The demographic and genetic dynamics of both within and between breeding groups offers intriguing insights into such fundamental questions as the amount of gene flow during different periods, mate choice, and paternity analysis. Large numbers of microsatellites markers have already been developed (Mullen *et al.* 2005). Thus, laboratory developmental work that is both expensive and time consuming would be minimal. Further and more extensive analyses of genetical spatial structure with the population of Alabama beach mice are warranted.

Fig. 1 Vet Village grids established during the fall of 1994. Each grid is approximately 25 X 13 m. The grids were divided into four corner, north/south and east/west quadrants to model subdivision within each grid. Water borders the north boundary of Vet Village grid.

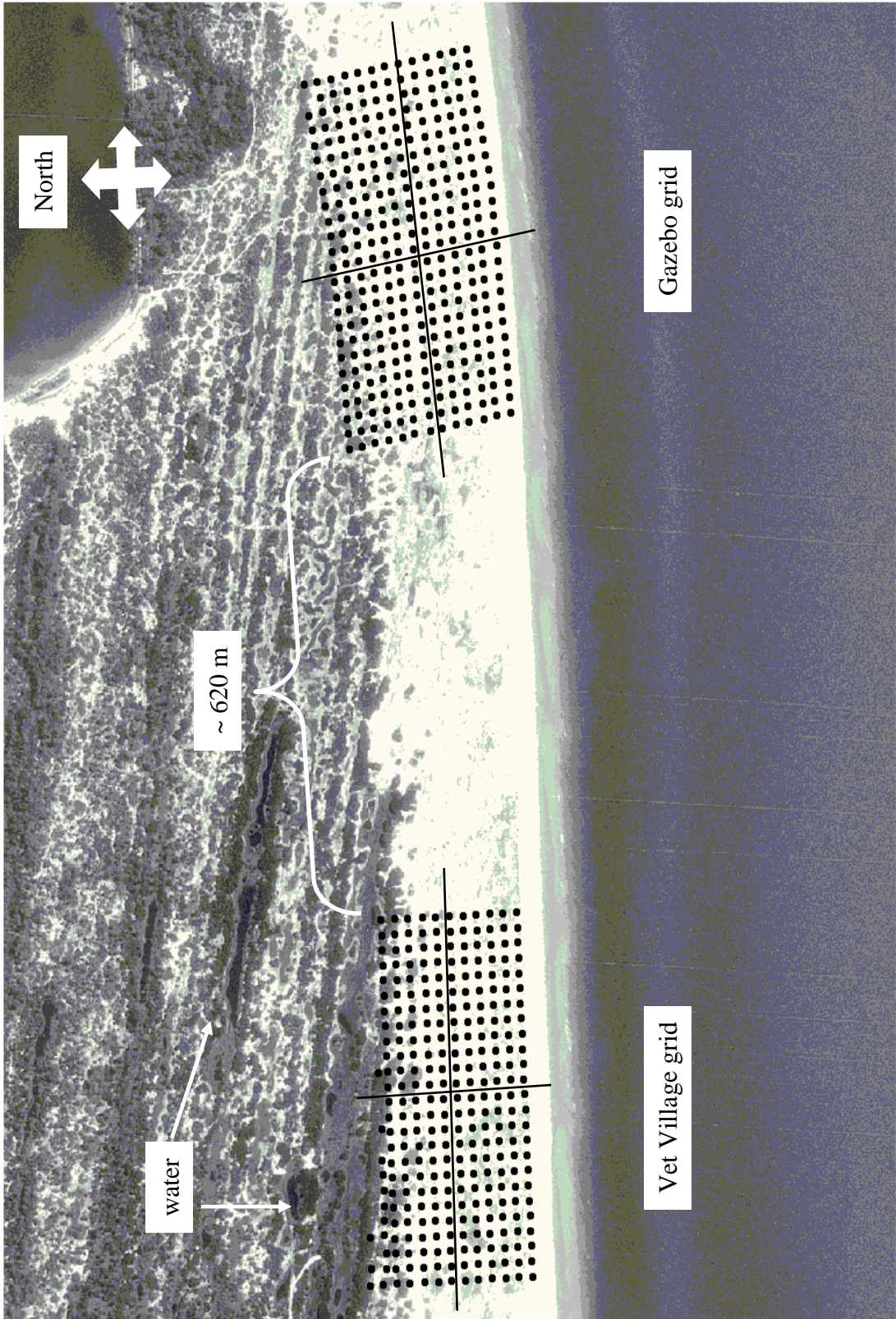


Fig. 2 The reduction of both grids increased the distance between them to approximately 920 m.

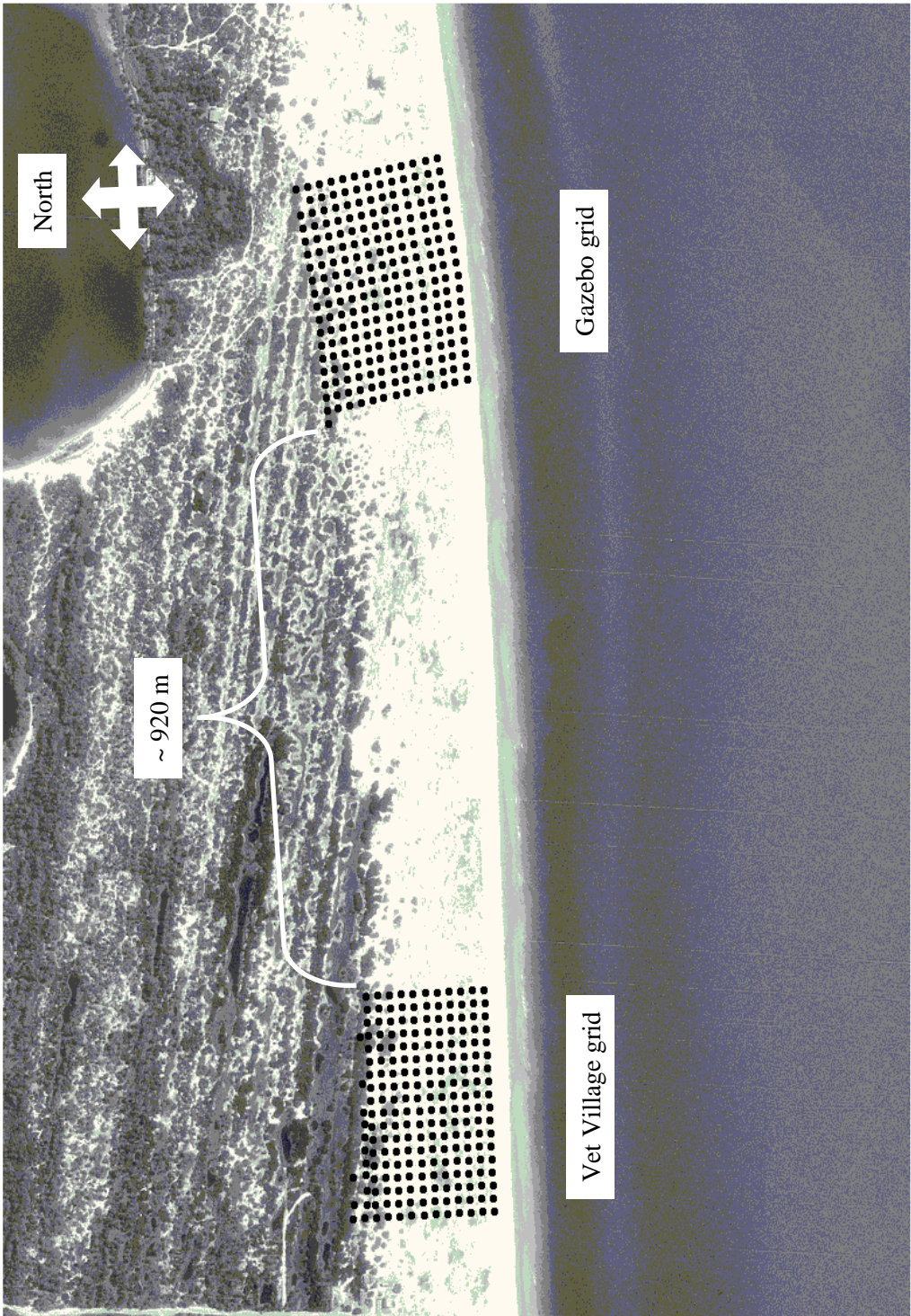


Fig. 3 Gazebo grid observed heterozygosity (H_o) for each trapping period along with the predicted heterozygosity (H_t) for each trapping period. Predicted heterozygosity is based on equation 7.14 in Hartl & Clark (1997). Observed heterozygosity increases following hurricane Opal in October 1995 while predicted heterozygosity declines.

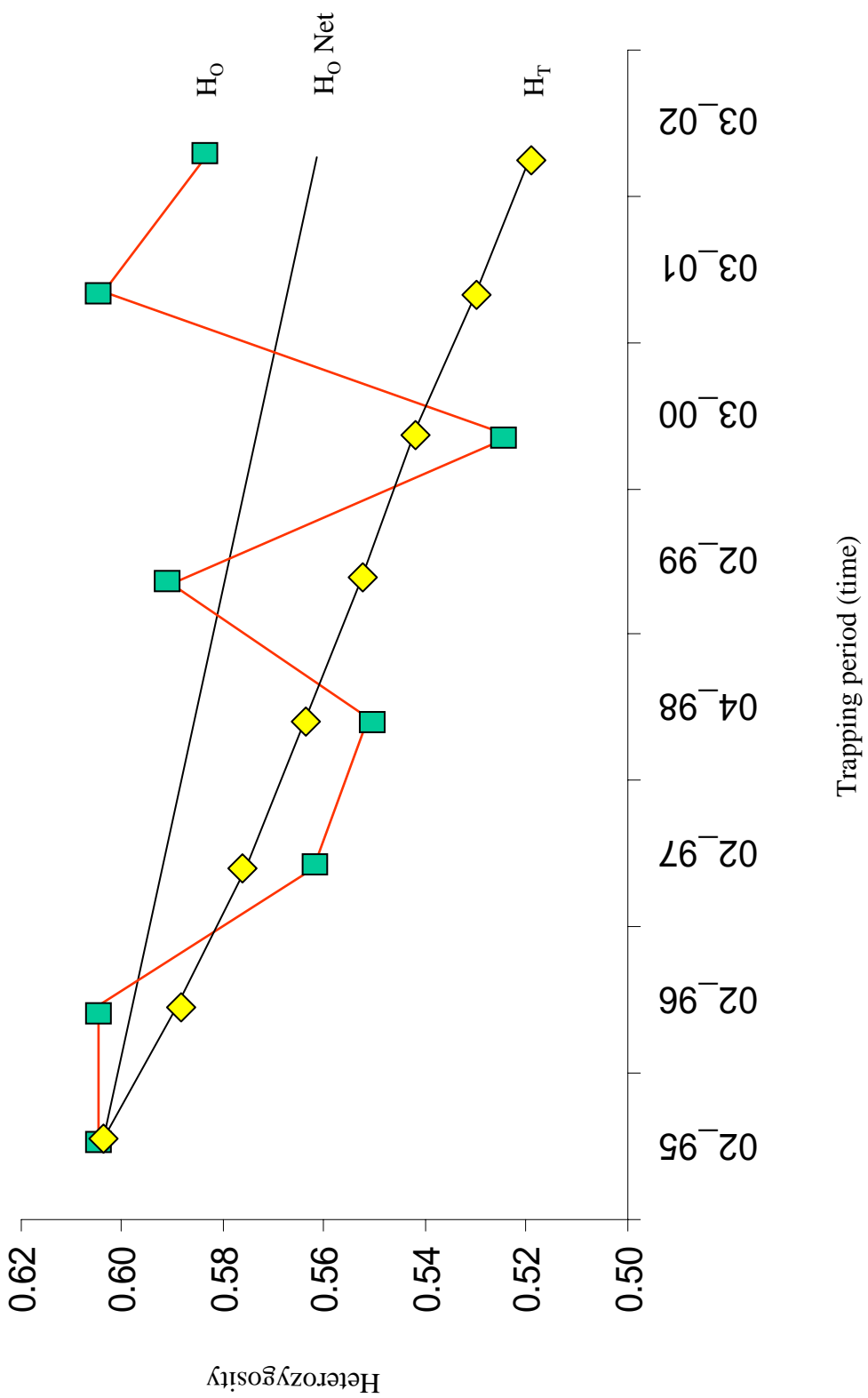


Fig. 4 Vet Village observed heterozygosity (H_o) for each trapping period along with the predicted heterozygosity (H_t) for each trapping period. Predicted heterozygosity is based on equation 7.14 in Hartl & Clark (1997). Observed heterozygosity increases following hurricane Opal in October 1995 while predicted heterozygosity declines.

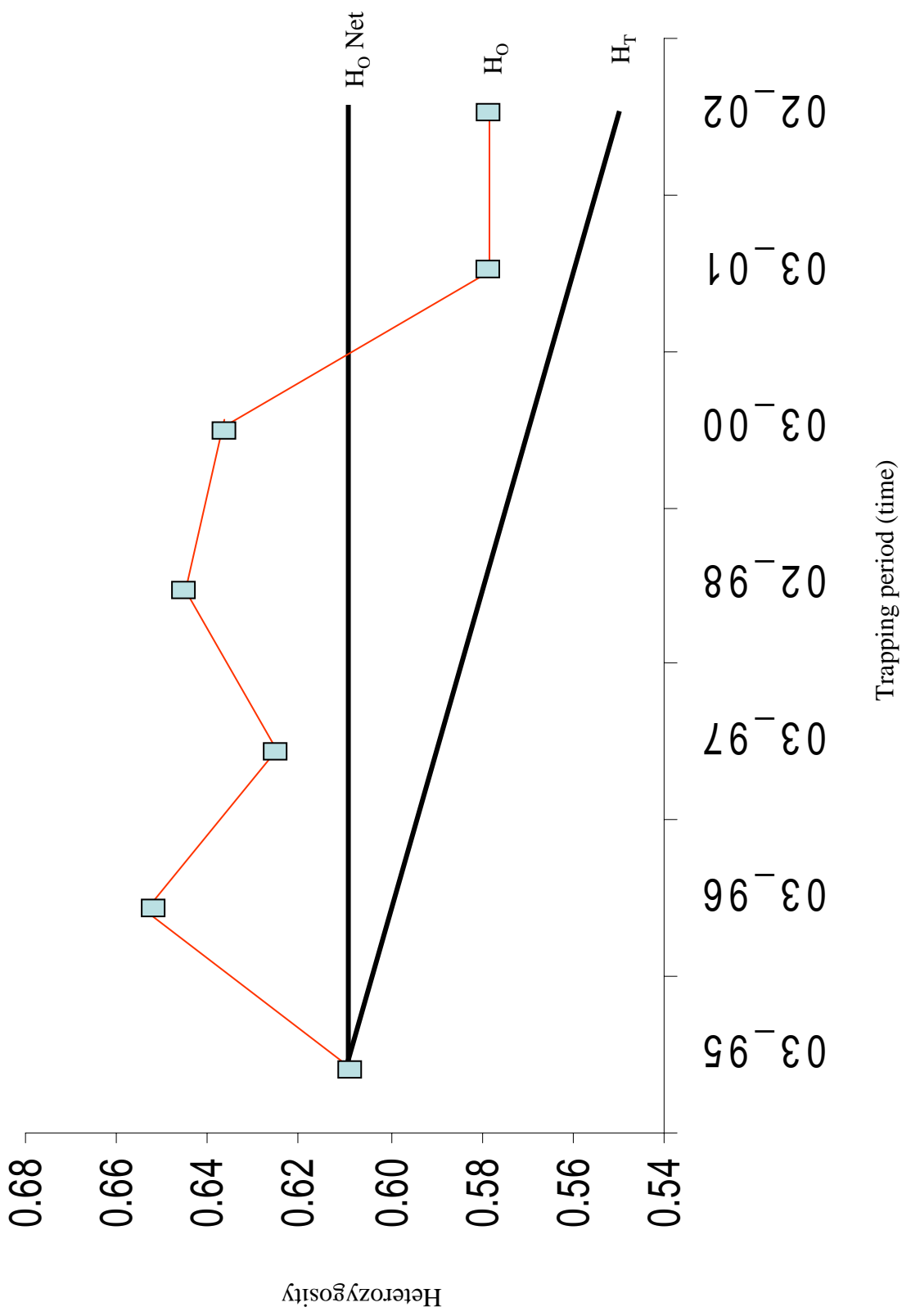


Fig. 5 Correlograms of Gazebo grid for the trapping period of February 1995 shows genetic correlation (r) as a function of distance and the 95% CI about a null hypothesis of randomly distributed genotypes. The 95% CI intervals about r are estimated by bootstrapping. Autocorrelation analysis are presented for distance class sizes of 20 m (A), 100 m (B) and 250 m (C).

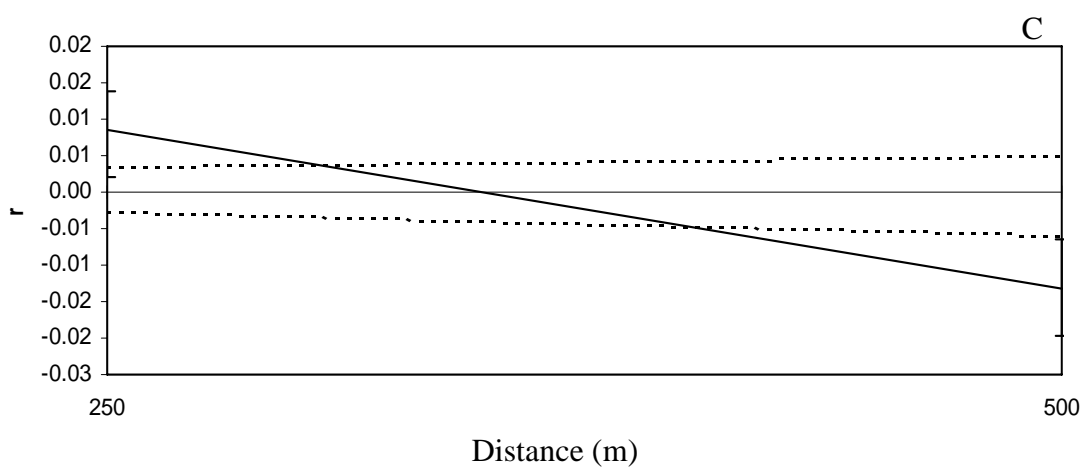
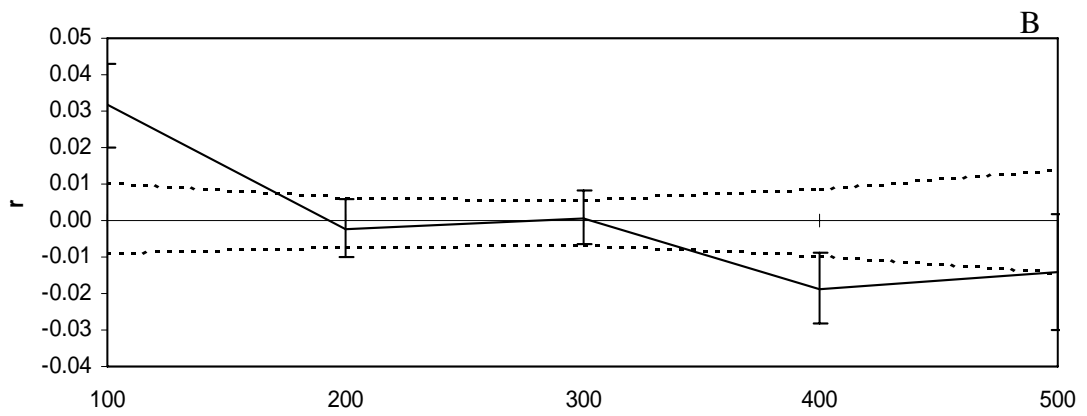
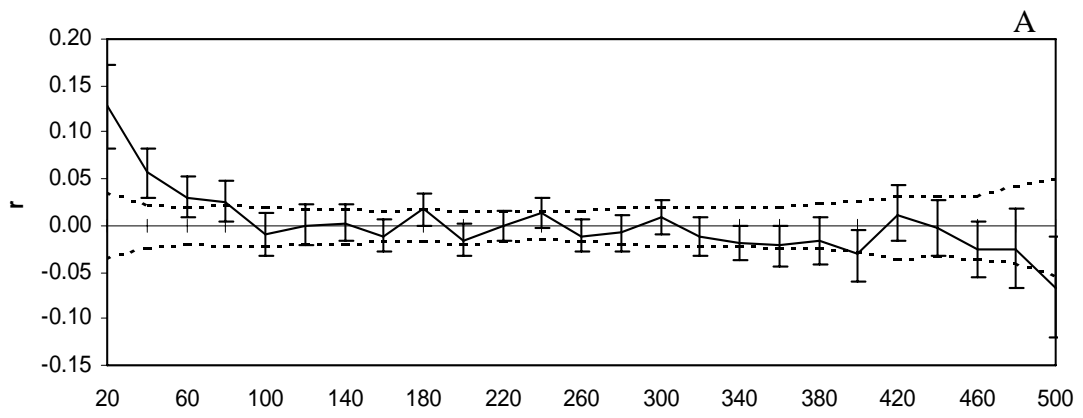


Fig. 6 Correlograms of Gazebo grid for the trapping period of April 1995 shows genetic correlation (r) as a function of distance and the 95% CI about a null hypothesis of randomly distributed genotypes. The 95% CI intervals about r are estimated by bootstrapping. Autocorrelation analysis are presented for distance class sizes of 20 m (A), 100 m (B) and 250 m (C).

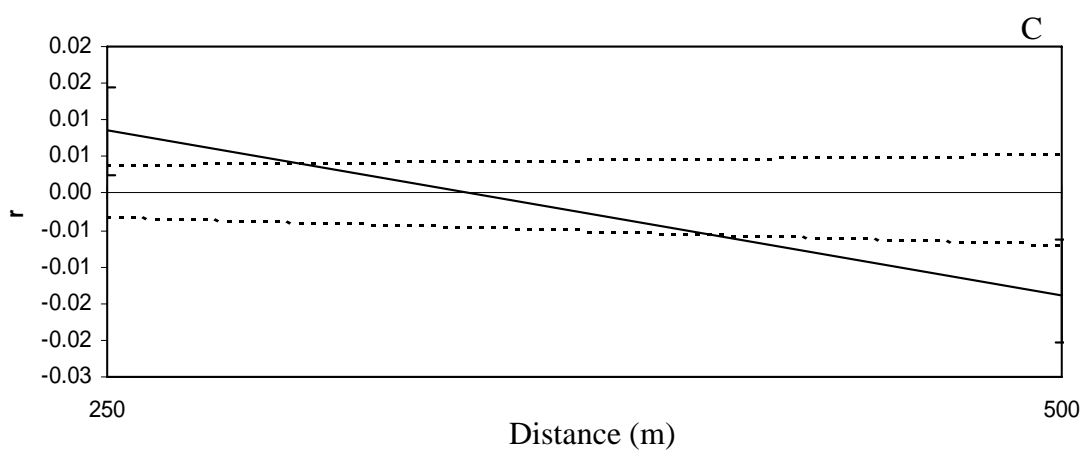
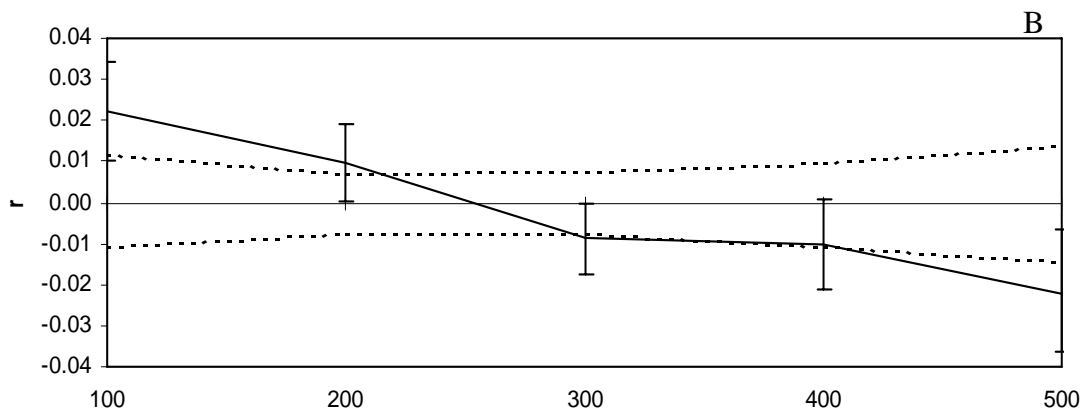
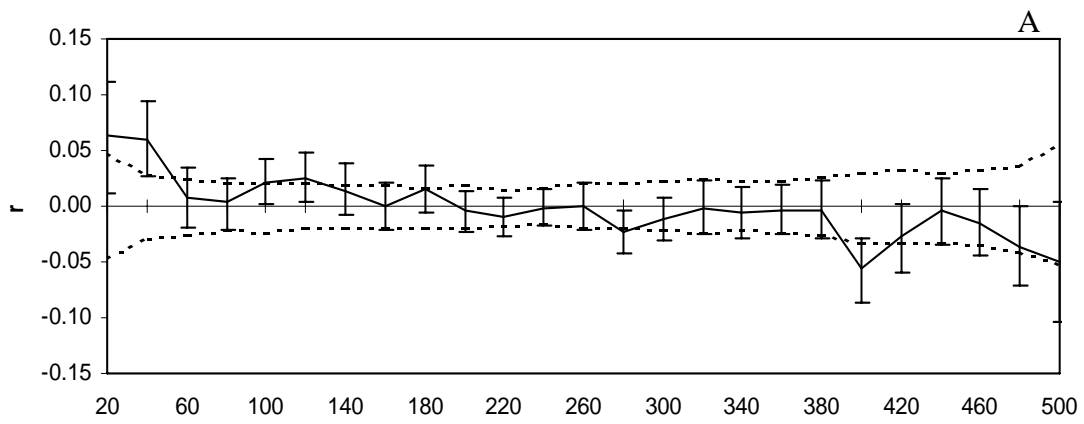


Fig. 7 Correlograms of Gazebo grid for the trapping period of June 1995 shows genetic correlation (r) as a function of distance and the 95% CI about a null hypothesis of randomly distributed genotypes. The 95% CI intervals about r are estimated by bootstrapping. Autocorrelation analysis are presented for distance class sizes of 20 m (A), 100 m (B) and 250 m (C).

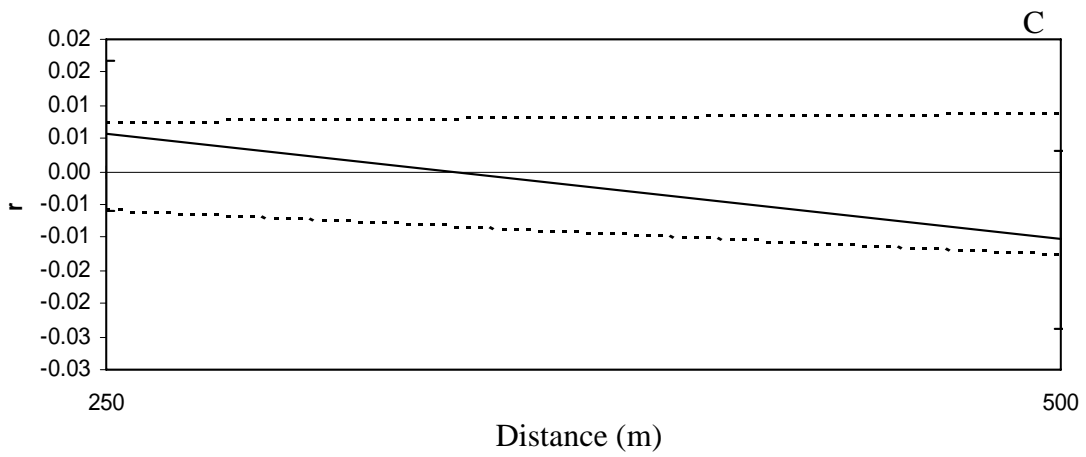
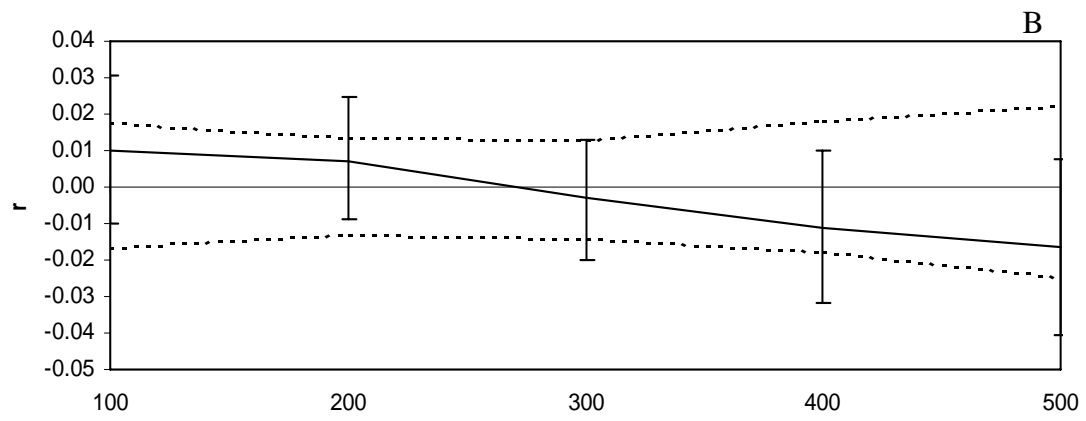
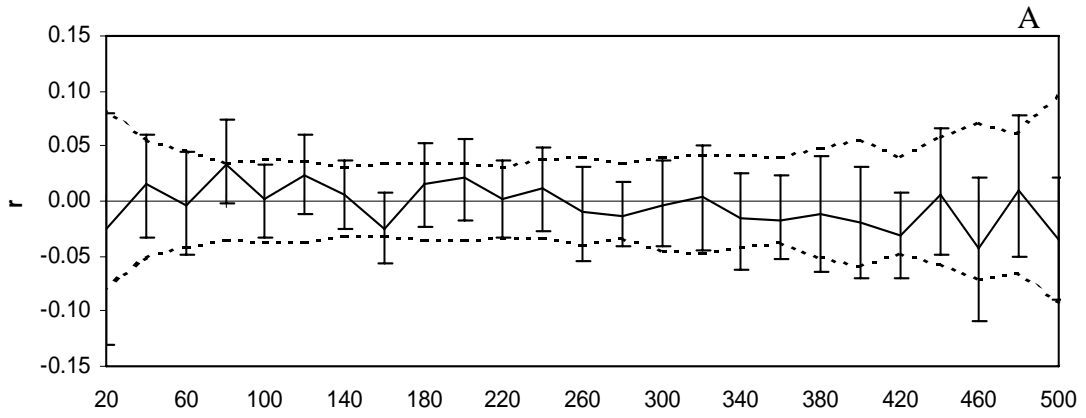


Fig. 8 Correlograms of Gazebo grid for the trapping period of February 1996 shows genetic correlation (r) as a function of distance and the 95% CI about a null hypothesis of randomly distributed genotypes. The 95% CI intervals about r are estimated by bootstrapping. Autocorrelation analysis are presented for distance class sizes of 20 m (A), 100 m (B) and 250 m (C).

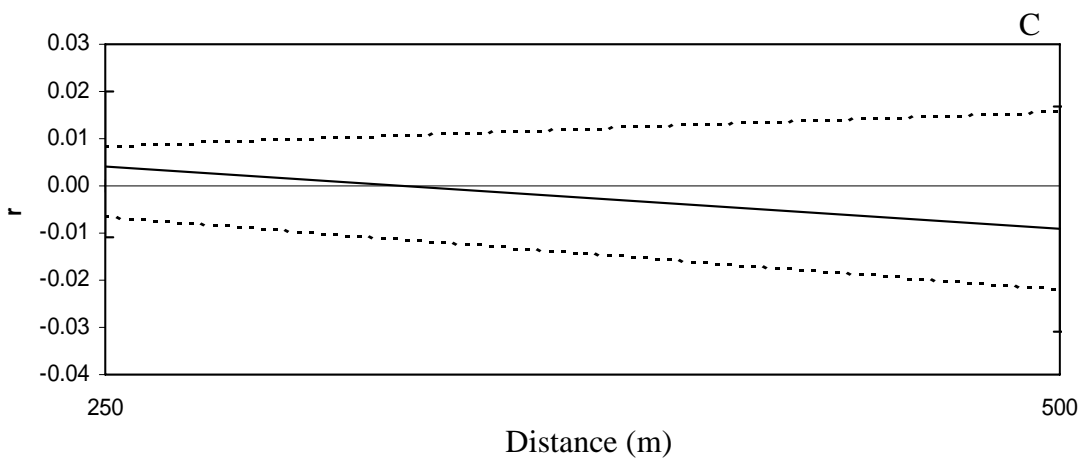
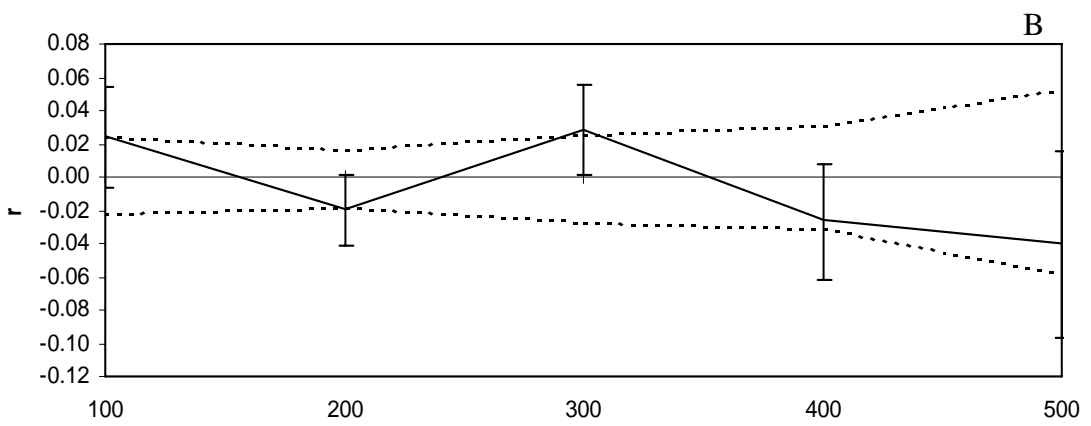
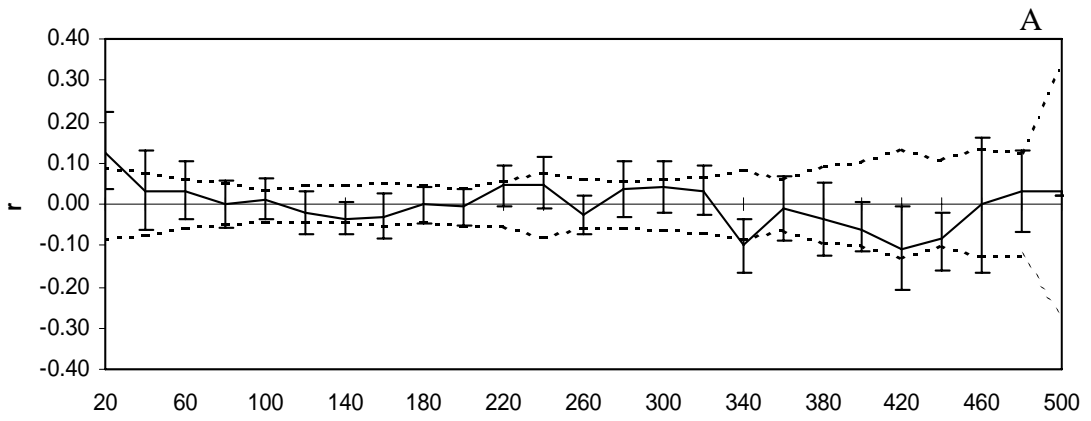


Fig. 9 Correlograms of Gazebo grid for the trapping period of April 1996 shows genetic correlation (r) as a function of distance and the 95% CI about a null hypothesis of randomly distributed genotypes. The 95% CI intervals about r are estimated by bootstrapping. Autocorrelation analysis are presented for distance class sizes of 20 m (A), 100 m (B) and 250 m (C).

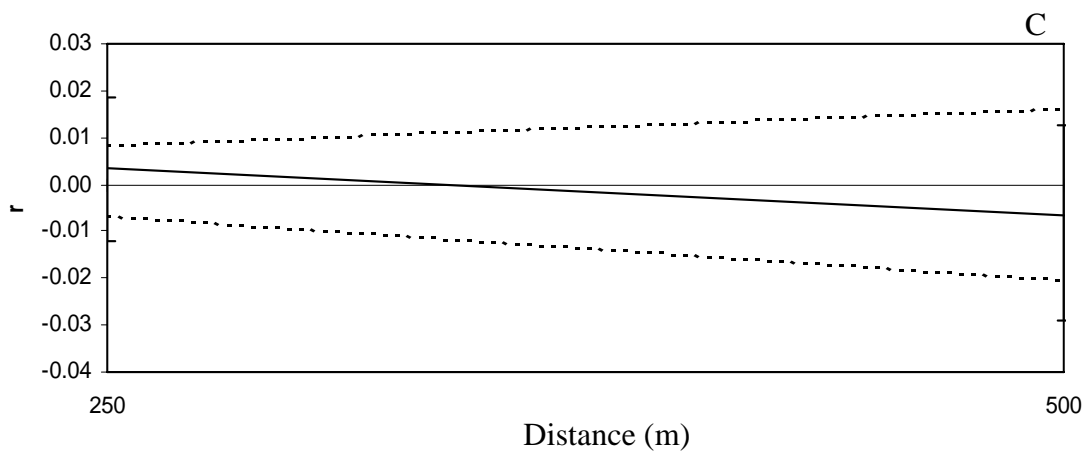
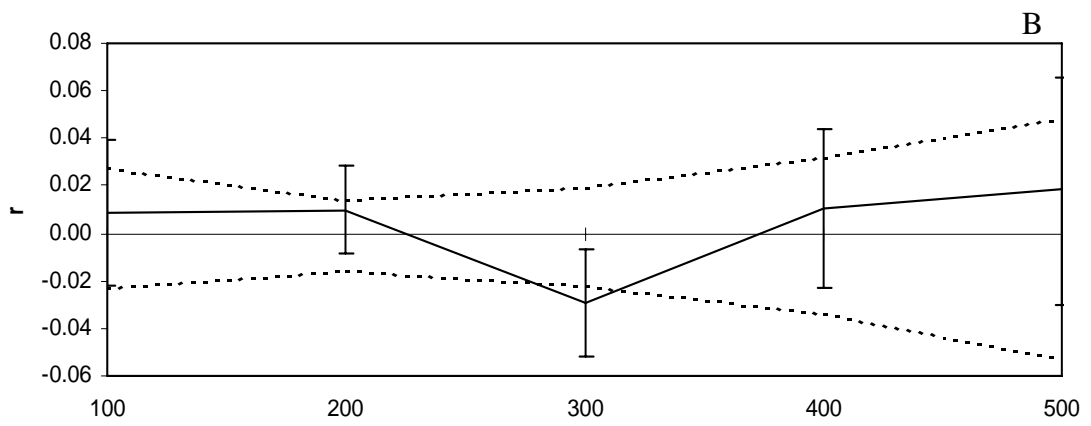
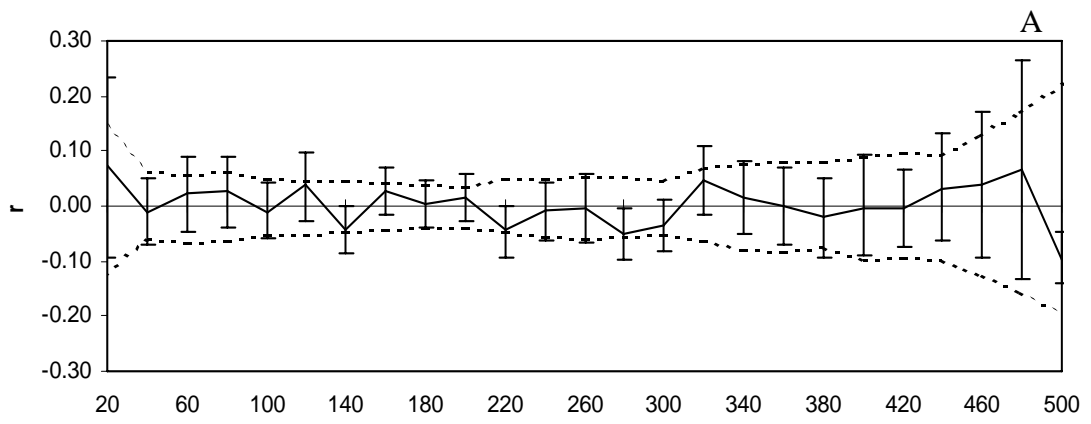


Fig. 10 Correlograms of Gazebo grid for the trapping period of June 1996 shows genetic correlation (r) as a function of distance and the 95% CI about a null hypothesis of randomly distributed genotypes. The 95% CI intervals about r are estimated by bootstrapping. Autocorrelation analysis are presented for distance class sizes of 20 m (A), 100 m (B) and 250 m (C).

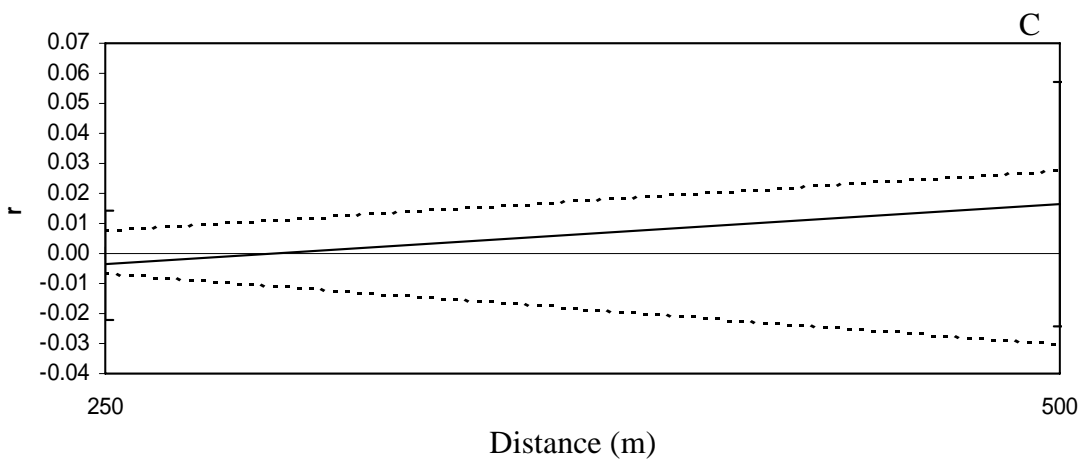
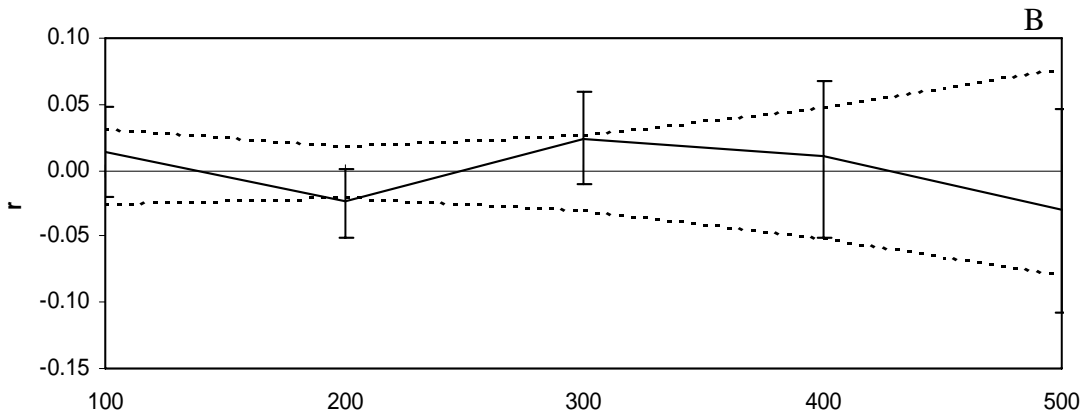
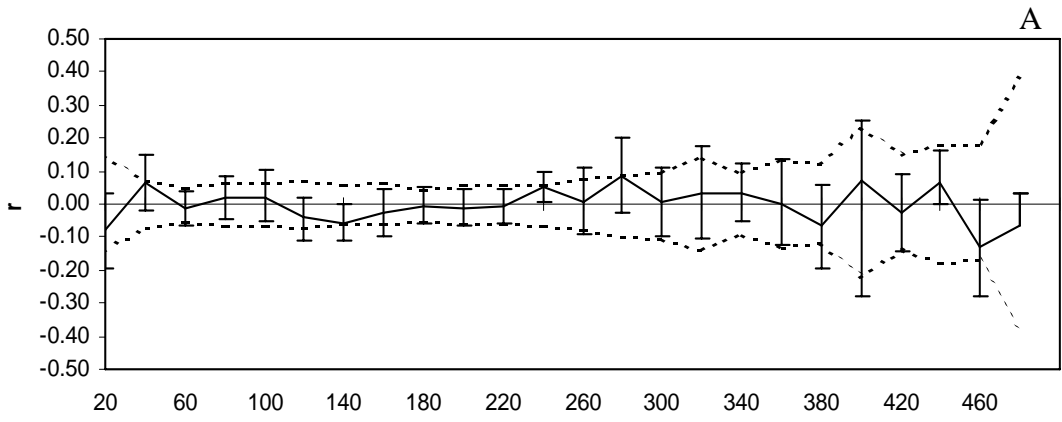


Fig. 11 Correlograms of Gazebo grid for the trapping period of March 2002 shows genetic correlation (r) as a function of distance and the 95% CI about a null hypothesis of randomly distributed genotypes. The 95% CI intervals about r are estimated by bootstrapping. Autocorrelation analysis are presented for distance class sizes of 20 m (A), 100 m (B) and 250 m (C).

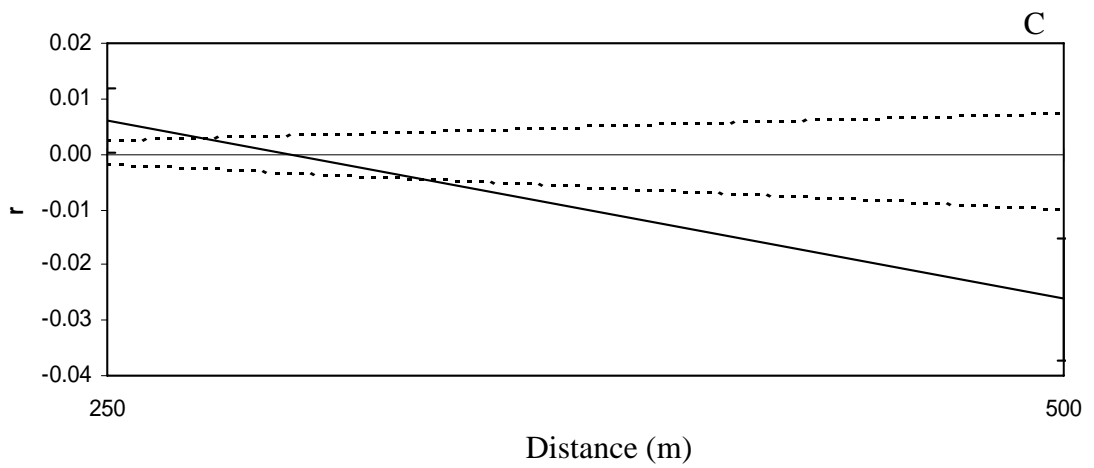
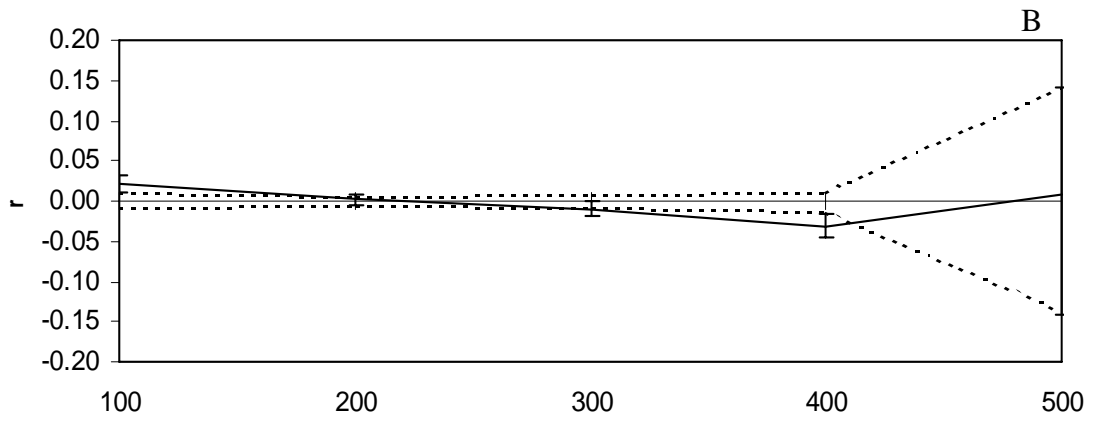
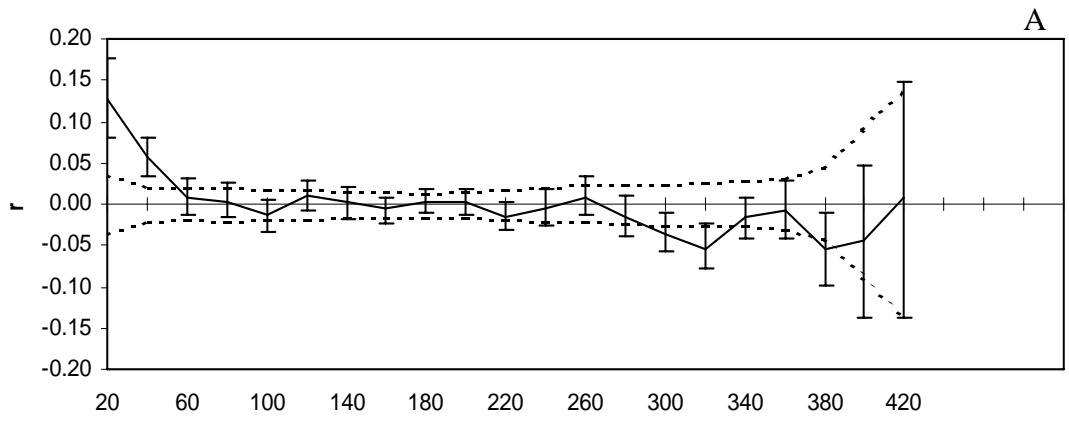


Fig. 12 Correlograms of Vet Village grid for the trapping period of March 1995 shows genetic correlation (r) as a function of distance and the 95% CI about a null hypothesis of randomly distributed genotypes. The 95% CI intervals about r are estimated by bootstrapping. Autocorrelation analysis are presented for distance class sizes of 20 m (A), 100 m (B) and 250 m (C).

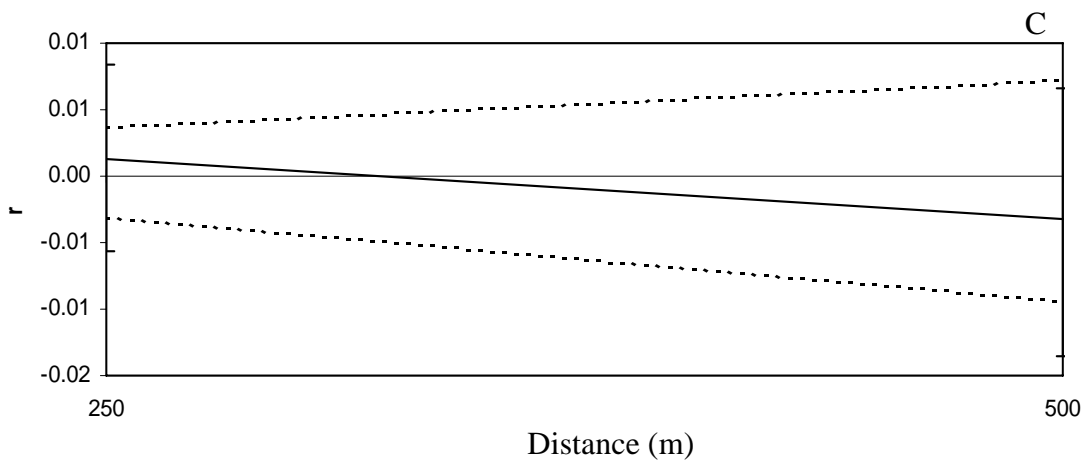
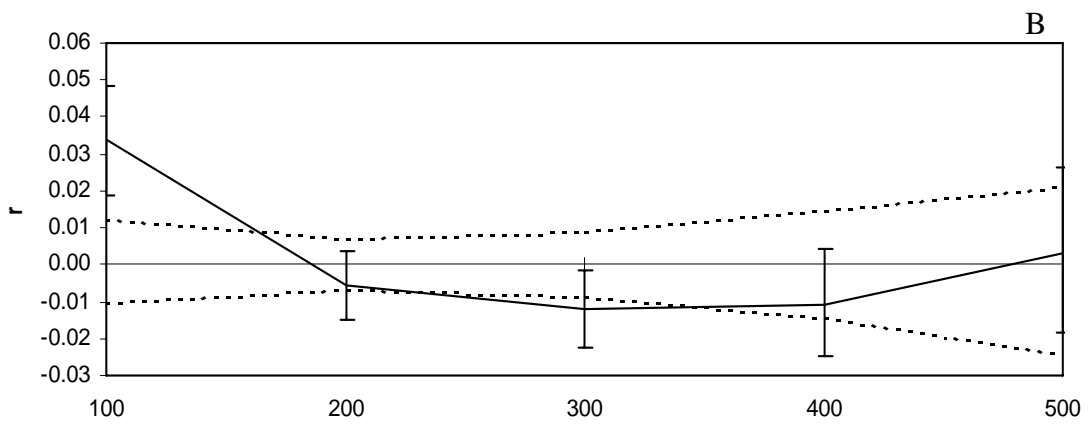
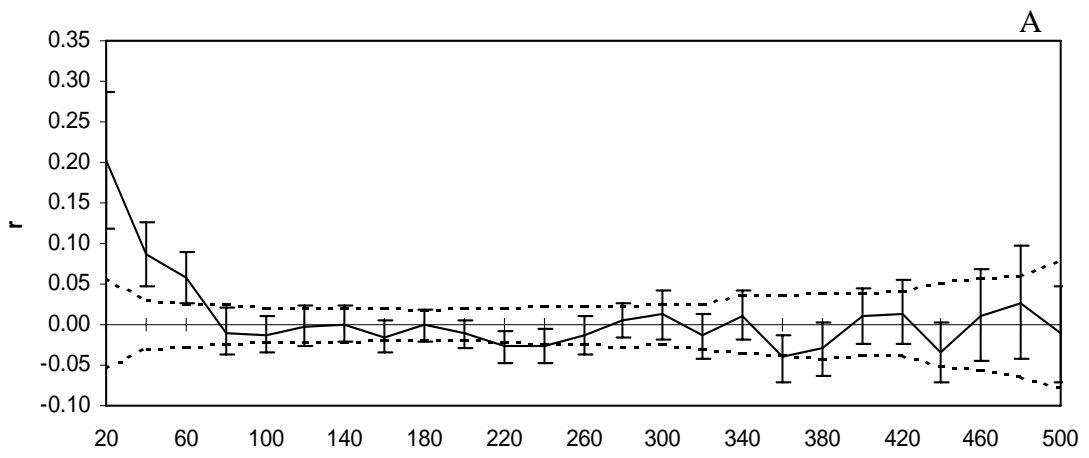


Fig. 13 Correlograms of Vet Village grid for the trapping period of April 1995 shows genetic correlation (r) as a function of distance and the 95% CI about a null hypothesis of randomly distributed genotypes. The 95% CI intervals about r are estimated by bootstrapping. Autocorrelation analysis are presented for distance class sizes of 20 m (A), 100 m (B) and 250 m (C).

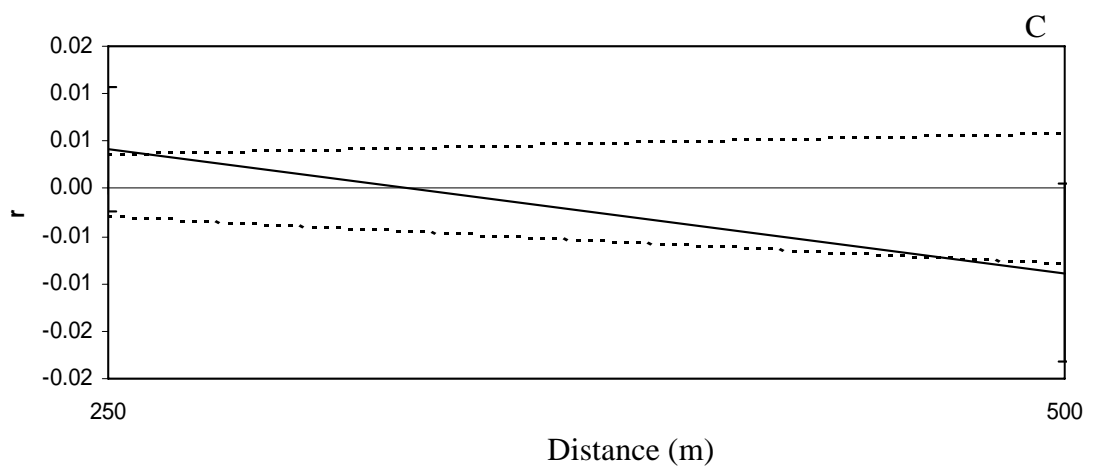
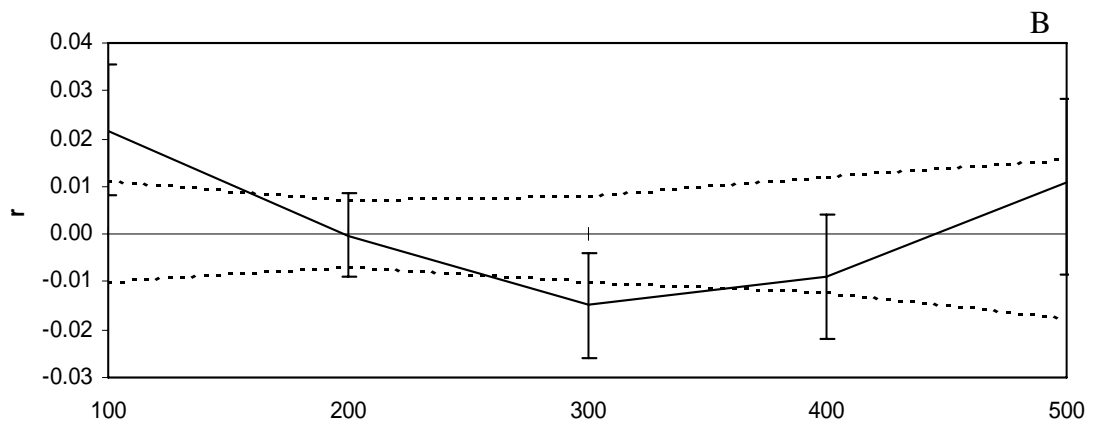
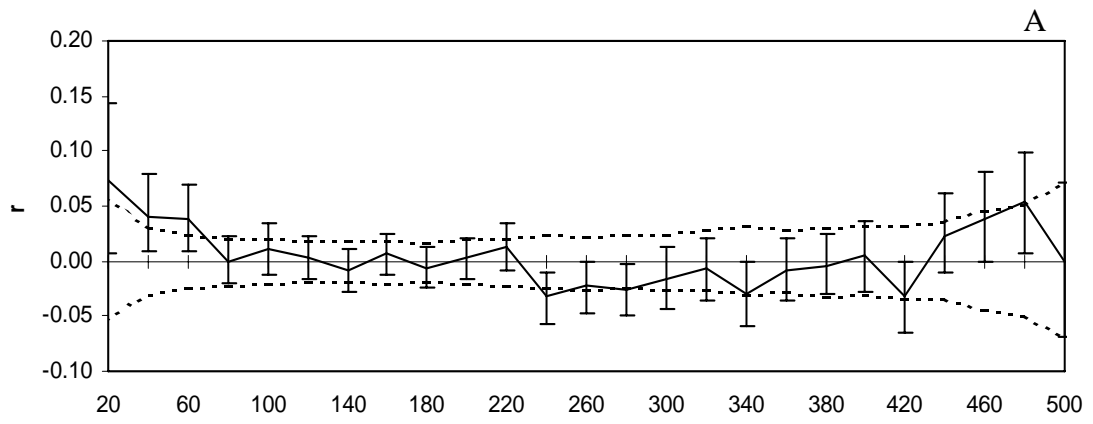


Fig. 14 Correlograms of Vet Village grid for the trapping period of June 1995 shows genetic correlation (r) as a function of distance and the 95% CI about a null hypothesis of randomly distributed genotypes. The 95% CI intervals about r are estimated by bootstrapping. Autocorrelation analysis are presented for distance class sizes of 20 m (A), 100 m (B) and 250 m (C).

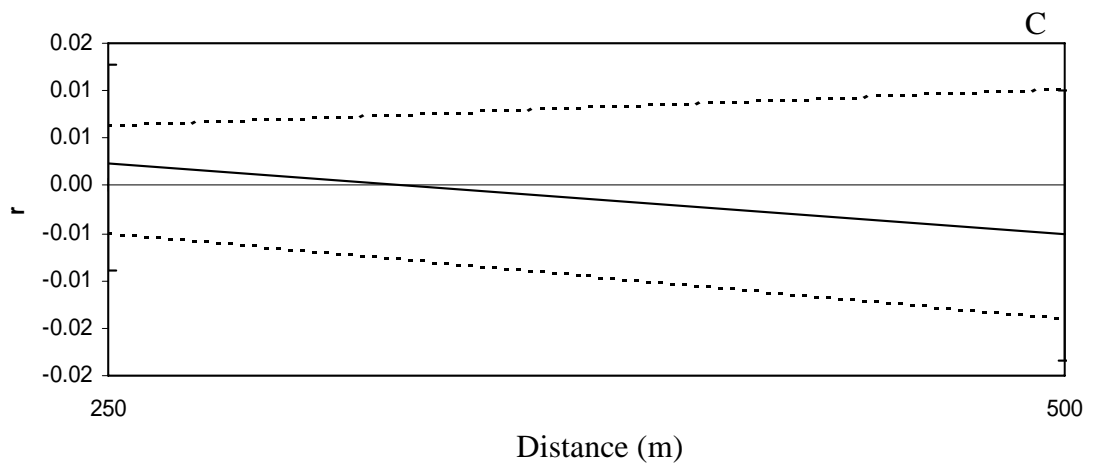
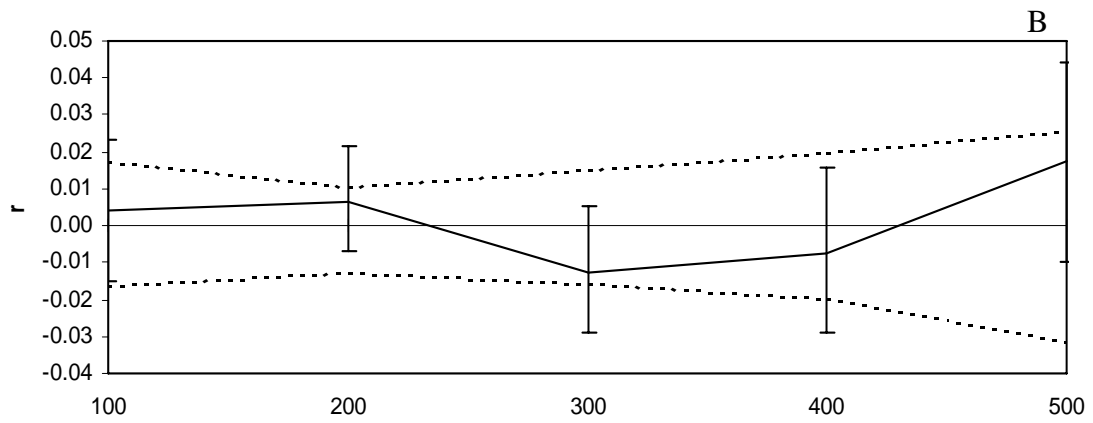
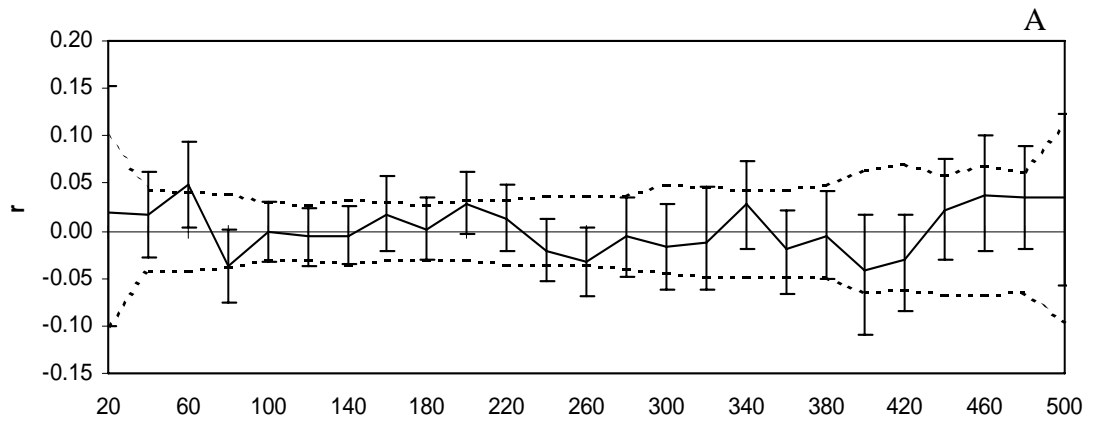


Fig. 15 Correlograms of Vet Village grid for the trapping period of March 1996 shows genetic correlation (r) as a function of distance and the 95% CI about a null hypothesis of randomly distributed genotypes. The 95% CI intervals about r are estimated by bootstrapping. Autocorrelation analysis are presented for distance class sizes of 20 m (A), 100 m (B) and 250 m (C).

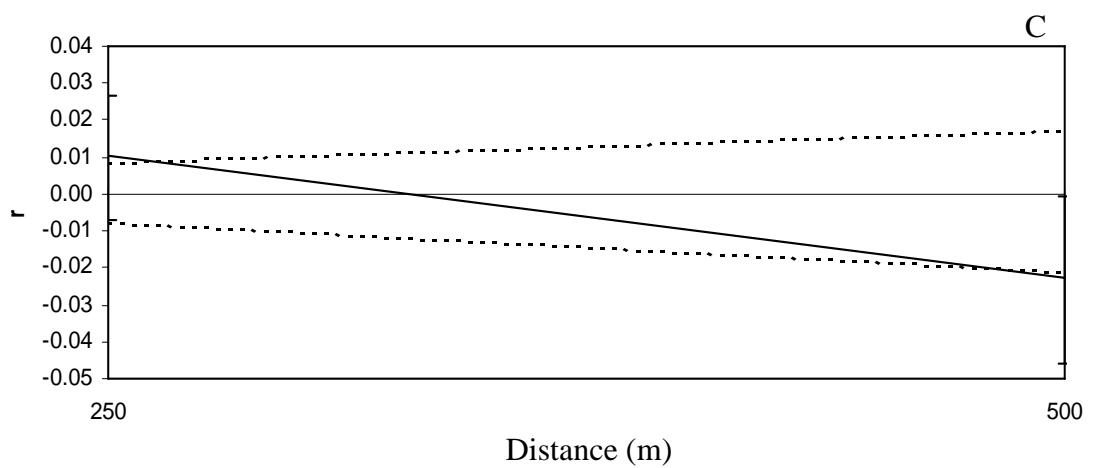
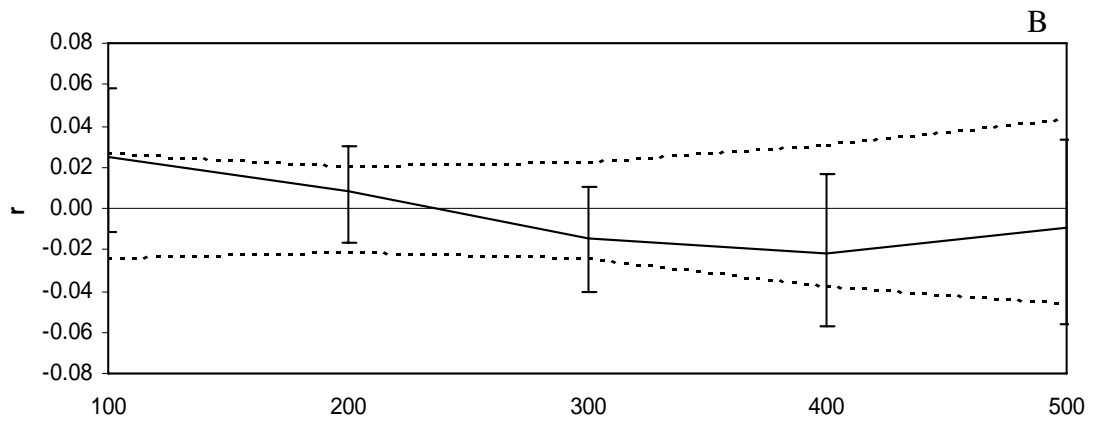
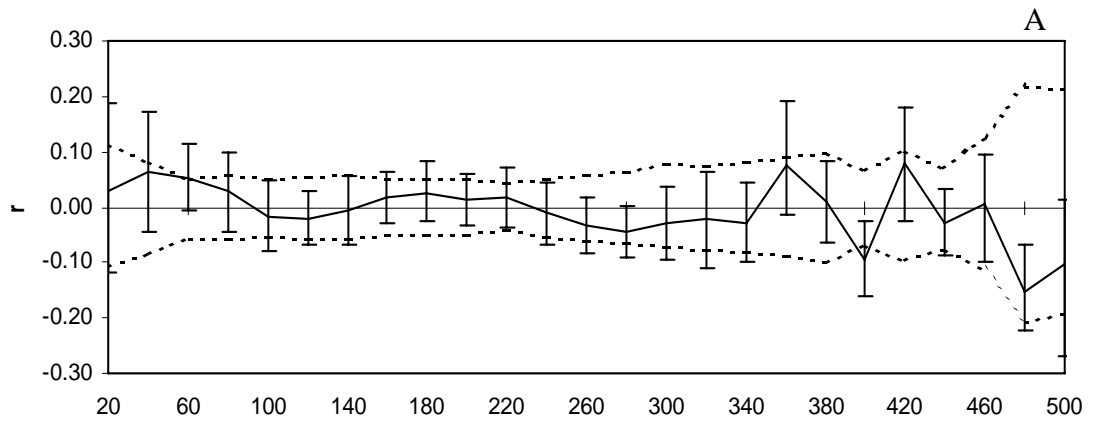


Fig. 16 Correlograms of Vet Village grid for the trapping period of April 1996 shows genetic correlation (r) as a function of distance and the 95% CI about a null hypothesis of randomly distributed genotypes. The 95% CI intervals about r are estimated by bootstrapping. Autocorrelation analysis are presented for distance class sizes of 20 m (A), 100 m (B) and 250 m (C).

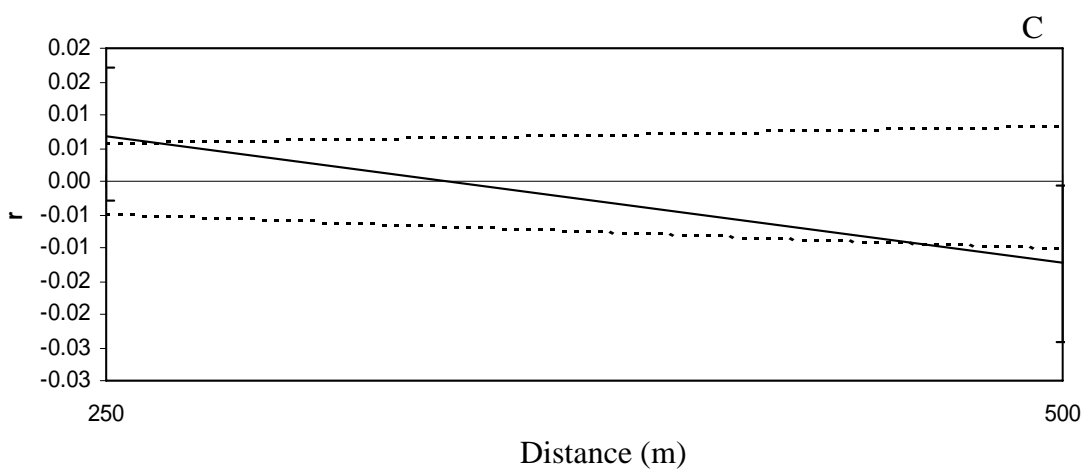
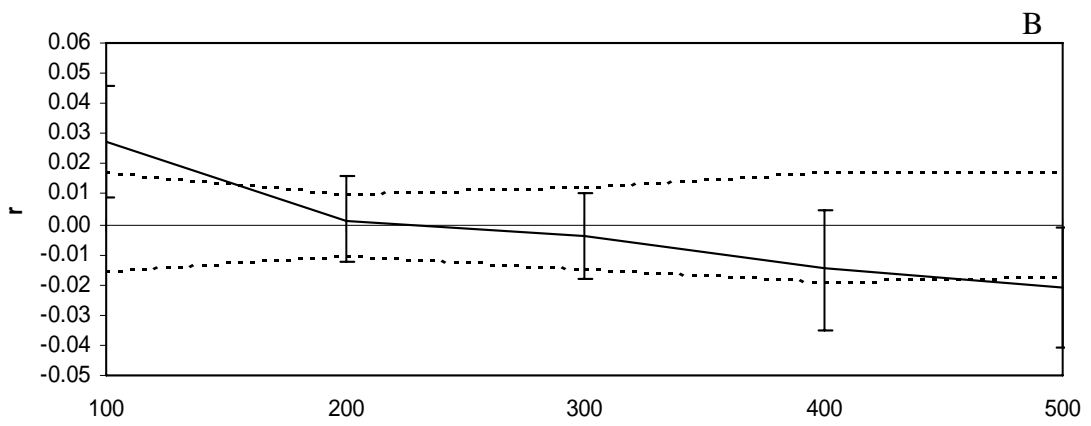
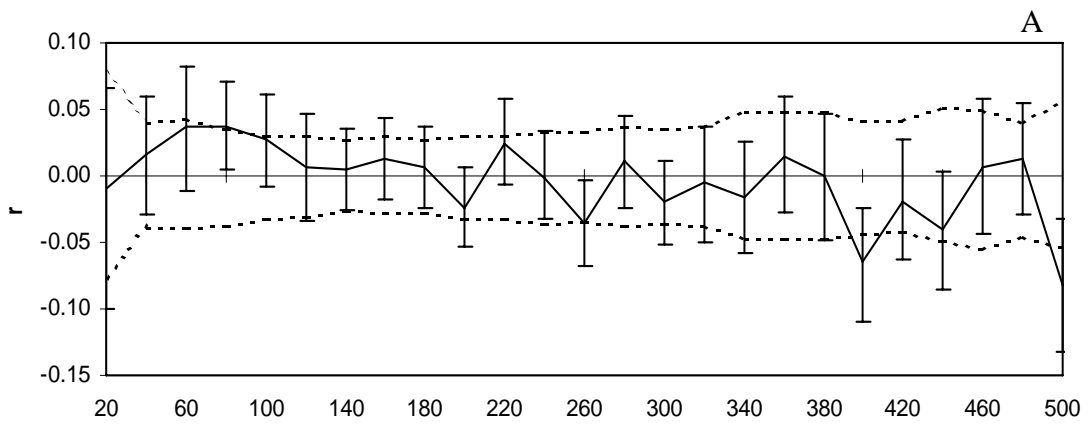


Fig. 17 Correlograms of Vet Village grid for the trapping period of June 1996 shows genetic correlation (r) as a function of distance and the 95% CI about a null hypothesis of randomly distributed genotypes. The 95% CI intervals about r are estimated by bootstrapping. Autocorrelation analysis are presented for distance class sizes of 20 m (A), 100 m (B) and 250 m (C).

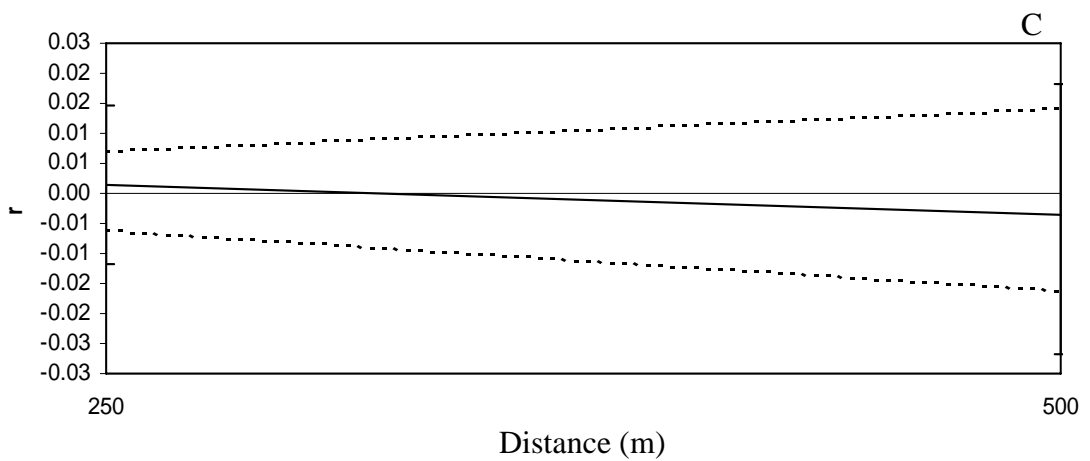
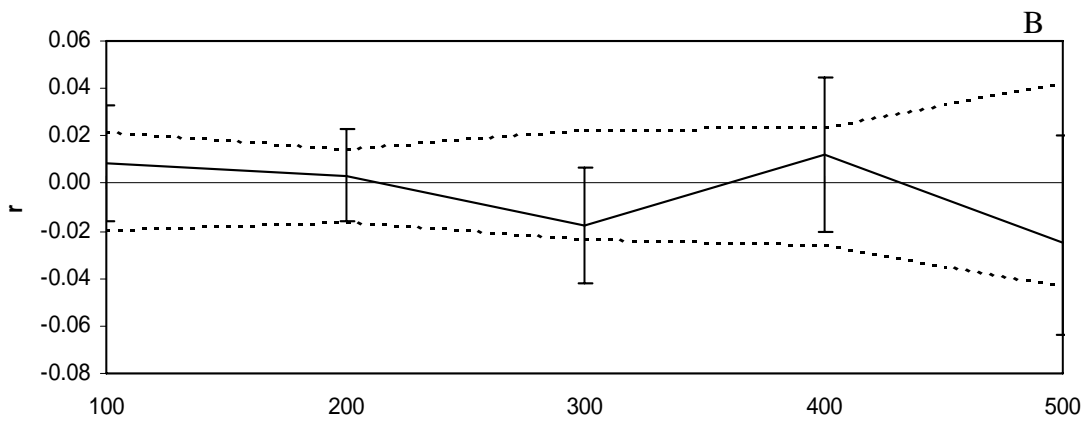
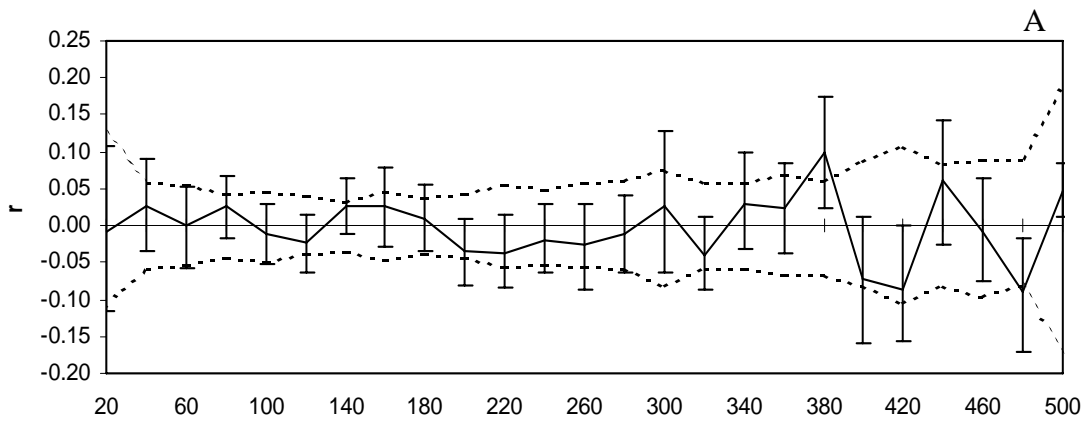


Fig. 18 Correlograms of Vet Village grid for the trapping period of February 2002 shows genetic correlation (r) as a function of distance and the 95% CI about a null hypothesis of randomly distributed genotypes. The 95% CI intervals about r are estimated by bootstrapping. Autocorrelation analysis are presented for distance class sizes of 20 m (A), 100 m (B) and 250 m (C).

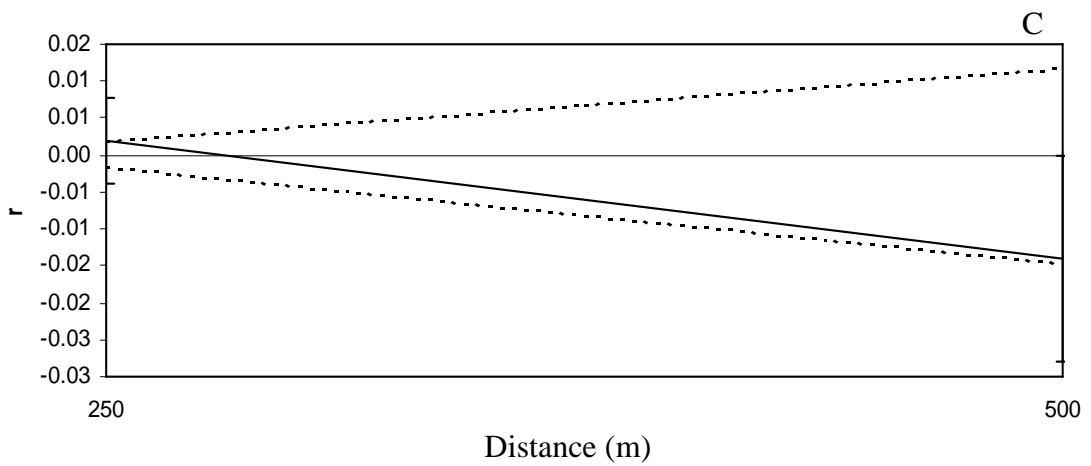
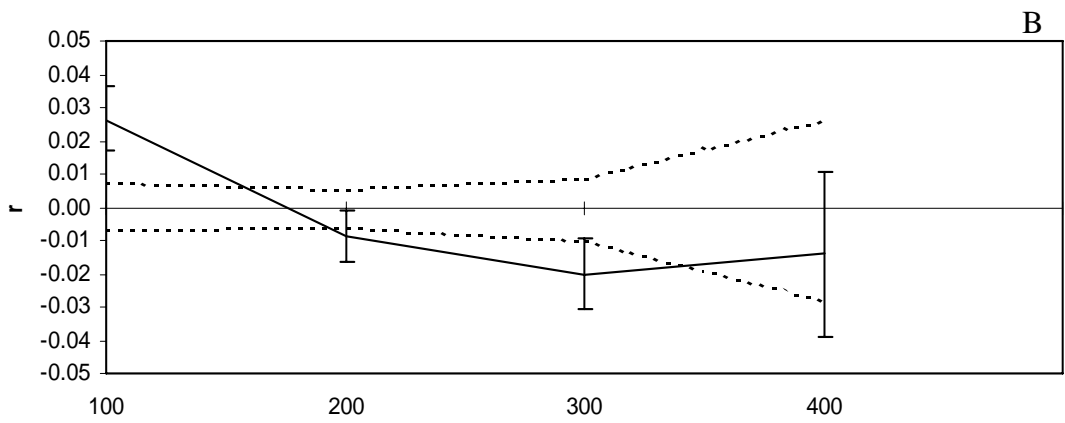
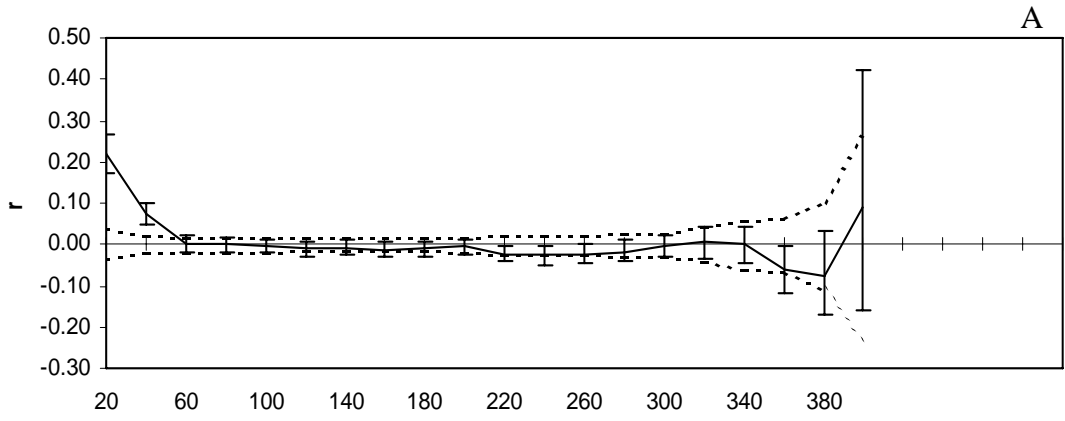


Fig. 19 Correlograms from combined trapping periods of February 1995 on Gazebo grid and March 1995 on Vet Village grid demonstrating genetic correlation (r) as a function of distance and the 95% CI about a null hypothesis of randomly distributed genotypes. The 95% CI intervals about r are estimated by bootstrapping. Autocorrelation analysis are presented for distance class sizes of 50 m (A), 200 m (B) and 800 m (C).

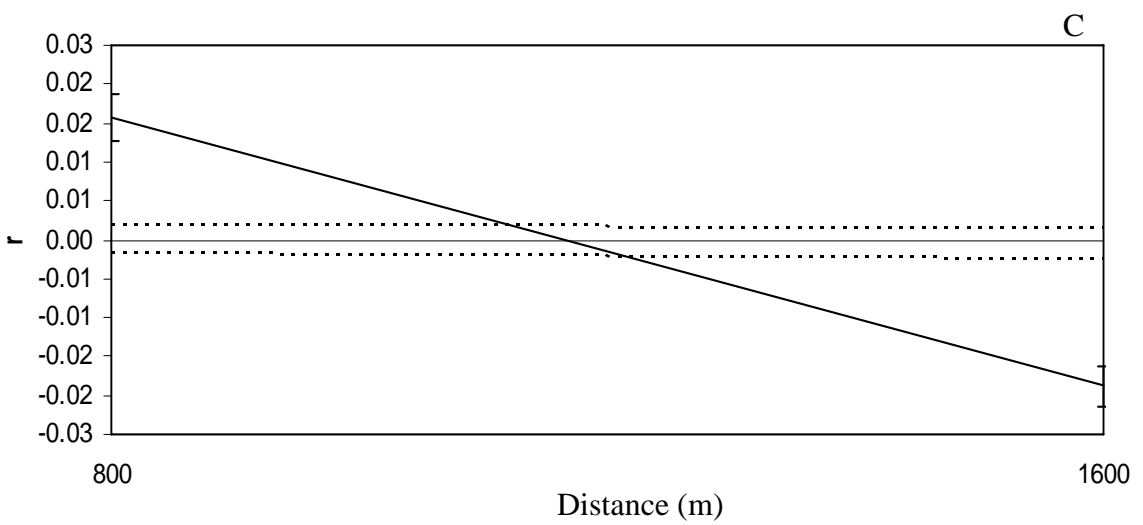
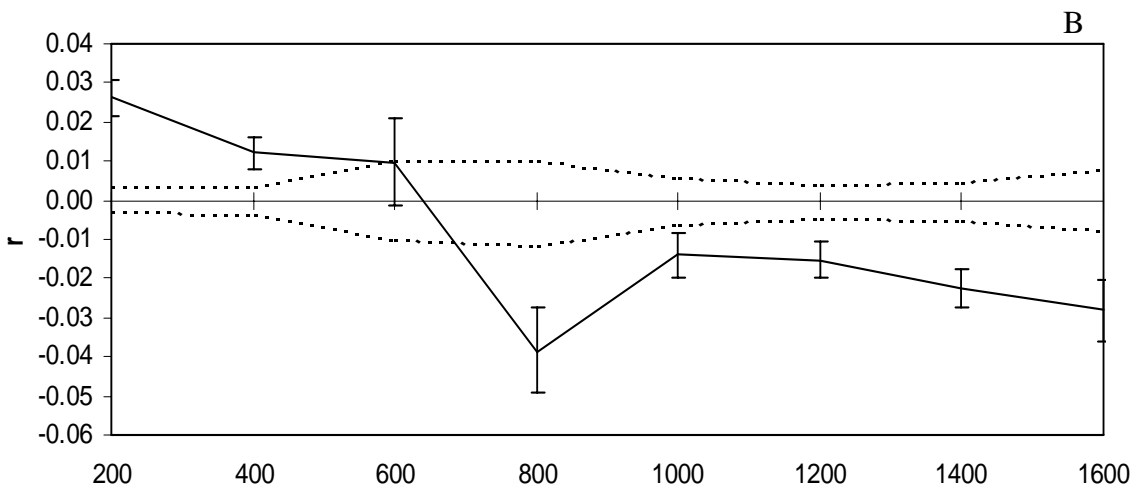
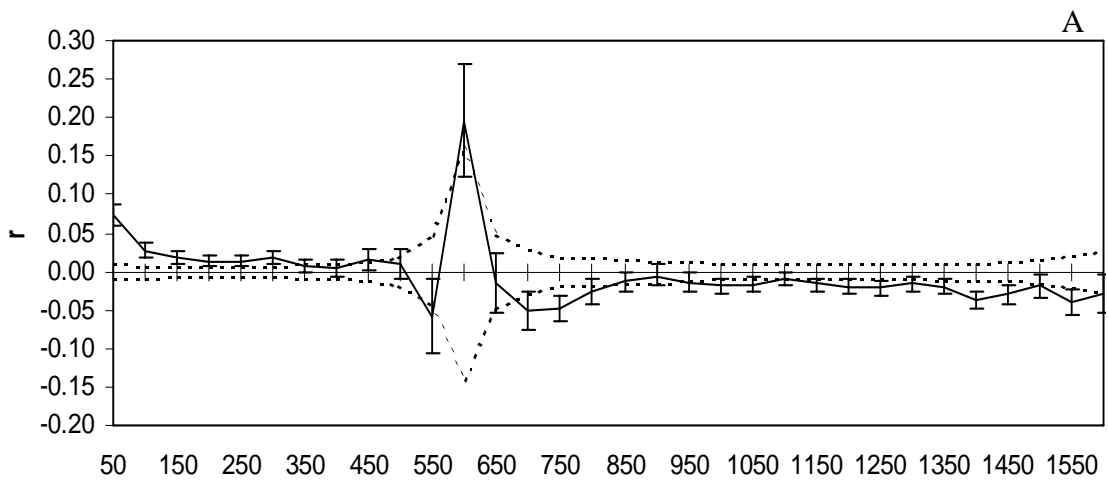


Fig. 20 Correlograms from combined trapping periods of April 1995 on both Gazebo and Vet Village grids demonstrating genetic correlation (r) as a function of distance and the 95% CI about a null hypothesis of randomly distributed genotypes. The 95% CI intervals about r are estimated by bootstrapping. Autocorrelation analysis are presented for distance class sizes of 50 m (A), 200 m (B) and 800 m (C).

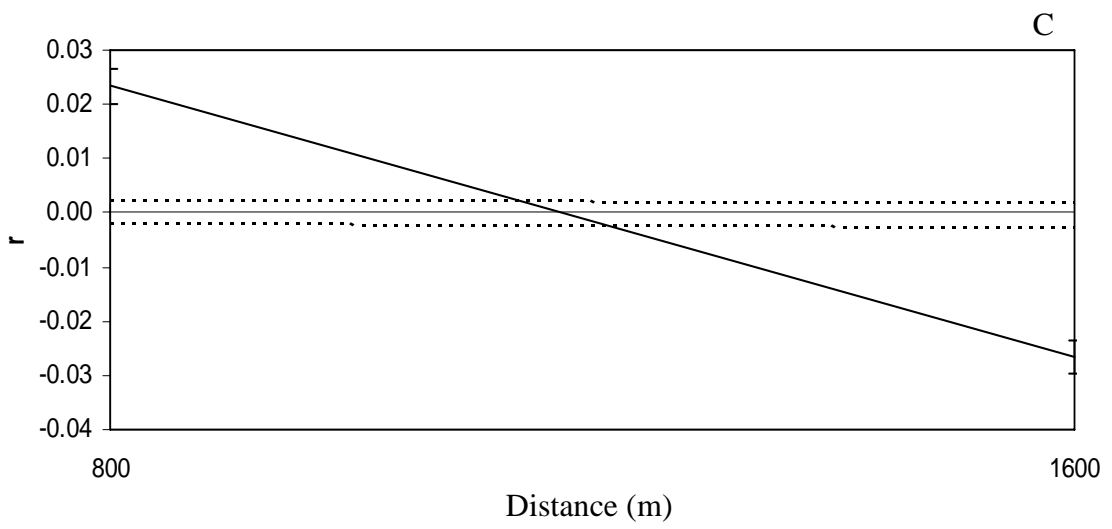
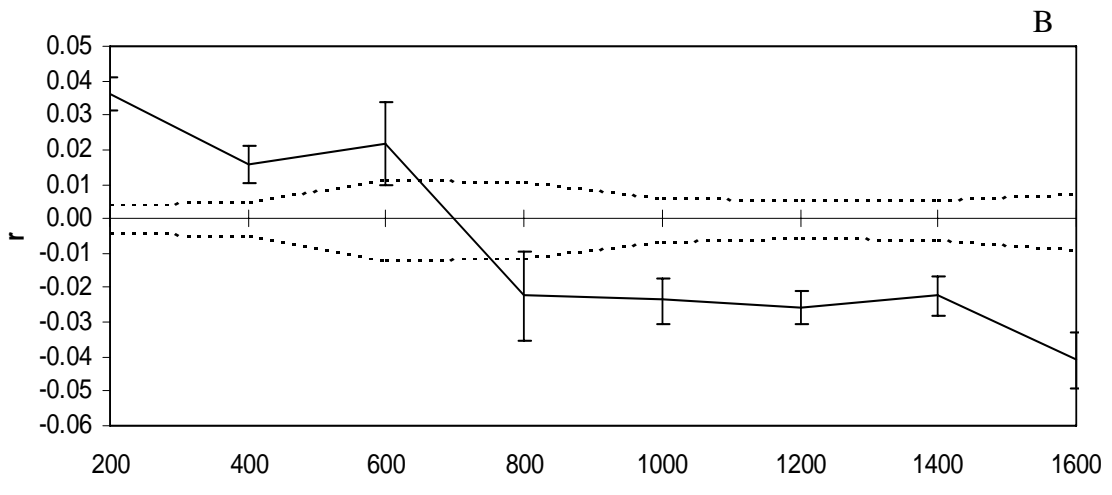
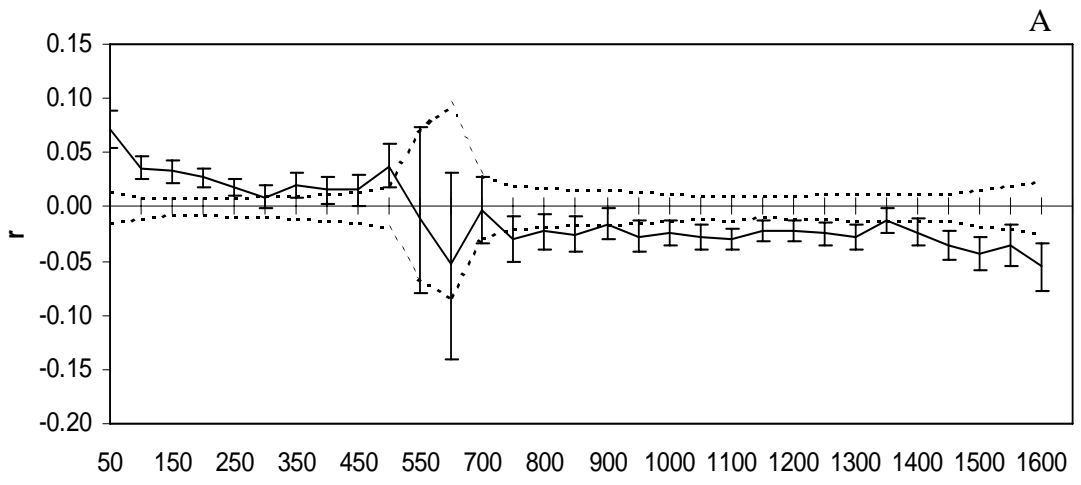


Fig. 21 Correlograms from combined trapping periods of June 1995 on both Gazebo and Vet Village grids demonstrating genetic correlation (r) as a function of distance and the 95% CI about a null hypothesis of randomly distributed genotypes. The 95% CI intervals about r are estimated by bootstrapping. Autocorrelation analysis are presented for distance class sizes of 50 m (A), 200 m (B) and 800 m (C).

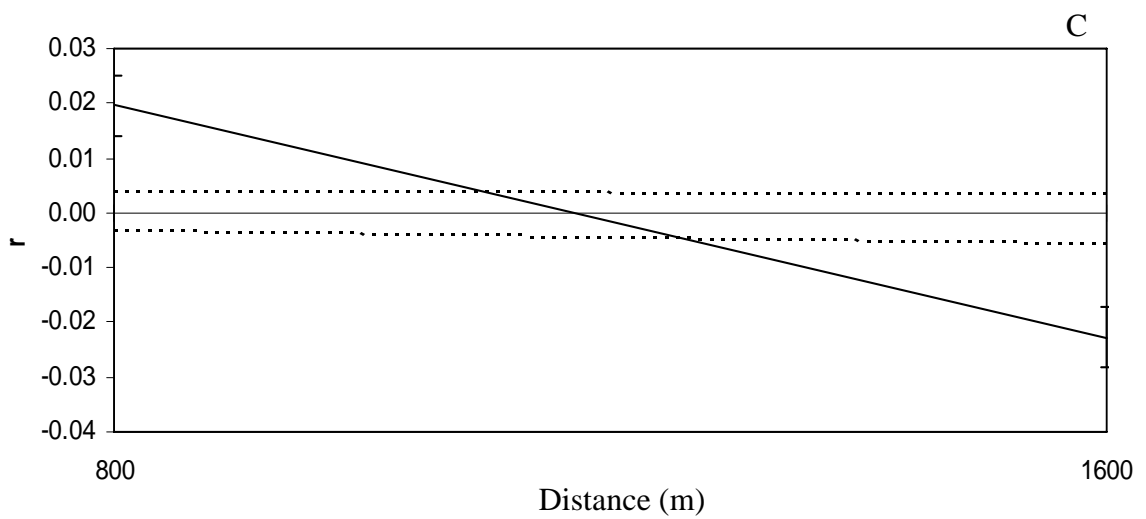
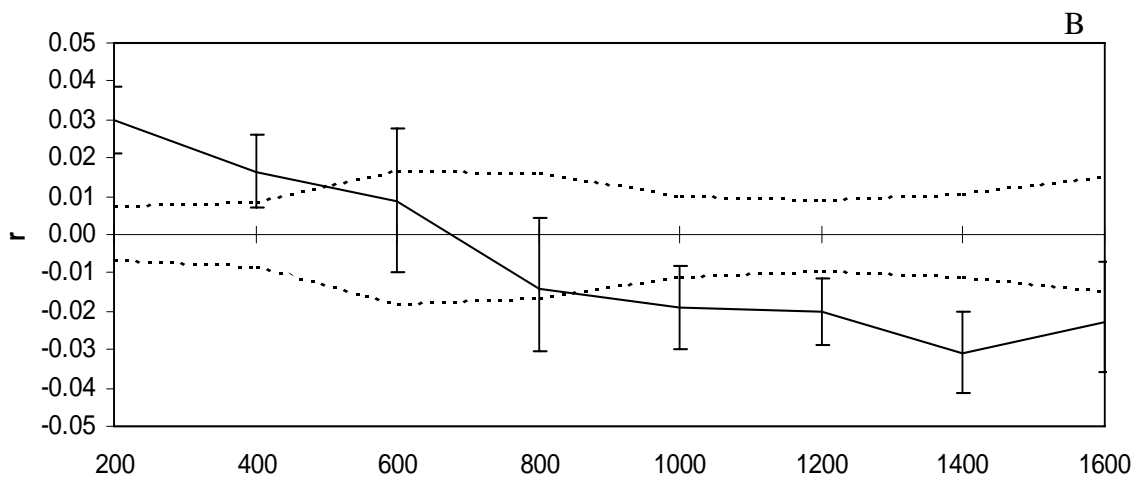
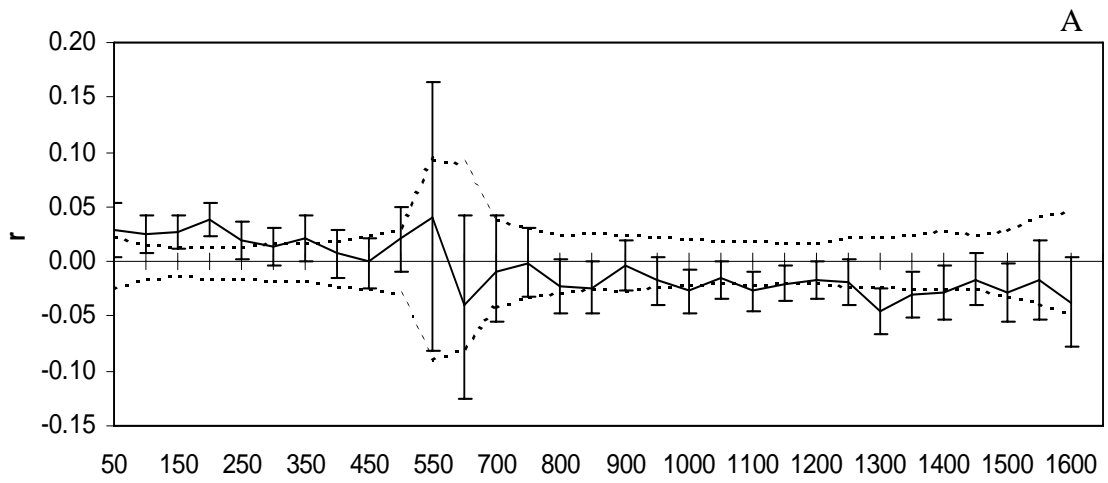


Fig. 22 Correlograms from combined trapping periods of February 1996 on Gazebo grid and March 1996 on Vet Village grid demonstrating genetic correlation (r) as a function of distance and the 95% CI about a null hypothesis of randomly distributed genotypes. The 95% CI intervals about r are estimated by bootstrapping. Autocorrelation analysis are presented for distance class sizes of 50 m (A), 200 m (B) and 800 m (C).

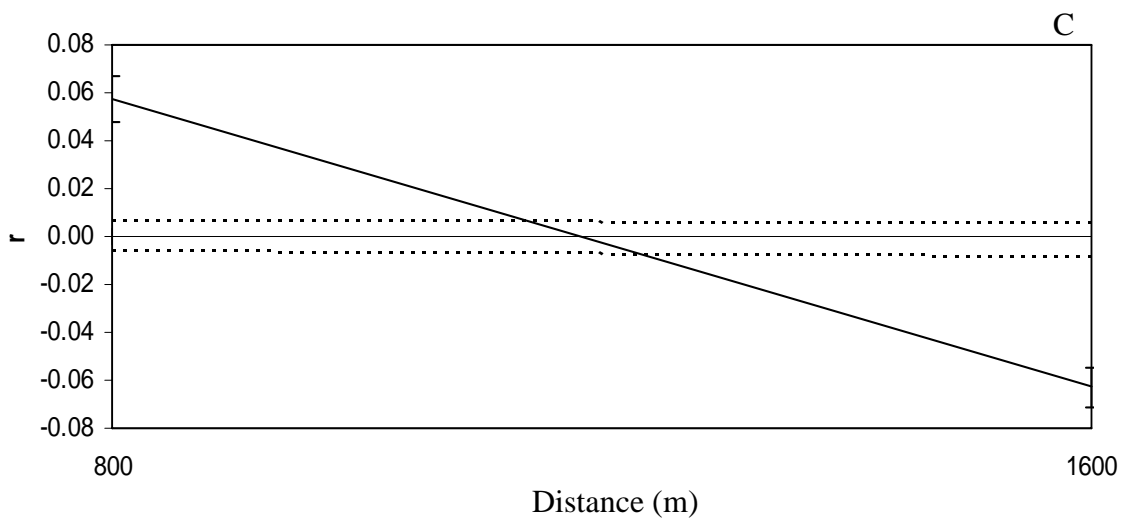
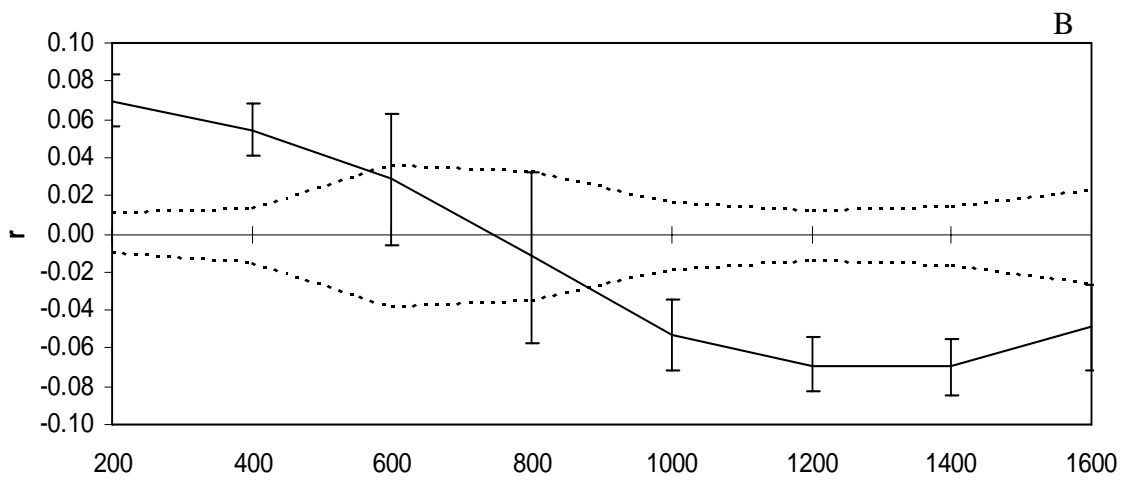
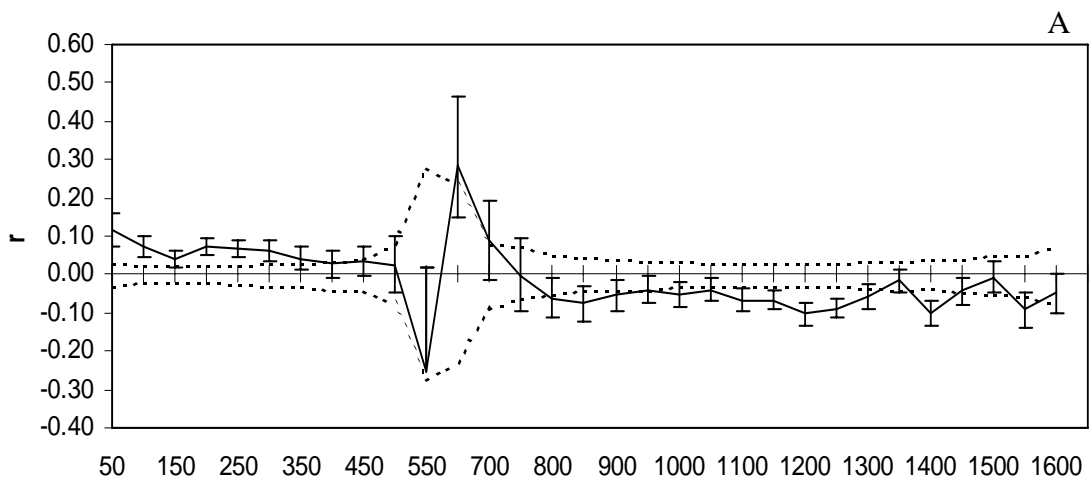


Fig. 23 Correlograms from combined trapping periods of April 1996 on both Gazebo and Vet Village grids demonstrating genetic correlation (r) as a function of distance and the 95% CI about a null hypothesis of randomly distributed genotypes. The 95% CI intervals about r are estimated by bootstrapping. Autocorrelation analysis are presented for distance class sizes of 50 m (A), 200 m (B) and 800 m (C).

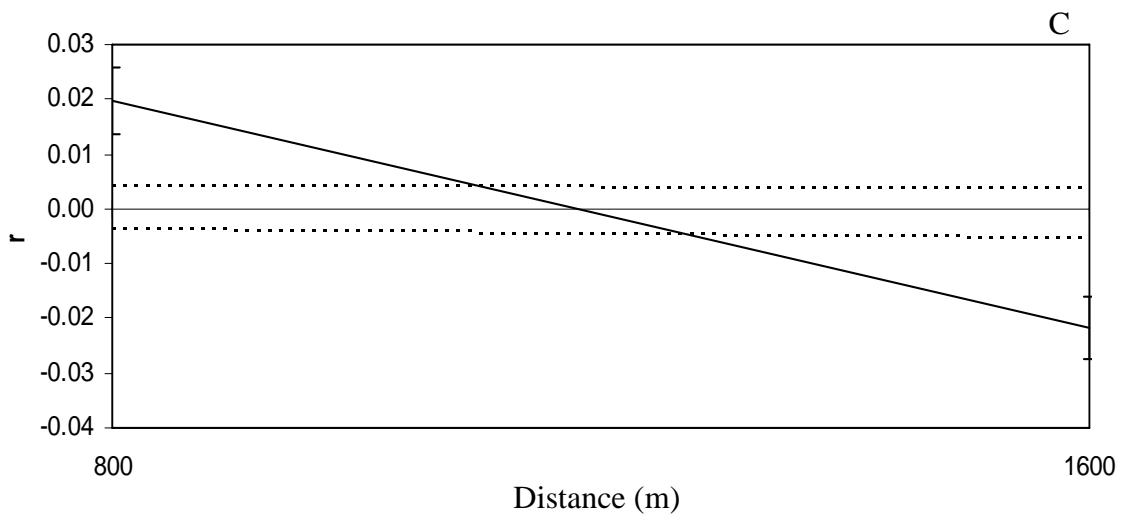
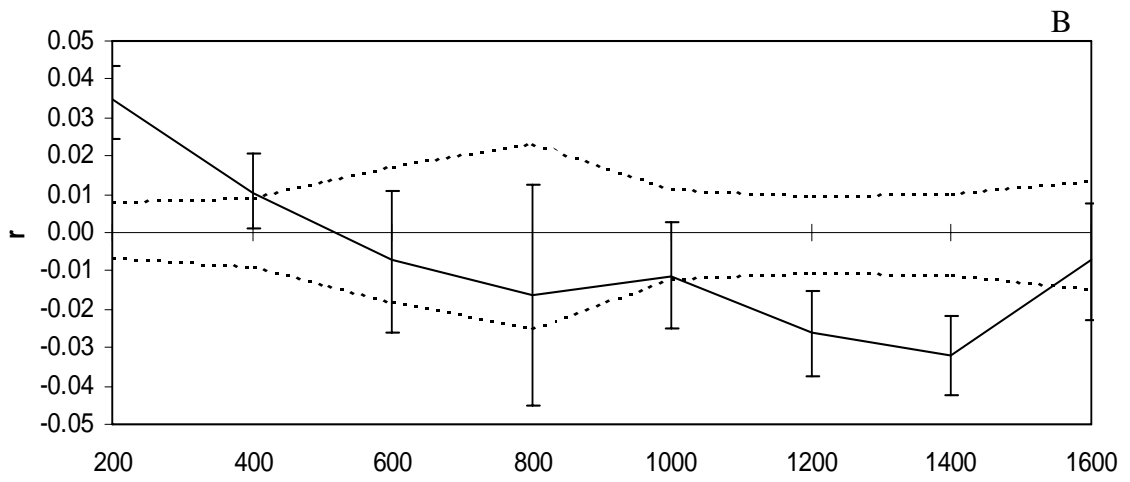
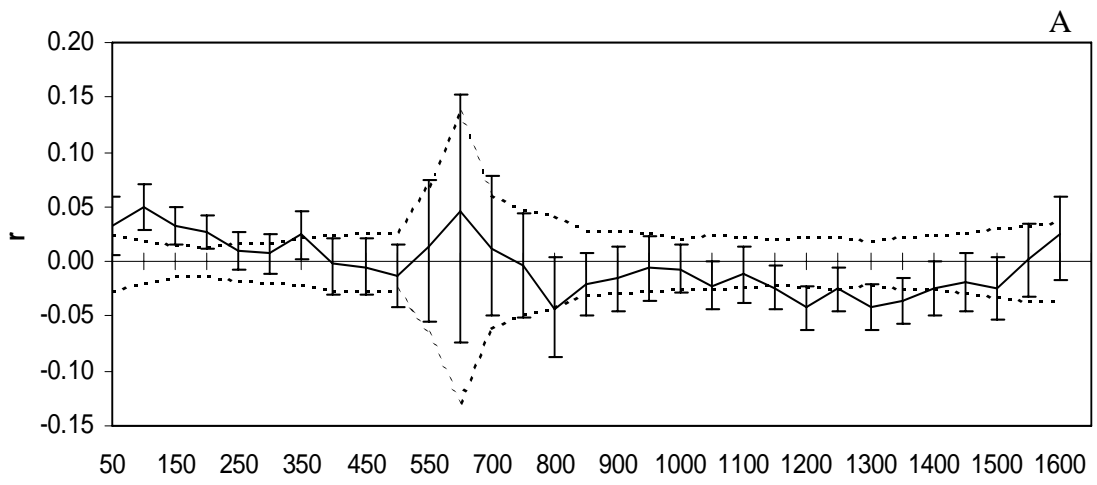


Fig. 24 Correlograms from combined trapping periods of June 1996 on both Gazebo and Vet Village grids demonstrating genetic correlation (r) as a function of distance and the 95% CI about a null hypothesis of randomly distributed genotypes. The 95% CI intervals about r are estimated by bootstrapping. Autocorrelation analysis are presented for distance class sizes of 50 m (A), 200 m (B) and 800 m (C).

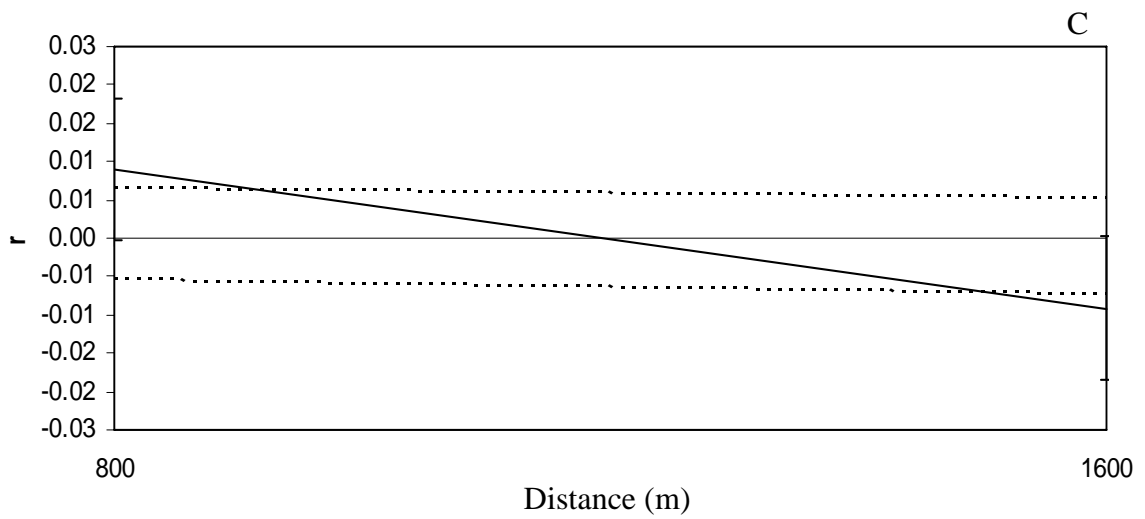
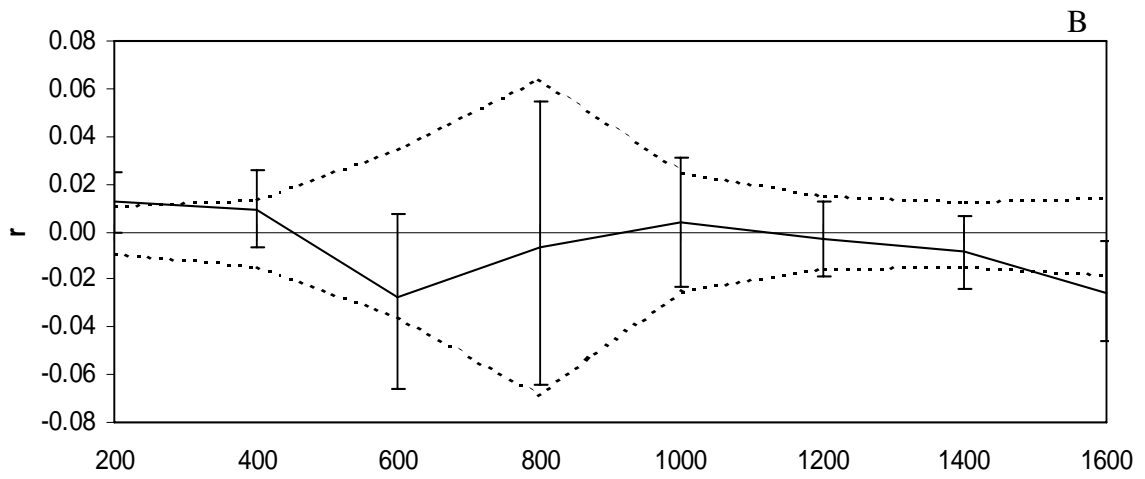
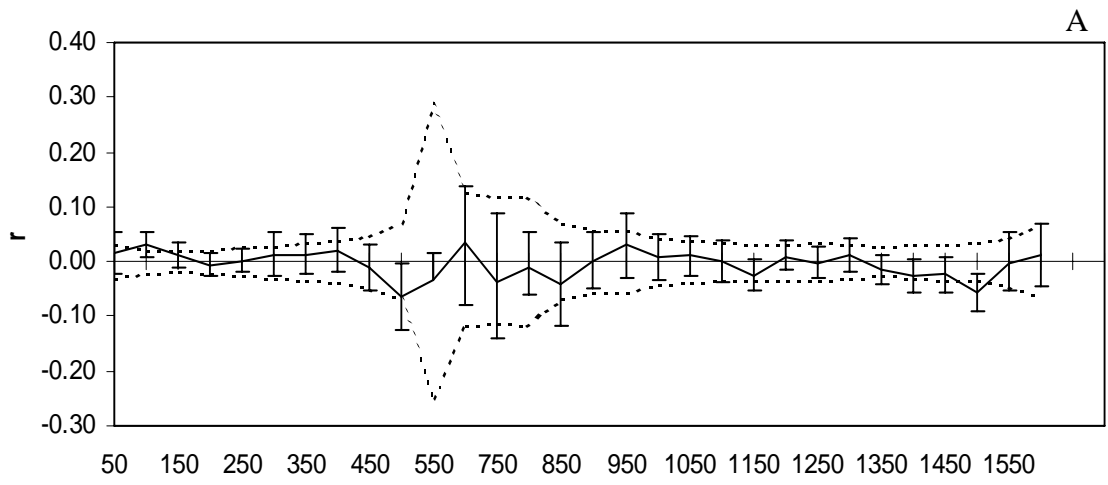


Fig. 25 Correlograms from combined trapping periods of March 2002 on Gazebo grid and February 2002 on Vet Village grid demonstrating genetic correlation (r) as a function of distance and the 95% CI about a null hypothesis of randomly distributed genotypes. The 95% CI intervals about r are estimated by bootstrapping. Autocorrelation analysis are presented for distance class sizes of 50 m (A), 200 m (B) and 800 m (C).

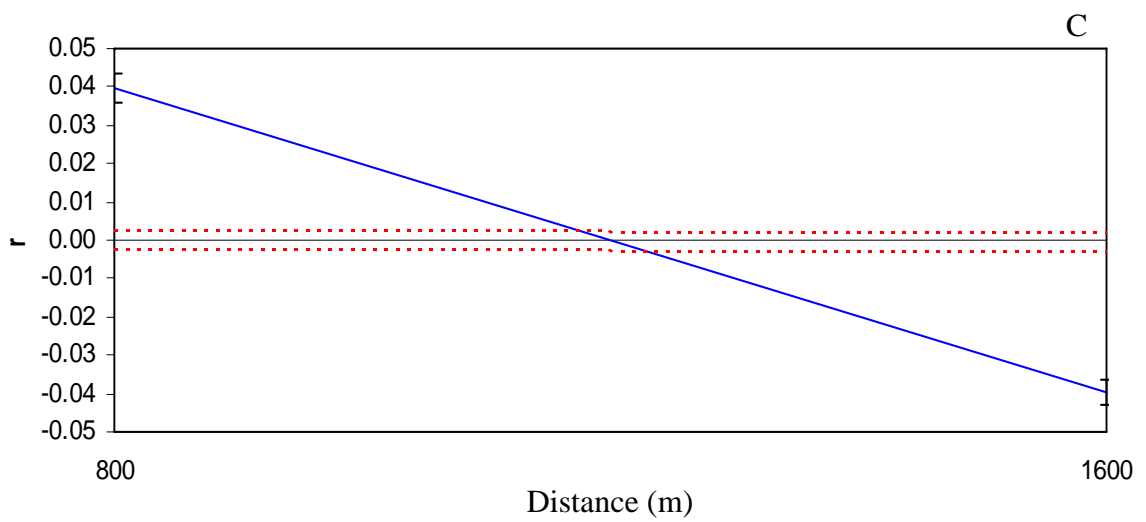
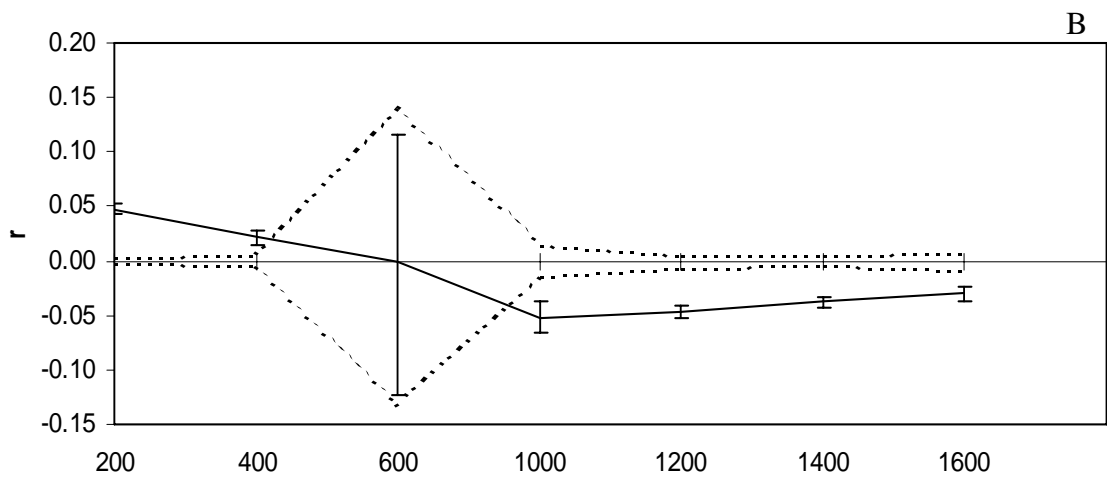
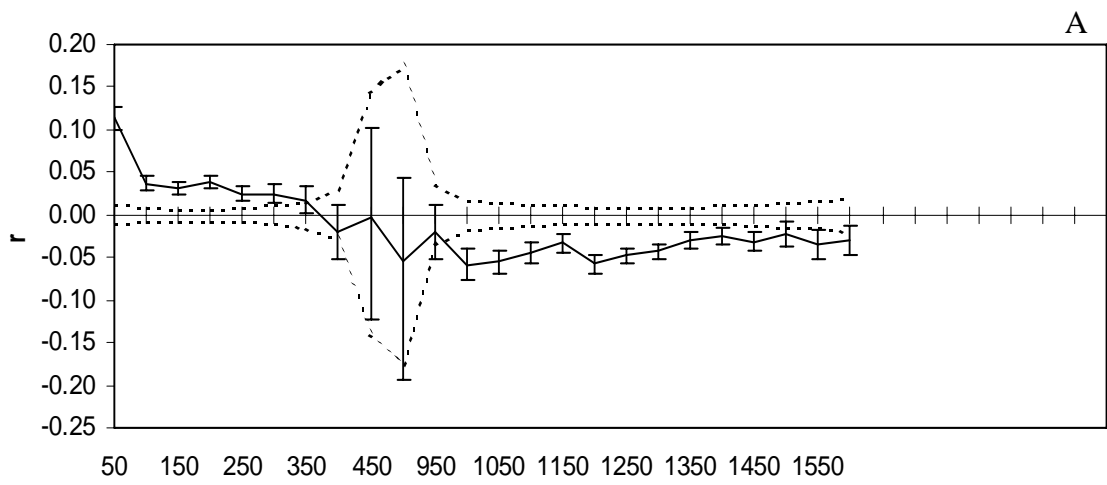


Table 1 Characterization of 11 microsatellite used for *Peromyscus polionotus ammobates* including primer sequences, Accession number, repeat motif, annealing temperature (T_a) and number of observed alleles.

Locus	Accession no.	Repeat motif	Primer sequence (5' - 3')	T_a (°C)	Alleles
Ppa01	AF016855	(AC) ₂₄	F:ATGTGCAGCTTTGTTGAGTTA R:ATTTCCATCTTGTGTCTTTCCCTA	58	3
Ppa12	AF016858	(AG) ₃₇	F:TGCCAAACTACACAAAGAGACCCCT R:GGACACAGAAAGGTCTCAAAGCTGA	58	9
Ppa46	AF016860	(GT) ₆ TT(GT) ₁₈	F:AGTCCACAGAGGGAGCTTCTAAG R:TTTTACAGAAAGGCAACATTTC	58	6
PO-25	AF380236	(AG) ₂₃	F:GGACAGCCAGGACTGTTACAC R:CCCACCTCATCTCAATGCC	65	8
PO-71	AF380240	(AC) ₁₀ (AG) ₄ AA(AG) ₂₈	F:CAGCCAGAAACAAAATAGCACT R:AGCTTCAATGCCCTCCTATATTC	64	10
PO3-68	AF380248	(TG) ₂₂₊	F:GTAGTCTGAGAAAGCGAAAGG R:TTTATTTGGGTCAGCTCGAC	58	8
PO3-85	AF380250	(AC) ₂₁	F:TGGCAAGGCTGATAAC R:CTCCCTCTTGGTCATCAGTA	58	6
Pm103	AF251777	(CA) ₂₂	F:GCCATTAGTCTATGTGACAG R:GCGATGTACCCAGAAAT	54	8
Pm104	AF251778	(CA) ₂₇	F:CATAAGGTGGCTCGGAATCA R:CAGGAAAGGGAATGACCCAT	57	5
Pm106	AF251780	(CA) ₂₄	F:CAGGGCTGTAGAGGGAGAAC R:ACTGGAGCAGAGGCATTTG	54	3
Pm111	AF251785	(CA) ₂₃	F:ACCCCCGAGTGTGAGATT R:GCCAACCCATTTCTTCAAGTG	57	7

Table 2 Total captures, new captures per trapping period and the number of individuals from which tissue was obtained.

Trap period	Captures	Tissue	New captures	Tissue
1st-95	322	248	322	248
2nd-95	329	235	98	89
3rd-95	189	138	15	14
1st-96	134	92	78	73
2nd-96	178	124	78	65
3rd-96	115	78	31	30
1st-97	45	37	39	34
1st-98	33	31	31	30
1st-99	16	15	16	15
1st-00	64	58	62	58
2nd-00	26	21	22	18
1st-01	83	65	71	56
2nd-01	61	48	48	43
1st-02	274	237	253	234
Totals	1869	1427	1163	1007

Table 3 Total captures, new captures and the number of individuals from which tissue was obtained on Gazebo grid.

Gazebo				
Trap period	Captures	Tissue	New captures	Tissue
Feb-95	170	145	170	145
Apr-95	166	122	41	38
Jun-95	91	68	6	6
Feb-96	77	48	41	37
Apr-96	75	52	25	24
Jun-96	53	34	12	12
Feb-97	11	9	9	8
Apr-98	10	9	9	9
Feb-99	9	9	9	9
Mar-00	33	32	33	32
Nov-00	16	13	14	11
Mar-01	29	22	24	18
Nov-01	12	12	11	11
Mar-02	138	120	135	117
Totals	890	695	539	477

Table 4 Total captures, new captures and the number of individuals from which tissue was obtained on Vet Village grid.

Vet Village				
Trap period	Captures	Tissue	New captures	Tissue
Mar-95	152	103	152	103
Apr-95	163	113	57	51
Jun-95	98	70	9	8
Mar-96	57	44	37	36
Apr-96	103	72	53	41
Jun-96	62	44	19	18
Mar-97	34	28	30	26
Feb-98	23	22	22	21
Feb-99	7	6	7	6
Mar-00	31	26	29	26
Dec-00	10	8	8	7
Mar-01	54	43	47	38
Oct-01	49	36	37	32
Feb-02	136	117	118	117
Totals	979	732	625	530

Table 5 The total number of alleles observed for each trapping period on each grid.

Locus	Gazebo	Vet Village	Total
Ppa-01	3	3	3
Ppa-12	8	6	9
Ppa-46	6	3	6
PO3-85	6	6	6
PO3-68	8	7	8
PO-25	8	6	8
Pml-03	7	6	8
Pml-11	7	7	7
Pml-04	4	4	5
PO-71	10	8	10
Pml-06	3	3	3
Total	70	59	73

Table 6 Summary statistics from Gazebo trap period February 1995 and Vet Village trap period March, 1995 included are sample size (N), number of alleles, effective number of alleles (N_e), observed heterozygosity (H_{OBS}), expected heterozygosity (H_{EXP}), and the fixation index (F).

Gazebo (Feb-95)						
Locus	N	Alleles	N_e	H_{OBS}	H_{EXP}	F
Ppa-01	142	3.0	1.6632	0.3485	0.3987	0.1260
Ppa-12	142	4.0	2.4367	0.6761	0.5896	-0.1466
Ppa-46	97	3.0	2.2040	0.5979	0.5463	-0.0946
PO3-85	143	5.0	2.2975	0.6014	0.5647	-0.0649
PO3-68	141	7.0	4.1798	0.7305	0.7608	0.0398
PO-25	145	5.0	2.6969	0.6069	0.6292	0.0355
Pml-03	142	5.0	2.4608	0.5435	0.5936	0.0845
Pml-11	142	6.0	4.0243	0.7042	0.7515	0.0629
Pml-04	118	3.0	1.9340	0.5508	0.4829	-0.1406
PO-71	142	8.0	3.2747	0.6831	0.6946	0.0166
Pml-06	143	3.0	2.6326	0.6643	0.6202	-0.0712
Mean	136	4.73	2.7096	0.6095	0.6031	-0.0140
St. Dev		1.74	0.8046	0.1062	0.1084	0.0936
Vet Village (Mar-95)						
Locus	N	Alleles	N_e	H_{OBS}	H_{EXP}	F
Ppa-01	100	2.0	1.8247	0.4100	0.4520	0.0928
Ppa-12	98	5.0	2.9451	0.6531	0.6605	0.0112
Ppa-46	94	3.0	2.0406	0.4894	0.5100	0.0404
PO3-85	102	5.0	3.4061	0.7353	0.7064	-0.0409
PO3-68	101	6.0	4.4682	0.8119	0.7762	-0.0460
PO-25	100	4.0	2.5777	0.7000	0.6120	-0.1437
Pml-03	103	4.0	2.5521	0.5534	0.6082	0.0900
Pml-11	103	6.0	4.1727	0.7282	0.7603	0.0423
Pml-04	103	3.0	1.6303	0.4175	0.3866	-0.0798
PO-71	86	8.0	3.3489	0.6395	0.7014	0.0882
Pml-06	101	3.0	2.7656	0.6040	0.6384	0.0540
Mean	99	4.45	2.8848	0.6128	0.6191	0.0097
St. Dev		1.75	0.9102	0.1328	0.1243	0.0780

Table 7 Summary statistics from Gazebo trap period April, 1995 and Vet Village trap period April, 1995 included are sample size (N), number of alleles, effective number of alleles (N_e), observed heterozygosity (H_{OBS}), expected heterozygosity (H_{EXP}), and the fixation index (F).

Gazebo (Apr-95)						
Locus	N	Alleles	N_e	H_{OBS}	H_{EXP}	F
Ppa-01	112	3.0	1.7174	0.4286	0.4177	-0.0260
Ppa-12	119	4.0	2.5075	0.6218	0.6012	-0.0344
Ppa-46	95	3.0	1.8742	0.5263	0.4664	-0.1284
PO3-85	121	5.0	2.2361	0.5785	0.5528	-0.0465
PO3-68	119	7.0	4.2886	0.7227	0.7668	0.0576
PO-25	121	5.0	2.6654	0.5950	0.6248	0.0477
Pml-03	91	5.0	2.5247	0.4835	0.6039	0.1994
Pml-11	118	6.0	4.0553	0.7288	0.7534	0.0326
Pml-04	106	3.0	1.8863	0.5094	0.4699	-0.0842
PO-71	122	7.0	3.5400	0.7131	0.7175	0.0061
Pml-06	121	3.0	2.5957	0.6612	0.6147	-0.0755
Mean	113	4.64	2.7173	0.5973	0.5991	-0.0045
St. Dev.		1.57	0.8758	0.1028	0.1167	0.0890
Vet Village (Apr-95)						
Locus	N	Alleles	N_e	H_{OBS}	H_{EXP}	F
Ppa-01	111	2.0	1.8804	0.4955	0.4682	-0.0583
Ppa-12	108	5.0	2.9710	0.6667	0.6634	-0.0049
Ppa-46	111	3.0	2.0790	0.5135	0.5190	0.0106
PO3-85	113	6.0	3.2783	0.6726	0.6950	0.0322
PO3-68	112	7.0	4.8545	0.8214	0.7940	-0.0345
PO-25	113	5.0	2.6153	0.6903	0.6176	-0.1176
Pml-03	113	4.0	2.4888	0.5664	0.5982	0.0532
Pml-11	113	7.0	3.8271	0.7434	0.7387	-0.0063
Pml-04	113	3.0	1.7451	0.4425	0.4270	-0.0363
PO-71	98	8.0	3.0916	0.6837	0.6765	-0.0105
Pml-06	113	3.0	2.7445	0.5664	0.6356	0.1090
Mean	111	4.82	2.8704	0.6237	0.6213	-0.0058
St. Dev.		1.99	0.9042	0.1157	0.1124	0.0595

Table 8 Summary statistics from Gazebo trap period June, 1995 and Vet Village trap period June, 1995 included are sample size (N), number of alleles, effective number of alleles (N_e), observed heterozygosity (H_{OBS}), expected heterozygosity (H_{EXP}), and the fixation index (F).

Gazebo (Jun-95)						
Locus	N	Alleles	N_e	H_{OBS}	H_{EXP}	F
Ppa-01	60	3.0	1.7557	0.4167	0.4304	0.0319
Ppa-12	66	3.0	2.5407	0.6970	0.6064	-0.1493
Ppa-46	53	3.0	2.0700	0.5283	0.5169	-0.0220
PO3-85	67	5.0	2.3441	0.6567	0.5734	-0.1453
PO3-68	65	6.0	4.3467	0.7385	0.7699	0.0409
PO-25	66	5.0	2.3357	0.5606	0.5719	0.0197
Pml-03	47	5.0	2.5060	0.4255	0.6010	0.2919
Pml-11	64	6.0	4.2314	0.6875	0.7637	0.0997
Pml-04	61	2.0	1.7698	0.5410	0.4350	-0.2437
PO-71	66	7.0	3.1114	0.7121	0.6786	-0.0494
Pml-06	67	3.0	2.6578	0.6418	0.6237	-0.0289
Mean	62	4.36	2.6972	0.6006	0.5974	-0.0139
St. Dev.		1.63	0.8777	0.1130	0.1127	0.1424
Vet Village (Jun-95)						
Locus	N	Alleles	N_e	H_{OBS}	H_{EXP}	F
Ppa-01	68	2.0	1.9490	0.4265	0.4869	0.1241
Ppa-12	67	5.0	2.8358	0.7015	0.6474	-0.0836
Ppa-46	68	3.0	2.0805	0.5441	0.5194	-0.0477
PO3-85	70	5.0	3.1705	0.6571	0.6846	0.0401
PO3-68	70	6.0	4.5837	0.8286	0.7818	-0.0598
PO-25	70	5.0	2.5708	0.6857	0.6110	-0.1222
Pml-03	70	4.0	2.7169	0.5143	0.6319	0.1862
Pml-11	70	7.0	3.8750	0.7286	0.7419	0.0180
Pml-04	70	3.0	1.6228	0.4000	0.3838	-0.0423
PO-71	60	8.0	3.1607	0.7000	0.6836	-0.0240
Pml-06	70	3.0	2.7754	0.5571	0.6397	0.1290
Mean	69	4.64	2.8493	0.6130	0.6194	0.0106
St. Dev.		1.86	0.8524	0.1344	0.1159	0.0987

Table 9 Summary statistics from Gazebo trap period February, 1996 and Vet Village trap period March, 1996 included are sample size (N), number of alleles, effective number of alleles (N_e), observed heterozygosity (H_{OBS}), expected heterozygosity (H_{EXP}), and the fixation index (F).

Gazebo (Feb-96)						
Locus	N	Alleles	N_e	H_{OBS}	H_{EXP}	F
Ppa-01	47	3.0	1.7858	0.3830	0.4400	0.1296
Ppa-12	47	3.0	2.7121	0.5745	0.6313	0.0900
Ppa-46	48	3.0	2.3963	0.5208	0.5827	0.1061
PO3-85	48	4.0	2.5815	0.6458	0.6126	-0.0542
PO3-68	46	6.0	4.5850	0.8261	0.7819	-0.0565
PO-25	47	5.0	2.6598	0.6383	0.6240	-0.0229
Pml-03	10	4.0	2.6667	0.5000	0.6250	0.2000
Pml-11	48	6.0	3.6923	0.7083	0.7292	0.0286
Pml-04	48	3.0	2.1294	0.6250	0.5304	-0.1784
PO-71	47	5.0	2.8284	0.7021	0.6464	-0.0861
Pml-06	48	3.0	2.6995	0.5833	0.6296	0.0734
Mean	44	4.09	2.7943	0.6096	0.6212	0.0209
St. Dev.		1.22	0.7568	0.1186	0.0900	0.1111
Vet Village (Mar-96)						
Locus	N	Alleles	N_e	H_{OBS}	H_{EXP}	F
Ppa-01	44	2.0	1.8615	0.5455	0.4628	-0.1786
Ppa-12	43	4.0	3.1286	0.6512	0.6804	0.0429
Ppa-46	44	3.0	2.2776	0.5455	0.5610	0.0276
PO3-85	44	5.0	3.3876	0.7955	0.7048	-0.1286
PO3-68	44	6.0	4.5877	0.8409	0.7820	-0.0753
PO-25	43	5.0	2.3569	0.5349	0.5757	0.0709
Pml-03	43	4.0	2.9141	0.5349	0.6568	0.1857
Pml-11	42	6.0	4.3557	0.8140	0.7704	-0.0565
Pml-04	44	3.0	1.8447	0.4773	0.4579	-0.0423
PO-71	41	7.0	4.2883	0.8049	0.7668	-0.0497
Pml-06	44	3.0	2.8038	0.7045	0.6433	-0.0951
Mean	43	4.36	3.0735	0.6589	0.6420	-0.2720
St. Dev.		1.57	0.9867	0.1375	0.1158	0.1025

Table 10 Summary statistics from Gazebo trap period April, 1996 and Vet Village trap period April, 1996 included are sample size (N), number of alleles, effective number of alleles (N_e), observed heterozygosity (H_{OBS}), expected heterozygosity (H_{EXP}), and the fixation index (F).

Gazebo (Apr-96)						
Locus	N	Alleles	N_e	H_{OBS}	H_{EXP}	F
Ppa-01	52	3.0	1.9616	0.5192	0.4902	-0.0592
Ppa-12	52	3.0	2.7217	0.6154	0.6326	0.0272
Ppa-46	52	3.0	2.3482	0.6538	0.5741	-0.1388
PO3-85	52	5.0	2.1367	0.4615	0.5320	0.1324
PO3-68	52	6.0	4.8372	0.8269	0.7933	-0.0424
PO-25	51	5.0	2.8964	0.6667	0.6547	-0.0182
Pml-03	29	5.0	1.7376	0.4483	0.4245	-0.0560
Pml-11	51	6.0	3.9290	0.7059	0.7455	0.0531
Pml-04	49	3.0	1.9433	0.5306	0.4854	-0.0931
PO-71	51	5.0	2.7685	0.7451	0.6388	-0.1664
Pml-06	49	3.0	2.3714	0.5306	0.5783	0.0825
Mean	49	4.27	2.6956	0.6095	0.5953	-0.0254
St. Dev.		1.27	0.9334	0.1219	0.1121	0.0921
Vet Village (Apr-96)						
Locus	N	Alleles	N_e	H_{OBS}	H_{EXP}	F
Ppa-01	72	3.0	1.7089	0.4167	0.4148	-0.0044
Ppa-12	71	4.0	3.0276	0.6620	0.6697	0.0116
Ppa-46	72	3.0	2.3409	0.6806	0.5728	-0.1881
PO3-85	72	5.0	3.0903	0.7361	0.6764	-0.0883
PO3-68	72	6.0	5.2390	0.8333	0.8091	-0.0299
PO-25	69	5.0	2.4803	0.6522	0.5968	-0.0927
Pml-03	71	5.0	3.1774	0.6761	0.6853	0.0135
Pml-11	70	6.0	4.1315	0.7286	0.7580	0.0388
Pml-04	72	4.0	1.9304	0.5139	0.4820	-0.0662
PO-71	69	8.0	3.6595	0.7826	0.7267	-0.0769
Pml-06	72	3.0	2.7234	0.6528	0.6328	-0.0316
Mean	71	4.73	3.0462	0.6669	0.6386	-0.0467
St. Dev.		1.56	1.0168	0.1167	0.1167	0.0646

Table 11 Summary statistics from Gazebo trap period June, 1996 and Vet Village trap period June, 1996 included are sample size (N), number of alleles, effective number of alleles (N_e), observed heterozygosity (H_{OBS}), expected heterozygosity (H_{EXP}), and the fixation index (F).

Gazebo (Jun-96)						
Locus	N	Alleles	N_e	H_{OBS}	H_{EXP}	F
Ppa-01	34	3.0	1.9744	0.5294	0.4935	-0.0727
Ppa-12	34	5.0	2.8508	0.6765	0.6492	-0.0420
Ppa-46	34	4.0	2.3616	0.6765	0.5766	-0.1733
PO3-85	34	5.0	2.4083	0.4706	0.5848	0.1953
PO3-68	34	7.0	5.2785	0.8824	0.8106	-0.0886
PO-25	34	8.0	3.0542	0.7059	0.6726	-0.0495
Pml-03	25	6.0	2.1259	0.5200	0.5296	0.0181
Pml-11	33	7.0	3.8077	0.7273	0.7374	0.0137
Pml-04	34	4.0	2.2468	0.7353	0.5549	-0.3250
PO-71	29	5.0	2.7894	0.7241	0.6415	-0.1288
Pml-06	31	3.0	2.2045	0.4375	0.5464	0.1993
Mean	32	5.18	2.8275	0.6440	0.6180	-0.0414
St. Dev.		1.66	0.9676	0.1360	0.0954	0.1513
Vet Village (Jun-96)						
Locus	N	Alleles	N_e	H_{OBS}	H_{EXP}	F
Ppa-01	43	2.0	1.7018	0.5798	0.4124	-0.1843
Ppa-12	42	4.0	3.0309	0.5952	0.6701	0.1117
Ppa-46	43	3.0	2.3420	0.5349	0.5730	0.0665
PO3-85	42	5.0	3.2015	0.7857	0.6876	-0.1426
PO3-68	43	6.0	5.0727	0.7674	0.8029	0.0441
PO-25	41	5.0	3.0018	0.7073	0.6669	-0.0607
Pml-03	43	6.0	2.8100	0.6047	0.6441	0.0613
Pml-11	42	6.0	3.8983	0.7143	0.7435	0.0393
Pml-04	44	4.0	1.7209	0.5227	0.4189	-0.2478
PO-71	42	8.0	4.2000	0.7857	0.7619	-0.0312
Pml-06	42	3.0	2.5658	0.4524	0.6103	0.2587
Mean	42	4.73	3.0496	0.6409	0.6355	-0.0077
St. Dev.		1.74	1.0265	0.1165	0.1273	0.1453

Table 12 Summary statistics from Gazebo trap period February, 1997 and Vet Village trap period March, 1997 included are sample size (N), number of alleles, effective number of alleles (N_e), observed heterozygosity (H_{OBS}), expected heterozygosity (H_{EXP}), and the fixation index (F).

Gazebo (Feb-97)						
Locus	N	Alleles	N_e	H_{OBS}	H_{EXP}	F
Ppa-01	9	2.0	1.9059	0.5556	0.4753	-0.1688
Ppa-12	8	4.0	3.2821	0.3750	0.6953	0.4607
Ppa-46	9	2.0	1.9059	0.5556	0.4753	-0.1688
PO3-85	9	3.0	2.4179	0.6667	0.5864	-0.1368
PO3-68	8	6.0	4.4138	0.7500	0.7734	0.0303
PO-25	9	4.0	3.1765	0.6667	0.6852	0.0270
Pml-03	8	4.0	2.9767	0.5000	0.6641	0.2471
Pml-11	9	4.0	2.9455	1.0000	0.6605	-0.5140
Pml-04	9	3.0	2.1600	0.3333	0.5370	0.3793
PO-71	6	3.0	1.4118	0.3333	0.2917	-0.1429
Pml-06	9	3.0	2.0506	0.4444	0.5123	0.1325
Mean	8	3.45	2.6704	0.5619	0.5776	0.0132
St. Dev.		1.13	0.8515	0.2017	0.1365	0.2820
Vet Village (Mar-97)						
Locus	N	Alleles	N_e	H_{OBS}	H_{EXP}	F
Ppa-01	28	2.0	1.9382	0.5357	0.4841	-0.1067
Ppa-12	28	3.0	2.2958	0.6429	0.5644	-0.1390
Ppa-46	28	3.0	1.6915	0.3929	0.4088	0.0390
PO3-85	28	4.0	3.2464	0.6429	0.6920	0.0710
PO3-68	27	6.0	4.4316	0.8519	0.7743	-0.1001
PO-25	28	4.0	2.5496	0.5357	0.6078	0.1186
Pml-03	28	4.0	3.1173	0.7500	0.6792	-0.1042
Pml-11	28	5.0	3.2131	0.6786	0.6888	0.0148
Pml-04	28	4.0	1.8044	0.5000	0.4458	-0.1216
PO-71	28	6.0	3.4161	0.8214	0.7073	-0.1614
Pml-06	28	3.0	2.3473	0.5714	0.5740	0.0044
Mean	28	4.00	2.7318	0.6295	0.6023	-0.0441
St. Dev.		1.26	0.8336	0.1404	0.1183	0.0959

Table 13 Summary statistics from Gazebo trap period April, 1998 and Vet Village trap period February, 1998 included are sample size (N), number of alleles, effective number of alleles (N_e), observed heterozygosity (H_{OBS}), expected heterozygosity (H_{EXP}), and the fixation index (F).

Gazebo (Apr-98)						
Locus	N	Alleles	N_e	H_{OBS}	H_{EXP}	F
Ppa-01	8	2.0	1.8824	0.5000	0.4688	-0.0667
Ppa-12	7	4.0	3.1613	0.4286	0.6837	0.3731
Ppa-46	9	4.0	2.2817	0.4444	0.5617	0.2088
PO3-85	8	3.0	1.8551	0.2500	0.4609	0.4576
PO3-68	8	5.0	3.7647	1.0000	0.7344	-0.3617
PO-25	8	4.0	3.1220	1.0000	0.6797	-0.4713
Pml-03	9	4.0	3.2400	0.3333	0.6914	0.5179
Pml-11	8	4.0	2.8444	0.3750	0.6484	0.4217
Pml-04	9	3.0	1.7419	0.3333	0.4259	0.2174
PO-71	8	5.0	2.6667	0.6250	0.6250	0.0000
Pml-06	8	3.0	2.4151	0.7500	0.5859	-0.2800
Mean	8	3.73	2.6341	0.5490	0.5969	0.0925
St. Dev		0.90	0.6593	0.2634	0.1053	0.3504
Vet Village (Feb-98)						
Locus	N	Alleles	N_e	H_{OBS}	H_{EXP}	F
Ppa-01	22	3.0	2.0907	0.5909	0.5217	-0.1327
Ppa-12	22	3.0	2.1753	0.4545	0.5403	0.1587
Ppa-46	22	3.0	2.1802	0.4545	0.5413	0.1603
PO3-85	22	4.0	3.8413	0.7273	0.7397	0.0168
PO3-68	22	5.0	3.7231	0.6818	0.7314	0.0678
PO-25	22	3.0	2.4631	0.6364	0.5940	-0.0713
Pml-03	22	4.0	3.6255	0.8182	0.7242	-0.1298
Pml-11	22	4.0	3.3495	0.7727	0.7014	-0.1016
Pml-04	22	3.0	1.7505	0.5909	0.4287	-0.3783
PO-71	20	5.0	2.6936	0.7500	0.6287	-0.1928
Pml-06	22	3.0	2.2830	0.6818	0.5620	-0.2132
Mean	22	3.64	2.7431	0.6509	0.6103	-0.0742
St. Dev		0.81	0.7520	0.1202	0.1029	0.1646

Table 14 Summary statistics from Gazebo trap period March, 2000 and Vet Village trap period March, 2000 included are sample size (N), number of alleles, effective number of alleles (N_e), observed heterozygosity (H_{OBS}), expected heterozygosity (H_{EXP}), and the fixation index (F).

Gazebo (Mar-00)						
Locus	N	Alleles	N_e	H_{OBS}	H_{EXP}	F
Ppa-01	32	2.0	1.8824	0.3750	0.4688	0.2000
Ppa-12	31	3.0	2.0253	0.3871	0.5062	0.2354
Ppa-46	32	3.0	2.2165	0.5938	0.5488	-0.0819
PO3-85	31	5.0	2.6732	0.6452	0.6259	-0.0308
PO3-68	31	5.0	3.7539	0.6452	0.7336	0.1206
PO-25	31	4.0	2.0869	0.5161	0.5208	0.0090
Pml-03	32	4.0	1.3412	0.2500	0.2544	0.0173
Pml-11	32	5.0	3.3964	0.7500	0.7056	-0.0630
Pml-04	32	2.0	1.9692	0.4375	0.4922	0.1111
PO-71	27	6.0	2.1378	0.4815	0.5322	0.0954
Pml-06	32	3.0	2.5473	0.6250	0.6074	-0.0289
Mean	31	3.82	2.3662	0.5187	0.5451	0.0530
St. Dev.		1.33	0.6947	0.1485	0.1295	0.1064
Vet Village (Mar-00)						
Locus	N	Alleles	N_e	H_{OBS}	H_{EXP}	F
Ppa-01	26	2.0	1.9737	0.6538	0.4933	-0.3253
Ppa-12	25	3.0	2.5667	0.6400	0.6104	-0.0485
Ppa-46	26	3.0	1.9123	0.6538	0.4771	-0.3705
PO3-85	26	4.0	2.5851	0.6538	0.6132	-0.0663
PO3-68	26	4.0	2.3032	0.6538	0.5658	-0.1556
PO-25	24	4.0	3.1911	0.7917	0.6866	-0.1530
Pml-03	26	4.0	2.5037	0.6538	0.6006	-0.0887
Pml-11	26	6.0	3.1369	0.8462	0.6812	-0.2421
Pml-04	25	3.0	1.6513	0.2000	0.3944	0.4929
PO-71	24	6.0	3.7770	0.7083	0.7352	0.0366
Pml-06	25	3.0	2.0227	0.6000	0.5056	-0.1867
Mean	26	3.82	2.5113	0.6415	0.5785	-0.1006
St. Dev.		1.25	0.6430	0.1632	0.1032	0.2307

Table 15 Summary statistics from Gazebo trap period November, 2000 and Vet Village trap period December, 2000 included are sample size (N), number of alleles, effective number of alleles (N_e), observed heterozygosity (H_{OBS}), expected heterozygosity (H_{EXP}), and the fixation index (F).

Gazebo (Nov-00)						
Locus	N	Alleles	N_e	H_{OBS}	H_{EXP}	F
Ppa-01	8	2.0	1.8824	0.5000	0.4688	-0.0667
Ppa-12	11	3.0	2.3725	0.3636	0.5785	0.3714
Ppa-46	11	2.0	1.5414	0.0909	0.3512	0.7412
PO3-85	10	3.0	1.9417	0.5000	0.4850	-0.0309
PO3-68	11	5.0	3.7231	0.9091	0.7314	-0.2429
PO-25	10	4.0	3.7736	0.6000	0.7350	0.1837
Pml-03	11	4.0	2.2000	0.4545	0.5455	0.1667
Pml-11	11	4.0	3.5072	0.8182	0.7149	-0.1445
Pml-04	11	2.0	1.8615	0.5455	0.4628	-0.1786
PO-71	11	6.0	4.0333	0.6364	0.7521	0.1538
Pml-06	9	3.0	2.3143	0.5556	0.5679	0.0217
Mean	10	3.45	2.6501	0.5431	0.5812	0.0885
St. Dev.		1.29	0.9163	0.2167	0.1354	0.2835
Vet Village (Dec-00)						
Locus	N	Alleles	N_e	H_{OBS}	H_{EXP}	F
Ppa-01	8	2.0	1.6000	0.2500	0.3750	0.3333
Ppa-12	8	3.0	2.8444	0.7500	0.6484	-0.1566
Ppa-46	8	3.0	2.1333	0.5000	0.5313	0.0588
PO3-85	8	3.0	2.6122	0.8750	0.6172	-0.4177
PO3-68	8	6.0	2.3704	0.5000	0.5781	0.1351
PO-25	7	4.0	2.9697	0.5714	0.6633	0.1385
Pml-03	8	1.0	1.0000	0.0000	0.0000	#N/A
Pml-11	8	4.0	3.1220	0.6250	0.6797	0.0805
Pml-04	8	2.0	1.9692	0.1250	0.4922	0.7460
PO-71	8	6.0	3.7647	0.5000	0.7344	0.3191
Pml-06	8	3.0	1.6623	0.2500	0.3984	0.3725
Mean	8	3.36	2.3679	0.4496	0.5196	0.1608
St. Dev.		1.57	0.7964	0.2667	0.2069	0.3156

Table 16 Summary statistics from Gazebo trap period March, 2001 and Vet Village trap period March, 2001 included are sample size (N), number of alleles, effective number of alleles (N_e), observed heterozygosity (H_{OBS}), expected heterozygosity (H_{EXP}), and the fixation index (F).

Gazebo (Mar-01)						
Locus	N	Alleles	N_e	H_{OBS}	H_{EXP}	F
Ppa-01	20	2.0	1.8824	0.4500	0.4688	0.0400
Ppa-12	22	3.0	2.2776	0.5000	0.5610	0.1087
Ppa-46	22	3.0	2.0125	0.5000	0.5031	0.0062
PO3-85	22	4.0	2.9877	0.6364	0.6653	0.0435
PO3-68	22	6.0	4.3214	0.7273	0.7686	0.0538
PO-25	21	4.0	2.4845	0.7619	0.5975	-0.2751
Pml-03	22	4.0	1.7441	0.4091	0.4267	0.0412
Pml-11	22	5.0	3.8876	0.7273	0.7428	0.0209
Pml-04	22	2.0	1.8161	0.5000	0.4494	-0.1126
PO-71	21	7.0	2.7477	0.6667	0.6361	-0.0481
Pml-06	22	3.0	2.7115	0.8182	0.6312	-0.2962
Mean	21	3.91	2.6248	0.6087	0.5865	-0.0380
St. Dev.		1.58	0.8441	0.1414	0.1159	0.1352
Vet Village (Mar-01)						
Locus	N	Alleles	N_e	H_{OBS}	H_{EXP}	F
Ppa-01	43	2.0	1.4947	0.3721	0.3310	-0.1242
Ppa-12	39	3.0	2.8298	0.6154	0.6466	0.0483
Ppa-46	43	3.0	2.1525	0.4419	0.5354	0.1747
PO3-85	42	4.0	2.3758	0.5476	0.5791	0.0543
PO3-68	43	6.0	2.7618	0.6279	0.6379	0.0157
PO-25	32	4.0	2.8967	0.6875	0.6548	-0.0500
Pml-03	43	4.0	1.9443	0.4884	0.4857	-0.0056
Pml-11	40	5.0	3.3862	0.7250	0.7047	-0.0288
Pml-04	43	3.0	2.0330	0.5581	0.5081	-0.0985
PO-71	43	6.0	3.6796	0.7907	0.7282	-0.0858
Pml-06	43	3.0	1.9210	0.5349	0.4794	-0.1156
Mean	42	3.91	2.4979	0.5809	0.5719	-0.0196
St. Dev.		1.30	0.6724	0.1245	0.1177	0.0900

Table 17 Summary statistics from Gazebo trap period November, 2001 and Vet Village trap period October, 2001 included are sample size (N), number of alleles, effective number of alleles (N_e), observed heterozygosity (H_{OBS}), expected heterozygosity (H_{EXP}), and the fixation index (F).

Gazebo (Nov-01)						
Locus	N	Alleles	N_e	H_{OBS}	H_{EXP}	F
Ppa-01	12	2.0	1.9459	0.6667	0.4861	-0.3714
Ppa-12	12	3.0	1.6457	0.5000	0.3924	-0.2743
Ppa-46	12	3.0	2.0719	0.6667	0.5174	-0.2886
PO3-85	11	3.0	1.7536	0.3636	0.4298	0.1538
PO3-68	12	6.0	3.8919	0.8333	0.7431	-0.1215
PO-25	12	5.0	2.4828	0.6667	0.5972	-0.1163
Pml-03	12	3.0	2.1333	0.5833	0.5313	-0.0980
Pml-11	12	4.0	3.2360	0.8333	0.6910	-0.2060
Pml-04	12	3.0	1.9862	0.5833	0.4965	-0.1748
PO-71	11	3.0	2.1416	0.7273	0.5331	-0.3643
Pml-06	12	3.0	2.6422	0.6667	0.6215	-0.0726
Mean	12	3.45	2.3575	0.6446	0.5490	-0.1757
St. Dev.		1.13	0.6767	0.1368	0.1061	0.1513
Vet Village (Oct-01)						
Locus	N	Alleles	N_e	H_{OBS}	H_{EXP}	F
Ppa-01	35	2.0	1.4706	0.2286	0.3200	0.2857
Ppa-12	34	3.0	2.6544	0.5294	0.6233	0.1506
Ppa-46	35	3.0	1.9460	0.4000	0.4861	0.1772
PO3-85	36	4.0	3.1116	0.5278	0.6786	0.2223
PO3-68	35	5.0	3.3243	0.7143	0.6992	-0.0216
PO-25	32	5.0	3.8861	0.7188	0.7427	0.0322
Pml-03	34	4.0	1.7088	0.4412	0.4148	-0.0636
Pml-11	33	5.0	3.6667	0.7273	0.7273	0.0000
Pml-04	36	2.0	1.7693	0.5833	0.4348	-0.3416
PO-71	36	5.0	2.9827	0.7500	0.6647	-0.1283
Pml-06	36	3.0	1.9445	0.5278	0.4857	-0.0866
Mean	35	3.73	2.5877	0.5589	0.5707	0.0205
St. Dev.		1.19	0.8770	0.1630	0.1462	0.1809

Table 18 Summary statistics from Gazebo trap period March, 2002 and Vet Village trap period February, 2002 included are sample size (N), number of alleles, effective number of alleles (N_e), observed heterozygosity (H_{OBS}), expected heterozygosity (H_{EXP}), and the fixation index (F).

Gazebo (Mar-02)						
Locus	N	Alleles	N_e	H_{OBS}	H_{EXP}	F
Ppa-01	119	2.0	1.8491	0.4622	0.4592	-0.0065
Ppa-12	110	5.0	2.0748	0.4364	0.5180	0.1576
Ppa-46	120	3.0	1.9907	0.5167	0.4977	-0.0382
PO3-85	120	4.0	2.5473	0.6083	0.6074	-0.0015
PO3-68	117	6.0	4.5630	0.7607	0.7808	0.0258
PO-25	118	5.0	3.3986	0.6610	0.7058	0.0634
Pml-03	88	4.0	2.1863	0.5455	0.5426	-0.0052
Pml-11	117	6.0	4.4539	0.8462	0.7755	-0.0911
Pml-04	119	3.0	1.8318	0.3866	0.4541	0.1487
PO-71	113	8.0	2.3280	0.5575	0.5704	0.0227
Pml-06	117	3.0	2.8569	0.6496	0.6500	0.0006
Mean	114	4.45	2.7346	0.5846	0.5965	0.0253
St. Dev.		1.76	0.9922	0.1390	0.1181	0.0742
Vet Village (Feb-02)						
Locus	N	Alleles	N_e	H_{OBS}	H_{EXP}	F
Ppa-01	117	2.0	1.4950	0.3162	0.3311	0.0449
Ppa-12	113	4.0	2.8442	0.5752	0.6484	0.1129
Ppa-46	117	3.0	1.7828	0.4103	0.4391	0.0656
PO3-85	116	4.0	2.9129	0.5603	0.6567	0.1467
PO3-68	117	5.0	3.1329	0.7350	0.6808	-0.0797
PO-25	103	5.0	3.2830	0.6602	0.6954	0.0506
Pml-03	117	3.0	1.8017	0.4914	0.4450	-0.1043
Pml-11	112	6.0	3.5216	0.7857	0.7160	-0.0973
Pml-04	115	3.0	1.9856	0.5826	0.4964	-0.1737
PO-71	115	7.0	3.4257	0.7391	0.7081	-0.0438
Pml-06	117	3.0	1.8590	0.5385	0.4621	-0.1653
Mean	114	4.09	2.5496	0.5812	0.5707	-0.0220
St. Dev.		1.51	0.7658	0.1438	0.1375	0.1114

Table 19 Mantel tests for Gazebo and Vet Village grids along with the number of samples for each trapping period. Individuals from the March 1999 trapping period did not amplify well during PCR reactions and were not used.

Gazebo				Vet Village			
Period	N	Rxy	P	Period	N	Rxy	P
Feb-95	145	0.076	0.003	Mar-95	103	0.049	0.081
Apr-95	122	0.045	0.057	Apr-95	113	-0.010	0.651
Jun-95	68	0.015	0.314	Jun-95	70	-0.089	0.994
Feb-96	48	0.041	0.218	Mar-96	44	0.158	0.004
Apr-96	52	0.028	0.281	Apr-96	72	0.059	0.058
Jun-96	34	-0.095	0.872	Jun-96	44	-0.071	0.836
Feb-97	9	-0.054	0.587	Mar-97	28	0.090	0.077
Apr-98	9	-0.017	0.488	Feb-98	22	0.133	0.057
Feb-99	9	-0.100	0.700	Mar-99	8		
Mar-00	32	0.011	0.099	Mar-00	26	0.160	0.053
Nov-00	11	0.063	0.329	Dec-00	8	0.053	0.397
Mar-01	22	0.365	0.001	Mar-01	43	0.240	0.001
Nov-01	12	0.266	0.029	Oct-01	36	0.127	0.037
Mar-02	120	0.052	0.023	Feb-02	117	0.106	0.001

Table 20 F_{ST} values based on various models of subdivision within Gazebo and Vet Village grids. The four corner, north/south and east/west models are based on sectioning the grid (**Fig. 1**). The four other models are based on randomly assigning individuals into the four corner, north/south and east/west quadrants, random one two subpopulations (R12P), random one four subpopulations (R14P), random two two subpopulations (R22P) and random two four subpopulations.

Gazebo

	Feb-95	Jun-95	Feb-96	Jun-96	Mar-02
	F_{ST}	F_{ST}	F_{ST}	F_{ST}	F_{ST}
Four corner	0.0143	0.0005	0.0050	0.0187	0.0159
North/South	0.0112	0.0048	0.0104	0.0220	0.0098
East/West	0.0046	0.0069	0.0125	-0.0096	0.0151
R12P	-0.0042	-0.0111	-0.0037	0.0203	-0.0016
R14P	-0.0002	-0.0189	-0.0173	0.0006	-0.0009
R22P	-0.0020	0.0219	0.0098	-0.0057	-0.0012
R24P	0.0002	0.0102	0.0080	-0.0107	-0.0005

Vet Village

	Mar-95	Jun-95	Mar-96	Jun-96	Mar-02
	F_{ST}	F_{ST}	F_{ST}	F_{ST}	F_{ST}
Four corner	0.0247	0.0009	0.0369	0.0082	0.0210
North/South	0.0165	-0.0028	0.0244	-0.0026	-0.0029
East/West	0.0125	0.0008	0.0092	0.0070	0.0231
R12P	0.0025	0.0050	0.0034	0.0002	0.0005
R14P	0.0008	0.0005	-0.0000	-0.0054	-0.0004
R22P	0.0007	0.0015	0.0064	0.0337	0.0025
R24P	-0.0030	0.0078	0.0068	0.0158	0.0010

Table 21 Summary statistics for the combined trapping periods of February 1995 on Gazebo grid and March 1995 on Vet Village grid (1st-95) and April 1995 on both Gazebo and Vet Village grids (2nd_95). Included are sample size (N), number of alleles (Na), effective number of alleles (N_e), observed heterozygosity (H_o), expected heterozygosity (H_e) and the fixation index (F_{IS}).

1st-95						
Locus	N	Na	N _e	H _o	H _e	F
Ppa-01	232	3.00	1.737	0.375	0.424	0.116
Ppa-12	240	5.00	2.719	0.667	0.632	-0.055
Ppa-46	191	3.00	2.138	0.545	0.532	-0.023
PO3-85	245	5.00	2.731	0.657	0.634	-0.037
PO3-68	242	7.00	4.503	0.764	0.778	0.017
PO-25	245	5.00	2.650	0.645	0.623	-0.036
Pml-03	195	5.00	2.538	0.549	0.606	0.095
Pml-11	245	6.00	4.282	0.714	0.766	0.068
Pml-04	221	3.00	1.821	0.489	0.451	-0.084
PO-71	228	9.00	3.337	0.667	0.700	0.048
Pml-06	244	3.00	2.690	0.639	0.628	-0.018
Mean	230	4.909	2.832	0.610	0.616	0.008
St. Dev.	19	1.921	0.895	0.111	0.113	0.652
2nd-95						
Locus	N	Na	N _e	H _o	H _e	F
Ppa-01	223	3.00	1.811	0.462	0.448	-0.032
Ppa-12	227	5.00	2.785	0.643	0.641	-0.003
Ppa-46	206	3.00	2.016	0.519	0.504	-0.031
PO3-85	234	6.00	2.704	0.624	0.630	0.010
PO3-68	231	7.00	4.725	0.771	0.788	0.023
PO-25	234	6.00	2.644	0.641	0.622	-0.031
Pml-03	204	5.00	2.519	0.529	0.603	0.122
Pml-11	231	7.00	4.250	0.736	0.765	0.038
Pml-04	219	3.00	1.832	0.475	0.454	-0.045
PO-71	220	8.00	3.384	0.700	0.705	0.006
Pml-06	234	3.00	2.681	0.615	0.627	0.018
Mean	224	5.090	2.850	0.611	0.617	0.007
St. Dev.	10	1.868	0.937	0.104	0.113	0.467

Table 22 Summary statistics for the combined trapping periods of June 1995 on Gazebo grid and Vet Village grid (3rd-95) along with February 1996 on Gazebo grid and March 1996 on Vet Village grid (1st-96). Included are sample size (N), number of alleles (Na), effective number of alleles (N_e), observed heterozygosity (H_o), expected heterozygosity (H_e) and the fixation index (F_{IS}).

3rd-95						
Locus	N	Na	N _e	H _o	H _e	F
Ppa-01	128	3.00	1.891	0.422	0.471	0.105
Ppa-12	133	5.00	2.738	0.699	0.635	-0.102
Ppa-46	121	3.00	2.086	0.537	0.521	-0.032
PO3-85	137	5.00	2.741	0.657	0.635	-0.034
PO3-68	135	6.00	4.600	0.785	0.783	-0.003
PO-25	136	5.00	2.483	0.625	0.597	-0.046
Pml-03	117	5.00	2.645	0.479	0.622	0.230
Pml-11	134	7.00	4.184	0.709	0.761	0.068
Pml-04	131	3.00	1.714	0.466	0.417	-0.118
PO-71	126	8.00	3.218	0.706	0.689	-0.025
Pml-06	137	3.00	2.727	0.599	0.633	0.055
Mean	130	4.818	2.821	0.608	0.615	0.009
St. Dev.	7	1.722	0.893	0.118	0.112	0.100
1st-96						
Locus	N	Na	N _e	H _o	H _e	F
Ppa-01	91	3.00	1.837	0.462	0.456	-0.013
Ppa-12	90	4.00	2.955	0.611	0.662	0.076
Ppa-46	92	3.00	2.355	0.533	0.575	0.074
PO3-85	92	5.00	2.966	0.717	0.663	-0.082
PO3-68	90	6.00	4.929	0.833	0.797	-0.045
PO-25	90	5.00	2.554	0.589	0.608	0.032
Pml-03	53	4.00	2.883	0.528	0.653	0.191
Pml-11	91	6.00	4.138	0.758	0.758	0.000
Pml-04	92	3.00	2.008	0.554	0.502	-0.104
PO-71	88	7.00	3.514	0.750	0.715	-0.048
Pml-06	92	3.00	2.762	0.641	0.638	-0.005
Mean	87	4.455	2.991	0.634	0.639	0.007
St. Dev.	11	1.440	0.911	0.116	0.102	0.084

Table 23 Summary statistics for the combined trapping periods of April 1996 on both Gazebo and Vet Village grids (2nd-96) along with June 1996 on both Gazebo and Vet Village grids (3rd-96). Included are sample size (N), number of alleles (Na), effective number of alleles (N_e), observed heterozygosity (H_o), expected heterozygosity (H_e) and the fixation index (F_{IS}).

2nd-96						
Locus	N	Na	N _e	H _o	H _e	F
Ppa-01	124	3.00	1.812	0.460	0.448	-0.026
Ppa-12	123	4.00	2.937	0.642	0.660	0.026
Ppa-46	124	3.00	2.345	0.669	0.574	-0.167
PO3-85	124	5.00	2.661	0.621	0.624	0.005
PO3-68	124	6.00	5.212	0.831	0.808	-0.028
PO-25	120	5.00	2.667	0.658	0.625	-0.053
Pml-03	100	5.00	2.792	0.610	0.642	0.050
Pml-11	121	6.00	4.213	0.719	0.763	0.057
Pml-04	121	4.00	1.942	0.521	0.485	-0.073
PO-71	120	8.00	3.270	0.767	0.694	-0.104
Pml-06	121	3.00	2.592	0.603	0.614	0.018
Mean	120	4.727	2.949	0.646	0.631	-0.027
St. Dev.	7	1.555	0.990	0.104	0.106	0.069
3rd-96						
Locus	N	Na	N _e	H _o	H _e	F
Ppa-01	77	3.00	1.820	0.506	0.450	-0.125
Ppa-12	76	6.00	2.997	0.632	0.666	0.052
Ppa-46	77	4.00	2.351	0.597	0.575	-0.039
PO3-85	76	5.00	2.850	0.645	0.649	0.007
PO3-68	77	7.00	5.449	0.818	0.816	-0.002
PO-25	75	8.00	3.049	0.707	0.672	-0.052
Pml-03	68	7.00	2.618	0.574	0.618	0.072
Pml-11	75	7.00	3.893	0.720	0.743	0.031
Pml-04	78	5.00	1.959	0.615	0.490	-0.257
PO-71	71	8.00	3.652	0.761	0.726	-0.047
Pml-06	74	3.00	2.417	0.446	0.586	0.239
Mean	75	5.727	3.005	0.638	0.636	-0.011
St. Dev.	3	1.849	1.030	0.109	0.108	0.124

Table 24 Summary statistics for the combined trapping periods of February 1997 on Gazebo grid and March 1997 on Vet Village grid (1st-97) along with April 1998 on Gazebo grid and February 1998 on Vet Village grid (1st-98). Included are sample size (N), number of alleles (Na), effective number of alleles (N_e), observed heterozygosity (H_o), expected heterozygosity (H_e) and the fixation index (F_{IS}).

1st-97						
Locus	N	Na	N _e	H _o	H _e	F
Ppa-01	37	2.00	1.931	0.541	0.482	-0.121
Ppa-12	36	4.00	2.546	0.583	0.607	0.039
Ppa-46	37	3.00	1.899	0.432	0.473	0.086
PO3-85	37	4.00	3.195	0.649	0.687	0.056
PO3-68	35	6.00	4.605	0.829	0.783	-0.058
PO-25	37	4.00	2.733	0.568	0.634	0.105
Pml-03	36	4.00	3.149	0.694	0.682	-0.018
Pml-11	37	5.00	3.154	0.757	0.683	-0.108
Pml-04	37	4.00	1.892	0.459	0.472	0.026
PO-71	34	6.00	2.934	0.735	0.659	-0.115
Pml-06	37	3.00	2.651	0.541	0.623	0.132
Mean	36	4.090	2.790	0.617	0.617	0.002
St. Dev.	1	1.221	0.785	0.126	0.102	0.092
1st-98						
Locus	N	Na	N _e	H _o	H _e	F
Ppa-01	30	3.00	2.062	0.567	0.515	-0.100
Ppa-12	29	4.00	2.470	0.448	0.595	0.247
Ppa-46	31	4.00	2.232	0.452	0.552	0.182
PO3-85	30	4.00	3.377	0.600	0.704	0.148
PO3-68	30	5.00	3.774	0.767	0.735	-0.043
PO-25	30	4.00	2.635	0.733	0.621	-0.182
Pml-03	31	4.00	3.579	0.677	0.721	0.060
Pml-11	30	5.00	3.279	0.667	0.695	0.041
Pml-04	31	3.00	1.750	0.516	0.429	-0.204
PO-71	28	6.00	2.751	0.714	0.636	-0.122
Pml-06	30	3.00	2.469	0.700	0.595	-0.176
Mean	30	4.090	2.762	0.622	0.618	-0.014
St. Dev.	1	0.944	0.657	0.113	0.095	0.159

Table 25 Summary statistics for the combined trapping periods of March 2000 on Gazebo and Vet Village grids (1st-00) along with November 2000 on Gazebo grid and December 2000 on Vet Village grid (2nd-00). Included are sample size (N), number of alleles (Na), effective number of alleles (N_e), observed heterozygosity (H_o), expected heterozygosity (H_e) and the fixation index (F_{IS}).

1st-00						
Locus	N	Na	N _e	H _o	H _e	F
Ppa-01	58	2.00	1.931	0.500	0.482	-0.037
Ppa-12	56	3.00	2.305	0.500	0.566	0.117
Ppa-46	58	3.00	2.086	0.621	0.521	-0.192
PO3-85	57	5.00	2.841	0.649	0.648	-0.002
PO3-68	57	5.00	3.272	0.649	0.694	0.065
PO-25	55	4.00	2.606	0.636	0.616	-0.033
Pml-03	58	4.00	1.822	0.431	0.451	0.044
Pml-11	58	6.00	3.528	0.793	0.717	-0.107
Pml-04	57	3.00	1.875	0.333	0.467	0.286
PO-71	51	6.00	2.998	0.588	0.666	0.117
Pml-06	57	3.00	2.346	0.614	0.574	-0.070
Mean	56	4.00	2.510	0.574	0.582	0.017
St. Dev.	2	1.342	0.586	0.125	0.094	0.130
2nd-00						
Locus	N	Na	N _e	H _o	H _e	F
Ppa-01	16	2.00	1.753	0.375	0.430	0.127
Ppa-12	19	3.00	2.625	0.526	0.619	0.150
Ppa-46	19	3.00	1.774	0.263	0.436	0.397
PO3-85	18	4.00	2.445	0.667	0.591	-0.128
PO3-68	19	6.00	3.297	0.737	0.697	-0.058
PO-25	17	4.00	3.879	0.588	0.742	0.207
Pml-03	19	4.00	1.563	0.263	0.360	0.269
Pml-11	19	4.00	3.557	0.737	0.719	-0.025
Pml-04	19	2.00	1.978	0.368	0.494	0.255
PO-71	19	6.00	4.102	0.579	0.756	0.234
Pml-06	17	3.00	2.014	0.412	0.503	0.182
Mean	18	3.727	2.635	0.501	0.577	0.146
St. Dev.	1	1.348	0.923	0.176	0.140	0.158

Table 26 Summary statistics for the combined trapping periods of March 2001 on both Gazebo and Vet Village grids (1st-01) along with November 2001 on Gazebo grid and October 2001 on Vet Village grid (2nd-01). Included are sample size (N), number of alleles (Na), effective number of alleles (N_e), observed heterozygosity (H_o), expected heterozygosity (H_e) and the fixation index (F_{IS}).

1st-01						
Locus	N	Na	N _e	H _o	H _e	F
Ppa-01	63	2.00	1.630	0.397	0.387	-0.026
Ppa-12	61	3.00	2.657	0.574	0.624	0.080
Ppa-46	65	3.00	2.109	0.462	0.526	0.122
PO3-85	64	4.00	2.654	0.578	0.623	0.072
PO3-68	65	6.00	3.303	0.662	0.697	0.051
PO-25	53	4.00	2.853	0.717	0.650	-0.104
Pml-03	65	4.00	1.875	0.462	0.467	0.011
Pml-11	62	6.00	3.710	0.726	0.730	0.006
Pml-04	65	3.00	1.978	0.538	0.495	-0.089
PO-71	64	7.00	3.542	0.750	0.718	-0.045
Pml-06	65	3.00	2.305	0.631	0.566	-0.114
Mean	63	4.090	2.602	0.591	0.589	-0.003
St. Dev.	4	1.578	0.698	0.118	0.111	0.080
2nd-01						
Locus	N	Na	N _e	H _o	H _e	F
Ppa-01	48	2.00	1.627	0.354	0.385	0.081
Ppa-12	48	3.00	2.395	0.542	0.582	0.070
Ppa-46	48	3.00	1.957	0.458	0.489	0.063
PO3-85	48	4.00	2.748	0.479	0.636	0.247
PO3-68	48	6.00	3.583	0.750	0.721	-0.040
PO-25	48	6.00	3.689	0.708	0.729	0.028
Pml-03	48	5.00	1.863	0.479	0.463	-0.034
Pml-11	48	5.00	3.704	0.771	0.730	-0.056
Pml-04	48	3.00	1.822	0.583	0.451	-0.293
PO-71	48	6.00	2.810	0.750	0.644	-0.164
Pml-06	48	3.00	2.182	0.563	0.542	-0.038
Mean	48	4.182	2.580	0.585	0.579	-0.012
St. Dev.	0	1.471	0.785	0.141	0.122	0.140

Table 27 Summary statistics for the combined trapping periods of March 2002 on Gazebo grid and February 2002 on Vet Village grid (1st-02). Included are sample size (N), number of alleles (Na), effective number of alleles (N_e), observed heterozygosity (H_o), expected heterozygosity (H_e) and the fixation index (F_{IS}).

1st-02						
Locus	N	Na	N_e	H_o	H_e	F
Ppa-01	236	2.00	1.685	0.390	0.407	0.041
Ppa-12	223	5.00	2.568	0.507	0.611	0.170
Ppa-46	237	3.00	1.887	0.464	0.470	0.013
PO3-85	236	4.00	2.737	0.585	0.635	0.079
PO3-68	234	6.00	3.917	0.748	0.745	-0.004
PO-25	221	6.00	3.412	0.661	0.707	0.065
Pml-03	204	4.00	1.961	0.515	0.490	-0.050
Pml-11	229	6.00	4.138	0.817	0.758	-0.077
Pml-04	234	4.00	1.928	0.483	0.481	-0.003
PO-71	228	9.00	2.957	0.649	0.662	0.019
Pml-06	234	3.00	2.426	0.594	0.588	-0.011
Mean	229	4.727	2.692	0.583	0.596	0.022
St. Dev.	10	1.954	0.840	0.128	0.120	0.067

Table 28 Mantel tests for the combined trapping periods along with the number of samples for each trapping period.

Period	N	Rxy	P
1st-95	248	0.079	0.001
2nd-95	235	0.113	0.001
3rd-95	138	0.099	0.001
1st-96	92	0.268	0.001
2nd-96	124	0.108	0.001
3rd-96	78	0.034	0.096
1st-97	37	0.326	0.001
1st-98	31	0.254	0.003
1st-00	58	0.128	0.001
2nd-00	19	0.070	0.153
1st-01	65	0.127	0.001
2nd-01	48	0.444	0.001
1st-02	237	0.140	0.001

Table 29 Between grid measures of differentiation that include F_{ST} and R_{ST} and the number of migrants per generation based on F_{ST} ranges from 9.90 to infinity. Also, between grid genetic differentiation as estimated by AMOVA (% variation).

Period	N	F_{ST}	P-value	SE	R_{ST}	$N_M(F_{ST})$	% Var.
1st-95	248	0.019	0.000	0.000	0.019	25.66	1.91
2nd-95	235	0.019	0.000	0.000	0.019	25.97	1.89
3rd-95	138	0.009	0.002	0.001	0.010	52.46	0.94
1st-96	92	0.012	0.009	0.003	0.012	41.22	1.20
2nd-96	124	0.006	0.013	0.003	0.006	80.59	0.62
3rd-96	78	0.004	0.137	0.013	0.004	127.34	0.39
1st-97	37	0.046	0.009	0.003	0.048	10.44	4.57
1st-98	31	-0.004	0.568	0.016	0.000	Inf.	0.00
1st-00	58	0.051	0.000	0.000	0.053	9.40	5.05
2nd-00	19	0.038	0.128	0.012	0.039	12.68	3.79
1st-01	65	0.032	0.001	0.001	0.033	15.15	3.19
2nd-01	48	0.033	0.011	0.003	0.034	14.64	3.30
1st-02	237	0.038	0.000	0.000	0.040	12.66	3.80

Table 30 Population assignment using the jackknife method within program WHICHRUN (Banks & Eichert 2000) for each grid by trapping period.

Trap period	Grid	n	% correct
1st-95	Gazebo	145	77.2
1st-95	Vet Village	103	71.8
2nd-95	Gazebo	122	76.2
2nd-95	Vet Village	113	74.3
3rd-95	Gazebo	68	67.6
3rd-95	Vet Village	70	67.1
1st-96	Gazebo	48	64.5
1st-96	Vet Village	44	59.1
2nd-96	Gazebo	52	67.3
2nd-96	Vet Village	72	69.4
3rd-96	Gazebo	34	64.7
3rd-96	Vet Village	44	70.5
1st-00	Gazebo	32	75.0
1st-00	Vet Village	26	73.1
1st-01	Gazebo	22	63.6
1st-01	Vet Village	43	69.8
1st-02	Gazebo	120	81.7
1st-02	Vet Village	117	81.2

CUMULATIVE REFERENCES

- Albrecht I, Schulte-Hostedde H, Gibbs L, *et al.* (2001) Microgeographic genetic structure in the yellow-pine chipmunk (*Tamias amoenus*). *Molecular Ecology*, **10**, 1625-1631.
- Arbogast BS (1999) Mitochondrial DNA phylogeography of the New World flying squirrels (*Glaucomys*): implications for Pleistocene biogeography. *Journal of Mammalogy*, **80**, 142-155.
- Avise JC (2000) History and purview of phylogeography. In: *Phylogeography: The History and Formation of Species* (ed. Avise JC), pp. 3-36. Harvard University Press, London.
- Avise JC, Arnold J, Ball RM, Jr *et al.* (1987) Intraspecific phylogeography: the mitochondrial DNA bridge between population genetics and systematics. *Annual Review of Ecology and Systematics*, **18**, 489-522.
- Avise JC, Lansman RA, Shade RO (1979) The use of restriction endonucleases to measure mitochondrial DNA sequence relatedness in natural populations. I. Population structure and evolution in the genus *Peromyscus*. *Genetics*, **92**, 279-295.
- Avise JC, Shapira JF, Daniel SW, Aquadro CF, Lansman RA (1983) Mitochondrial DNA differentiation during the speciation process in *Peromyscus*. *Molecular Biology and Evolution*, **1**, 38-56.

- Avise JC, Walker D, Johns GC (1998) Speciation durations and Pleistocene effects on vertebrate phylogeography. *Proceedings of the Royal Society of London*, **B 267**, 1707-1712.
- Avise JC (1996) Space and time as axes in intraspecific phylogeography. In: *Past and Future Environmental Changes: The Spatial and Evolutionary Responses of Terrestrial Biota* (eds Huntly B, Cramer W, Morgan AV, Prentice HC, Allen JRM), pp. 381-388. Springer-Verlag, New York.
- Banks MA, Eichert W (2000) WHICHRUN (version 4.1) a computer program for population assignment of individuals based on multilocus genotype data. *Journal of Heredity*, **91**, 87-89
- Bengtsson BO (1978) Avoid inbreeding: At what cost? *Journal of Theoretical Biology*, **73**, 439-444.
- Blair WF (1950) Ecological factors in speciation of *Peromyscus*. *Evolution*, **4**, 253-275.
- Blondel J, Aronson J (1999) *Biology and wildlife of the Mediterranean region*. Oxford University Press, New York.
- Bowen WW (1968) Variation and Evolution of Gulf Coast populations of beach mice, *Peromyscus polionotus*. *Bulletin of the Florida State Museum*, **12**, 1-91.
- Brookfield JFY (1996) A simple new method for estimating null allele frequency from heterozygote deficiency. *Molecular Ecology*, **56**, 45-47.
- Brown WM, George M, Jr, Wilson AC (1979) Rapid evolution of animal mitochondrial DNA. *Proceedings of the National Academy of Sciences of the USA*, **76**, 1967-1971.
- Cain SA (1944) *Foundations of plant geography*. Harper and Brothers, New York.

- Chesser RK, Smith MH, Brisbin Jr IL (1980) Management and maintenance of genetic variability in endangered species. *International Zoo Yearbook*, **20**, 146-154.
- Chesser RK, Smith MH, Brisbin Jr IL (1980) Management and maintenance of genetic variability in endangered species. *International Zoo Yearbook*, **20**, 146-154.
- Chesser RK (1983) Genetic variability within and among populations of the black-tailed prairie dog. *Evolution*, **37**, 320-331.
- Chesser RK (1991a) Gene diversity and female philopatry. *Genetics*, **127**, 437-447.
- Chesser RK (1991b) Influence of gene flow and breeding tactics on gene diversity within populations. *Genetics*, **129**, 573-583.
- Chesser RK (1998) Relativity of Behavioral Interactions in Socially Structured Populations. *Journal of Mammalogy*, **79**, 713-724.
- Chirhart SE, Honeycutt RL, Greenbaum IF (2000) Microsatellite markers for the deer mouse *Peromyscus maniculatus*. *Molecular Ecology*, **9**, 1669-1671.
- Christiansen FB (1974) Sufficient conditions for protected polymorphism in a subdivided population. *The American Naturalist*, **108**, 157-166.
- Clement M, Posada D and Crandall K. 2000. TCS: a computer program to estimate gene genealogies. *Molecular Ecology* 9(10): 1657-1660
- Delcourt PA, Delcourt HR (1981) Vegetation for eastern North America: 40,000 yr B. P. to the present. In *Geobotany II* (ed. Roamns RC), pp. 123-165. Plenum Press, New York.
- Dobson FS (1998) Social structure and gene dynamics in mammals. *Journal of Mammalogy*, **79**, 667-670.

- Donoghue JF, Stapor FW, Tanner WF (1998) Discussion of: Otvos EG (1995) Multiple Pliocene-Quaternary marine highstands, northeast Gulf coastal plain - fallacies and facts. *Journal of Coastal Research*, **11**, 984-1002. *Journal of Coastal Research*, **14**, 669-674.
- Double MC, Peakall R, Beck NR, Cockburn A (2005) Dispersal, philopatry, and infidelity: dissecting local genetic structure in superb fairy-wrens (*Malurus cyaneus*). *Evolution*, **59**, 625-635.
- Ellsworth DL, Honeycutt RL, Silvy NJ, Bickham JW, Klimstra WD (1994) Historical biogeography and contemporary patterns of mitochondrial DNA variation in white-tailed Deer from the Southeastern United States. *Evolution*, **48**, 122-136.
- Emerson BC, Paradis E, Thébaud C (2001) Revealing the demographic histories of species using DNA sequences. *Trends in Ecology and Evolution*, **16**, 707-716.
- Epperson BK (1990) Spatial autocorrelation of genotypes under directional selection. *Genetics*, **124**, 757-771.
- Epperson BK, Li TQ (1997) Gene dispersal and spatial genetic structure. *Evolution*, **51**, 672-681.
- Excoffier L, Smouse P, et Quattro, JM (1992) Analysis of molecular variance inferred from metric distances among DNA haplotypes: Application to human mitochondrial DNA restriction data. *Genetics*, **131**, 479-491.
- Felsenstein J (1981) Evolutionary trees from DNA sequences: a maximum likelihood approach. *Journal of Molecular Evolution*, **17**, 368-376.
- Felsenstein J (1985) Confidence limits on phylogenies: an approach using the bootstrap. *Evolution*, **39**, 783-791.

- Fisher RA (1930) *The Genetical Theory of Natural Selection*. Clarendon Press, Oxford.
- Foltz DW (1981) Genetic Evidence for long-term monogamy in a small rodent, *Peromyscus polionotus*. *The American Naturalist*, **117**, 665-675.
- Ford EB (1954) Problems in the evolution of geographic races. In: *Evolution as a process* (eds. Huxley J, Hardy AC, Ford EB), pp.99-108. Allen and Unwin, London.
- Ford EB (1960) Evolution in process. In: *Evolution after Darwin* (ed. Sol Tax), pp. 181-196. University of Chicago Press, Chicago.
- Fu Y-X, Li W-H (1993) Statistical tests of neutrality of mutations. *Genetics*, **133**, 693-709.
- Fu Y-X (1997) Statistical tests of neutrality of mutations against population growth, hitchhiking and background selection. *Genetics*, **147**, 915-925.
- Gates DM (1993) *Climate Change and its Biological Consequences*. Sinauer Associates, Sunderland Massachusetts.
- Gerlach G, Musolf K (2000) Fragmentation of landscape as a cause for genetic subdivision in bank voles. *Conservation Biology*, **14**, 1066-1074.
- Gibbs HL, Prior KA, Weatherhead PJ, *et al.* (1997) Genetic structure of populations of the threatened eastern massasauga rattlesnake, *Sistrurus c. catenatus*: evidence from microsatellite DNA markers. *Molecular Ecology*, **6**, 1123-1132.
- Giles BE, Goudet J (1997) Genetics differentiation in *Silene dioica* metapopulations: estimation of spatio-temporal effects in a successional plant species. *American Naturalist*, **149**, 507-526.

- Graham RW, Lundelius EL Jr. (1984) Coevolutionary disequilibrium and Pleistocene extinctions. In: *Quaternary Extinctions* (eds. Martin PS, Klein RG), pp. 223-249. University of Arizona Press, Tucson.
- Greenwood PJ (1980) Mating systems, philopatry and dispersal in birds and mammals. *Animal Behavior*, **28**, 1140-1162.
- Guo SW, Thompson EA (1992) Performing the exact test of Hardy-Weinberg proportions for multiple alleles. *Biometrics*, **48**, 361-372.
- Haldane JBS (1948) The theory of a cline. *Journal of Genetics*, **48**, 227-284.
- Hall ER (1981) The mammals of North America. New York, John Wiley and Sons.
- Hall TA (1999) BioEdit: a user-friendly biological sequence alignment editor and analysis program for Windows 95/98/NT. *Nucleic Acids Symposium Series*, **41**, 95-98.
- Hamrick JL, Nason JD (1996) Consequences of dispersal in plants. In: *Spatial and Temporal Aspects of Population Processes*. (eds. Rhodes OE, Chesser R, Smith M), pp. 203-236. University of Chicago Press, Chicago.
- Haffer J (1969) Speciation in Amazonian forest birds. *Science*, **165**, 131-137.
- Hartl DL, Clark AG (1989) Principles of population genetics. Sinauer, Sunderland Massachusetts.
- Hasegawa M, Kishino H, Yano T (1985) Dating of the human-ape splitting by a molecular clock of mitochondrial DNA. *Journal of Molecular Evolution*, **22**, 160-174.
- Hays JP, Harrison RG (1992) Variation in mitochondrial DNA and the biogeographic history of woodrats (*Neotoma*) of the Eastern United States. *Systematic Biology*, **43**, 331-344.

- Hewitt G M (1996) Some genetic consequences of ice ages, and their role in divergence and speciation. *Biological Journal of the Linnean Society*, **58**, 247-276.
- Hewitt G M (2000) The genetic legacy of the Quaternary ice ages. *Nature*, **405**, 907-913.
- Hewitt G M (1993) Postglacial distribution and species substructure: lessons from pollen, insects and hybrid zones. In: *Evolutionary Patterns and Processes* (eds. Lees DR, Edwards D), pp. 97-123. Academic Press, San Diego, California.
- Hibbard CW (1968) Paleontology, in Biology of Peromyscus (Rodentia). In: *Special Publication Number 2* (ed. King JA), pp. 27-74. American Society of Mammalogists.
- Hoffman EA, Blouin MS (2004) Evolutionary history of the Northern leopard frog: reconstruction of phylogeny, phylogeography, and historical changes in population demography from mitochondrial DNA. *Evolution*, **58**, 145-159.
- Howell AH (1920) Description of a new species of beach mouse from Florida. *Journal of Mammalogy*, **1**, 237-240.
- Hudson RR (1989) How often are polymorphic sites due to a single mutation? *Theoretical Population Biology*, **36**, 23-33.
- Huelsenbeck JP, Ronquist FR (2001) MrBayes: Bayesian inference for phylogeny. *Biometrics* **17**, 754-756.
- Huelsenbeck JP, Bull JJ, Cunningham CW (2002) Combining data in phylogenetic analysis. *Trends in Evolution and Ecology*, **11**, 152-158.
- Huxley JS (1943) *Evolution; the modern synthesis*. Harper and Brothers, New York.
- Jarne P, Lagoda PJJ (1996) Microsatellites, from molecules to populations and back. *Trends in Ecology and Evolution*, **11**, 424-429.

- Karlin S, Campbell RB (1980) Polymorphism in subdivided populations characterized by a major and subordinate demes. *Heredity*, **44**, 151-168.
- Kimura M (1955) Solution of a process of random genetic drift with a continuous model. *Proceedings of the National Academy of Science of the USA*, **41**, 144-150.
- Kimura M, Weiss GH (1964) The stepping stone model of population structure and the decrease of genetic correlation with distance. *Genetics*, **49**, 561-576.
- Kretzmann MB, Gemmell NJ, Meyer A (2001) microsatellite analysis of population structure in the endangered Hawaiian monk seal. *Conservation Biology*, **15**, 457-466.
- Kuhner MK, Yamato J, Felsenstein (1998) Maximum likelihood estimation of population growth rates based on the coalescent. *Genetics*, **149**, 429-434.
- Kuhner MK, Yamato J, Felsenstein J (1995) Estimating effective population size and mutation rate from sequence data using Metropolis-Hastings sampling. *Genetics*, **140**, 1421-1430.
- Lanave C, Preparata G, Saccone C, Serio G (1984) A new method for calculating evolutionary substitution rates. *Journal of molecular evolution*, **20**, 86-93.
- Levins R (1969) Some demographic and genetic consequences of environmental heterogeneity for biological control. *Bulletin of the Entomological Society of America*, **15**, 237-240.
- Li W-H, Graur D (1991) *Fundamentals of Molecular Evolution*. Sinauer Associates, Sunderland, Massachusetts.
- Maruyama T (1970) Rate of decrease of genetic variability in a subdivided population. *Biometrika*, **57**, 299-311.

- Mayr E (1942) *Systematics in the origin of species*. Columbia University Press. New York.
- Mayr E (1954) Change of genetic environment and evolution. In: *Evolution as a process* (eds. Huxley J, Hardy AC, Ford EB), pp. 157-180. Allen and Unwin, London.
- McDonald JH, Kreitman M (1991) Adaptive protein evolution at the *Adh* locus in *Drosophila*. *Nature*, **351**, 652-654.
- Mullen LM, Hirschmann RJ, Prince KL *et al.* (2005) Sixty polymorphic microsatellite markers for the oldfield mouse developed in *Peromyscus polionotus* and *Peromyscus maniculatus*. *Molecular Ecology Notes*, *in press*.
- Nei M, Maruyama T, Chakraborty R (1975) The bottleneck effect and genetic variability in populations. *Evolution*, **29**, 1-10.
- Nei M (1987) *Molecular Evolutionary Genetics*. Columbia University Press, New York.
- Nylander J.A.A. (2002) MrModeltest version 1.1b. <http://morphbank.ebc.uu.se/systzoo/staff/nylander.html>.
- Oli MK, Holler NR, Wooten MC (2001) Viability analysis of endangered Gulf Coast beach mice (*Peromyscus polionotus*) populations. *Biological Conservation*, **97**, 107-118.
- Osgood WH (1909) Revision of the mice the American genus *Peromyscus polionotus*. *North American Fauna*, **28**, 1-285.
- Otis DL, Burnham KP, White GC *et al.* (1978) Statistical inference from capture data on closed animal populations. *Wildlife Monographs*, **62**, 1-135.
- Otvos EG (1995) Multiple Pliocene-Quaternary marine highstands, northeast Gulf coastal-plain-fallacies and facts. *Journal of Coastal Research*, **11**, 984-1002.

- Paetkau D, Calvert W, Stirling I, Strobeck C (1995) Microsatellite analysis of population structure in polar bears. *Molecular Ecology*, **4**, 347-354.
- Palumbi, JP, Martin A, Romano S *et al.* (1991) Simple fool's guide to PCR. Department of Zoology and Kewalo Marine Laboratory, University of Hawaii, Honolulu, HI.
- Patton JL, Yang SY (1977) Genetic variation in *Thomomys bottae* pocket gophers: macrogeographic patterns. *Evolution*, **31**, 697-720.
- Peakall R, Smouse PE (2005) GenAlEx 6: Genetic Analysis in Excel. Population genetic software for teaching and research. Australian National University, Canberra, Australia. <http://www.anu.edu.au/BoZo/GenAlEx/>
- Peakall R, Ruibal M, Lindenmayer DB (2003) Spatial autocorrelation analysis offers new insights into gene flow in the Australian bush rat, *Rattus fuscipes*. *Evolution*, **57**, 1182-1195.
- Petit JR, Jouzel J, Raynaud D (1999) Climate and atmospheric history of the past 420,000 years from the Vostok ice core, Antarctica. *Nature*, **399**, 429-436.
- Pfenninger M, Posada D (2002) Phylogeographic history of the land snail *Candidula unifasciata* (Helicellinae, Stylommatophora): fragmentation, corridor migration, and secondary contact. *Evolution*, **56**, 1776-1788.
- Pielou EC (1991) *After the ice age: return of life to glaciated North America*. University of Chicago Press, Chicago, Illinois.
- Posada D, Crandall KA (1998) MODELTEST: testing the model of DNA substitution. *Bioinformatics*, **14**, 817-818.

- Posada D, Crandall KA, Templeton AR (2000) GeoDis: a program for the cladistic nested analysis of the geographical distribution of genetic haplotypes. *Molecular Ecology*, **9**, 487-488.
- Prince KL, Glenn TC, Dewey MJ (2002) Cross-species amplification among peromyscines of new microsatellite DNA loci from the oldfield mouse (*Peromyscus polionotus subgriseus*) *Molecular Ecology Notes*, **2**, 133-136.
- Raymond M, Rousset F (1995) GENEPOP, version 3.4: an updated version of GENEPOP (version 1.2), population genetics software for exact tests and ecumenism. *Journal of Heredity*, **86**, 248-249.
- Rohlf FJ, Schnell GD (1971) An investigation of the isolation-by-distance model. *The American Naturalist*, **19**, 473-511.
- Root JJ, Black WC IV, Calisher CH *et al.* (2003) Analyses of gene flow among populations of deer mice (*Peromyscus polionotus*) at sites near hantavirus pulmonary syndrome case-patient residences. *Journal of Wildlife Diseases*, **39**, 287-298.
- Ross KG, Krieger MJB, Shoemaker DD, *et al.* (1997) Hierarchical analysis of genetic structure in native fire ant populations: results from three classes of molecular markers. *Genetics*, **147**, 643-655.
- Rozas J, Sánchez-DelBarrio JC, Messeguer X, Rozas R (2003) DnaSP, DNA polymorphism analysis by the coalescent and other methods. *Bioinformatics*, **19**, 2496-2497.
- Ruez DR, Jr (2001) Early Irvingtonian (latest Pliocene) rodents from Inglis 1C, Citrus County, Florida. *Journal of Vertebrate Paleontology*, **21**, 153-171.
- SAS Institute (2000) SAS System for Windows v.9.10. SAS Institute, Cary, NC, USA.

- Sbisa E, Tanzariello F, Reyes A, *et al.* (1997) Mammalian mitochondrial D-loop region structural analysis: identification of new conserved sequences and their functional and evolutionary implications. *Gene*, **205**, 125-140.
- Schneider S, Roessli D, Excoffier L (2000) ARLEQUIN v. 2.0 A software for population genetic data analysis. University of Geneva: Genetics and Biometry Laboratory.
- Scribner KT, Chesser RK (1993) Environmental and demographic correlates of spatial and seasonal genetic structure in the eastern cottontail (*Sylvilagus floridanus*). *Journal of Mammalogy*, **74**, 1026-1044.
- Selander RK (1970a) Biochemical polymorphism in populations of the house mouse and old-field mouse. *Symposium of the Zoological Society of London*, **26**, 73-91.
- Selander RK (1970b) Behavior and genetic variation in natural populations. *American Zoologist*, **10**, 53-66.
- Selander RK, Smith MH, Yang SY, Johnson WE, Gentry JB (1971) Biochemical polymorphism and systematics in the genus *Peromyscus*. I. Variation in the oldfield mouse (*Peromyscus polionotus*). *Studies in Genetics*, **6**, 49-90.
- Slatkin M (1976) The rate and spread of an advantageous allele in a subdivided population. In: *Population Genetics and Ecology* (eds Karlin S, Nevo E), pp. 767-780. Academic Press. New York.
- Slatkin M (1977) Gene flow and genetic drift in a species subject to frequent local extinctions. *Theoretical Population Biology*, **12**, 253-262.
- Slatkin M (1985) Gene flow in natural population. *Annual review of Ecology and Systematics*, **16**, 393-430.

- Smouse PE, Long JC (1992) Matrix correlation analysis in anthropology and genetics. *Yearbook of Physical Anthropology*, **35**, 187-213.
- Smouse PE, Peakall R (1999) Spatial autocorrelation analysis of individual multiallele and multilocus genetic structure, *Heredity*, **82**, 561-773.
- Smouse PE, Long JC, Sokal RR (1986) Multiple regression and correlation extensions of the Mantel test of matrix correspondence. *Systematic Zoology*, **35**, 627-632.
- Sober E (1988) *Reconstructing the past: Parsimony, Evolution, and Inference*. MIT Press, Cambridge, Mass.
- Sokal RR, Oden NL (1978a) Spatial autocorrelation in biology. 1. Methodology. *Biological Journal of the Linnean Society*, **10**, 199-228.
- Sokal RR, Oden NL (1978b) Spatial autocorrelation in biology. 2. Some biological implications and four applications of evolutionary and ecological interest. *Biological Journal of the Linnean Society*, **10**, 229-249.
- Sokal RR, Wartenberg DE (1983) A test of spatial autocorrelation analysis using an isolation-by-distance model. *Genetics*, **105**, 219-237.
- Sokal RR, Jacquez GL, Wooten MC (1989) Spatial autocorrelation analysis of migration and selection. *Genetics*, **121**, 845-855.
- Sumner FB (1926) An analysis of geographic variation in mice of the *Peromyscus polionotus* group from Florida and Alabama. *Journal of Mammalogy*, **7**, 149-184.
- Sumner FB (1929) An analysis of a concrete case of intergradation between two subspecies. *Proceedings of the National Academy of Sciences of the USA*, **15**, 11-120.

- Swilling RS Jr, Wooten MC, Holler NR, Lynn WJ (1998) Population dynamics of Alabama beach mice (*Peromyscus polionotus ammobates*) following hurricane Opal. *The American Midland Naturalist*, **140**, 287-298.
- Swilling RS Jr, Wooten MC (2000) Subadult dispersal in a monogamous species: the Alabama beach mouse (*Peromyscus polionotus ammobates*). *Journal of Mammalogy*, **83**, 252-259.
- Swofford DL (2002) PAUP*: phylogenetic analysis using parsimony (* and other methods). Ver. 4.0b10. Sinauer Associates, Sunderland, MA.
- Tajima F (1989) Statistical method for testing the neutral mutation hypothesis by DNA polymorphism. *Genetics*, **123**, 585-595.
- Templeton AR (1998) Nested clade analyses of phylogeographic data: testing hypotheses about gene flow and population history. *Molecular Ecology*, **7**, 381-397.
- Templeton AR, Boerwinkle E, Sing CF (1987) A cladistic analysis of phenotypic associations with haplotypes inferred from restriction endonuclease mapping. I. Basic theory and an analysis of alcohol dehydrogenase activity in *Drosophila*. *Genetics* **117**, 343-351.
- Templeton AR, Crandall A, Sing CF (1992) A cladistic analysis of phenotypic associations with haplotypes inferred from restriction endonuclease mapping and DNA sequence data. III. Cladogram estimation. *Genetics* **132**, 619-633.
- Templeton AR, Sing CF (1993) A cladistic analysis of phenotypic associations with haplotypes inferred from restriction endonuclease mapping. IV. Nested analysis with cladogram uncertainty and recombination. *Genetics*, **134**, 659-669.

- Templeton AR, Routman E, Phillips CA (1995) Separating population structure from population history: a cladistic analysis of the geographical distribution of mitochondrial DNA haplotypes in the tiger salamander, *Ambystoma tigrinum*. *Genetics*, **140**, 767-782.
- Thompson, J.D., Gibson, T.J., Plewniak, F., Jeanmougin, F. and Higgins, D.G. (1997) The ClustalX windows interface: flexible strategies for multiple sequence alignment aided by quality analysis tools. *Nucleic Acids Research*, *24*:4876-4882.
- Tiedemann R, Hardy O, Vekemans X, Milinkovitch MC (2000) Higher impact of female than male migration on population structure in large mammals. *Molecular Ecology*, **9**, 1159-1163.
- Turner ME, Stephens JC, Anderson WW (1982) Homozygosity and patch structure in plant populations as a result of nearest-neighbor pollination. *Proceedings of the National Academy of Science of the USA*, **79**, 203-207.
- van Oosterhout C, Hutchinson WF, Wills DPM, Shipley P (2004) MICRO-CHECKER: software for identifying and correcting genotyping errors in microsatellite data. *Molecular Ecology Notes*, **4**, 535-538.
- van Staaden MJ, Michener GR, Chesser RK (1996) Spatial analysis of microgeographic genetic structure in Richardson's ground squirrels. *Canadian Journal of Zoology*, **74**, 1187-1195.
- Veith M, Kosuch J, Vences M (2003) Climatic oscillations triggered post-Messinian speciation of Western Palearctic brown frogs (Amphibia, Ranidae). *Molecular Phylogenetics and Evolution*, **26**, 310-327.

- Vigilant LA, Stoneking M, Harpending H, Hawkes K, Wilson AC (1991) African populations and the evolution of mitochondrial DNA. *Science*, **253**, 1503-1507.
- Wahlund S (1928) Composition of populations from the perspective of the theory of heredity. *Hereditas*, **11**, 65-105 (in German).
- Walker D, Avise JC (1998) Principles of phylogeography as illustrated by freshwater and terrestrial turtles in the Southeastern United States. *Annual Review of Ecology and Systematics*, **29**, 23-58.
- Wanless HR (1989) The inundation of our coastlines Past, present and future with a focus on south Florida, *Sea Frontiers*, **September-October**, 264-271.
- Wanless HR, Parkinson RW, Tedesco LP (1994) Sea level control on stability of Everglades wetlands. In *Everglades: The Ecosystem and Its Restoration*, (eds. Davis S, Ogden J) pp. 199-223. St. Lucie Press, Delray Beach, Florida.
- Waser J (1993) Sex, mating Systems, Inbreeding, and Outbreeding. In: *The Natural History of Inbreeding and Outbreeding* (ed. Thornhill NW) pp. 1-13. University of Chicago Press, Chicago.
- Waser PM, Elliot LF (1991) Dispersal and genetic structure in Kangaroo rats. *Evolution*, **45**, 935-943.
- Waser PM, Strobeck C (1998) Genetic signatures of interpopulation dispersal. *Trends in Ecology and Evolution*, **13**, 43-44.
- Watterson GA (1975) On the number of segregating sites in genetic models without recombination. *Theoretical Population Biology*, **7**, 256-276.
- Webb SD (1974) Chronology of Florida Pleistocene mammals, In: *Pleistocene Mammals of Florida* (ed. Webb SD), pp. 5-31. University Presses of Florida, Gainesville.

- Webb SD, Wilkins KT (1984) Historical biogeography of Florida Pleistocene Mammals. In: *Special Publication of Carnegie Museum of Natural History* (Genoways HH, Dawson), pp. 370-383. Pittsburgh, PA.
- Williams CL, Serfass TL, Cogan R, *et al.* (2002) Microsatellite variation in the reintroduced Pennsylvania elk herd. *Molecular Ecology*, **11**, 1299-1310.
- Winker CD, Howard JD (1977) Plio-Pleistocene paleogeography of the Florida Gulf Coast interpreted from relict shorelines. *Transactions-Gulf Coast Association of Geological Societies*, **XXVII**, 409-420.
- Wooten MC, Holler NR (1999) Genetic analysis within and among natural populations of beach mice. *Final Report, United States Fish and Wildlife Service*.
- Wooten MC, Scribner KT, Krehling JT (1999) Isolation and characterization of microsatellite loci from the endangered beach mouse *Peromyscus polionotus*. *Molecular Ecology*, **8**, 167-168.
- Wright S (1931) Evolution in Mendelian populations. *Genetics*, **16**, 97-159.
- Wright S (1940) The statistical consequences of Mendelian heredity in relation to speciation. In: *The new systematics* (Huxley J), pp. 161-183. Clarendon Press, Oxford.
- Wright S (1943) Isolation by distance. *Genetics*, **28**, 114-138.
- Wright S (1951) The genetical structure of populations. *Annals of Eugenics*, **15**, 323-354.
- Wright S (1969) Evolution and the genetics of populations, In: *The theory of gene frequencies*, Vol 2. University of Chicago Press, Chicago.
- Wright S (1978) Evolution and the genetics of populations, In: *Variability within and among natural populations*, Vol 4. University of Chicago Press, Chicago.

- Yang Z (1996) Among-site rate variation and its impact on phylogenetic analyses. *Trends in Ecology and Evolution*, **11**, 367-372.
- Zamudio KR, Savage WK (2003) Historical isolation, range expansion, and secondary contact of two highly divergent mitochondrial lineages in spotted salamanders (*Ambystoma maculatum*). *Evolution*, **57**, 1631-1652.
- Zhang XS, Wang J, Hill WG (2004) Redistribution of gene frequency and changes of genetic variation following a bottleneck in population size. *Genetics*, **167**, 1475-1492.

APPENDICES

Appendix 1 Allele frequencies for each locus by trapping period from Gazebo, Vet Village and combined grids from a population of Alabama beach mice (*Peromyscus polionotus annobates*).

Locus	Allele	Feb-95	Apr-95	Jun-95	Feb-96	Apr-96	Jun-96	Feb-97	Apr-98	Feb-99	Mar-00	Nov-00	Mar-01	Nov-01	Mar-02
Ppa-01	152	0.0040	0.0180	0.0330	0.0430	0.0670	0.0440	-	-	-	-	-	-	-	-
	184	0.2690	0.2680	0.2580	0.2550	0.2790	0.3240	0.3890	0.6250	0.5630	0.3750	0.3750	0.3750	0.4170	0.3570
	186	0.7270	0.7140	0.7080	0.7020	0.6540	0.6320	0.6110	0.3750	0.4380	0.6250	0.6250	0.6250	0.5830	0.6430
Ppa-12	229	-	-	-	-	-	0.0150	-	-	-	-	-	-	-	-
	234	-	-	-	-	-	-	-	-	-	-	-	-	-	0.0050
	237	-	-	-	-	-	0.0150	-	-	-	-	-	-	-	-
	242	-	-	-	-	-	-	-	-	-	-	-	-	-	0.0050
Ppa-46	244	0.3490	0.3570	0.3710	0.3940	0.4130	0.2940	0.3130	0.4290	0.1250	0.3060	0.4550	0.4770	0.2080	0.2450
	248	0.5250	0.5040	0.4850	0.4260	0.4040	0.4710	0.3750	0.2860	0.8750	0.6290	0.4550	0.4550	0.7500	0.6410
	250	0.0110	0.0080	-	-	-	-	0.0630	0.0710	-	-	-	-	-	-
	252	0.1160	0.1300	0.1440	0.1810	0.1830	0.2060	0.2500	0.2140	-	0.0650	0.0910	0.0680	0.0420	0.1050
	222	-	-	-	-	-	-	-	-	0.2500	-	-	-	-	-
PO3-85	226	-	-	-	-	-	-	-	0.1110	0.2500	-	-	-	-	-
	229	0.2890	0.2630	0.3400	0.5210	0.4330	0.3680	0.6110	0.2220	0.0630	0.4060	0.2270	0.2950	0.2920	0.3040
	231	0.5980	0.6790	0.6040	0.3650	0.4810	0.5290	0.3890	0.6110	0.3750	0.5310	0.7730	0.6360	0.6250	0.6370
	235	0.1130	0.0580	0.0570	0.1150	0.0870	0.0880	-	0.0560	0.0630	0.0630	-	0.0680	0.0830	0.0580
	239	-	-	-	-	-	0.0150	-	-	-	-	-	-	-	-
Ppa-46	227	0.0520	0.0450	0.0520	0.0210	0.0380	0.0440	-	-	-	0.0320	-	0.0450	-	0.0290
	229	0.0070	0.0080	0.0070	-	0.0100	0.0290	-	-	-	-	-	-	-	-
	231	0.5730	0.5830	0.5370	0.5210	0.6350	0.5740	0.5560	0.6880	0.7500	0.4840	0.3000	0.3640	0.7270	0.5460
	233	-	-	-	-	-	-	-	-	-	0.0160	-	-	-	-
	235	0.3180	0.3220	0.3660	0.3020	0.2400	0.2790	0.1670	0.2500	0.2500	0.3550	0.6500	0.4090	0.1820	0.2540
237	0.0490	0.0410	0.0370	0.1560	0.0770	0.0740	0.2780	0.0630	-	0.1130	0.0500	0.1820	0.0910	0.1710	

Locus	Allele	Feb-95	Apr-95	Jun-95	Feb-96	Apr-96	Jun-96	Feb-97	Apr-98	Feb-99	Mar-00	Nov-00	Mar-01	Nov-01	Mar-02
PO3-68	263	-	-	-	-	-	0.0150	-	-	-	-	-	-	-	-
	270	0.3580	0.3400	0.3230	0.3150	0.3170	0.2790	0.1250	0.3130	0.7500	0.3390	0.3640	0.3410	0.3750	0.2740
	272	0.0040	0.0040	-	-	-	-	-	-	-	-	-	-	-	-
	276	0.1210	0.0970	0.0850	0.1090	0.1150	0.1180	0.1880	0.3130	-	0.2420	0.2730	0.1820	0.0830	0.2260
	278	0.1280	0.1430	0.1620	0.1960	0.2020	0.1910	0.3750	0.2500	-	0.2900	0.0910	0.1590	0.2080	0.1970
	280	0.0500	0.0460	0.0540	0.0980	0.0870	0.1030	0.1250	-	-	-	-	0.0230	0.0420	0.0470
	282	0.0710	0.0920	0.0920	0.0430	0.0870	0.0880	0.0630	0.0630	-	0.0810	0.2270	0.2270	0.2500	0.2260
	284	0.2700	0.2770	0.2850	0.2390	0.1920	0.2060	0.1250	0.0630	0.2500	0.0480	0.0450	0.0680	0.0420	0.0300
	PO-25	143	-	-	-	-	-	0.0150	-	-	-	-	-	-	-
	145	-	-	-	-	-	0.0290	-	-	-	-	-	-	-	-
Pml-03	147	0.3240	0.3310	0.3110	0.3190	0.3430	0.3680	0.3890	0.3750	0.3750	0.6610	0.2500	0.2860	0.1250	0.3690
	149	0.1140	0.1200	0.0910	0.0640	0.1470	0.0740	0.2220	0.1880	0.1250	0.0650	0.3000	0.1430	0.2080	0.1530
	151	0.0520	0.0370	0.0230	0.0960	0.0490	0.0590	0.0560	0.0630	0.1250	0.1290	0.1500	0.0240	0.0420	0.1310
	153	-	-	0.0080	0.0110	0.0100	0.0150	-	-	-	-	-	-	-	-
	163	0.0100	0.0120	-	-	-	0.0150	-	-	-	-	-	-	0.0420	0.0040
	169	0.5000	0.5000	0.5680	0.5110	0.4510	0.4260	0.3330	0.3750	0.3750	0.1450	0.3000	0.5480	0.5830	0.3430
	237	0.5920	0.5820	0.5850	0.5500	0.7410	0.6600	0.5000	0.4440	0.4000	0.8590	0.6360	0.7270	0.5420	0.6140
	249	-	-	-	-	-	0.0200	-	-	-	-	-	-	-	-
	251	0.1300	0.1260	0.1060	0.2000	0.1030	0.0600	0.1880	0.1110	-	0.0310	0.1820	0.0450	-	0.0570
253	0.0050	0.0050	0.0110	-	-	-	-	-	-	-	-	-	-	-	
255	0.1630	0.1370	0.1700	0.1500	0.0170	0.0600	0.1250	0.2220	0.4000	0.0470	0.0910	0.0230	0.0420	0.0570	
257	-	-	-	-	0.0170	0.0400	-	-	-	-	-	-	-	-	
259	0.1090	0.1480	0.1280	0.1000	0.1210	0.1600	0.1880	0.2220	0.2000	0.0630	0.0910	0.2050	0.4170	0.2730	

Locus	Allele	Feb-95	Apr-95	Jun-95	Feb-96	Apr-96	Jun-96	Feb-97	Apr-98	Feb-99	Mar-00	Nov-00	Mar-01	Nov-01	Mar-02
Pml-11	256	0.2180	0.1990	0.2420	0.3440	0.2840	0.3180	0.5000	0.5000	0.6250	0.3440	0.3640	0.2500	0.4580	0.3290
	258	-	-	-	-	-	0.0150	-	-	-	-	-	-	-	-
	260	0.0670	0.0590	0.0630	0.0310	0.0290	0.0300	-	0.0630	0.1250	0.0310	-	0.0450	-	0.0430
	262	0.2540	0.2500	0.2270	0.1770	0.2160	0.1820	0.1670	0.1880	0.1250	0.2340	0.3180	0.3640	0.1670	0.2390
	264	0.3560	0.3640	0.3360	0.3330	0.3430	0.3480	0.2220	0.2500	0.1250	0.3440	0.1820	0.2050	0.2080	0.1970
	266	0.0560	0.0680	0.0860	0.0940	0.0490	0.0450	0.1110	-	-	-	-	-	-	0.0980
	268	0.0490	0.0590	0.0470	0.0210	0.0780	0.0610	-	-	-	0.0470	0.1360	0.1360	0.1670	0.0940
	222	0.3430	0.3350	0.3200	0.3540	0.3370	0.3820	0.2780	0.2220	0.5000	0.4380	0.3640	0.3410	0.3330	0.3150
	226	0.6310	0.6460	0.6800	0.5830	0.6330	0.5440	0.6110	0.7220	0.5000	0.5630	0.0636	0.6590	0.6250	0.6680
	228	0.0250	0.0190	-	0.0630	0.0310	0.0440	0.1110	0.0560	-	-	-	-	0.0420	0.0170
230	-	-	-	-	-	0.0290	-	-	-	-	-	-	-	-	
PO-71	237	-	-	-	-	-	-	-	-	-	-	-	-	-	0.0040
	241	0.0180	0.0250	0.0300	-	-	-	-	0.0630	-	0.0930	0.0910	0.0240	-	0.0090
	243	0.4330	0.4060	0.4620	0.5210	0.5100	0.5170	0.8330	0.5630	0.7500	0.6670	0.4090	0.5480	0.5450	0.5930
	245	0.2990	0.2910	0.2950	0.2450	0.2940	0.2590	0.0830	0.1880	0.1250	0.0560	0.1820	0.2140	0.4090	0.2700
	247	0.0110	0.0120	0.0080	-	-	-	-	0.0630	0.1250	0.0560	0.0450	0.0480	-	-
	249	0.0560	0.0780	0.0450	0.0850	0.0780	0.0690	-	-	-	0.0560	0.1360	0.1190	-	0.0580
	251	0.1550	0.1600	0.1290	0.1170	0.0880	0.1380	0.0830	0.1250	-	0.0740	0.1360	0.0240	-	0.0270
	253	0.0250	0.0290	0.0300	0.0320	0.0290	0.0170	-	-	-	-	-	0.0240	0.0450	0.0310
	258	0.0040	-	-	-	-	-	-	-	-	-	-	-	-	-
	262	-	-	-	-	-	-	-	-	-	-	-	-	-	0.0090
Pml-06	133	0.4790	0.4630	0.4180	0.4270	0.5310	0.6090	0.0560	0.2500	0.5000	0.2190	0.3330	0.4320	0.4580	0.3630
	148	0.1750	0.1530	0.1640	0.1770	0.1120	0.1410	0.3330	0.1880	0.1000	0.2500	0.1110	0.1820	0.1670	0.2310
	152	0.3460	0.3840	0.4180	0.3960	0.3570	0.2500	0.6110	0.5630	0.4000	0.5310	0.5560	0.3860	0.3750	0.4060

Vet Village

Locus	Allele	Feb-95	Apr-95	Jun-95	Feb-96	Apr-96	Jun-96	Feb-97	Apr-98	Mar-00	Nov-00	Mar-01	Nov-01	Mar-02
Ppa-01	152	-	-	-	-	0.0140	-	-	0.0230	-	-	-	-	-
	184	0.3450	0.3740	0.4190	0.3640	0.2710	0.2910	0.4110	0.4770	0.4420	0.2500	0.2090	0.2000	0.2090
	186	0.6550	0.6260	0.5810	0.6360	0.7150	0.7090	0.5890	0.5000	0.5580	0.7500	0.7910	0.8000	0.7910
Ppa-12	234	-	-	-	-	-	-	-	-	-	-	-	-	0.0090
	244	0.4540	0.4440	0.4550	0.3490	0.3590	0.3810	0.5360	0.3640	0.4200	0.3130	0.3850	0.2790	0.2120
	248	0.3210	0.3330	0.3360	0.3260	0.3310	0.3570	0.3750	0.5680	0.4400	0.4380	0.3970	0.5000	0.4290
	250	0.0200	0.0090	0.0070	0.0230	-	0.0240	-	-	-	-	-	-	-
	252	0.1680	0.1570	0.1790	0.3020	0.3030	0.2380	0.0890	0.0680	0.1400	0.2500	0.2180	0.2210	0.3500
	254	0.0360	0.0560	0.0220	-	0.0070	-	-	-	-	-	-	-	-
Ppa-46	229	0.3830	0.4100	0.4190	0.4770	0.4510	0.3600	0.2320	0.3180	0.3460	0.2500	0.3490	0.3140	0.2740
	231	0.5850	0.5590	0.5510	0.4550	0.4650	0.5350	0.7320	0.5910	0.6350	0.6250	0.5810	0.6430	0.6970
	235	0.0320	0.0320	0.0290	0.0680	0.0830	0.1050	0.0360	0.0910	0.0190	0.1250	0.0700	0.0430	0.0300
PO3-85	227	0.1370	0.1190	0.1140	0.1360	0.1040	0.1310	0.2320	0.1820	0.1150	0.1880	0.0360	0.0560	0.0300
	229	0.0250	0.0350	0.0430	0.0110	0.0280	0.0360	-	-	-	-	-	-	-
	231	0.4070	0.4250	0.4360	0.4200	0.4720	0.4290	0.4290	0.3180	0.2310	0.5000	0.5710	0.4310	0.4570
	233	-	0.0040	-	-	-	-	-	-	-	-	-	-	-
	235	0.3040	0.3140	0.3210	0.2730	0.2710	0.3210	0.2500	0.2730	0.5580	0.3130	0.2860	0.2780	0.2890
	237	0.1270	0.1020	0.0860	0.1590	0.1250	0.0830	0.0890	0.2270	0.0960	-	0.1070	0.2360	0.2240

Locus	Allele	Feb-95	Apr-95	Jun-95	Feb-96	Apr-96	Jun-96	Feb-97	Apr-98	Mar-00	Nov-00	Mar-01	Nov-01	Mar-02
PO3-68	270	0.1830	0.1830	0.1930	0.1250	0.2150	0.1630	0.2220	0.2500	0.6150	0.6250	0.5230	0.4430	0.4490
	272	-	0.0040	-	-	-	-	-	-	-	-	-	-	-
	276	0.1290	0.1430	0.1500	0.2270	0.2080	0.2790	0.2960	0.3860	0.0960	0.1250	0.2670	0.2570	0.2990
	278	0.2130	0.2190	0.1570	0.2500	0.1670	0.1740	0.2410	0.2050	0.0960	0.0630	0.0470	0.1710	0.1030
	280	0.0640	0.0490	0.0710	0.0340	0.0690	0.0700	0.0370	-	-	0.0630	0.0230	0.0430	0.0170
	282	0.0640	0.0980	0.0790	0.0800	0.0970	0.0930	0.0370	0.1140	0.1920	0.0630	0.1160	0.0860	0.1320
	284	0.3470	0.3040	0.3500	0.2840	0.2430	0.2210	0.1670	0.0450	-	0.0630	0.0230	-	-
	145	-	-	-	-	-	-	-	-	-	-	-	0.0310	0.0050
PO-25	147	0.3600	0.3540	0.4070	0.4650	0.4200	0.4270	0.4640	0.4320	0.4380	0.4290	0.4530	0.3130	0.4420
	149	0.1100	0.0930	0.0710	0.0230	0.0580	0.1100	0.0540	0.1140	0.2500	0.0710	0.1250	0.2030	0.1170
	151	0.0350	0.0530	0.0500	0.0350	0.0290	0.0610	0.0710	-	0.0830	0.3570	0.0780	0.1410	0.2040
	153	-	0.0040	0.0070	0.0230	0.0220	0.0370	-	-	-	-	-	-	-
	169	0.4950	0.4960	0.4640	0.4530	0.4710	0.3660	0.4110	0.4550	0.2290	0.1430	0.3440	0.3130	0.2330
	235	-	-	-	-	-	0.0120	-	-	-	-	-	-	-
	237	0.5580	0.5800	0.5430	0.4770	0.4370	0.5230	0.4460	0.3410	0.5380	1.0000	0.6740	0.7350	0.7030
	251	0.2480	0.2080	0.1930	0.2910	0.2890	0.1860	0.1790	0.1820	0.0380	-	0.0700	0.0440	0.0560
Pml-11	255	0.1020	0.1060	0.1570	0.1630	0.1830	0.2090	0.2860	0.1590	0.1150	-	0.0230	0.0150	-
	257	-	-	-	-	0.0070	0.0120	-	-	-	-	-	-	-
	259	0.0920	0.1060	0.1070	0.0700	0.0850	0.0580	0.0890	0.3180	0.3080	-	0.2330	0.2060	0.2410
	256	0.3450	0.4070	0.3860	0.3260	0.3930	0.3570	0.4460	0.3640	0.1730	0.1880	0.2000	0.3030	0.2190
	258	-	0.0040	0.0070	-	-	-	-	-	-	-	-	-	-
	260	0.0290	0.0440	0.0360	0.0580	0.0710	0.0600	0.0180	-	0.0380	-	-	-	0.0090
	262	0.2430	0.1990	0.2210	0.1630	0.1500	0.2140	0.1790	0.2050	0.4620	0.3750	0.3000	0.3480	0.4060
	264	0.2040	0.2040	0.2210	0.1980	0.2070	0.2740	0.2680	0.3410	0.2690	0.3750	0.4000	0.2270	0.2540
Pml-03	266	0.1310	0.1060	0.0930	0.2330	0.1140	0.0480	0.0890	0.0910	0.0380	-	0.0380	0.0760	0.0580
	268	0.0490	0.0350	0.0360	0.0230	0.0640	0.0480	-	-	0.0190	0.0630	0.0630	0.0450	0.0540

Locus	Allele	Feb-95	Apr-95	Jun-95	Feb-96	Apr-96	Jun-96	Feb-97	Apr-98	Mar-00	Nov-00	Mar-01	Nov-01	Mar-02
Pml-04	222	0.1650	0.2040	0.1640	0.2390	0.2640	0.2610	0.1960	0.2730	0.2400	0.5630	0.4530	0.3190	0.4350
	224	-	-	-	-	0.0070	0.0110	0.0180	-	0.0200	-	0.0120	-	0.0040
	226	0.7620	0.7260	0.7640	0.6930	0.6670	0.7160	0.7140	0.7050	0.7400	0.4380	0.5350	0.6810	0.5610
	228	0.0730	0.0710	0.0710	0.0680	0.0630	0.0110	0.0710	0.0230	-	-	-	-	-
PO-71	241	0.0170	0.0050	0.0080	-	0.0070	0.0120	0.0360	-	0.0830	0.0630	0.0470	0.0280	0.0430
	243	0.3720	0.3720	0.3500	0.3290	0.3990	0.3100	0.4640	0.5500	0.3750	0.3750	0.3140	0.4440	0.3830
	245	0.3780	0.4130	0.4250	0.2800	0.2830	0.3210	0.2140	0.0500	0.3130	0.0630	0.3020	0.3060	0.2740
	247	0.0410	0.0200	0.0330	0.0490	0.0140	0.0240	-	0.0750	0.0830	0.0630	0.0350	0.0140	0.0130
	249	0.0640	0.0660	0.0670	0.1830	0.1590	0.1430	0.1250	0.1000	0.1040	0.3130	0.2790	0.2080	0.2610
	251	0.1050	0.0920	0.0830	0.0850	0.0870	0.1190	0.1070	0.2250	0.0420	0.1250	0.0230	-	-
	253	0.0170	0.0260	0.0250	0.0490	0.0290	0.0600	0.0540	-	-	-	-	-	0.0170
Pml-06	262	0.0060	0.0050	0.0080	0.0240	0.0220	0.0120	-	-	-	-	-	-	0.0090
	133	0.4500	0.4650	0.4360	0.4430	0.4380	0.5120	0.5360	0.5450	0.2800	0.1880	0.1740	0.2920	0.2090
	148	0.2130	0.2170	0.2070	0.2270	0.1880	0.1790	0.1070	0.0910	0.0800	0.0630	0.1400	0.0560	0.0940
	152	0.3370	0.3190	0.3570	0.3300	0.3750	0.3100	0.3570	0.3640	0.6400	0.7500	0.6860	0.6530	0.6970

Combined grids

Locus	Allele	1st-95	2nd-95	3rd-95	1st-96	2nd-96	3rd-96	1st-97	1st-98	1st-99	1st-00	2nd-00	1st-01	2nd-01	1st-02
Ppa-01	152	0.0022	0.0090	0.0156	0.0220	0.0363	0.0195	-	0.0167	-	-	-	-	-	-
	184	0.3017	0.3206	0.3438	0.3077	0.2742	0.3052	0.4054	0.5167	0.5630	0.4052	0.3125	0.2619	0.2604	0.2839
	186	0.6961	0.6704	0.6406	0.6703	0.6895	0.6753	0.5946	0.4667	0.4380	0.5948	0.6875	0.7381	0.7396	0.7161
Ppa-12	229	-	-	-	-	-	0.0066	-	-	-	-	-	-	-	-
	237	-	-	-	-	-	0.0066	-	-	-	-	-	-	-	-
	234	-	-	-	-	-	-	-	-	-	-	-	-	-	0.0067
Ppa-46	242	-	-	-	-	-	-	-	-	-	-	-	-	-	0.0022
	244	0.3917	0.3987	0.4135	0.3722	0.3821	0.3421	0.4861	0.3793	0.1250	0.3571	0.3947	0.4180	0.2708	0.2287
	248	0.4417	0.4229	0.4098	0.3778	0.3618	0.4079	0.3750	0.5000	0.8750	0.5446	0.4474	0.4180	0.5625	0.5336
Ppa-46	250	0.0146	0.0088	0.0038	0.0111	-	0.0132	0.0139	0.0172	-	-	-	-	-	-
	252	0.1375	0.1432	0.1617	0.2389	0.2520	0.2237	0.1250	0.1034	-	0.0982	0.1579	0.1639	0.1667	0.2287
	254	0.0146	0.0264	0.0113	-	0.0041	-	-	-	-	-	-	-	-	-
PO3-85	222	-	-	-	-	-	-	-	-	0.2500	-	-	-	-	-
	226	-	-	-	-	-	-	0.0323	0.2500	-	-	-	-	-	-
	229	0.3351	0.3422	0.3843	0.5000	0.4435	0.3636	0.3243	0.2903	0.0630	0.3793	0.2368	0.3308	0.3021	0.2890
PO3-68	231	0.5916	0.6141	0.5744	0.4076	0.4718	0.5325	0.6486	0.5968	0.3750	0.5776	0.7105	0.6000	0.6458	0.6667
	235	0.0733	0.0437	0.0413	0.0924	0.0847	0.0974	0.0270	0.0806	0.0630	0.0431	0.0526	0.0692	0.0521	0.0443
	239	-	-	-	-	-	0.0065	-	-	-	-	-	-	-	-
PO3-68	227	0.0878	0.0812	0.0839	0.0761	0.0766	0.0921	0.1757	0.1333	-	0.0702	0.0833	0.0391	0.0417	0.0297
	229	0.0143	0.0214	0.0255	0.0054	0.0202	0.0329	-	-	-	-	-	-	-	-
	231	0.5041	0.5064	0.4854	0.4728	0.5403	0.4934	0.4595	0.4167	0.7500	0.3684	0.3889	0.5000	0.5104	0.5021
PO3-68	233	0.3122	0.0021	-	-	-	-	-	-	-	0.0088	-	-	-	-
	235	-	0.3184	0.3431	0.2880	0.2581	0.3026	0.2297	0.2667	0.2500	0.4474	0.5000	0.3281	0.2500	0.2712
	237	0.0816	0.0705	0.0620	0.1576	0.1048	0.0789	0.1351	0.1833	-	0.1053	0.0278	0.1328	0.1979	0.1970
PO3-68	263	-	-	-	-	-	0.0065	-	-	-	-	-	-	-	-
	270	0.2851	0.2641	0.2556	0.2222	0.2581	0.2143	0.2000	0.2667	0.7500	0.4649	0.4737	0.4615	0.4271	0.3611
	272	0.0021	0.0043	-	-	-	-	-	-	-	-	-	-	-	-
PO3-68	276	0.1240	0.1190	0.1185	0.1667	0.1694	0.2078	0.2714	0.3667	-	0.1754	0.2105	0.2385	0.2188	0.2628
	278	0.1632	0.1797	0.1593	0.2222	0.1815	0.1818	0.2714	0.2167	-	0.2018	0.0789	0.0846	0.1771	0.1496
	280	0.0558	0.0476	0.0630	0.0667	0.0766	0.0844	0.0571	-	-	-	0.0263	0.0231	0.0417	0.0321
PO3-68	282	0.0682	0.0952	0.0852	0.0611	0.0927	0.0909	0.0429	0.1000	-	0.1316	0.1579	0.1538	0.1250	0.1795
	284	0.3017	0.2900	0.3185	0.2611	0.2218	0.2143	0.1571	0.0500	0.2500	0.0263	0.0526	0.0385	0.0104	0.0150

Locus	Allele	1st-95	2nd-95	3rd-95	1st-96	2nd-96	3rd-96	1st-97	1st-98	1st-99	1st-00	2nd-00	1st-01	2nd-01	1st-02
PO-25	143	-	-	-	-	-	0.0067	-	-	-	-	-	-	-	-
	145	-	-	-	-	-	0.0133	-	-	-	-	-	-	0.0208	0.0023
	147	0.3388	0.3419	0.3603	0.3889	0.3875	0.4000	0.4459	0.4167	0.3750	0.5636	0.3235	0.3868	0.2708	0.4027
	149	0.1122	0.1068	0.0809	0.0444	0.0958	0.0933	0.0946	0.1333	0.1250	0.1455	0.2059	0.1321	0.2083	0.1357
	151	0.0449	0.0449	0.0368	0.0667	0.0375	0.0600	0.0676	0.0167	0.1250	0.1091	0.2353	0.0566	0.1146	0.1652
Pml-03	153	-	0.0021	0.0074	0.0167	0.0167	0.0267	-	-	-	-	-	-	-	-
	163	0.0061	0.0064	-	-	-	0.0067	-	-	-	-	-	-	0.0104	0.0023
	169	0.4980	0.4979	0.5147	0.4833	0.4625	0.3933	0.3919	0.4333	0.3750	0.1818	0.2353	0.4245	0.3750	0.2919
	235	-	-	-	-	-	0.0074	-	-	-	-	-	-	-	-
	237	0.5744	0.5809	0.5598	0.4906	0.5250	0.5735	0.4583	0.3710	0.4000	0.7155	0.7895	0.6923	0.6875	0.6642
Pml-11	249	-	-	-	-	-	0.0074	-	-	-	-	-	-	-	-
	251	0.1923	0.1716	0.1581	0.2736	0.2350	0.1397	0.1806	0.1613	-	0.0345	0.1053	0.0615	0.0313	0.0564
	253	0.0026	0.0025	0.0043	-	0.1350	0.1544	0.2500	0.1774	0.4000	0.0776	0.0526	0.0231	0.0208	0.0245
	255	0.1308	0.1201	0.1624	0.1604	0.0100	0.0221	-	-	-	-	-	-	0.0104	-
	259	0.1000	0.1250	0.1154	0.0755	0.0950	0.0956	0.1111	0.2903	0.2000	0.1724	0.0526	0.2231	0.2500	0.2549
Pml-04	256	0.2714	0.3009	0.3172	0.3352	0.3471	0.3400	0.4595	0.4000	0.6250	0.2672	0.2895	0.2177	0.3438	0.2751
	258	-	0.0022	0.0037	-	-	0.0067	-	-	-	-	-	-	-	-
	260	0.0510	0.0519	0.0485	0.0440	0.0537	0.0467	0.0135	0.0167	0.1250	0.0345	-	0.0161	-	0.0262
	262	0.2490	0.2251	0.2239	0.1703	0.1777	0.2000	0.1757	0.2000	0.1250	0.3362	0.3421	0.3226	0.3021	0.3210
	264	0.2918	0.2857	0.2761	0.2692	0.2645	0.3067	0.2568	0.3167	0.1250	0.3103	0.2632	0.3306	0.2292	0.2249
Pml-04	266	0.0878	0.0866	0.0896	0.1593	0.0868	0.0467	0.0946	0.0667	-	0.0172	-	0.0242	0.0521	0.0786
	268	0.0490	0.0476	0.0410	0.0220	0.0702	0.0533	-	-	-	0.0345	0.1053	0.0887	0.0729	0.0742
	222	0.2602	0.2671	0.2366	0.2989	0.2934	0.3141	0.2162	0.2581	0.5000	0.3509	0.4474	0.4154	0.3229	0.3739
	224	-	-	-	-	0.0041	0.0064	0.0135	-	-	0.0088	-	0.0077	-	0.0021
	226	0.6923	0.6872	0.7252	0.6359	0.6529	0.6410	0.6892	0.7097	0.5000	0.6404	0.5526	0.5769	0.6667	0.6154
228	0.0475	0.0457	0.0382	0.0652	0.0496	0.0256	0.0811	0.0323	-	-	-	-	-	0.0104	
230	-	-	-	-	-	0.0128	-	-	-	-	-	-	-	-	

Locus	Allele	1st-95	2nd-95	3rd-95	1st-96	2nd-96	3rd-96	1st-97	1st-98	1st-99	1st-00	2nd-00	1st-01	2nd-01	1st-02
PO-71	237	-	-	-	-	-	-	-	-	-	-	-	-	-	0.0022
	241	0.0175	0.0159	0.0198	-	0.0042	0.0070	0.0294	0.0179	-	0.0882	0.0789	0.0391	0.0208	0.0263
	243	0.4101	0.3909	0.4087	0.4318	0.4458	0.3944	0.5294	0.5536	0.7500	0.5294	0.3947	0.3906	0.4688	0.4868
	245	0.3289	0.3455	0.3571	0.2614	0.2875	0.2958	0.1912	0.0893	0.1250	0.1765	0.1316	0.2734	0.3333	0.2719
	247	0.0219	0.0159	0.0198	0.0227	0.0083	0.0141	-	0.0714	0.1250	0.0686	0.0526	0.0391	0.0104	0.0066
	249	0.0592	0.0727	0.0556	0.1307	0.1250	0.1127	0.1029	0.0714	-	0.0784	0.2105	0.2266	0.1563	0.1601
	251	0.1360	0.1295	0.1071	0.1023	0.0875	0.1268	0.1029	0.1964	-	0.0588	0.1316	0.0234	-	0.0132
	253	0.0219	0.0273	0.0278	0.0398	0.0292	0.0423	0.0441	-	-	-	-	0.0078	0.0104	0.0241
	258	0.0022	-	-	-	-	-	-	-	-	-	-	-	-	-
	262	0.0022	0.0023	0.0040	0.0114	0.0125	0.0070	-	-	-	-	-	-	-	-
Pml-06	133	0.4672	0.4637	0.4270	0.4348	0.4752	0.5541	0.4189	0.4667	0.5000	0.2456	0.2647	0.2615	0.3333	0.2863
	148	0.1906	0.1838	0.1861	0.2011	0.1570	0.1622	0.1622	0.1167	0.1000	0.1754	0.0882	0.1538	0.0833	0.1624
	152	0.3422	0.3526	0.3869	0.3641	0.3678	0.2838	0.4189	0.4167	0.4000	0.5789	0.6471	0.5846	0.5833	0.5513

Appendix 2 Exact tests of Hardy-Weinberg equilibrium for each locus based on the Markov chain method for Gazebo grid, Vet Village grid and the combined grids.

Locus	Feb-95		Apr-95		Jun-95		Feb-96	
	P-val	S. E.	P-val	S. E.	P-val	S. E.	P-val	S. E.
Ppa-01	0.2288	0.0104	0.4896	0.0072	0.5848	0.0057	0.3343	0.0060
Ppa-12	0.2065	0.0097	0.3433	0.0103	0.1007	0.0034	0.1624	0.0042
Ppa-46	0.4577	0.0066	0.3382	0.0060	1.0000	0.0000	0.5810	0.0058
PO3-85	0.9699	0.0026	0.9462	0.0043	0.2097	0.0102	0.7855	0.0059
PO3-68	0.5631	0.0165	0.1711	0.0131	0.3816	0.0109	0.1778	0.0085
PO-25	0.6123	0.0131	0.1725	0.0099	0.4500	0.0136	0.9837	0.0017
Pml-03	0.6292	0.0106	0.0030	0.0008	0.0072	0.0019	0.3409	0.0078
Pml-11	0.7762	0.0098	0.9454	0.0041	0.2777	0.0104	0.2638	0.0120
Pml-04	0.3704	0.0082	0.7154	0.0067	0.0794	0.0021	0.5474	0.0050
PO-71	0.0228	0.0100	0.4276	0.0168	0.5623	0.0171	0.5719	0.0108
Pml-06	0.5402	0.0076	0.4787	0.0066	0.9165	0.0020	0.8098	0.0028

Locus	Apr-96		Jun-96		Feb-97		Apr-98	
	P-val	S. E.	P-val	S. E.	P-val	S. E.	P-val	S. E.
Ppa-01	0.8144	0.0029	1.0000	0.0000	1.0000	0.0000	1.0000	0.0000
Ppa-12	0.8170	0.0031	0.1498	0.0105	0.0694	0.0038	0.0507	0.0031
Ppa-46	0.4150	0.0053	0.2037	0.0074	1.0000	0.0000	0.0535	0.0039
PO3-85	0.3576	0.0115	0.1377	0.0082	0.6089	0.0035	0.0819	0.0032
PO3-68	0.2950	0.0100	0.4190	0.0132	0.8349	0.0085	0.6304	0.0073
PO-25	0.9784	0.0017	0.2544	0.0177	0.9244	0.0029	0.5183	0.0073
Pml-03	0.4475	0.0129	0.3929	0.0172	0.0060	0.0011	0.0608	0.0035
Pml-11	0.3516	0.0111	0.1080	0.0098	0.1637	0.0050	0.1467	0.0054
Pml-04	0.5692	0.0043	0.0006	0.0003	0.0343	0.0021	0.5272	0.0054
PO-71	0.3274	0.0092	0.8708	0.0061	1.0000	0.0000	0.7904	0.0087
Pml-06	0.2463	0.0054	0.0668	0.0030	0.6433	0.0046	1.0000	0.0000

	Feb-99		Mar-00		Nov-00		Mar-01	
	P-val	S. E.	P-val	S. E.	P-val	S. E.	P-val	S. E.
Ppa-01	0.1419	0.0017	0.2688	0.0030	1.0000	0.0000	1.0000	0.0000
Ppa-12			0.0867	0.0031	0.1474	0.0042	0.2960	0.0044
Ppa-46	0.0643	0.0054	0.4778	0.0052	0.0375	0.0011	1.0000	0.0000
PO3-85	1.0000	0.0000	0.1409	0.0089	1.0000	0.0000	0.7804	0.0050
PO3-68	1.0000	0.0000	0.1632	0.0074	0.6754	0.0067	0.8412	0.0070
PO-25	1.0000	0.0000	0.1627	0.0066	0.0767	0.0032	0.0578	0.0040
Pml-03	1.0000	0.0000	0.2473	0.0082	0.3758	0.0083	0.6636	0.0092
Pml-11	0.4225	0.0096	0.4980	0.0088	0.9551	0.0019	0.5460	0.0087
Pml-04	1.0000	0.0000	0.4949	0.0030	1.0000	0.0000	1.0000	0.0000
PO-71	1.0000	0.0000	0.0785	0.0090	0.1473	0.0084	0.5519	0.0180
Pml-06	0.6134	0.0043	0.0739	0.0026	1.0000	0.0000	0.2811	0.0046

	Nov-01		Mar-02	
	P-val	S. E.	P-val	S. E.
Ppa-01	0.5512	0.0018	1.0000	0.0000
Ppa-12	1.0000	0.0000	0.1109	0.0102
Ppa-46	0.5440	0.0045	0.9230	0.0025
PO3-85	0.0880	0.0029	0.3258	0.0079
PO3-68	0.9029	0.0061	0.0579	0.0055
PO-25	0.7880	0.0093	0.4546	0.0144
Pml-03	1.0000	0.0000	0.0337	0.0024
Pml-11	0.4736	0.0062	0.2997	0.0111
Pml-04	1.0000	0.0000	0.1799	0.0068
PO-71	0.3735	0.0045	0.4160	0.0255
Pml-06	0.6127	0.0037	0.2393	0.0065

Vet Village

Locus	Mar-95		Apr-95		Jun-95		Mar-96	
	P-val	S. E.	P-val	S. E.	P-val	S. E.	P-val	S. E.
Ppa-01	0.3787	0.0044	0.6855	0.0032	0.3293	0.0044	0.3337	0.0031
Ppa-12	0.4883	0.0113	0.6210	0.0105	0.1742	0.0095	0.1240	0.0060
Ppa-46	0.8974	0.0028	0.9564	0.0017	0.9322	0.0019	0.6720	0.0046
PO3-85	0.6941	0.0088	0.4593	0.0137	0.4320	0.0099	0.5999	0.0102
PO3-68	0.2067	0.0106	0.0141	0.0030	0.0312	0.0033	0.7798	0.0079
PO-25	0.3299	0.0085	0.7419	0.0100	0.6670	0.0115	0.5865	0.0123
Pml-03	0.2089	0.0066	0.5165	0.0081	0.0540	0.0038	0.2572	0.0063
Pml-11	0.1602	0.0100	0.8883	0.0075	0.5782	0.0155	0.0372	0.0038
Pml-04	0.8792	0.0027	0.8793	0.0029	1.0000	0.0000	0.9108	0.0022
PO-71	0.3897	0.0228	0.4188	0.0194	0.8770	0.0137	0.3458	0.0125
Pml-06	0.6656	0.0062	0.3584	0.0073	0.4557	0.0060	0.3145	0.0051

	Apr-96		Jun-96		Mar-97		Feb-98	
	P-val	S. E.	P-val	S. E.	P-val	S. E.	P-val	S. E.
Ppa-01	0.7587	0.0047	0.4516	0.0027	0.7045	0.0018	0.6671	0.0054
Ppa-12	0.9211	0.0039	0.2764	0.0081	0.8975	0.0021	0.6325	0.0045
Ppa-46	0.1819	0.0050	0.6590	0.0048	0.7852	0.0043	0.4997	0.0047
PO3-85	0.1805	0.0084	0.5789	0.0085	0.6562	0.0065	0.0868	0.0031
PO3-68	0.7815	0.0070	0.4180	0.0098	0.5078	0.0100	0.1422	0.0063
PO-25	0.9261	0.0044	0.9372	0.0036	0.2076	0.0060	0.5295	0.0051
Pml-03	0.9822	0.0017	0.2323	0.0126	0.7001	0.0054	0.6606	0.0056
Pml-11	0.5217	0.0109	0.5828	0.0112	0.1891	0.0076	0.1986	0.0047
Pml-04	0.9325	0.0034	0.3136	0.0105	0.8638	0.0043	0.1658	0.0054
PO-71	0.7827	0.0164	0.5339	0.0200	0.2859	0.0122	0.3059	0.0100
Pml-06	0.4677	0.0066	0.0895	0.0032	1.0000	0.0000	0.6678	0.0037

	Mar-00		Dec-00		Mar-05		Oct-05	
	P-val	S. E.	P-val	S. E.	P-val	S. E.	P-val	S. E.
Ppa-01	0.2260	0.0024	0.3849	0.0022	0.6590	0.0016	0.1072	0.0020
Ppa-12	1.0000	0.0000	1.0000	0.0000	0.7099	0.0038	0.5790	0.0039
Ppa-46	0.1284	0.0052	0.0804	0.0028	0.3597	0.0052	0.4289	0.0062
PO3-85	0.6830	0.0056	0.7797	0.0031	0.4003	0.0084	0.1579	0.0048
PO3-68	0.6758	0.0063	0.2386	0.0201	0.5548	0.0134	0.4579	0.0105
PO-25	0.3779	0.0050	0.7362	0.0052	0.0940	0.0036	0.0193	0.0022
Pml-03	0.8657	0.0041			0.5356	0.0077	1.0000	0.0000
Pml-11	0.7286	0.0095	0.8127	0.0070	0.6413	0.0076	0.7186	0.0068
Pml-04	0.0090	0.0013	0.0475	0.0011	0.8668	0.0034	0.0609	0.0016
PO-71	0.2945	0.0118	0.0025	0.0011	0.2970	0.0121	0.3734	0.0118
Pml-06	0.6542	0.0028	0.3972	0.0066	0.4161	0.0047	0.5388	0.0050

	Feb-02	
	P-val	S. E.
Ppa-01	0.5824	0.0035
Ppa-12	0.0714	0.0073
Ppa-46	0.0388	0.0024
PO3-85	0.0692	0.0045
PO3-68	0.8749	0.0058
PO-25	0.0000	0.0000
Pml-03	0.6490	0.0061
Pml-11	0.1683	0.0109
Pml-04	0.0930	0.0075
PO-71	0.4676	0.0173
Pml-06	0.1981	0.0059

Combined grids

	1st-95		2nd-95		3rd-95		1st-96	
Locus	P-val	S. E.	P-val	S. E.	P-val	S. E.	P-val	S. E.
Ppa-01	0.1230	0.0106	0.6417	0.0079	0.3458	0.0088	0.7392	0.0043
Ppa-12	0.2794	0.0127	0.2323	0.0114	0.0224	0.0033	0.0846	0.0056
Ppa-46	0.4917	0.0081	0.6616	0.0067	0.9685	0.0013	0.7227	0.0056
PO3-85	0.7769	0.0106	0.6798	0.0141	0.6057	0.0104	0.5558	0.0122
PO3-68	0.7693	0.0153	0.4678	0.0166	0.0703	0.0061	0.3431	0.0101
PO-25	0.4322	0.0128	0.1720	0.0120	0.7719	0.0085	0.8471	0.0067
Pml-03	0.5185	0.0145	0.0889	0.0076	0.0017	0.0008	0.1138	0.0046
Pml-11	0.1208	0.0081	0.7553	0.0134	0.2308	0.0151	0.1759	0.0117
Pml-04	0.5349	0.0084	0.5381	0.0068	0.4287	0.0077	0.7405	0.0046
PO-71	0.0487	0.0091	0.8589	0.0137	0.5346	0.0213	0.0475	0.0061
Pml-06	0.9758	0.0014	0.8759	0.0043	0.7371	0.0060	0.7062	0.0052

	2nd-96		3rd-96		1st-97		1st-98	
	P-val	S. E.	P-val	S. E.	P-val	S. E.	P-val	S. E.
Ppa-01	1.0000	0.0000	0.0618	0.0072	0.7317	0.0016	0.8522	0.0034
Ppa-12	0.8708	0.0059	0.0498	0.0070	0.3148	0.0080	0.0476	0.0030
Ppa-46	0.0459	0.0034	0.2800	0.0102	0.5259	0.0059	0.0378	0.0027
PO3-85	0.8266	0.0071	0.3061	0.0107	0.6720	0.0064	0.0057	0.0008
PO3-68	0.3691	0.0103	0.1436	0.0107	0.5292	0.0109	0.3076	0.0080
PO-25	0.9861	0.0014	0.3174	0.0195	0.4224	0.0075	0.3496	0.0078
Pml-03	0.5597	0.0117	0.0991	0.0106	0.6035	0.0067	0.5068	0.0056
Pml-11	0.1380	0.0098	0.3515	0.0155	0.5305	0.0094	0.2378	0.0088
Pml-04	0.8849	0.0062	0.0009	0.0005	0.8039	0.0061	0.5311	0.0056
PO-71	0.2874	0.0188	0.3864	0.0216	0.2978	0.0115	0.2423	0.0125
Pml-06	0.4187	0.0067	0.0110	0.0009	0.6121	0.0049	0.7764	0.0034

	1st-00		2nd-00		1st-01		2nd-01	
	P-val	S. E.	P-val	S. E.	P-val	S. E.	P-val	S. E.
Ppa-01	1.0000	0.0000	0.5875	0.0019	1.0000	0.0000	0.7078	0.0017
Ppa-12	0.3559	0.0054	0.4690	0.0045	0.4950	0.0053	0.8102	0.0030
Ppa-46	0.2171	0.0049	0.0169	0.0015	0.5061	0.0046	0.7635	0.0042
PO3-85	0.4645	0.0127	0.9207	0.0029	0.3234	0.0071	0.1101	0.0050
PO3-68	0.1870	0.0069	0.6540	0.0115	0.6084	0.0113	0.5726	0.0128
PO-25	0.8311	0.0042	0.1031	0.0033	0.1869	0.0063	0.0166	0.0027
Pml-03	0.4665	0.0088	0.1072	0.0065	0.8196	0.0066	1.0000	0.0000
Pml-11	0.6800	0.0113	0.8773	0.0031	0.6046	0.0124	0.5246	0.0084
Pml-04	0.0362	0.0036	0.3509	0.0021	0.7617	0.0050	0.0681	0.0044
PO-71	0.0211	0.0036	0.0068	0.0012	0.2366	0.0165	0.1224	0.0109
Pml-06	0.4605	0.0051	0.4438	0.0047	0.5308	0.0054	0.5698	0.0048

	1st-02	
	P-val	S. E.
Ppa-01	0.5269	0.0051
Ppa-12	0.0002	0.0002
Ppa-46	0.3938	0.0092
PO3-85	0.4740	0.0120
PO3-68	0.1666	0.0117
PO-25	0.0006	0.0006
Pml-03	0.0786	0.0045
Pml-11	0.7342	0.0119
Pml-04	1.0000	0.0000
PO-71	0.4960	0.0248
Pml-06	0.3584	0.0088

Appendix 3 Spatial autocorrelation analysis for each trapping period on Gazebo, Vet Village and the combined grids after Peakall *et al.* (2003). The distance classes used in the analysis are 20, 50, 100 and 250 m for Gazebo and Vet Village grids. The distance classes used for the combined grids were 20, 50, 100, 200, 320 and 800 m. The number of pairwise comparisons (n), the correlation coefficient (r), 95% CI upper (U) and lower bounds (L), bootstrap resampling upper (Ur) and lower (Lr) bounds about r, the probability based on a one-tailed test (P) and the estimated x-intercept. For distance classes where significance was not found the x-intercept was made zero.

Feb-95	Apr-95							
	20	50	100	250	20	50	100	250
D	20	50	100	250	20	50	100	250
n	127	658	1733	6576	74	397	1152	4617
r	0.131	0.061	0.031	0.008	0.063	0.046	0.022	0.008
U	0.042	0.018	0.011	0.003	0.048	0.021	0.012	0.004
L	-0.038	-0.017	-0.009	-0.003	-0.046	-0.018	-0.011	-0.003
P	0.001	0.001	0.001	0.001	0.008	0.001	0.002	0.002
Ur	0.178	0.082	0.043	0.014	0.111	0.069	0.034	0.015
Lr	0.083	0.044	0.020	0.002	0.012	0.022	0.010	0.002
Int	95	150	193	348	196	215	252	346

Jun-95	Feb-96							
	20	50	100	250	20	50	100	250
D	20	50	100	250	20	50	100	250
n	24	130	401	1395	24	84	274	806
r	-0.025	-0.009	0.010	0.006	0.123	0.053	0.025	0.004
U	0.083	0.035	0.018	0.008	0.088	0.048	0.025	0.009
L	-0.080	-0.032	-0.017	-0.006	-0.081	-0.041	-0.022	-0.007
P	0.723	0.678	0.134	0.063	0.005	0.017	0.027	0.153
Ur	0.079	0.022	0.030	0.017	0.223	0.104	0.054	0.020
Lr	-0.131	-0.044	-0.010	-0.006	0.035	-0.002	-0.007	-0.011
Int	0	0	0	0	107	0	0	0

Apr-96					Jun-96			
D	20	50	100	250	20	50	100	250
n	13	92	241	926	7	56	147	451
r	0.074	-0.007	0.008	0.003	-0.078	-0.005	0.014	-0.004
U	0.145	0.047	0.027	0.009	0.146	0.053	0.032	0.008
L	-0.123	-0.046	-0.023	-0.007	-0.143	-0.047	-0.025	-0.007
P	0.131	0.612	0.246	0.186	0.855	0.562	0.159	0.857
Ur	0.233	0.042	0.039	0.019	0.034	0.055	0.048	0.014
Lr	-0.095	-0.059	-0.022	-0.012	-0.193	-0.061	-0.02	-0.022
Int	0	0	0	0	0	0	0	0

Feb-97					Apr-98			
D	20	50	100	250	20	50	100	250
n	3	4	5	25	1	3	14	29
r	0.415	0.273	0.339	-0.056	0.281	0.147	-0.011	-0.010
U	0.414	0.312	0.245	0.055	0.517	0.183	0.067	0.023
L	-0.211	-0.216	-0.209	-0.053	-0.329	-0.177	-0.053	-0.023
P	0.021	0.039	0.007	0.986	0.071	0.056	0.645	0.820
Ur	0.455	0.443	0.527	0.053	0.128	0.276	0.065	0.046
Lr	0.342	-0.026	0.071	-0.157	0.128	0.064	-0.080	-0.065
Int	48	0	173	0	0	0	0	0

Feb-99					Mar-00			
D	20	50	100	250	20	50	100	250
n	4	6	9	32	14	55	150	433
r	0.277	0.033	-0.021	0.006	0.091	0.107	0.018	0.010
U	0.774	0.623	0.410	0.073	0.135	0.070	0.035	0.007
L	-0.330	-0.196	-0.169	-0.069	-0.122	-0.058	-0.030	-0.007
P	0.154	0.277	0.375	0.385	0.085	0.006	0.139	0.006
Ur	0.954	0.529	0.449	0.231	0.237	0.186	0.064	0.035
Lr	-0.394	-0.447	-0.451	-0.192	-0.057	0.038	-0.033	-0.014
Int	0	0	0	0	0	88	0	0

	Nov-00				Mar-01			
D	20	50	100	250	20	50	100	250
n	2	5	14	50	5	20	57	186
r	0.230	0.001	-0.015	0.001	0.061	0.111	0.083	0.015
U	0.342	0.250	0.120	0.017	0.198	0.093	0.047	0.011
L	-0.317	-0.173	-0.099	-0.018	-0.176	-0.075	-0.039	-0.011
P	0.092	0.448	0.568	0.464	0.244	0.013	0.002	0.007
Ur	0.093	0.356	0.138	0.073	0.287	0.209	0.141	0.043
Lr	0.093	-0.256	-0.139	-0.071	-0.149	0.009	0.026	-0.015
Int	0	0	0	0	0	204	218	0

	Nov-01				Mar-02			
D	20	50	100	250	20	50	100	250
n	3	5	15	55	138	707	1711	5766
r	0.312	0.225	0.093	0.030	0.127	0.058	0.021	0.006
U	0.186	0.164	0.090	0.018	0.037	0.016	0.010	0.002
L	-0.168	-0.154	-0.084	-0.016	-0.035	-0.015	-0.008	-0.002
P	0.001	0.001	0.017	0.001	0.001	0.001	0.001	0.001
Ur	0.381	0.323	0.172	0.071	0.176	0.075	0.031	0.012
Lr	0.247	0.135	0.019	-0.013	0.081	0.039	0.010	0.000
Int	78	128	219	0	85	95	216	297

Vet Village grid

	Mar-95				Apr-95			
D	20	50	100	250	20	50	100	250
n	56	376	1005	3739	55	398	1234	4276
r	0.202	0.091	0.034	0.001	0.073	0.040	0.022	0.004
U	0.059	0.021	0.012	0.004	0.057	0.021	0.011	0.004
L	-0.053	-0.019	-0.010	-0.003	-0.054	-0.019	-0.010	-0.003
P	0.001	0.001	0.001	0.196	0.011	0.001	0.001	0.012
Ur	0.286	0.117	0.048	0.008	0.143	0.066	0.035	0.011
Lr	0.117	0.064	0.019	-0.006	0.008	0.013	0.008	-0.002
Intercept	77	99	186	0	80	147	198	0

Jun-95	Mar-96							
D	20	50	100	250	20	50	100	250
n	19	156	479	1649	15	81	209	663
r	0.019	0.031	0.004	0.002	0.029	0.046	0.025	0.011
U	0.099	0.033	0.018	0.006	0.115	0.049	0.027	0.009
L	-0.099	-0.032	-0.016	-0.005	-0.105	-0.043	-0.024	-0.008
P	0.353	0.035	0.326	0.174	0.268	0.029	0.038	0.013
Ur	0.152	0.071	0.023	0.013	0.186	0.103	0.058	0.027
Lr	-0.099	-0.004	-0.015	-0.009	-0.117	-0.013	-0.012	-0.007
Intercept	0	0	0	0	0	0	0	0

Apr-96	Jun-96							
D	20	50	100	250	20	50	100	250
n	25	157	457	1610	9	66	202	653
r	-0.010	0.030	0.027	0.007	-0.007	0.011	0.009	0.002
U	0.077	0.033	0.017	0.006	0.124	0.047	0.022	0.007
L	-0.077	-0.030	-0.015	-0.005	-0.111	-0.039	-0.020	-0.006
P	0.585	0.041	0.005	0.015	0.539	0.307	0.208	0.323
Ur	0.067	0.064	0.046	0.017	0.108	0.057	0.033	0.015
Lr	-0.100	-0.003	0.009	-0.003	-0.115	-0.032	-0.016	-0.012
Intercept	0	0	225	0	0	0	0	0

Mar-97	Feb-98							
D	20	50	100	250	20	50	100	250
n	5	28	86	261	5	16	48	186
r	0.287	0.183	0.084	0.010	0.083	0.013	0.058	0.030
U	0.235	0.093	0.045	0.017	0.225	0.124	0.066	0.016
L	-0.194	-0.078	-0.039	-0.012	-0.212	-0.115	-0.058	-0.011
P	0.009	0.001	0.003	0.097	0.232	0.419	0.041	0.001
Ur	0.517	0.297	0.135	0.041	0.400	0.142	0.125	0.065
Lr	0.008	0.068	0.026	-0.019	-0.117	-0.078	-0.015	-0.004
Intercept	106	121	174	0	0	0	0	0

Mar-00					Dec-00			
D	20	50	100	250	20	50	100	250
n	4	33	104	252	2	3	4	22
r	0.112	0.005	0.054	0.013	-0.197	-0.007	-0.066	-0.021
U	0.258	0.084	0.040	0.015	0.366	0.269	0.267	0.037
L	-0.240	-0.083	-0.034	-0.010	-0.318	-0.168	-0.181	-0.037
P	0.192	0.452	0.004	0.043	0.896	0.508	0.681	0.846
Ur	0.309	0.122	0.109	0.048	0.149	0.320	0.180	0.082
Lr	-0.146	-0.100	-0.003	-0.021	0.149	-0.352	-0.280	-0.120
Intercept	0	0	0	0	0	0	0	0

Mar-01					Oct-01			
D	20	50	100	250	20	50	100	250
n	43	154	261	752	12	79	195	552
r	0.197	0.069	0.050	0.009	0.109	0.110	0.036	0.002
U	0.070	0.034	0.025	0.007	0.121	0.046	0.023	0.006
L	-0.058	-0.028	-0.020	-0.006	-0.117	-0.040	-0.021	-0.005
P	0.001	0.002	0.001	0.004	0.044	0.001	0.006	0.197
Ur	0.267	0.114	0.080	0.024	0.235	0.167	0.068	0.021
Lr	0.127	0.029	0.021	-0.008	-0.013	0.053	0.005	-0.015
Intercept	60	126	164	0	0	94	172	0

Feb-02				
D	20	50	100	250
n	133	821	2234	6012
r	0.22	0.075	0.026	0.002
U	0.037	0.014	0.007	0.002
L	-0.036	-0.013	-0.007	-0.002
P	0.001	0.001	0.001	0.028
Ur	0.267	0.095	0.036	0.008
Lr	0.17	0.056	0.017	-0.004
Intercept	0	99	175	0

Combined grids

1st-95

D	20	50	100	200	320	800
n	183	1034	2738	7586	12753	16562
r	0.146	0.074	0.045	0.026	0.022	0.016
U	0.027	0.011	0.007	0.004	0.003	0.002
L	-0.025	-0.011	-0.006	-0.003	-0.002	-0.002
P	0.001	0.001	0.001	0.001	0.001	0.001
Ur	0.181	0.087	0.052	0.031	0.026	0.019
Lr	0.109	0.059	0.037	0.022	0.019	0.013
Intercept	341	506	524	639	704	1166

2nd-95

D	20	50	100	200	320	800
n	129	795	2386	6778	10918	14643
r	0.096	0.072	0.048	0.036	0.028	0.023
U	0.038	0.014	0.007	0.004	0.003	0.002
L	-0.033	-0.014	-0.007	-0.004	-0.002	-0.002
P	0.001	0.001	0.001	0.001	0.001	0.001
Ur	0.140	0.088	0.056	0.041	0.032	0.026
Lr	0.053	0.054	0.039	0.031	0.024	0.020
Intercept	400	539	576	701	777	1175

3rd-95

D	20	50	100	200	320	800
n	43	286	880	2377	3708	5151
r	0.013	0.029	0.026	0.030	0.026	0.020
U	0.058	0.024	0.013	0.008	0.005	0.004
L	-0.057	-0.025	-0.012	-0.007	-0.004	-0.003
P	0.324	0.010	0.001	0.001	0.001	0.001
Ur	0.093	0.053	0.040	0.039	0.032	0.025
Lr	-0.068	0.004	0.013	0.021	0.019	0.014
Intercept	398	449	672	674	775	1172

1st-96						
D	20	50	100	200	320	800
n	39	165	483	1176	1741	2204
r	0.156	0.117	0.087	0.069	0.068	0.057
U	0.068	0.031	0.016	0.012	0.009	0.007
L	-0.068	-0.031	-0.017	-0.010	-0.007	-0.006
P	0.002	0.001	0.001	0.001	0.001	0.001
Ur	0.240	0.159	0.111	0.083	0.078	0.067
Lr	0.081	0.073	0.065	0.057	0.057	0.048
Intercept	336	506	512	740	768	1181

2nd-96						
D	20	50	100	200	320	800
n	38	249	698	2036	3100	4075
r	0.037	0.033	0.044	0.035	0.027	0.020
U	0.068	0.025	0.013	0.008	0.006	0.005
L	-0.059	-0.026	-0.014	-0.007	-0.055	-0.004
P	0.128	0.007	0.001	0.001	0.001	0.001
Ur	0.111	0.060	0.060	0.043	0.034	0.026
Lr	-0.041	0.005	0.028	0.024	0.020	0.014
Intercept	291	396	458	518	614	1178

3rd-96						
D	20	50	100	200	320	800
n	16	122	349	919	1275	1535
r	-0.029	0.015	0.025	0.012	0.010	0.009
U	0.087	0.033	0.017	0.011	0.008	0.007
L	-0.090	-0.030	-0.017	-0.009	-0.007	-0.005
P	0.741	0.170	0.003	0.011	0.011	0.006
Ur	0.045	0.053	0.045	0.025	0.020	0.018
Lr	-0.105	-0.022	0.006	0.000	0.000	0.000
Intercept	113	185	438	450	1207	1196

1st-97

D	20	50	100	200	320	800
n	8	32	91	239	354	429
r	0.410	0.227	0.119	0.027	0.018	0.018
U	0.160	0.080	0.046	0.022	0.015	0.011
L	-0.142	-0.074	-0.040	-0.019	-0.011	-0.008
P	0.001	0.001	0.001	0.008	0.014	0.004
Ur	0.524	0.329	0.173	0.061	0.043	0.041
Lr	0.219	0.098	0.061	-0.008	-0.006	-0.005
Intercept	109	130	181	750	778	1110

1st-98

D	20	50	100	200	320	800
n	6	19	62	168	257	267
r	0.109	0.043	0.038	0.035	0.006	0.004
U	0.176	0.100	0.055	0.025	0.017	0.017
L	-0.164	-0.087	-0.045	-0.019	-0.012	-0.011
P	0.116	0.179	0.070	0.006	0.199	0.261
Ur	0.330	0.134	0.093	0.069	0.035	0.032
Lr	-0.071	-0.047	-0.021	0.000	-0.023	-0.021
Intercept	80	245	248	284	347	1180

1st-00

D	20	50	100	200	320	800
n	18	88	254	612	778	821
r	0.113	0.138	0.095	0.065	0.051	0.047
U	0.116	0.060	0.032	0.018	0.016	0.015
L	-0.107	-0.050	-0.024	-0.033	-0.010	-0.009
P	0.029	0.001	0.001	0.001	0.001	0.001
Ur	0.227	0.202	0.133	0.086	0.069	0.068
Lr	-0.019	0.072	0.056	0.044	0.033	0.030
Intercept	219	272	298	389	564	1202

2nd-00						
D	20	50	100	200	320	800
n	2	8	18	68	80	83
r	0.248	-0.038	-0.017	0.016	0.020	0.017
U	0.320	0.168	0.105	0.048	0.046	0.050
L	-0.285	-0.145	-0.090	-0.037	-0.032	-0.029
P	0.071	0.663	0.626	0.209	0.154	0.174
Ur	0.065	0.223	0.106	0.087	0.072	0.079
Lr	0.065	-0.234	-0.132	-0.041	-0.032	-0.034
Intercept	31	197	364	870	434	1230

1st-01						
D	20	50	100	200	320	800
n	48	174	318	745	1107	1134
r	0.224	0.107	0.089	0.039	0.025	0.024
U	0.060	0.029	0.023	0.012	0.009	0.009
L	-0.052	-0.025	-0.018	-0.010	-0.006	-0.006
P	0.001	0.001	0.001	0.001	0.001	0.001
Ur	0.286	0.144	0.114	0.055	0.038	0.037
Lr	0.157	0.067	0.062	0.022	0.012	0.010
Intercept	169	176	294	389	602	1161

2nd-01						
D	20	50	100	200	320	800
n	15	84	210	526	695	696
r	0.232	0.188	0.111	0.078	0.078	0.077
U	0.125	0.055	0.028	0.012	0.010	0.010
L	-0.117	-0.044	-0.023	-0.010	-0.006	-0.006
P	0.001	0.001	0.001	0.001	0.001	0.001
Ur	0.394	0.250	0.146	0.099	0.094	0.094
Lr	0.071	0.133	0.078	0.057	0.060	0.060
Intercept	255	958	917	836	1014	1123

1st-02						
	20	50	100	200	320	800
D	271	1528	3945	9745	13290	13926
n	0.208	0.114	0.067	0.048	0.041	0.040
r	0.025	0.011	0.006	0.004	0.003	0.003
U	-0.023	-0.010	-0.006	-0.003	-0.002	-0.002
L	0.001	0.001	0.001	0.001	0.001	0.001
P	0.243	0.126	0.075	0.052	0.045	0.043
Ur	0.173	0.100	0.060	0.043	0.037	0.036
Lr	372	373	806	591	751	1201
Intercept						